

Selective Extraction of Naturally Occurring Radioactive Ra²⁺ from Aqueous Waste Streams

Extractants Based on Thiacalix[4]arene and (Iso)guanosine



This research was supported by the Technology Foundation STW, applied science division of NWO and the technology program of the Ministry of Economic Affairs, grant number TCS. 5291.

Publisher:

Print Partners Ipskamp, Postbus 33, 7500 AH Enschede, The Netherlands,

<http://www.ppi.nl>

© Fijs van Leeuwen, Enschede, 2005

No Part of this work may be reproduced by print, photocopy, or any other means without the permission in writing from the publisher.

Thesis University of Twente, Enschede, The Netherlands

ISBN 90-365-2172-6

**SELECTIVE EXTRACTION OF NATURALLY
OCCURRING RADIOACTIVE RA²⁺ FROM
AQUEOUS WASTE STREAMS**

EXTRACTANTS BASED ON THIACALIX[4]ARENE AND
(ISO)GUANOSINE

PROEFSCHRIFT

ter verkrijging van
de graad van doctor aan de Universiteit Twente,
op gezag van de rector magnificus,
prof. dr. W. H. M. Zijm,
volgens besluit van het College van Promoties
in het openbaar te verdedigen
op donderdag 31 maart 2005 om 15.00 uur

door

Fijs Willem Bernhard van Leeuwen

geboren op 29 oktober 1977
te Leiderdorp

Dit proefschrift is goedgekeurd door:

Promotor: Prof. dr. ir. D. N. Reinhoudt

Assistent-Promotor: Dr. W. Verboom

“..... these substances contain a small quantity of a strongly radioactive body, differing from uranium and thorium and the simple bodies actually known. I thought that if this were indeed the case, I might hope to extract this substance by the ordinary methods of chemical analysis”

Mme. Curie

Aan Lieke, Sven en Zoë

Contents

Chapter 1

General Introduction	1
-----------------------------	---

Chapter 2

Naturally Occurring Radioactive Ra²⁺ Nuclides in Waste Streams and their Removal	5
2.1 Introduction	6
2.2 NORM Occurrence	7
2.3 Technologically Enhanced Natural Radioactive Material (TENORM)	8
2.3.1 Introduction	8
2.3.2 Ores	9
2.3.3 Energy Production	9
2.3.3.1 Coal	9
2.3.3.2 Oil and Gas Production	10
2.3.4 Water Supplies	11
2.3.5 General Ra ²⁺ Occurrence in Aqueous TENORM streams	12
2.4 Ra ²⁺ Toxicity	12
2.5 General Ra ²⁺ Separation Techniques	13
2.6 Organic Ra ²⁺ Extractants	15
2.6.1	15
2.6.2 Resin-based Ra ²⁺ Extraction	15
2.6.3 Anionic Polydentate Extractants	16
2.6.4 Synergistic Ra ²⁺ Extractants	19
2.6.5 Combining Acids and Crown Ethers on a Platform	21
2.7 Outlook	23
References	24

Chapter 3

Synthesis and Conformational Evaluation of <i>p</i>-<i>tert</i>-Butylthiacalix[4]crowns	29
3.1 Introduction	30
3.2 Results and Discussion	30
3.2.1 Direct Bridging of Thiacalix[4]arene	30
3.2.2 Diametrically Substituted Thiacalix[4]monocrowns	33
3.2.3 Indirect Synthesis of Dihydroxythiacalix[4]crowns	35
3.2.4 Assignment of the Conformation	36
3.2.4.1 Thiacalix[4]biscrowns	36
3.2.4.2 Rigid Thiacalix[4]monocrowns	38
3.2.4.3 Conformationally Flexible Dihydroxy- and Dimethoxythiacalix[4]monocrowns	42
3.3 Conclusions	45
3.4 Experimental	46
References	54

Chapter 4

Ionizable (Thia)calix[4]crowns as Highly Selective Ra^{2+} Extractants	57
4.1 Introduction	58
4.2 Results and Discussion	59
4.2.1 Synthesis	59
4.2.2 Extraction of Alkali(ne Earth) Cations by (Thia)calix[4]crown Dicarboxylic Acids	60
4.2.3 Precipitation of Ra^{2+}	61
4.2.4 Competitive Ra^{2+} Extraction Experiments in the Presence of Alkali and Alkaline Earth Cations	63
4.2.5 Dissolution of Precipitated Ra^{2+} Salts	68
4.2.6 Effective pH Range of Thiacalix[4]crown-6 Dicarboxylic Acid	68
4.2.7 Loading and Regeneration of Thiacalix[4]crown-6 Dicarboxylic Acid by pH Variation	69
4.3 Conclusions	70
4.4 Experimental	71
4.4.1 Synthesis	71

4.4.2 Extraction	73
References	76
 <i>Chapter 5</i>	
Thiacalix[4]arene Derivatives as Ra²⁺ Extractants: a Systematic Study on the Requirements for Ra²⁺ Extraction	79
5.1 Introduction	80
5.2 Results and Discussion	81
5.2.1 Synthesis and Characterization of Extractants	81
5.2.2 The Role of Covalently Attached Carboxylic Acid Groups	84
5.2.3 Ra ²⁺ Extraction by Thiacalix[4]arene Derivatives	86
5.3 Conclusions	92
5.4 Experimental	92
5.4.1 Synthesis	92
5.4.2 Extraction	96
References	98
 <i>Appendix Chapter 5</i>	
Derivation of Extraction Constants and Ra²⁺ Selectivity Coefficients	101
A.1 Introduction	101
A.2 General	101
A.3 Singly Charged Extractants, 1: 1 Stoichiometry	102
A.4 Doubly or Triply Charged Extractants, 1: 1 Stoichiometry	104
A.5 Quadruply Charged Extractants, 1: 2 Stoichiometry	106
References	108
 <i>Chapter 6</i>	
Selective Ra²⁺ Extractants Provided by Self-assembly of Guanosine and Isoguanosine Derivatives	109
6.1 Introduction	110
6.2 Results and Discussion	111
6.2.1 Non-competitive Ra ²⁺ Extraction Experiments	111
6.2.2 Binding Potential of Guanosine-Picrate and Isoguanosine Assemblies for Divalent Alkaline Earth Cations	112

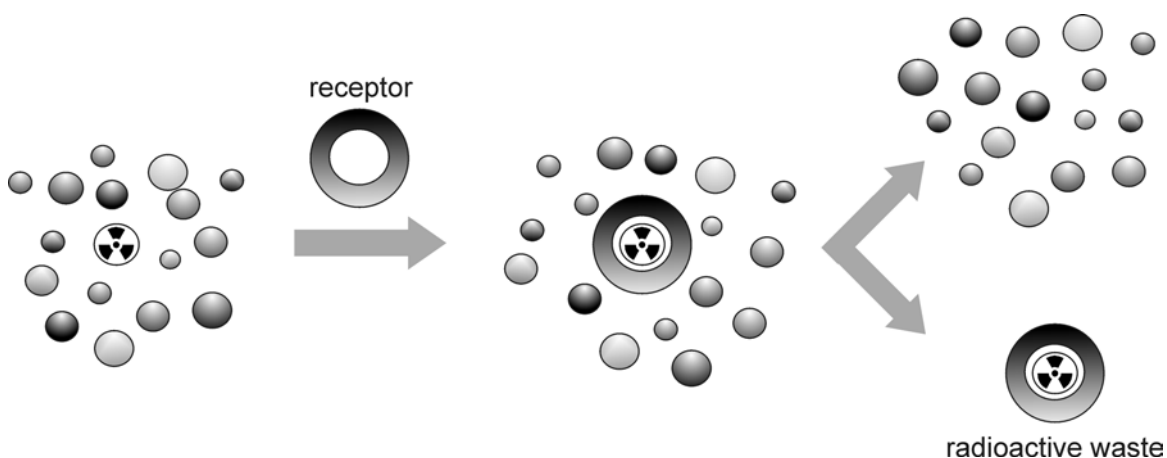
6.2.3 Competitive Ra ²⁺ Extraction Experiments in the Presence of Alkaline Earth Cations	113
6.2.4 Competitive Ra ²⁺ Extraction Experiments in the Presence of Alkali Cations	116
6.2.5 Determination of the Effective pH Range	119
6.3 Conclusions	120
6.4 Experimental	120
References	123
<i>Chapter 7</i>	
Selective Removal of Ra²⁺ from Produced Waters of the Gas Industry	125
7.1 Introduction	126
7.2 Results and Discussion	127
7.2.1 Metal Ion Constituents of Gas-field Produced Water	127
7.2.2 Ra ²⁺ Extraction from a Produced Water Sample	128
7.2.3 Stripping of the Organic Phases	130
7.3 Conclusions	131
7.4 Experimental	131
References	133
<i>Outlook</i>	135
<i>Summary</i>	141
<i>Samenvatting</i>	143
<i>Acknowledgments/Dankwoord</i>	

Chapter 1

General Introduction

Radioactivity can cause environmental problems, since a relatively small quantity of (long-lived) radioactive material is able to give a widespread contamination.¹ Efficient removal/concentration of radioactive pollutants would prevent exposure of the world's population to their radioactivity.

Advances in molecular (metal ion) recognition are reflected in the Nobel Prize for Pedersen, Cram, and Lehn.²⁻⁴ However, implementing molecular recognition in the selective removal of radioactive metal ions from aqueous (waste) streams is still a big challenge. One of the reasons for this is that receptors must be able to differentiate between highly similar metal ions (Scheme 1).⁵ Furthermore, many different types of radioactive cations are found, often in very low concentrations and in the presence of a significant excess of other metal ions.¹



Scheme 1. Schematic representation of radioactive metal ion recognition and separation in the presence of competing metal ions.

The research described in this thesis is based on the design and evaluation of new selective receptor molecules, which can be used for the removal of naturally occurring⁶ radioactive radium (Ra^{2+}) from waste streams of non-nuclear industries.⁷ Because of the nature of these waste streams, the molecular recognition of Ra^{2+} must be selective in the presence of an excess of the other alkali(ne earth) cations such as Na^+ , K^+ , Ba^{2+} , and Ca^{2+} .

Chapter 2 gives an introduction in the radioactive Ra^{2+} contaminations found in non-nuclear industries, as well as the radiotoxicity of Ra^{2+} . Recent developments in the removal of Ra^{2+} from (aqueous) solutions and in particular the current advances in the design of Ra^{2+} selective receptor molecules (extractants) are reported.

The synthesis of various thiacalix[4](bis)crown derivatives, and their conformational assignment based on both 2D NMR spectroscopy and X-ray crystal structures is discussed in **Chapter 3**.

In **Chapter 4** the synthesis of new *thiacalix*[4]crown-5 and -6 dicarboxylic acids and their Ra^{2+} selectivity in a significant excess of other alkali(ne earth) cations is reported. Additionally, the Ra^{2+} selectivity of known calix[4]crown-5 and -6 dicarboxylic acids was determined under identical conditions, to allow direct comparison of thiacalix[4]crowns and calix[4]crowns. In addition, both the effective pH range and the pH dependent loading and stripping of thiacalix[4]crown-6 dicarboxylic acid are described.

A systematic study on the essential features of thiacalix[4]arene-based Ra^{2+} receptors is reported in **Chapter 5**. The first part of this chapter deals with the synthesis of new trisubstituted thiacalix[4]arene derivatives. The second part describes the improved Ra^{2+} extraction by the combination of a crown ether and carboxylic acid substituents on a thiacalix[4]arene platform over that by a mixture containing both a crown-ether derivative and an acid derivative. The third part evaluates the influence that crown-ether bridges and (carboxylic) acid groups have on the Ra^{2+} extraction of thiacalix[4]crown dicarboxylic acids. The appendix of Chapter 5 describes the proof for the complex stoichiometries and models used to determine both the K_{ex}^{M} values and the Ra^{2+} selectivity coefficients $[\log(K_{\text{ex}}^{\text{Ra}}/K_{\text{ex}}^{\text{M}})]$.

Chapter 6 deals with the alkaline earth cation affinities of noncovalent assemblies of guanosine and isoguanosine at equimolar metal ion and ionophore concentrations, followed by the Ra^{2+} selectivity in the presence of excesses of alkali(ne earth) cations. Furthermore, the prevention of Ra^{2+} salt formation and the effective pH range in which Ra^{2+} is extracted are described.

In **Chapter 7** both the thiacalix[4]crown-5 and -6 dicarboxylic acids and the noncovalent assemblies of guanosine and isoguanosine are examined for their Ra^{2+} extraction ability from actual produced water from the gas industry. The metal ion content of the produced water was determined, after which extractions were performed with a produced water sample and a metal ion-based model solution. The chapter ends with Ra^{2+} recovery experiments.

In the **outlook**, suggestions are given for modifications/implementations of the extractants described in Chapters 4 and 6.

References

1. Eisenbud, M.; Gesell, T. F. *Environmental Radioactivity – From Natural, Industrial, and Military Sources*, 4th ed.; Academic Press: New York, 1997.
2. Pederson, C. J. *Angew. Chem. Int. Ed. Engl.* **1988**, *27*, 1021-1027.
3. Cram, D. J. *Angew. Chem. Int. Ed. Engl.* **1988**, *27*, 1009-1020.
4. Lehn, J.-M. *Angew. Chem. Int. Ed. Engl.* **1988**, *27*, 89-112.
5. Izatt, R. M.; Bradshaw, J. S.; Bruening, R. L.; Taret, B. J.; Bruening, M. L. *Pure Appl. Chem.* **1995**, *67*, 1069-1074.
6. Kathren, R. L. *Appl. Radiat. Isot.* **1998**, *49*, 149-168.
7. Heaton, B.; Lambley, J. *Appl. Radiat. Isot.* **1995**, *46*, 577-581.

Chapter 2

Naturally Occurring Radioactive Ra^{2+} Nuclides in Waste Streams and their Removal by Selective extraction

Abstract: The behavior of the naturally occurring radioactive metal ion Ra^{2+} in sediments is discussed together with the industries producing Ra^{2+} holding waste. The radiotoxicity of Ra^{2+} and the need for its (selective) removal from abundant (competing) metal ions is outlined. This chapter concludes with the currently most common Ra^{2+} extraction techniques, in particular those based on organic extractants.

2.1 Introduction

Nearly all rocks, soils, and water streams contain small amounts of Naturally Occurring Radioactive Material (NORM). The term NORM includes more than twenty primordial nuclides, e.g. ^{40}K , ^{87}Rb , ^{232}Th , ^{235}U , and ^{238}U .¹ This chapter focuses on the natural radioactive elements uranium (^{238}U and ^{235}U) and thorium (^{232}Th), and their daughter products (Figure 2.1).

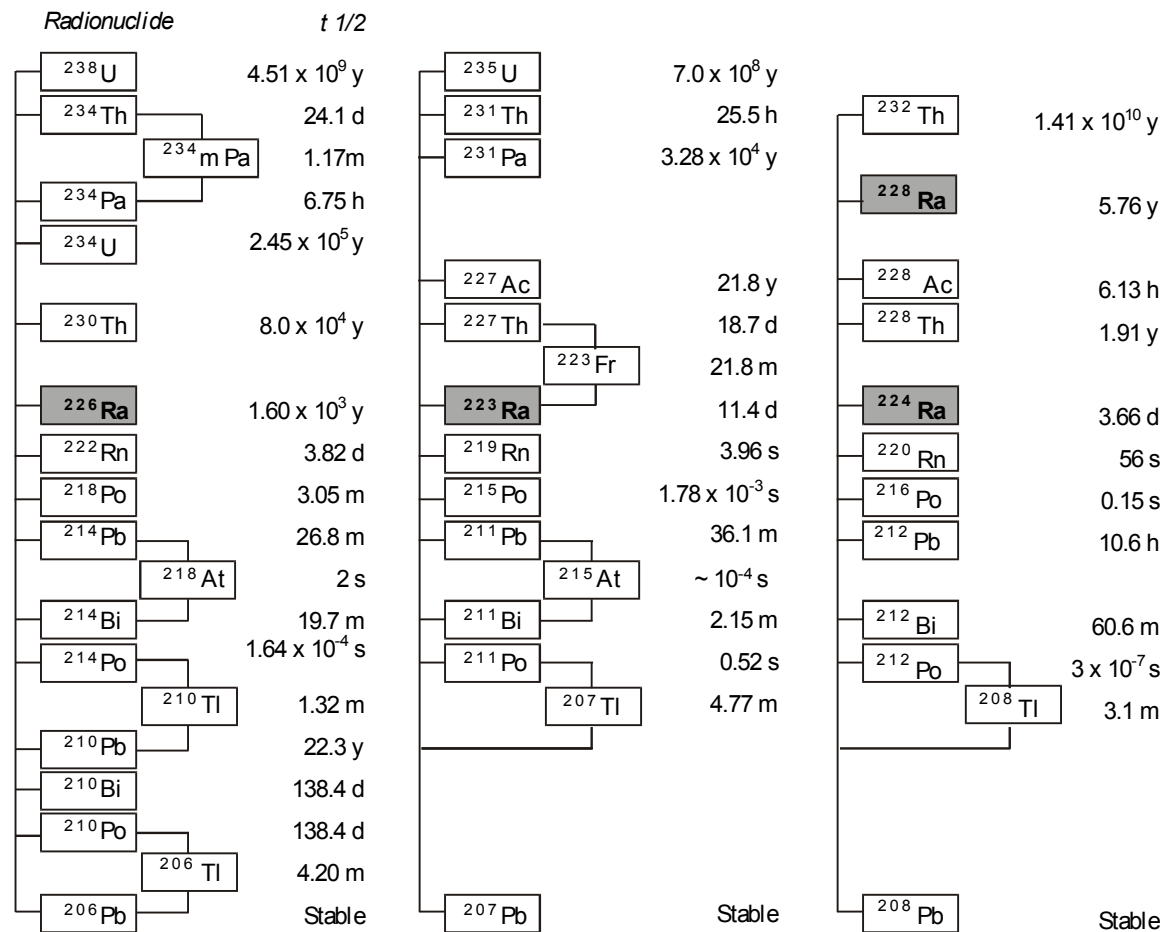


Figure 2.1. Decay processes of ^{238}U , ^{235}U , and ^{232}Th , in which the daughter nuclides ^{226}Ra , ^{228}Ra , ^{224}Ra , and ^{223}Ra are formed.¹

Due to industries that utilize NORM containing sediments, this natural form of radioactive contamination has - over the years - contributed to the release of significant amounts ($\sim 10^4 \text{ GBq/a}$)² of radioactive material into the environment. To reduce the future dose, research is ongoing for the separation of the most radiotoxic

and long-living nuclides, in particular that of the highly water soluble radium (²²⁶Ra²⁺; t_{1/2} = 1600 y).

In this chapter, the Ra²⁺-waste generating industries and their Ra²⁺ containing waste streams are described, as well as the current Ra²⁺ extraction techniques, with the focus on organic extractants.

2.2 NORM Occurrence

The parent NORM nuclides U and Th are associated with many different minerals and rock types. Because, the soil geology is decisive for the U and Th content, their abundance varies worldwide. On average U concentrations range from 0-59 Bq/kg and Th from 7-81 Bq/kg (Table 2.1) and of all rock types, salic rock holds the highest background levels (Bq = nuclear decay per second).² Mobilization by water makes transport to sedimentary rocks (shales, sandstones, and carbonate rocks) and soil possible, increasing their NORM contents.

Table 2.1. Average background levels of U and Th in crustal rocks (Bq/kg).³

Rock type	²³⁸ U (Bq/kg)	²³² Th (Bq/kg)
<i>Igneous</i>		
Acidic (Granite)	59	81
Intermediate (Diorite)	23	32
Mafic (Basalt)	11	11
Ultra basic (durite)	0.4	24
<i>Sedimentary</i>		
Limestone	27	7
Carbonate	26	8
Sandstone	18	11
Shale	44	44
Upper crust average	34	45
Soil	25	25

Due to their high temperatures and chemically reducing (low redox potential) nature, highly mineralized formation waters or brines that occur in subsurface formations, may have a high NORM content. This formation water, of which the

constituents may vary greatly around the world, holds minerals that have been leached from the rocks.⁴ The saline conditions of these waters allow for solvation of alkali(ne earth) cations. However, together with adsorption onto rock particles (FeO), this reduces the levels of U and Th.^{3,5} Consequently, the alkaline earth cation Ra^{2+} is the most widely encountered form of NORM in saline waters. There are four possible processes that transport Ra^{2+} from the rock to the water, namely leaching, diffusion, alpha-recoil, and ion exchange. Of these four examples, the latter seems to be the most feasible way to give high Ra^{2+} concentrations. Ra^{2+} is desorbed from the surface of minerals and replaced, mainly by Ca^{2+} , Ba^{2+} , and Sr^{2+} ,⁶ and to a lesser extent by Na^+ and K^+ . Elution experiments have shown that besides the ion-exchange process, the type and amount of anions present also have an influence on the immobilization of Ra^{2+} . Larger anions like NO_3^- interfere with the hydrate ion shell around minerals and enhance the ion exchange process.⁷

2.3 Technologically Enhanced Naturally Occurring Radioactive Material (TENORM)

2.3.1 Introduction

The term “Technologically Enhanced NORM” (TENORM) is used to describe any form of NORM of which the radionuclide concentrations are increased above levels present in the natural state as a result of human activities.^{8,9} In general, TENORM wastes are often included in (by-)products from industrial activities such as mining, phosphate production, coal burning, oil and natural gas production, and water treatment (for some examples of $^{226}\text{Ra}^{2+}$ emissions see Table 2.2).⁹⁻¹¹

Table 2.2. Average annual ore throughput (10^6 kg/a) and annual release of $^{226}\text{Ra}^{2+}$ to water (GBq/a).²

Industry	Ore throughput	Release to water
Phosphor	1645	7.4×10^2
Coal	2355	1.1×10^{-2}
Mineral sands	1.8×10^{2a}	6.8×10^{-2}
Oil extraction	3.5×10^3	1.7×10^2
Gas extraction	7.2×10^{4a}	3.2×10^1

^a $10^6 \text{ m}^3/\text{a}$.

2.3.2 Ores

Uranium minerals are found in association with many primary metal deposits such as those of copper, lead, and precious metal sulfide ores.¹² Geologists generally agree that the presence of NORM within a particular ore deposit depends on the regional geology, the minerals, and the geological formation, rather than on the mining type or classification.¹² For example, lanthanides are mined as bastnasite [(Ce, La, Y)CO₃F], monazite [(Ce, La, Th, Nd, Y)PO₄], and xenotime (YPO₄), which all contain the chemically similar actinides Th and U.¹¹ In the case of uranium mining, the presence of its daughter nuclides is evident. However, only the overburden and mine spoils have to be considered as TENORM-waste, since both the source materials as the mill tailings are specified as under the atomic energy act.¹¹

Phosphate ores contain both U and Th, together with a broad spectrum of other cations, e.g. Ca²⁺, Mg²⁺, Sr²⁺, Ba²⁺, Fe³⁺, Al³⁺, Na⁺, Mn²⁺, and Zr⁴⁺.^{13,14} It is assumed that in these ores Ra²⁺ exists as a sulfate salt with Ba²⁺ and possibly Sr²⁺.¹⁴ When phosphate ore is processed, it produces both elemental phosphorus and phosphoric acid.¹⁴ These are then used in the production of phosphate fertilizers, detergents, (animal and human) food products, and phosphorus chemicals, all of which may contain (TE)NORM. For example, phosphate fertilizers, obtained after direct mixing of phosphoric acid and phosphate rock, contain Ra²⁺ in their matrix and as such significantly contribute to the Ra²⁺ presence in crops, water streams, and lakes.¹⁵ One of the main side products in the production of phosphoric acid (wet process), phosphogypsum (gypsum = CaSO₄•2H₂O), contains about 80% of the Ra²⁺ present in the original phosphate ores. This side product is produced in 4.8 x 10¹⁰ kg per year (Table 2.2), and is often used for construction purposes.^{16,17}

2.3.3 Energy Production

Energy generating industries that use subsurface formations, coal, oil, and gas can also produce TENORM wastes.⁹

2.3.3.1 Coal

Coal tends to concentrate trace quantities of U³⁺ and Th⁴⁺, as well as their radioactive decay products.¹⁸ Waters produced from coalmines were estimated to contain 13 kBq/m³ of ²²⁶Ra²⁺. This would result in a total ²²⁶Ra²⁺ emanation of 37

GBq per year in the Ruhr district alone.¹⁹ When coal is burned to produce electricity, the non-flammable minerals are concentrated in the ash (0.14 Bq/kg; Table 2.2),²⁰ which is commonly used as an additive in constructing materials.²¹

A very important feature of Ra²⁺-containing coalmine pit waters, is the co-existence of significant excesses of other cations (total salinity 230 g/L).⁷ Moreover, the Ra²⁺ concentration increases with the salinity, caused by Na⁺, K⁺, Mg²⁺, Ca²⁺, Sr²⁺, and Ba²⁺ cations.²² Table 2.3 shows that alkali(ne earth) cations are present in huge excess compared to ²²⁶Ra²⁺ (< 63 Bq/L) and ²²⁸Ra²⁺ (< 28 Bq/L).

Table 2.3. The ionic composition (mg/L) of high-salinity pit waters at pH 6.5 containing ²²⁶Ra²⁺ (60 Bq/L; 1.6 x 10⁻⁶ mg/L).^{a,7}

Na ⁺	K ⁺	Ca ²⁺	Mg ²⁺	Sr ²⁺	Ba ²⁺	Cl ⁻	SO ₄ ²⁻	HCO ₃ ⁻	NO ₃ ⁻
70000	1200	9000	1500	700	1500	120000	< 5	120	20

^a Determined by ICP-OES.

2.3.3.2 Oil and Gas Production

One of the main industries with a TENORM problem is the petroleum industry. The sedimentary rocks, shales, within which oil and gas deposits are found have a high level of radioactivity (Table 2.1) and contain formation water in relatively large quantities. This Ra²⁺ containing formation water (Figure 2.2a) is transported to the surface together with e.g. sulphate-rich injected (sea) water.^{23,24} When the produced water is brought to the surface, both the pressure and the temperature drop, causing precipitation of some of the dissolved Ra²⁺ together with other cations such as Ba²⁺.^{24,25} This results in radioactive scales that block and contaminate the production pipes (Figure 2.2b).²⁶ In most cases Ra²⁺ co-precipitates with BaSO₄ or SrSO₄ scales,²⁴ but Ra²⁺ can also co-precipitate with CaCO₃.^{27,28} In addition, Ra²⁺ cations can be present in sludges, which are deposits that accumulate at the bottom of storage and process vessels. Although the majority of Ra²⁺ precipitates, produced water can still contain traces of Ra²⁺, together with an abundance of other cations and organic compounds (Table 2.4; Figure 2.2c).²⁹

Produced water contains a wide range of metal ions.^{30,34} In addition to the cations reported in Table 2.4, it holds traces of various other cations namely: Fe³⁺, Mn²⁺, Hg²⁺, Pb²⁺, Cd²⁺, Cu²⁺, Ni²⁺, Th⁴⁺, Zr⁴⁺, Zn²⁺, and Al³⁺.³⁰⁻³³

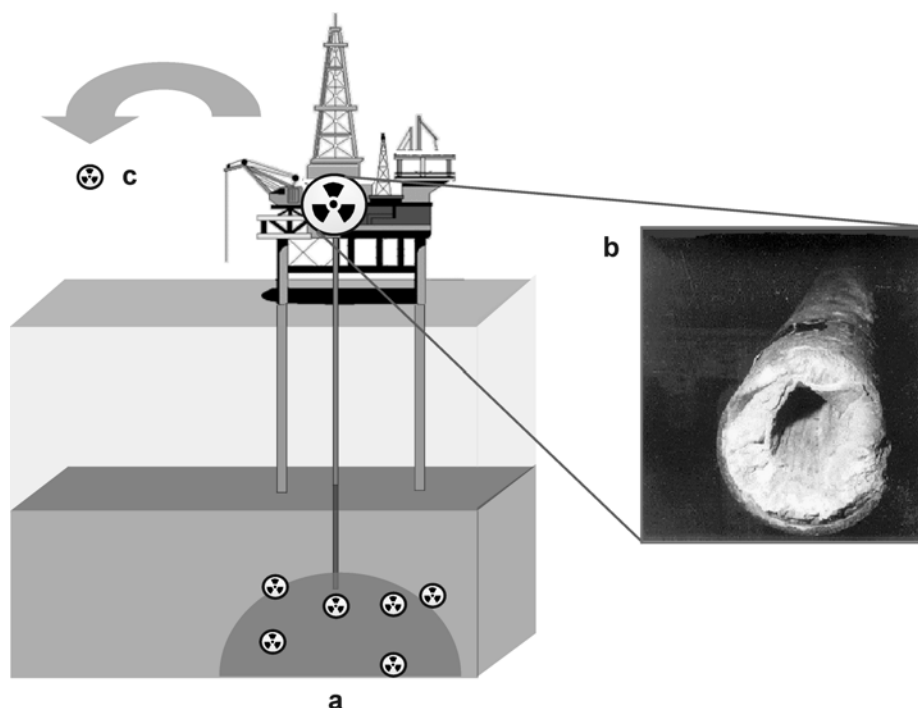


Figure 2.2. A schematic representation of the Ra²⁺ transport in the petroleum industry (left) and a production pipe with scales (right): (a) Ra²⁺ in formation water, (b) Ra²⁺ contamination of the production pipes, and (c) Ra²⁺ released with the produced water stream.

Table 2.4. Cationic composition (mg/L) of formation, sea, and production water (400 g/L of dissolved solids).²⁴

Ion	Formation water	Sea water	Produced water ³⁴
Na ⁺	31000	11000	35000
K ⁺	650	460	Not reported
Mg ²⁺	380	1400	910
Ca ²⁺	5000	430	3300
Sr ²⁺	770	0	130
Ba ²⁺	270	0	95

2.3.4 Water Supplies

Water supplies like streams, lakes, reservoirs, and aquifers contain varying levels of Ra²⁺ leached from surrounding rocks and sediments.^{35,36} Most drinking water sources, however, have such low levels of radioactive contaminants that they are not

considered a public health concern. However, a small percentage of drinking water samples, including bottled mineral waters,³⁷ contains α -radiation levels high enough to pose a health concern (> 100 Bq/L).^{3,38,39} Consequently, the waste produced by water treatment plants may result in TENORM containing sludges with up to 10^3 Bq/kg of $^{226}\text{Ra}^{2+}$.¹⁰

In different water supplies,⁴⁰⁻⁴² Ra^{2+} cations are present together with a wide range of other cations (for an example see Table 2.5). Studies on spring water from Slovenia show that Sr^{2+} can also be present in high concentrations.⁴³

Table 2.5. Example of the cationic contents (mg/L) of “raw” water (pH 7.3) taken from waters of the Jordan wells in Washington, Iowa (Ra^{2+} 2.7×10^{-1} Bq/L; 7.2×10^{-9} mg/L).⁴²

K^+	Na^+	Ca^{2+}	Fe^{3+}	Mg^{2+}	Total dissolved solids
22	200	110	0.8	47	1200

2.3.5 General Ra^{2+} Occurrence in Aqueous TENORM Streams

In general, Ra^{2+} is always found in saline waters to a significantly lesser degree compared with other common alkali(ne earth) cations such as Na^+ , K^+ , Mg^{2+} , Ca^{2+} , Sr^{2+} , Ba^{2+} , and traces of transition and heavy metal ions.

2.4 Radium (Ra) Toxicity

The element Ra can be ingested with food^{44,45} and inhaled.⁴⁶ Subsequently, it follows similar accumulation pathways as Ca^{2+} , namely to the mineral bone tissue, but not into the bone marrow,^{47,48} and contributes considerably to the internal dose of radioactivity.⁴⁹ Furthermore, the Ra daughter nuclide Rn (^{222}Rn , ^{219}Rn , and ^{220}Rn) is retained in the lungs as Po and (stable) Pb.⁵⁰

People that were exposed to internally deposited α -emitters such as ^{226}Ra nuclides, have shown abundant cancer at heavily contaminated sites.⁵¹⁻⁵³ Most important is the induction of lung cancer by inhaling the daughter nuclides of Ra, like ^{222}Rn (see Figure 2.1), which is present indoors and causes between 6,000 and 36,000 lung cancer deaths per year in the US.⁵²

$^{226}\text{Ra}^{2+}$ is considered to be among the most toxic long-lived α -emitters present in environmental samples, as well as one of the most widespread.⁵⁴ Furthermore, both

the ²²⁶Ra and ²²⁸Ra radiotoxicities are estimated to be about eight times higher than of ²²⁴Ra.⁵⁵

2.5 General Ra²⁺ Separation Techniques

The highly toxic nature of Ra²⁺ isotopes renders effective separation of these radionuclides from other non-toxic substances highly desirable.

Mme. Curie discovered that pitch-blend (U-oxide ore) contained a small amount of a new element, which was much more radioactive than U and Th. By isolating this element, she developed the first isolation method for Ra²⁺. However, her attempts based on the fractional precipitation of the RaCl₂ salt (Figure 2.3) from 50 kg of pitch-blend, did not yield pure RaCl₂ but mixtures with BaCl₂.⁵⁶



Figure 2.3. Ra²⁺ separation by fractional crystallization, performed by Mme. Curie and co-workers.⁵⁷

In the following quote Mme. Curie illustrates some of the experimental procedures involved in this Ra^{2+} isolation method.

“I went ahead with the chemical experiments, which had as their objective the preparation of pure radium salts. I had to work with as much as twenty kilograms of material at a time, so that the hangar was filled with great vessels full of precipitates and of liquids. It was exhausting work to move the containers about, to transfer the liquids, and to stir for hours at a time, with an iron bar, the boiling material in the cast-iron basin. I extracted from the mineral the radium-bearing barium and this, in the state of chloride, I submitted to a fractional crystallization.”

Mme. Curie⁵⁸

A typical preconcentration technique for Ra^{2+} involves an initial coprecipitation of Ra^{2+} with Ba^{2+} or Pb^{2+} sulfates, carbonates, or chromates.^{59,60} Elution from (ion exchange) columns, using e.g. ammonium citrate or EDTA, is another common way to isolate Ra^{2+} .^{61,62} A technique, often used to analyze the Ra^{2+} content of water-streams, is the non-specific binding of alkaline earth cations on manganese oxide⁶³ or hydrous titanium oxide.⁶⁴ Furthermore, the properties of Ra^{2+} cations can be used to immobilize them in synthetic clay. Na-4-mica ($\text{Na}_4\text{Al}_4\text{Si}_4\text{Mg}_6\text{O}_{20}\text{F}_4 \cdot x\text{H}_2\text{O}$) has a high Ra^{2+} selectivity;⁶⁵ its high charge density and special layer stacking allows for the uptake of the less hydrated cations⁶⁶ such as Ra^{2+} . This mica can be used both to separate Ra^{2+} from Na^+ and as fixation for safe disposal. Drinking water production units use separation technologies not specifically designed for the removal of Ra^{2+} such as ion exchange, reverse osmosis, lime softening, green sand filtration, coprecipitation with barium sulfate, hydrous manganese oxide filtration, electro dialysis reversal,⁴² activated alumina,⁶⁷ and enhanced coagulation/filtration.⁶⁷

With all these techniques Ra^{2+} cations can be removed from aqueous solutes, but they are not selective. An alternative approach to remove Ra^{2+} from aqueous streams is solvent extraction with a Ra^{2+} specific extractant.⁶⁸

2.6 Organic Ra²⁺ Extractants

2.6.1 Introduction

For the design of Ra²⁺ selective extractants there must be a difference in complexation properties compared to the alkali(ne earth) cations Na⁺, K⁺, Mg²⁺, Ca²⁺, Sr²⁺, and Ba²⁺.^{69,70} This is a substantial challenge, since, of all the alkaline earth cations, Ra²⁺ has the lowest tendency to form complexes.⁷¹

In this section the various approaches to complex Ra²⁺ using organic extractants are described. A direct comparison between the results of different studies is not often possible, since the reported results have been obtained with different extraction techniques and under different conditions. Some techniques use extractants dissolved in aqueous media to extract Ra²⁺ from complexes in organic media (Figure 2.4a), while other use extractants dissolved in organic media to extract Ra²⁺ cations from aqueous solutions (Figure 2.4b). Again other systems use the combination of water-soluble extractants and lipophilic extractants (Figure 2.4c), or a solid support (Figure 2.4d).

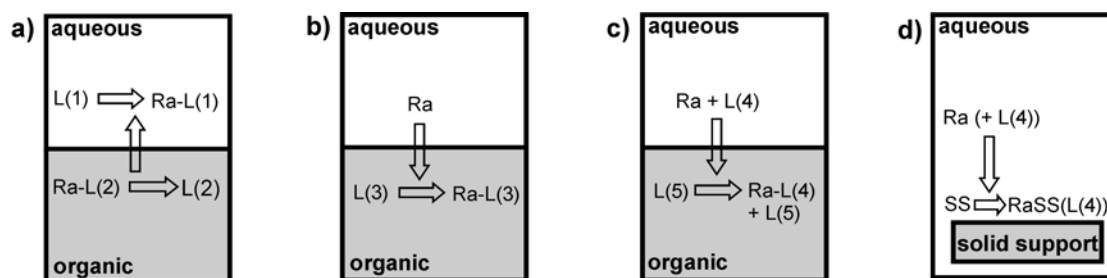


Figure 2.4. The four basic techniques used to determine the Ra²⁺ affinity of organic extractants.⁷²

2.6.2 Resin-based Ra²⁺ Extraction

There are two known methods that exploit the use of a solid support for Ra²⁺ extraction (Figure 2.4d). The first uses neutral extractant immobilized on a solid support. The complexation behavior of alkaline earth cations by neutral extractants (Chart 2.1) depends on matching of the size of cation and extractant.⁷³ The extractant should be large enough to incorporate Ra²⁺ cations (1.48–1.70 Å),⁷⁴ and should possess oxygen donor atoms, because Ra²⁺ is a hard Lewis-acid.⁷⁵

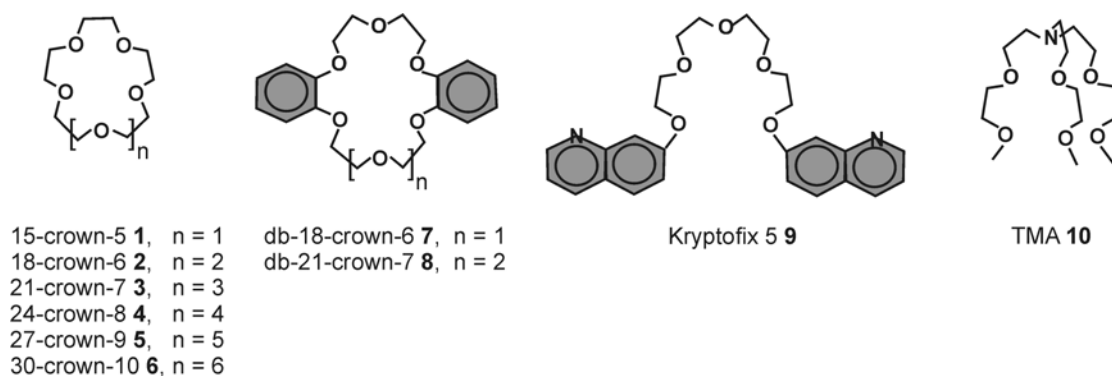


Chart 2.1

Benzi et al.⁷⁶ reported Ra^{2+} extraction by several podands and crown ethers on either Amberlite XAD resins or Kieselgel. 1,11-Bis(8-quinolyloxy)-6,9-trioxaundecane [Kryptofix 5 (**9**)], and tris(2-methoxyethoxyethyl)amine [TMA (**10**)] exhibit a high Ra^{2+} extraction under non-competitive conditions, whereas 18-crown-6 (**2**), 24-crown-8 (**4**), and dibenzo-18-crown-6 (**7**) are less effective. However, the amount of free extractant or Ra^{2+} complex in the aqueous solution has not been determined, although this could have a significant influence on the extraction percentages.

Using covalent attachment, the 3M company has immobilized crown ethers (type not specified) on a silica surface (3M EmporeTM),⁷⁷ to extract various cations, such as Ra^{2+} from aqueous solutions.^{78,79}

The second solid support based extraction technique uses a neutral extractant, dissolved in water, which forms a complex with a negatively charged support. Cation exchangers are negatively charged and as such can nonselectively bind cations, including Ra^{2+} . Addition of water-soluble crown ethers (**1-6**) gives rise to a synergistic effect, inducing selectivity by forming $[(\text{solid support})^n \cdot \text{Ra}^{2+} \cdot (\text{crown-ether})]^{n-2}$ complexes.⁸⁰ A cation exchanger in combination with a significant excess of a crown ether, resulted for 18-crown-6 (**2**) in higher formation constants ($\log \beta_1$) for Ra^{2+} (3.7) and Ba^{2+} (3.9), compared to Ca^{2+} (1.1) and Sr^{2+} (3.0).⁸⁰ The most efficient cation exchanger for the cooperative (synergistic) extraction of Ra^{2+} cations is Bio-Rad AG MP-50.⁸¹

2.6.3 Anionic Polydentate Extractants

Since Ra²⁺ cations are divalent, to form (neutral) complexes, the charges have to be compensated. Consequently, a common Ra²⁺ extraction technique is based on the use of electrostatic effects, applying amino carboxylic, alkyl phosphoric, sulfonic, and alkyl carboxylic acids (for some examples see Chart 2.2).^{71,82}

Amino carboxylic acids have Ra²⁺ stability constants with $\log K_{\text{ex}} \geq 5.6$ (Table 2.6). This resulted in efficient extraction of Ra²⁺ cations from an organic phase containing the non-selective extractants 2-thenoyltrifluoroacetone [TTA (**11**)]⁸³ and tributylphosphate (TBP). From Table 2.6 it is clear that in general the extraction constants of Ra²⁺ are lower than those of the other alkaline earth cations.⁸⁴ This indicates, that amino carboxylic acids cannot function as selective Ra²⁺ extractants in waste streams containing competing alkaline earth cations.

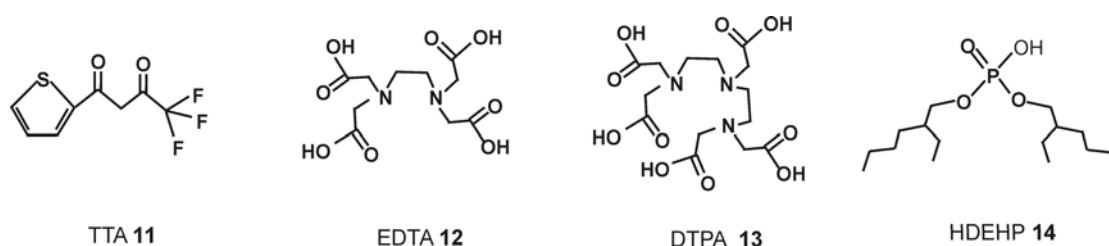


Chart 2.2

Table 2.6. Stability constants [$\log(K_{\text{ex}} = [\text{ML}^{2-}]/[\text{M}^{2+}][\text{L}^{-}])$] of the alkaline earth cations with various (water-soluble) amino carboxylic acids.⁸⁴

Extractant ^a	Mg ²⁺	Ca ²⁺	Sr ²⁺	Ba ²⁺	Ra ²⁺
CyDTA	10.3	12.5	10.0	8.0	8.3
DTPA	9.3	10.6	9.7	8.8	8.5
EDTA	8.7	10.7	8.6	7.8	7.5 ⁸⁵
EGTA	5.2	11.0	8.5	8.4	7.7
HEDTA	5.2	8.0	6.8	6.2	5.6

^a *trans*-1,2-Diaminocyclohexane-*N,N,N',N'*-tetraacetic acid, monohydrate (CyDTA), diethylenetriamine-*N,N,N',N'',N''*-pentaacetic acid [DTPA (**13**)], ethylenediamine-*N,N,N',N'*-tetraacetic acid [EDTA (**12**)], ethylene glycol bis(2-aminoethyl ether)-*N,N,N',N'*-tetraacetic acid (EGTA), and *N'*-(2-hydroxyethyl)ethylenediamine-*N,N,N'*-triacetic acid (HEDTA).

Alternatives to amino carboxylic acids are phosphoric acids. Nitrilotris(methylene)triphosphonic acid (NTTA) has a Ba^{2+} stability constant of $\log K_{\text{ex}} 6.5$ and it is concluded that it has a similar value for Ra^{2+} .⁹¹ Furthermore, bis(2-ethylhexyl)phosphoric acid [HDEHP (**14**)] extracts Ra^{2+} , at highly acidic conditions⁸⁶ from a mixture of ^{227}Ac , ^{223}Ra , ^{227}Th , and ^{233}Fr .⁸⁷ However, a similar extracting agent, *P,P'*-bis(2-ethylhexyl)ethanediphosphonic acid ($\text{H}_2\text{DEH}[\text{MDP}]$), is hardly selective for the alkaline earth series.⁸⁸ In general, the alkaline earth selectivity of phosphoric acids is assumed to decrease in the order $\text{Ca}^{2+} \gg \text{Sr}^{2+} > \text{Ba}^{2+} \geq \text{Ra}^{2+}$.⁸⁹

Despite their general lack of a Ra^{2+} selectivity in the alkaline earth series, both amino carboxylic acids and phosphoric acids are often used when no real selectivity is desired e.g. for the non-selective removal of Ra^{2+} from ion exchange resins.^{24,90,91}



Chart 2.3

Hendriksen et al.⁹² describe the use of *p-t*-butylcalix[4]arene tetracarboxylic acid [CTA (**17**)] as carboxylic acid-based Ra^{2+} extractant.⁹³ The relative extraction constants of CTA (**17**) have been obtained by back-extraction experiments using another water-soluble extractant, DTPA (**13**), 1,4,7,10-tetraazacyclododecan-1,4,7,10-tetraacetic acid [DOTA (**15**)], or 4,7,13,16,21,24-hexaoxa-1,10-diazabicyclo-[8.8.8]hexacosane [Kryptofix 2.2.2 (**16**)].⁹² The relative extraction constants of CTA (**17**) (K_{CTA}) are: $5.7 \cdot K_{\text{DTPA}}$, $2.2 \cdot K_{\text{DOTA}}$, and $3.5 \cdot K_{\text{Kryptofix 2.2.2}}$. The difference between the K -values of DTPA (**13**) and DOTA (**15**) might be due to either the difference in the number of carboxylic acid substituents or the macrocycle effect claimed for DOTA (**15**). A similar experiment with EDTA (**12**), rather than DTPA (**13**), would clarify which factor is the most decisive. These data also suggest that in aqueous media, a neutral strapped macrocyclic cage [Kryptofix 2.2.2 (**16**)] is almost as

important for effective Ra²⁺ complexation as the presence of four carboxylic acid groups on a macrocycle [DOTA (**15**)].

Unfortunately, extraction results for alkaline earth cations other than Ra²⁺ have not been reported, making it hard to conclude whether CTA (**17**) is Ra²⁺ selective. However, the kinetic stability of a Ra²⁺ complex with 2 mM CTA (**17**) in the presence of a mixture of Na⁺ (150 mM), K⁺ (2.5 mM), Mg²⁺ (2.5 mM), Ca²⁺ (2.5 mM), and Zn²⁺ (2.5 mM) has been studied. After extractions for 10 min, 5 h, and 15 h, about 62% of the Ra²⁺ cations remained in the organic phase, proving the high Ra²⁺ complex stability of this particular extractant. Overall, the extraction data seem to suggest, that electrostatic extractants provide stable Ra²⁺ complexes, but cannot be used for selective Ra²⁺ extraction in the presence of the other alkaline earth cations.

2.6.4 Synergistic Ra²⁺ Extractants

Since the dehydration and transfer of anions into organic solvents is difficult, neutral extractants are not very effective for the extraction of Ra²⁺ into organic solvents.⁹⁴ A way to improve both the extraction efficiency and selectivity is to make use of the cooperation (synergism) between two systems. This can be accomplished by using a non-selective electrostatic agent to drive the extraction in combination with a selective neutral complexing agent.^{94,95} One example is the combination of TTA (**11**) and TBP or trioctylphosphine oxide (TOPO) can be used to extract Ra²⁺ cations, resulting in (Ra(TTA)₂(L)_s)_{org} complexes (L = TBP or TOPO),⁹⁶ while TBP and TOPO alone do not give Ra²⁺ extraction.⁹⁷ The majority of the research on Ra²⁺ selective extractants, however, is based on “size-selective synergism”.^{98,99} This approach generally utilizes the macrocyclic cage of a crown ether for size selectivity, and complementary acidic groups for the neutralization of the divalent cations.⁹⁴

A 2:1 mixture of dicyclohexano-21-crown-7 (dc-21-crown-7) and 2-heptyl-2-methylnonanoic acid (HMHN) gave a Ra²⁺ distribution coefficient ($D_{Ra} = R_{a,org}/R_{a,aq}$) larger than 200.¹⁰⁰ In addition, this extractant combination also has good separation factors (D_{Ra}/D_M ; $D_M = M_{org}/M_{aq}$) with the other alkaline earth cations (Table 2.7).¹⁰¹ However, it should be noted that the high separation factors are in the presence of a fifty-fold excess of dc-21-crown-7 compared to the concentrations of the competing cations. Ra²⁺ extraction started to decrease significantly at M(NO₃)₂ concentrations

between 10^{-2} and 10^{-1} M. Nevertheless, Ra^{2+} extraction in the presence of large excesses of Na^+ is still effective.¹⁰⁰

Table 2.7. Separation factors ($D_{\text{Ra}}/D_{\text{M}}$) obtained with various crown-ether acid combinations.

Cation	Separation factor ($D_{\text{Ra}}/D_{\text{M}}$)			
	dc-21-crown-7 + HMHN ^a	15-crown-5 (1) + HDNNS ^b	18-crown-6 (2) + HDNNS ^b	21-crown-7 (3) + HDNNS ^b
Ba^{2+}	9.3	1.2	1.9	2.7
Sr^{2+}	12.3	6.2	2.8	5.5
Ca^{2+}	58	41	140	350
Mg^{2+}	560	-	-	-

^a The aqueous phase contained 5.0×10^{-8} M Ra^{2+} , 4 M Na^+ , and 0.01 M $\text{M}(\text{NO}_3)_2$ ($\text{M}^{2+} = \text{Be}^{2+}$, Ca^{2+} , Sr^{2+} , or Ba^{2+}) while the organic phase contained 0.10 M HMHN and 0.05 M dc-21-crown-7.¹⁰⁰ ^b The aqueous phase contained $^{45}\text{Ca}^{2+}$, $^{85}\text{Sr}^{2+}$, $^{133}\text{Ba}^{2+}$, and $^{223}\text{Ra}^{2+}$ tracers (very low concentrations expected), while the organic phase contained 0.01 M HDNNS and 0.001 M crown ether.¹⁰²

Ra^{2+} separation can also be achieved using water-soluble crown ethers in solvent extraction studies similar to the experiments performed with cation exchange resins (see paragraph 2.6.1; Figure 2.4d).⁸⁰ In this case an organic solution of dinonylnaphthalenesulfonic acid (HDNNS) has been used as neutralizing agent, and the Ra^{2+} selectivity of 15-crown-5 (1), 18-crown-6 (2), and 21-crown-7 (3) has been determined in the presence of the other alkaline earth cations (Table 2.7).¹⁰³ Since HDNNS alone showed very little selectivity along the series of the alkaline earth cations, the obtained Ra^{2+} selectivities have been attributed to the crown ethers. For Ca^{2+} , Ra^{2+} separation factors ($D_{\text{Ra}}/D_{\text{Ca}}$) between 40 and 350 have been found, while $D_{\text{Ra}}/D_{\text{Sr}}$ and $D_{\text{Ra}}/D_{\text{Ba}}$ were rather small (Table 2.7). Increasing the crown ether size from 15-crown-5 (1) to 21-crown-7 (3) improves the Ra^{2+} separation factors in the presence of Ca^{2+} , Sr^{2+} , and Ba^{2+} .^{103,104} Furthermore, it has been shown that an excess of TBP in the organic phase, compared to HDNNS, gave a decrease in extraction, suggesting that TBP competes in the synergism between the crown ether and HDNNS.

The combination of 18-crown-6 (**2**) and tungstosilicic acid (H₄SiW₁₂O₄₀•30H₂O; TSA) has been used to co-precipitate Ra²⁺ with Sr²⁺ or Ca²⁺ cations.¹⁰⁵ Compared to the stability constants of Ca²⁺ (18.2) and Sr²⁺ (776.2), that of ²²³Ra²⁺ has been estimated to be 2366. Ra²⁺ precipitates have only been observed when all components were present in equal ratios.

Although the synergistic systems described above are rather similar, they give slightly different results (Table 2.7). This may be caused by the lack of uniformity between the studies of different authors; there are differences in the experimental conditions (concentrations) used to determine the selectivity and in the description of the results. Nevertheless, it may be concluded that a 21-crown-7 gives the best Ra²⁺ selectivity.

2.6.5 Combining Acids and Crown Ethers on a Platform

In order to optimize the combination of electrostatic and macrocyclic effects, a logical step is the use of crown ethers functionalized with pendant acid groups.^{106,107} This system was first introduced by Bartsch et al.^{108,109} and gives an increased extraction of alkali(ne earth) cations compared to the crown ether alone.

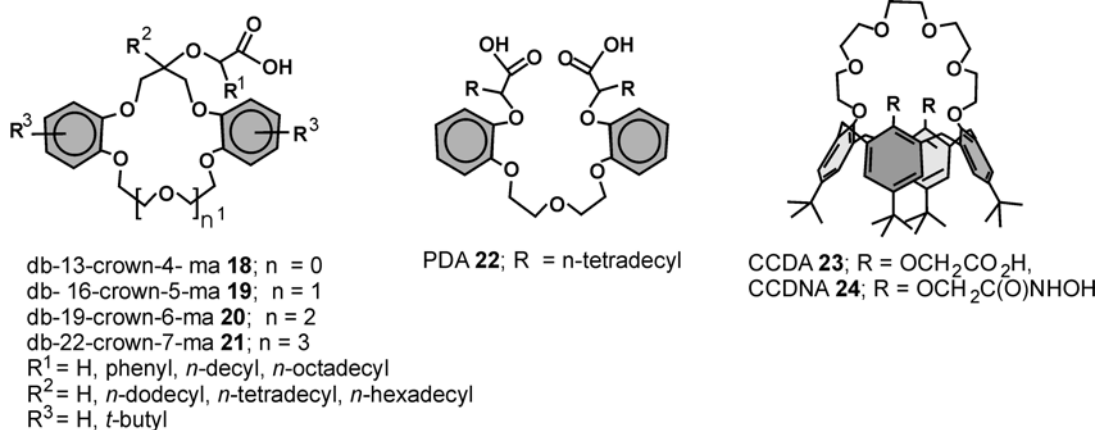


Chart 2.4

The non-competitive Ra²⁺ extraction behavior of eleven different crown-ether carboxylic acid derivatives (Chart 2.4; left) has been evaluated by Beklemishev et al.¹¹⁰ Unfortunately, no direct comparison between the combination of a crown ether-

carboxylic acid combination and a separate crown ether or carboxylic acid has been made.

First of all the crown ether cavity size has been evaluated, showing that dibenzo-22-crown-7 monocarboxylic acid (db-22-crown-7-ma (**21**); $n = 3$; $R^1 = R^2 = R^3 = H$) gave the highest distribution coefficient for Ra^{2+} ($D_{Ra} = 0.5$). Surprisingly, only the second smallest crown ether, db-16-crown-5-ma (**19**), has been further optimized by increasing the lipophilicity; with $R^1 = n$ -decyl ($R^2 = R^3 = H$) D_{Ra} is 2.0, with $R^2 = n$ -hexadecyl ($R^1 = R^3 = H$) D_{Ra} is 2.8, and with $R^3 = t$ -butyl ($R^1 = R^2 = H$) D_{Ra} is 23. These results reveal the positive influence of an increased crown ether lipophilicity on the Ra^{2+} extraction. In an extension of this study Chu et al.¹¹¹ reported the selectivity of db-16-crown-5-ma (**19**) ($R^1 = R^2 = H$ and $R^3 = t$ -butyl) towards the alkaline earth cations. Their reason for using db-16-crown-5-ma (**19**), instead of e.g. db-22-crown-7-ma (**21**) is the lower price, rather than an optimized macrocyclic effect. Using an excess of extractant (10^{-3} M), a significant competition in the Ra^{2+} extraction has been observed when the concentrations of the competing alkaline earth cations were 10^4 times higher than that of $^{226}Ra^{2+}$ (56 Bq/mL = 6.8×10^{-9} M). Chen et al.¹¹² reported that in competition experiments, the highest Ra^{2+} separation factor is found in the presence of Ca^{2+} cations (Table 2.8); the Ra^{2+} extraction percentage remains below 20% in all cases. Surprisingly, no competition has been observed for similar K^+ concentrations, a result that has been attributed to the different valency and chemical properties of K^+ cations.¹¹¹

Another possibility to combine a crown ether derivative with acidic groups is the attachment of two acidic substituents to a calix[4]crown.¹¹³ The two phenol groups of a calix[4]crown allow for two acid groups to be positioned adjacent to the crown-ether bridge, resulting in both complete neutralization and size selective complexation of alkaline earth cations.¹¹³ Chen et al.¹¹² reported the Ra^{2+} selectivity in the presence of alkaline earth cations, using a variety of acid-functionalized extractants (Chart 2.4; Table 2.8). Under the conditions used, the calix[4]crown diacids CCDA (**23**) and CCDNA (**24**) showed the highest Ba^{2+} and Ra^{2+} selectivities compared to db-16-crown-5-ma (**19**) ($R^1 = R^2 = H$ and $R^3 = t$ -butyl) and a podant containing two carboxylic acid groups (PDA (**22**); Table 2.8). Where CCDA (**23**) and CCDNA (**24**) only showed high affinities for Ba^{2+} and Ra^{2+} cations, db-16-crown-5-ma (**19**) and PDA (**22**) do not give distinct differentiation between the different alkaline earth cations.

Table 2.8. Separation factors ($D_{\text{Ra}}/D_{\text{M}}$)^a of various crown ethers; adapted from Chen et al.¹¹²

Extractant	Mg ²⁺	Ca ²⁺	Sr ²⁺	Ba ²⁺
db-16-crown-5-ma (19) ^b	1.1	0.71	0.97	1.1
PDA (22)	0.53	0.66	0.87	1.2
CCDA (23)	>998000	5405	360	13
CCDNA (24)	>998000	6867	277	8.1

^a Distribution coefficients were calculated based on $D_{\text{M}} = [M_{\text{org}}]/([M_{\text{single}}]_{\text{tot}} - [M_{\text{org}}])$, with $M^{2+} = \text{Mg}^{2+}, \text{Ca}^{2+}, \text{Sr}^{2+}, \text{Ba}^{2+}, \text{or Ra}^{2+}$. Extractions were performed using a solution of ²²³Ra²⁺ (1.3×10^{-7} M) with Mg²⁺, Ca²⁺, Sr²⁺, and Ba²⁺ cations (0.2 mM each), while having an excess of extractant (1 mM). ^b The concentration of db-16-crown-5-ma (**19**) is not corrected for the 1:2 stoichiometry.

Back extractions with the water-soluble extracting agent EDTA (**12**) have been used to determine the relative extraction constants of CCDA (**23**) and CCDNA (**24**) in chloroform: $K_{\text{CCDA}} = 0.561 \cdot K_{\text{EDTA}}$, while $K_{\text{CCDNA}} = 12.6 \cdot K_{\text{EDTA}}$.¹¹⁴ In addition, pre-formed ²²³Ra²⁺ complexes of both calix[4]crown-6 derivatives showed a high kinetic stability. Less than 5% of the Ra²⁺ cations were removed after back extraction with aqueous phases containing Na⁺, K⁺, Mg²⁺, Ca²⁺, and Zn²⁺ (1 M; a tenfold excess of each cation to extractant).

From these data it can be concluded that the combination of a crown ether and two acid groups, attached to a molecular platform, gives a high Ra²⁺ affinity/selectivity. CCDA (**23**) and CCDNA (**24**) are the best self-neutralizing systems for the extraction of Ra²⁺ cations.

2.7 Outlook

Although, various extractants have been reported and some of them are suggested to be Ra²⁺ selective, none is able to remove Ra²⁺ cations from the actual TENORM waste streams. To be applied under waste conditions (see section 2.3), the Ra²⁺ extractants should have large separation factors for cations ranging from Na⁺, K⁺, Mg²⁺, Ca²⁺, Sr²⁺ to Ba²⁺. Furthermore, they should be able to extract Ra²⁺ cations from solutions containing an excess of salts compared to the amount of extractant(s) used. In addition, efficient stripping of Ra²⁺ from the extractants, as well as their full

regeneration are both highly desirable. Therefore, the development of new Ra^{2+} extractants, which meet the mentioned requirements, is very desirable.

In this thesis, new Ra^{2+} extractants are described that were evaluated for their Ra^{2+} extraction behavior under highly competitive conditions. Chapters 3-5 focus on the synthesis and evaluation of new thiocalix[4]crown-based Ra^{2+} extractants to get insight into the most important requirements of a Ra^{2+} extractant. In Chapter 6, a completely new type of Ra^{2+} extractant is introduced, based on self-assembly. Finally, in Chapter 7 Ra^{2+} extractions are described under actual TENORM waste stream conditions.

References

1. Kathren, R. L. *Appl. Radiat. Isot.* **1998**, *49*, 149-168.
2. UNSCEAR, *Sources and Effects of Ionizing Radiation, Annex B: Exposures from Natural Radiation Sources*, United Nations, New York 1977.
3. <http://www.c5plus.com/norm.html>.
4. Shawky, S.; Amer, H.; Nada, A. A.; Abd El-Maksound, T. M.; Ibrahiem, N. M. *Appl. Radiat. Isot.* **2001**, *55*, 135-139.
5. Greeman, D. J.; Rose, A. W.; Washington, J. W.; Dobos, R. R.; Ciolkosz, E. J. *Appl. Geochem.* **1999**, *14*, 365-385.
6. Sturchio, N. C.; Banner, J. L.; Binz, C. M.; Heraty, L. B.; Musgrove, M. *Appl. Geochem.* **2001**, *16*, 109-122.
7. Wiegand, J.; Sebastian, F., *Origin of Radium in High-Mineralized Waters*, IAEA-TECDOC-1271 2002.
8. Heaton, B.; Lambley, J. *Appl. Radiat. Isot.* **1995**, *46*, 577-581.
9. United States Environmental Protection Agency, *Air and Radiation, Evaluation of EPA's Guideline for Technologically Enhanced Naturally Occurring Radioactive Materials (TENORM)*, 2000, EPA 402-R-00-01.
10. Leopold, K.; Peters, B.; Weiß, D.; Wiegand, J. *German national report to levels and inventory of TENORM*, 2002.
11. www.tenorm.com.
12. United States Environmental protection Agency, *Technologically Enhanced Naturally Occurring Radioactive Materials in the Southwestern Copper Belt of Arizona*, Washington D.C., 1999, EPA 402-R-99-002.
13. Ogunleye, P. O.; Mayaki, M. C.; Amapu, I. Y. *J. Environ. Radioact.* **2002**, *62*, 39-48.
14. Rutherford, P. M.; Dudas, M. J.; Arocena, J. M. *Sci. Total Environ.* **1996**, *180*, 201-209.
15. Ioannides, K. G.; Mertzimekis, T. J.; Papachristodoulou, C. A.; Tziialla, C. E. *Sci. Total Environ.* **1997**, *196*, 63-67.
16. Vanderhove, H. *International Congress Series* **2002**, *1225*, 307-315.
17. Haridasan, P. P.; Paul, A. C.; Desai, V. M. *J. Environ. Radioact.*, **2001**, *53*, 155-165.
18. Baba, A. *Environ. Geol.* **2002**, *41*, 916-921.

19. Skubacz, K.; Lebecka, J.; Chalupnik, S.; Wysocka M. *Possible Changes in the Background Radiation of the Natural Environment Caused by Coal Mining Activity* IAEA-SM-308/72 1998, 425-429.
20. Tadmor, J. *J. Environ. Radioact.* **1986**, *4*, 177-204.
21. *Radioactive Elements in Coal and Fly Ash: Abundance, Forms, and Environmental Significance*, U.S. Geological Survey Fact Sheet FS-163-97, October, 1997.
22. Tonza, I.; Lebecka, J. Radium-bearing waters in coal mines: occurrence, methods of measurements and radiation hazard. *Proceedings of International Conference on Radiation Hazards in Mining*, Golden, C. O. Kingsport Press, 1981, 945-948.
23. Sorbie, K. S.; Mackay, E. J. *J. Petr. Sci. Eng.* **2000**, *27*, 85-106.
24. Crabtree, M.; Eslinger, D.; Flecher, P.; Miller, M. Johnson, A.; King, G. *Oilfield Reviews* **1999**, 30-45.
25. Boerlage, S. F. E.; Kennedy, M. D.; Bremere, I.; Witkamp, G. J.; Van der Hoek, J. P.; Schipper, J. C. *J. Membr. Sci.* **2002**, *197*, 251-268.
26. <http://www.epa.gov/radiation/tenorm/sources.htm>.
27. Zhang, Y.; Dawe, R. *Appl. Geochem.* **1998**, *13*, 177-184.
28. Zielinski, R. A.; Otton, J. K.; Budahn, J. R. *Environ. Poll.* **2001**, *11*, 299-309.
29. Smith, K. P.; Arnish, J. J.; Williams, G. P.; Blunt, D. L. *Environ. Sci. Technol.* **2003**, *37*, 2060-2066.
30. Utvik, T. I. R. *Chemosphere* **1999**, *39*, 2593-2606.
31. W. Cretney, M. Yunker, P. Yeats, *Biogeochemical Benchmarks for Source Identification of Contaminants from an Offshore Oil and Gas Industry*, Research document 2002/129 of the Canadian Science Advisory Secretariat.
32. Cofino, W. P.; Slager, L. K.; van Hattum, B. *Environmental Aspects of Produced Water Discharges from Oil and Gas Production on the Dutch Continental Shelf. Part 1. Overview of Surveys on the Composition of Produced Waters Conducted on the Dutch Continental Shelf*. Institute for environmental studies, Vrije Universiteit Amsterdam in commissioned by the Netherlands Oil and Gas Exploration and Producing Association (NOGEP) 1992.
33. Hamlat, M. S.; Kadi, H.; Fellag, H. *Appl. Radiat. Isot.* **2003**, *59*, 95-99.
34. Bostick, D. T.; Luo, H.; Hindmarsh, B., *Characterization of Soluble Organics in Produced Water*, ORNL/TM-2001/78.
35. Jiménez, A.; De La Montaña Rufo, M. *Water Res.* **2002**, *6*, 1715-1724.
36. Rihs, S.; Condomines, M. *Chem. Geol.* **2002**, *182*, 409-421.
37. Somlai, J.; Horváth, B.; Kanyár, B.; Kovács, T.; Bodrogi, E.; Kávási, N. *J. Environ. Rad.* **2002**, *62*, 235-240.
38. Environmental Protection Agency, National Primary Drinking Water Regulations; Radionuclides; Final Rule *Federal Register* **2000**, *65*, 76707-76753.
39. World Health Organization, *Guidelines for Drinking Water Quality* 3rd ed. 2004, Vol 1, p. 203.
40. Lauria, D. C.; Godoy, J. M. *J. Environ. Rad.* **2002**, *61*, 159-168.
41. Almeida, R. M. R.; Lauria, D. C.; Ferreira, A. C.; Sracek, O. *J. Environ. Rad.* **2004**, *73*, 323-334.
42. Hays, J. *Desalination* **2000**, *132*, 161-165.
43. Popit, A.; Vaupotic, Kukar, N. *J. Environ. Rad.* **2004**, *76*, 337-347.
44. Pietrzak-Flis, Z.; Rosiak, L.; Suplinska, M. M.; Chrzanzanowski, E.; Dembinska, S. *Sci. Total Environ.* **2001**, *27*, 16-169.

45. Fisenne, I. M.; Perry, P. M.; Decker, K. M.; Keller, H. W. *Health Phys.* **1987**, *5*, 357-363.
46. Agency for Toxic Substances and Disease Registry U.S. Public Health Service and U.S. Environmental Protection Agency, *Toxicological Profile for Radium*, 1990.
47. Evans, R. D. *Health Phys.* **1974**, *27*, 497-510.
48. Boice Jr., J. D.; Lubin, J. H. *Cancer Causes and Control* **1997**, *8*, 309-322.
49. Radium, in *Health Risks of Radon and Other Internally Deposited Alpha-Emitters: BEIR IV*, 1988, Chap. 4, 176-244.
50. Shabana, E. I.; Al-Jaseem, Q. K. *J. Radioanal. Nucl. Chem. Lett.* **1995**, *200*, 233-245.
51. The National Academy of Sciences (NAS) *Biological Effects of Ionizing Radiation (BEIR) VI Report: The Health Effects of Exposure to Indoor Air* 1998.
52. Lubin, J. H.; Boice Jr, J. D.; Edling, C.; Hornung, R. W.; Howe, G. R.; Kunz, E.; Kusiak, R. A.; Morrison, H. I.; Radford E. P.; Samet, J. M. *JNCI*, **1995**, *87*, 817-827.
53. Spiers, F. W.; Lucas, H. F.; Rudo, J.; Anast, G. A. *Health Phys.* **1983**, *44*, 65-72.
54. Sill, C. W. *Nucl. Chem. Waste Manage.* **1987**, *7*, 239-256.
55. Unites States Environmental Protection agency, *Estimating Radiogenic Cancer Risks*, EPA 402-R-93-076 1994.
56. Curie, M. S. *Century Magazine* **1904**, 461-466.
57. Photo Credit: 'MATTER' - Life Science Library, Time Inc, N.Y. 1963.
58. Curie, M. *Pierre Curie-The Dream Becomes A Reality; The Discovery of Radium* 1923, Chap. 5, 93-106.
59. Clifford, D. A.; Higgins, E. A. *Health Phys.* **1992**, *62*, 413-422.
60. Salutsky, M. L.; Sites Jr., J. G. *Ind. Eng. Chem.* **1955**, 2162-2166.
61. Power, W. H.; Kirby, H. W.; McCluggage, W. C.; Nelson, G. D.; Payne Jr., J. H. *Anal. Chem.* **1959**, *1*, 1077-1079.
62. Tomkins, E. R. *J. Am. Chem. Soc.* **1948**, *70*, 3520-3522.
63. Moon, D. S.; Burnett, W. C.; Nour, S.; Horwitz, P.; Bond A. *Appl. Radiat. Isot.* **2003**, *59*, 255-262.
64. Andersen, T. C.; Black, R. A.; Blevis, I.; Boger, J.; Bonvin, E.; Chen, M.; Cleveland, B. T.; Dai, X.; Dalnoki-Veress, F.; Doucas, G.; Farine, J.; Fergani, H.; Fowler, M. M.; Hahn, R. L.; Hallman, E. D.; Hargrove, C. K.; Heron, H.; Hooper, E.; Howard, K. H.; Jagam, P.; Jolley, N. A.; Knox, A. B.; Lee, H. W.; Levine, I.; Locke, W.; Majerus, S.; McFarlane, K.; McGregor, G.; Miller, G. G.; Moorhead, M.; Noble, A. J.; Otori, M.; Rowley, J. K.; Shatkay, M.; Shewchuk, C.; Simpson, J. J.; Sinclair, D.; Tanner, N. W.; Taplin, R. K.; Trent, P. T.; Wang, J.-X.; Wilhelmy, J. B.; Yeh, M. *Nucl. Instrum. Methods Phys. Res., Sect. A* **2003**, *501*, 386-398.
65. Komarneni, S.; Kozai, N.; Paulus, J. W. *Nature* **2001**, *410*, 771.
66. Paulus, W. J.; Komarneni, S.; Roy, R. *Nature* **1992**, *357*, 571-573.
67. Gäfvert, T.; Ellmark, C.; Holm, E. *J. Environ. Rad.* **2002**, *63*, 105-115.
68. Kentish, S. E.; Stevens, G. W. *Chem. Eng. J.* **2001**, *84*, 149-159.
69. Comba, P. *Coord. Chem. Rev.* **1999**, *81*, 185-186.
70. Lindoy, L.F. *Pure Appl. Chem.* **1997**, *69*, 2179-2186.
71. Gmelin Handbuch der Anorganische Chemie, **1977**. Radium. 8th ed.; Springer, Berlin, p. 372.
72. The order in which organic and aqueous phases are depicted is random, since different organic solvents can cause reversal of the phase order.

73. Izatt, R. M.; Pawlak, K.; Bradshaw, J. S. *Chem. Rev.* **1995**, *95*, 2529-2586.
74. Shannon, R. D. *Acta Cryst. A* **1976**, *32*, 751-767.
75. Pearson, R. G. *J. Am. Chem. Soc.* **1963**, *85*, 3533-3539.
76. Benzi, P.; Reghetti, R.; Volpe, P. *J. Radioanal. Nucl. Chem. Lett.* **1992**, *164*, 211-220.
77. Goken, G. L.; Orlandini, K. A.; Erickson, M. D.; Haddad, L. C.; Seely, D. C.; Hoffman, K. M.; Dallas, S. K. *United States Patent* **2000**, 6,139,749.
78. Bradshaw, J. S.; Izatt, R. M. *Acc. Chem. Res.* **1997**, *30*, 338-345.
79. Izatt, R. M.; Bradshaw, J. S.; Bruening, R. L. *Pure Appl. Chem.* **1996**, *68*, 1237-1241.
80. Dietz, M. L.; Chiarizia, R.; Horwitz, E.P. *Anal. Chem.* **1997**, *69*, 3028-3037.
81. Chiarizia, R.; Ferraro, J. R.; D.Arcy, K. A.; Horwitz, E. P. *Solvent Extr. Ion Exch.* **1995**, *13*, 1063-1082.
82. Hendriksen, G.; Shoultz, B. W.; Michaelsen, T. E.; Bruland, Ø. S.; Larsen, R. H. *Nucl. Med. Biol.* **2004**, *31*, 441-449.
83. Jackson, W. M.; Gleason, G. I. *Anal. Chem.* **1973**, *45*, 2125-2129.
84. Sekine, T.; Kawashima, Y.; Unnai, T.; Sakairi, M. *Bull. Chem. Soc. Jpn.* **1968**, *41*, 3013-3015.
85. Nelson, F.; Day, R. A.; Kraus, K. A. *J. Inorg. Nucl. Chem.*, **1960**, *15*, 140-150.
86. Türler, A.; Wegmüller, F.; Von Gunten, H. R.; Gregorich, K. E.; Lee, D.; Hoffman, D. C.; Fowler, M. M. *Radiochim. Acta* **1988**, *43*, 149-152.
87. Mitsugashira, T.; Yamana, H.; Suzuki, S. *Bull. Chem. Soc. Jpn.* **1977**, *50*, 2913-2916.
88. Chiarizia, R.; Horwitz, E. P.; Rickert, P. G.; Herlinger, A. W. *Solvent Extr. Ion Exch.* **1996**, *14*, 773-792.
89. Fenton, D.E. *Alkali Metal and Group II Metals* in Comprehensive Coordination Chemistry, Wilkinson, Sir J.; Gillard, R. D.; McCleverty, J. A. eds., **1987**, Vol 3, p. 1-80.
90. Purkl, S.; Eisenhauer, A. *Appl. Radiat. Isot.* **2003**, *59*, 245-254.
91. Chao, J.-C.; Hong, A.; Okey, R. W.; Peters, R. W. Proceedings of the 1998 conference on hazardous waste research, 142-159.
92. Hendriksen, G.; Hoff, P.; Larsen, R. H. *Appl. Radiat. Isot.* **2002**, *56*, 667-671.
93. Although DOTA holds a crown ether, in this chapter it is considered as an acid-based extractant, because of the presence of four carboxylic acid groups, while in theory Ra²⁺ only requires two of these groups.
94. Bond, A. H.; Dietz, M. L.; Chiarizia, R. *Ind. Eng. Chem. Res.* **2000**, *39*, 3442-3464.
95. Ionova, G.; Ionov, S.; Rabbe, C.; Hill, C.; Madic, C.; Guillaumont, R.; Modolo, G.; Krupa, J. C. *New J. Chem.*, **2001**, *25*, 491-501.
96. Šebesta, F.; Havlik, B. J. *Radioanal. Chem.* **1975**, *24*, 337-343.
97. Gmelin Handbuch der Anorganische Chemie, **1977**. Radium. 8th ed., Springer, Berlin, p. 426.
98. Kinard, W. F.; McDowell, W. J.; Shoun, R. R. *Sep. Sci. Technol.* **1980**, *15*, 1013-1024.
99. McDowell, W. J.; Case, G. N.; Aldrup, D. W. *Sep. Sci. Technol.* **1983**, *18*, 1483-1507.
100. McDowell, W. J.; Arndsten, B. A.; Case, G. N. *Solvent Extr. Ion Exch.* **1989**, *7*, 377-393.
101. McDowell, W. J.; Case, G. N. *United States Patent* **1988**, 4,917,825.

102. McDowell, W. J.; Moyer, B. A.; Case, G. N.; Case, F. I. *Solvent Extr. Ion Exch.* **1986**, *4*, 217-236.
103. Chiarizia, R.; Horwitz, E.P.; Dietz, M.L.; Cheng, Y.D. *Reactive & Functional Polymers* **1998**, *38*, 249-257.
104. Chiarizia, R.; Dietz, M. L.; Horwitz, E. P.; Burnett, W. C.; Cable, P. H. *Sep. Sci. Technol.* **1999**, *34*, 931-950.
105. Rajec, P.; Mikulaj, V.; Švec, V. *J. Radioanal. Nucl. Chem.* **1997**, *219*, 123-125.
106. Uhlemann, E.; Bukowsky, H.; Dietrich, F.; Gloe, K.; Mühl, P.; Mosler, H. *Anal. Chim. Acta* **1989**, *224*, 47-53.
107. Uhlemann, E.; Geyer, H.; Gloe, K.; Mühl, P. *Anal. Chim. Acta* **1986**, *185*, 279-285.
108. Strzelbicki, J.; Bartsch, R. A. *Anal. Chem.* **1981**, *53*, 2251-2253.
109. Strzelbicki, J.; Bartsch, R. A. *Anal. Chem.* **1981**, *53*, 2247-2250.
110. Beklemishev, M. K.; Elshani, S.; Wai, C. M. *Anal Chem.* **1994**, *66*, 3521-3524.
111. Chu, T.-C.; Lin, C.-C. *Appl. Radiat. Isot.* **2001**, *55*, 609-616.
112. Chen X.; Ji, M.; Fisher, D. R.; Wai, C. M. *Inorg. Chem.* **1999**, *8*, 5449-5452.
113. Ungaro, R.; Pochini, A.; Andreetti, G. D. *J. Inclusion Phenom. Macrocyclic Chem.* **1984**, *2*, 199-206.
114. Adapted from Chen et al. ref 112.

Chapter 3

Synthesis and Conformational Evaluation of *p*-tert-Butylthiacalix[4]crowns*

Abstract Bridging of *p*-tert-butylthiacalix[4]arene afforded 1,3-dihydroxythiacalix[4]monocrown-5 (**3b**), 1,3-alternate thiacalix[4]biscrown-5 and -6 (**4a,b**), and 1,2-alternate thiacalix[4]biscrown-4 and -5 (**5a,b**), depending on the metal carbonates and oligoethylene glycol ditosylates used. Starting from 1,3-dialkylated thiacalix[4]arenes the corresponding bridging reaction yielded 1,3-alternate, partial-cone and cone conformers (**10-19**), depending on the substituents present. Temperature dependent studies revealed that the conformationally flexible 1,3-dimethoxythiacalix[4]crowns (**10a-c**) exclusively occupy the 1,3-alternate conformation. Demethylation exclusively gave the cone 1,3-dihydroxythiacalix[4]crowns (**3a,c**), which could not be obtained by direct bridging of thiacalix[4]arene. The different structures were determined on the basis of several X-ray crystal structures and extensive 2-D ¹H NMR studies.

* Parts of this work have been published: Van Leeuwen, F. W. B.; Beijleveld, H.; Kooijman, H.; Spek, A. L.; Verboom, W.; Reinhoudt, D. N. *Tetrahedron Lett.* **2002**, *43*, 9675-9678. Van Leeuwen, F. W. B.; Beijleveld, H.; Kooijman, H.; Spek, A. L.; Verboom, W.; Reinhoudt, D. N. *J. Org. Chem.* **2004**, *69*, 3928-3936.

3.1 Introduction

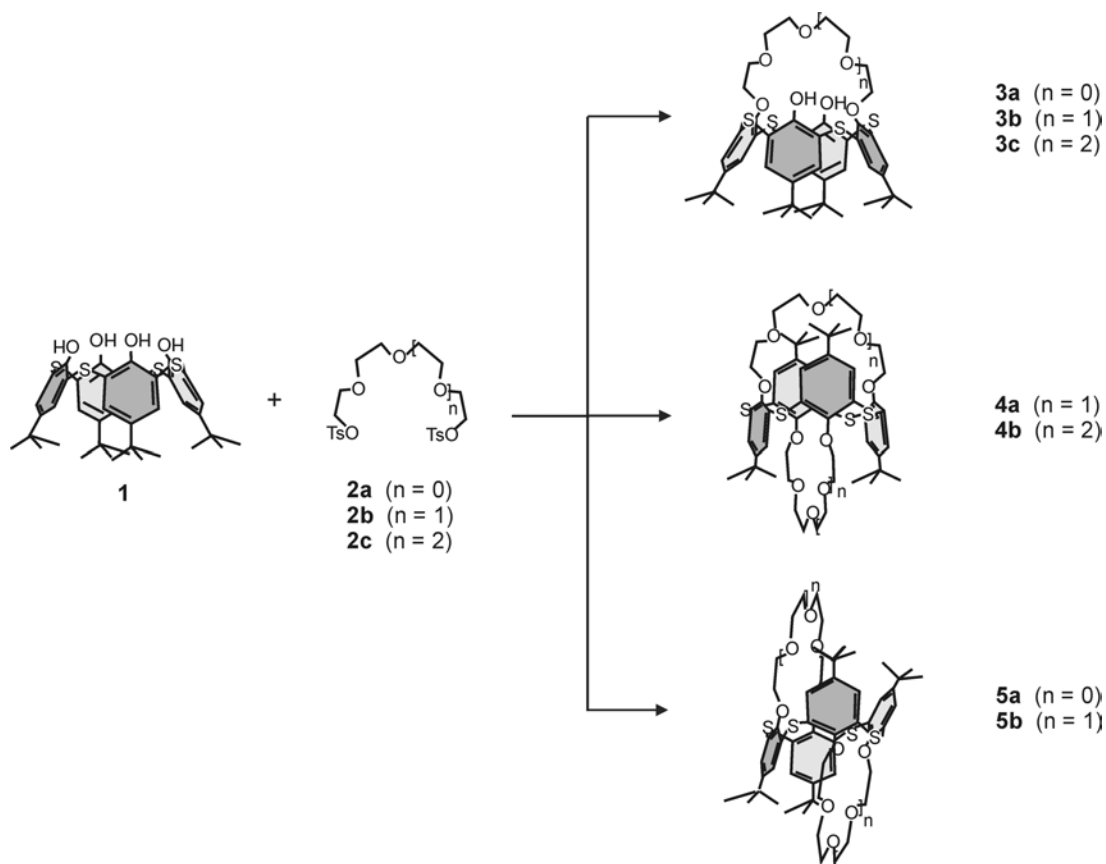
Thiacalix[4]arenes are being used more and more in supramolecular chemistry due to the additional features induced by the bridging sulfur atoms, compared to calix[4]arenes.¹⁻⁵ In the past, it was found that calix[4]crowns are highly selective extractants for e.g. K^+ and Cs^+ .⁶⁻⁷ Therefore one of the obvious classes of extractants suitable for selective complexation of alkali(ne earth) cations would be the thiacalix[4]crowns. A number of thiacalix[4]crowns have already been reported by several groups viz. 1,3-alternate thiacalix[4]biscrowns,^{8,9} diametrically bridged 1,3-alternate thiacalix[4]monocrowns,^{10,11} and proximally bridged thiacalix[4]monocrowns.¹² Similar to calix[4]arenes, thiacalix[4]arenes can adopt four different conformations viz. 1,2-alternate, 1,3-alternate, partial cone, and cone.^{4,13} Whereas the structures of calix[4]arenes can be assigned based on the positions of the bridging methylene groups in the 1H and ^{13}C NMR spectra,^{13,14} in the spectra of thiacalix[4]arenes these characteristic protons are not present. However, the conformation can often be established using 1H NMR spectroscopy in combination with X-ray crystal structures.¹⁵⁻¹⁷ In some cases, additional proof was obtained by 2D 1H NMR spectroscopy.¹⁸⁻²¹ Except for the X-ray crystal structures of the 1,3-alternate thiacalix[4]biscrown-5 and -6,⁸ there is little structural information on thiacalix[4]crown conformers.

In this chapter the results of a systematic study on the formation and conformations of *p-tert*-butylthiacalix[4](bis)crowns-4, -5, and -6 are reported.

3.2 Results and Discussion

3.2.1 Direct Bridging of Thiacalix[4]arene

The reactions of thiacalix[4]arene **1** with tri-, tetra-, and pentaethylene glycol ditosylates **2a-c** (Scheme 3.1) in acetonitrile were systematically studied by varying the reaction conditions. The results are summarized in Table 3.1.



Scheme 3.1

The reactions between **1** and **2** (1 equiv) with Na_2CO_3 as a base, gave diametrically bridged thiacalix[4]monocrowns **3**. The template effect induced by the sodium cation appears favorable for the formation of monocrown derivatives in the cone conformation. Only thiacalix[4]crown-5 (**3b**) could be isolated from the obtained reaction mixtures in low yield (10%). Reaction times of 11-15 days together with conversions of only 40-50%, indicate that Na_2CO_3 is not the optimal base for the direct bridging of thiacalix[4]arene.

Reactions of **1** with **2** (1.8 equiv), using K_2CO_3 as base, gave thiacalix[4]monocrowns (**3**), 1,3-alternate thiacalix[4]biscrowns (**4**), and 1,2-alternate thiacalix[4]biscrowns (**5**). The shorter reaction times and the formation of biscrowns show that K_2CO_3 is a more efficient base. Reaction of **1** with **2a** gave slow conversion to 1,2-alternate thiacalix[4]biscrown-4 **5a** (Table 3.1, entry 2). The reaction of **1** and **2b**

yielded exclusively the 1,3-alternate thiacalix[4]biscrown-5 (**4a**)⁹ (Table 3.1, entry 5), while **1** and **2c** afforded a mixture of **4b**⁹ and **3c** (Table 3.1, entry 8).

The reaction between **1** and **2** (1.8 equiv), with Cs₂CO₃ as base, only yielded thiacalix[4]biscrowns (**4** and **5**). The reaction of **1** with **2a** (Table 3.1, entry 3) exclusively afforded the 1,2-alternate thiacalix[4]biscrown-4 (**5a**; 72%). With **2b** as a bridging agent, a mixture of the 1,2-alternate thiacalix[4]biscrown-5 (**5b**; 27%) and the corresponding 1,3-alternate conformer **4a** (15%) was obtained (Table 3.1, entry 6). Bridging **1** using **2c** gave conversion to only **4b**⁹ (Table 1, entry 9).

Table 3.1. Direct functionalization of thiacalix[4]arene (**1**).

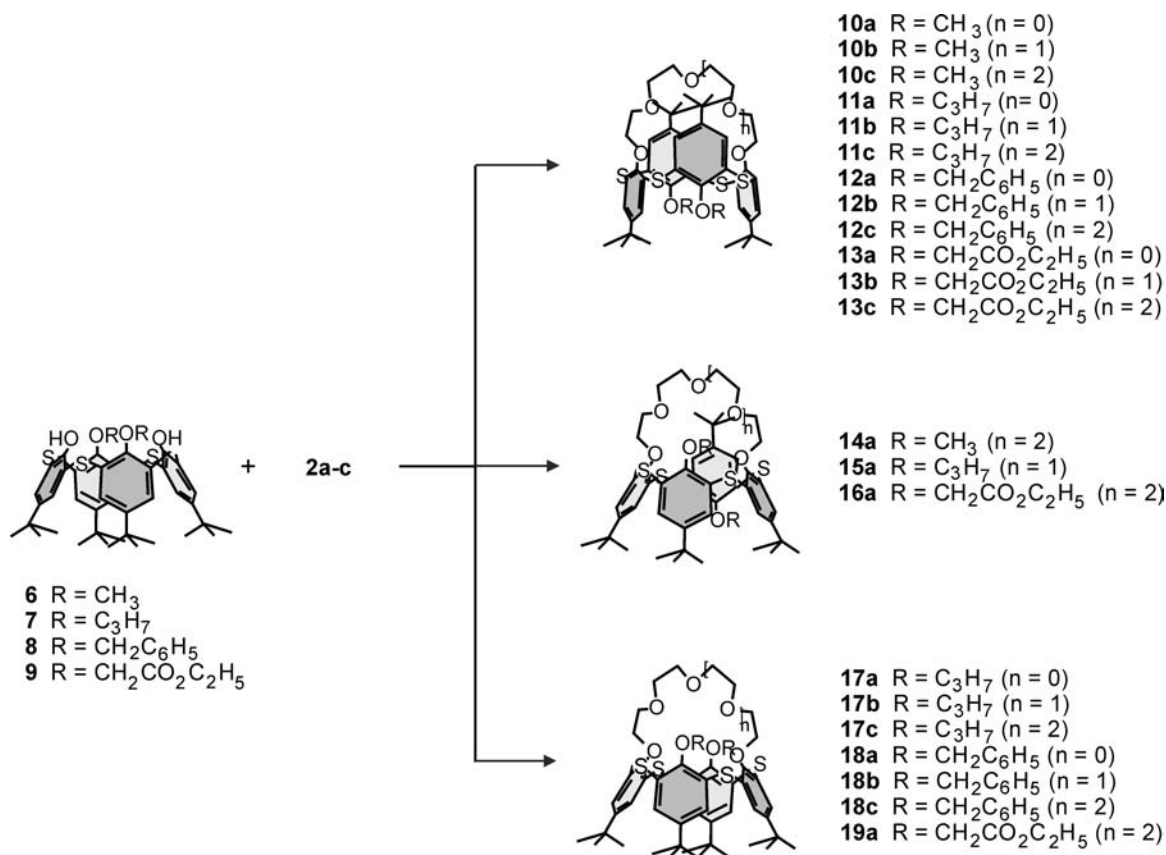
Entry	Crown	Base (equiv)	Reaction time	Conversion 1 (%) ^a	Products formed ^a (ratio)
1	2a (crown-4)	Na ₂ CO ₃ (12)	15 d	50	3a
2	2a	K ₂ CO ₃ (4)	2 d	40	5a
3	2a	Cs ₂ CO ₃ (4)	6 h	100	5a
4	2b (crown-5)	Na ₂ CO ₃ (12)	11 d	50	3b
5	2b	K ₂ CO ₃ (4)	12 h	100	4a
6	2b	Cs ₂ CO ₃ (4)	12 h	100	5b : 4a (1: 1)
7	2c (crown-6)	Na ₂ CO ₃ (1.2)	15 d	40	3c
8	2c	K ₂ CO ₃ (4)	7 d	100	4b : 3c (1: 4)
9	2c	Cs ₂ CO ₃ (4)	6 h	70	4b

^a Determined from the ¹H NMR spectra of the crude reaction mixtures.

Not only the metal carbonate, but also the number of ethylene glycol units in the bridging agent (**2**) influences the product formation. The smallest of the crown-ether bridges **2a** only forms diametrically bridged monocrown and proximally bridged 1,2-alternate biscrowns. Due to steric reasons, formation of diametrically bridged 1,3-alternate biscrown-4 products is unfavorable. However, tetraethylene glycol ditosylate **2b** gave all three products **3b**, **4a**, and **5b**. The largest of the ethylene glycol ditosylates used (**2c**) only gave rise to diametrically bridging.

3.2.2 Diametrically Substituted Thiacalix[4]monocrowns

In addition to the direct bridging of thiacalix[4]arene (**1**), various diametrically substituted thiacalix[4]arene derivatives (**6-9**) were reacted with **2** (Scheme 3.2).



Scheme 3.2

The known 1,3-dialkoxythiacalix[4]arenes **6-9**^{2,10,21,22} were reacted with 1 equiv of oligoethylene glycol ditosylates **2a-c** in the presence of 4 equiv of K₂CO₃ in acetonitrile to give the thiacalix[4]monocrowns **10-19**. K₂CO₃ turned out to be the most efficient base,²³ allowing the formation of all three conformers: 1,3-alternate, partial cone, and cone. The results are summarized in Table 3.2.

Reaction of 1,3-dimethoxythiacalix[4]arene (**6**) with **2a-c** gave exclusively the 1,3-alternate products **10a-c** (Table 3.2, entries 1, 2, and 3).^{10,24} Crystallization of **10c**

only gave crystals of the partial-cone conformer **14a**, underlining the conformational flexibility of this compound (vide infra).

The reaction of 1,3-dipropoxythiacalix[4]arene **7** with **2a** (Table 3.2, entry 4) mainly gave the 1,3-alternate conformer **11a**. Reacting **7** and **2b** yielded all possible conformers (Table 3.2, entry 5): 1,3-alternate (**11b**¹⁰; 59%), partial cone (**15a**; 2%), and cone (**17b**; 8%). Isolation of the partial cone conformer **15a** proves the ability of rotation by the propoxy groups through the annulus before rigidification by the crown-ether bridge. The largest ethylene glycol unit **2c** (Table 3.2, entry 6), as bridging agent, gave the 1,3-alternate conformer **11c**¹⁰ (57%).

Table 3.2. Diametrically substituted thiacalix[4]crowns.

Entry	Starting compound	Bridging agent	Reaction time	Conformers 1,3-alt: pc: cone (ratio) ^a
1	6	2a	5 d	10a : - : - (1: 0: 0)
2	6	2b	5 d	10b : - : - (1: 0: 0)
3	6	2c	5 d	10c : - : - (1: 0: 0)
4	7	2a	5 d	11a : - : 17a ^b (20: 0: 1)
5	7	2b	5 d	11b : 15a : 17b (15: 1: 1)
6	7	2c	5 d	11c : - : 17c ^b (20: 0: 1)
7	8	2a	5 d	12a : - : 18a ^b (2: 0: 1)
8	8	2b	5 d	12b : - : 18b (1: 0: 1)
9	8	2c	5 d	12c : - : 18c (1: 0: 1)
10	9	2a	12 h	13a : - : - (1: 0: 0)
11	9	2b	12 h	13b : - : - (1: 0: 0)
12	9	2c	12 h	13c : 16a ^b : 19a ^b (7: 10: 4)

^a Ratio obtained from ¹H NMR spectra of the crude reaction mixtures; 1,3-alternate (1,3-alt), partial cone (pc), and cone. ^b Formation deduced from ¹H NMR spectra of the crude reaction mixtures, but not supported by analytical data of the isolated compounds.

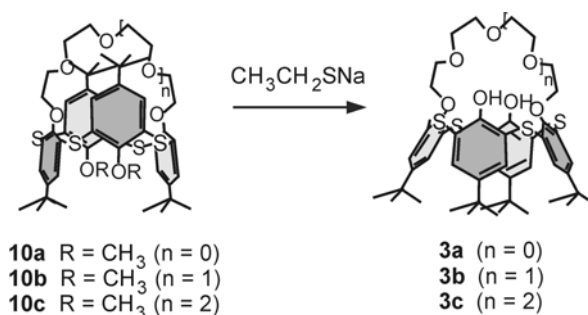
Bridging of 1,3-bis(benzyloxy)thiacalix[4]arene (**8**) gave in all cases a mixture of 1,3-alternate **12a-c** and cone conformers **18a-c** (Table 3.2, entries 7, 8, 9). The formation of only cone and 1,3-alternate products can be ascribed to the size of the benzyloxy groups, preventing them from rotating through the annulus.

Bridging of 1,3-thiacalix[4]arene diethyl ester (**9**) with crown-ether bridges **2a-c** proceeded much faster than with **6-8**, namely 12 hours instead of five days. The ethyl ester functionalities may bind the potassium cations,¹⁶ hence influencing product formation. Bridging with **2a,b** afforded the respective 1,3-alternate products **13a** (29%)²⁵ and **13b** (71%). Reacting **9** and **2c**, however, afforded a mixture of 1,3-alternate **13c**, partial cone **16a**, and cone conformer **19a** (Table 2, entry 12), of which only **13c** could be isolated (16%). The formation of **16a** suggests that the ethyl ester groups are able to rotate through the annulus, which is very surprising as they were considered to be bulky enough to prevent rotation.¹⁹

3.2.3 Indirect Synthesis of Dihydroxythiacalix[4]crowns

Of the diametrically bridged thiacalix[4]crowns (**3a-c**), only the crown-5 derivative **3b** could be obtained in pure form upon bridging of thiacalix[4]arene (**1**) using Na₂CO₃ as base (see above). Therefore, an alternative synthetic approach to synthesize diametrically bridged dihydroxythiacalix[4]crowns was developed by deprotection of the diametrically substituted dimethoxythiacalix[4]crowns (**10a-c**).^{7,26}

Attempts to remove the benzyl group in 1,3-bis(benzyloxy)thiacalix[4]crown-5 (**18b**) using acetic acid or trimethylsilyl iodide, as is common practice for the corresponding calix[4]arene-crowns,²⁷ were unsuccessful. Starting from 1,3-dimethoxythiacalix[4]crown-5 (**10a**), trimethylsilyl iodide also gave partial cleavage of the crown-ether bridge, which does not occur in the case of the corresponding 1,3-calix[4]arene-crowns,⁷ while the demethylation agent lithium diphenylphosphide²⁸ gave no conversion. Reacting 1,3-dimethoxythiacalix[4]crowns (**10a-c**) with 5 equiv of sodium ethanethiolate in DMF (Scheme 3.3), however, gave the corresponding 1,3-dihydroxythiacalix[4]crowns **3a** (18%), **3b** (25%), and **3c** (16%) in the cone conformation.²⁶



Scheme 3.3

3.2.4 Assignment of the Conformation

The structures of the different conformers of the thiacalix[4]crowns were determined by a combination of ¹H NMR spectroscopy and X-ray crystallography. Since the crown-5 derivatives were available in all the conformers, they were used for the conformational analysis. These conformers exhibit distinct differences in their ¹H NMR spectra. Using the knowledge obtained with the crown-5 derivatives, extrapolations towards the crown-4 and -6 derivatives were made.

3.2.4.1 Thiacalix[4]biscrowns

MS values and the double ¹H NMR crown-ether bridge peak intensities (see experimental) can be used to distinguish monocrown from biscrown products, after which the different conformers can be assigned. Only the 1,3-alternate (diametrical) and 1,2-alternate (proximal) biscrown conformers were obtained. For both the 1,2-alternate (**4**) and 1,3-alternate (**5**) thiacalix[4]biscrown-5 derivatives, X-ray crystal structures were obtained (Figure 3.1). The 1,3-alternate thiacalix[4]biscrown-5 (**4a**) is a highly symmetrical molecule (C₂, 2σ_h), consequently all the aromatic and *tert*-butyl hydrogen atoms are both present as only one signal in the ¹H NMR spectrum. Furthermore, the crown-ether bridge protons of **4a** give a highly symmetrical set of peaks (1: 1: 1: 1; Figure 3.1a). Compared to **4a**, the 1,2-alternate thiacalix[4]biscrown-5 (**5b**) has one plane of symmetry less and an inversion point in the thiacalix[4]arene annulus more (I, C₂, and σ_v). This results in two doublets for the ArH's (7.72 and 7.56 ppm; Figure 3.1b), whereas the *tert*-butyl groups appear as one peak (1.37 ppm), because they are equivalent. The

crown-ether bridge protons of **5b** show an asymmetrical pattern (1: 6: 1; Figure 3.1). Based on the assumption that the most downfield shifted crown-ether bridge proton peak belongs to its first methylene group, COSY correlations revealed that most upfield shifted crown-ether bridge proton peak, also belongs to the first methylene groups attached to the phenolic oxygens. Consequently, these methylene groups are diastereotopic; the rest of the methylene groups all appear as one broad multiplet (Figure 3.1). The observed differences in crown-ether bridge peak order, result in a second diagnostic tool in the ^1H NMR spectra to distinguish the 1,3-alternate conformer **4a** and 1,2-alternate conformer **5b**.

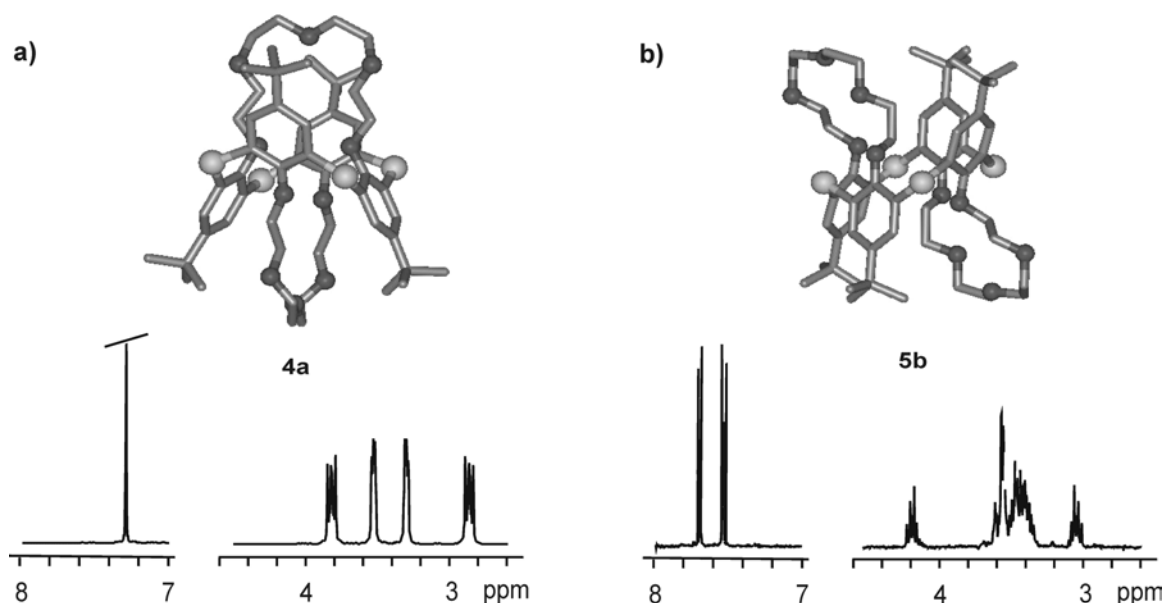


Figure 3.1. Top: X-ray crystal structures of 1,3-alternate thiocalix[4]biscrown-5 [**4a**, (a)] and 1,2-alternate thiocalix[4]biscrown-5 [**5b**, (b)]. Bottom: part of the ^1H NMR spectra for the ArH (left) and crown-ether bridge protons (right) of **4a** (a) and **5b** (b); CHCl_3 peak at 7.26 ppm has been removed for clarity).

Thiocalix[4]biscrown-6 (**4b**)⁹ shows a single peak for the ArH's and *tert*-butyl hydrogen atoms (at 7.38 and 1.34 ppm, respectively) in the ^1H NMR spectrum indicating a 1,3-alternate conformation. In addition, a symmetrical pattern of the crown-ether bridge protons was observed, also pointing to the 1,3-alternate conformation. Thiocalix[4]biscrown-4 (**5a**) exhibits two doublets for the ArH protons (7.77 and 7.52

ppm) and one for the *tert*-butyl groups (1.37 ppm) in the ^1H NMR spectrum. This ^1H NMR pattern shows a high degree of similarity to that of **5b**, indicating a 1,2-alternate conformation.

3.2.4.2 Rigid Thiacalix[4]monocrowns

Diametrically bridged 1,3-thiacalix[4]monocrowns, can be obtained in three different conformers, namely 1,3-alternate, partial cone, and cone. Both the 1,3-alternate and the cone conformers having the same symmetry elements (C_2 , $2\sigma_h$), show similar peak patterns of the protons of the thiacalix[4]arene platform. The pattern of the crown-ether bridge protons, however, is different. In the case of the partial cone conformation the C_2 rotational symmetry axes is lost, resulting in a distinctly different splitting pattern for the protons of the thiacalix[4]arene skeleton.

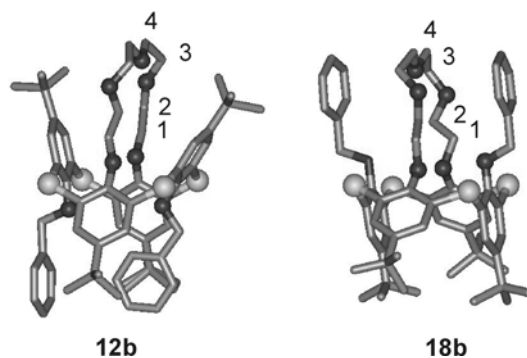


Figure 3.2. X-ray structures of 1,3-bis(benzyloxy)thiacalix[4]crown-5 1,3-alternate **12b** (left) and cone **18b** (right).

X-ray crystal structures of both 1,3-bis(benzyloxy)thiacalix[4]crown-5 conformers (**12b** and **18b**) were obtained (Figure 3.2). The benzyloxy groups are too large for rotation through the annulus, therefore, the conformation is identical both in the solid state and in solution.

The chemical environment of the crown-ether bridge of **12b** is very similar to that of the 1,3-alternate thiacalix[4]biscrown-5 (**4a**; Figures 3.1a and 3.2 left). The benzyloxy groups are positioned perpendicular to each other; one benzyloxy group fills the cavity between the two aromatic units of the thiacalix[4]arene. In the X-ray crystal structure of

the cone conformer **18b** (Figure 3.2), the benzyloxy groups are parallel and the crown-ether bridge fills the space between them. Furthermore, also the aromatic rings of the thiacalix[4]arene to which the benzyloxy groups are attached, are parallel, resulting in a pinched cone conformation.²⁹

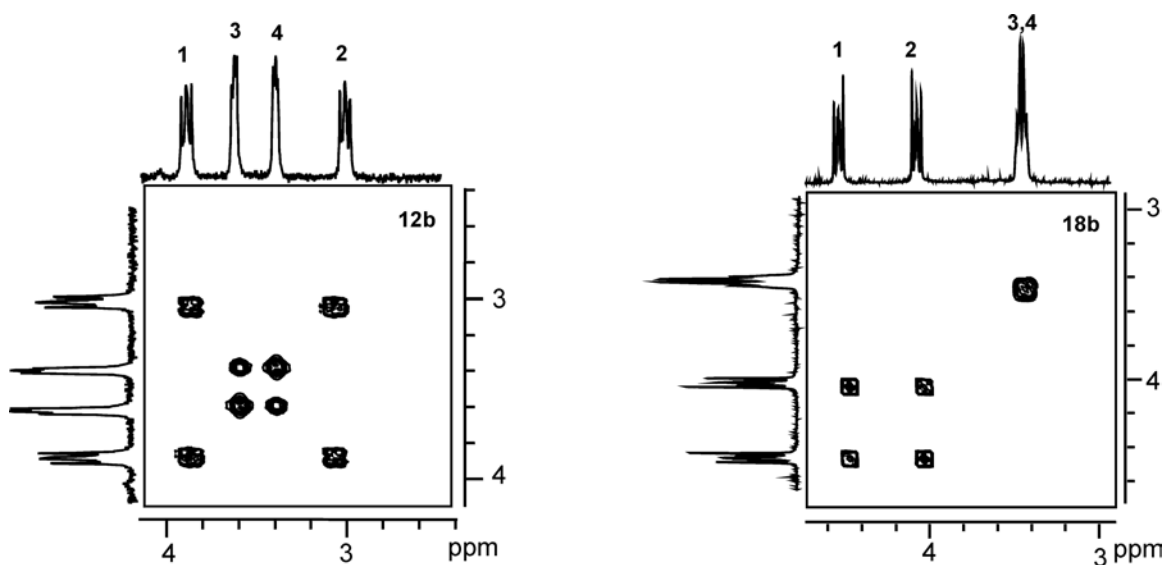


Figure 3.3. COSY ^1H NMR spectra and the peak order of the crown-ether bridge methylene units 1,3-bis(benzyloxy)thiacalix[4]crown-5, 1,3-alternate **12b** [(1)-(3)-(4)-(2), left] and cone **18b** [(1)-(2)-(3,4), right].

Differences between the ^1H NMR spectra of **12b** and **18b** are solely caused by the chemical environment of the different crown-ether bridges. Hence, the most obvious difference lies in the pattern of the crown-ether bridge protons between 3-5 ppm (Figure 3.3). The 1,3-alternate conformer **12b** gives four highly symmetrically spaced peaks (1: 1: 1: 1; Figure 3), resembling the ^1H NMR spectrum of **4a**. Since the benzyl substituents are at the other site of the molecule, they hardly have any influence on the chemical shifts of the crown-ether bridge. Additional COSY experiments revealed coupling between the outer peaks of the crown-ether bridge protons. Therefore, the outer peaks are those of the first two methylene groups of the crown-ether bridge (1 and 2; Figure 3.3). The inner two peaks also show correlation with each other, indicating they correspond to the second set of methylene groups (3 and 4; Figure 3.3). The large upfield shift of methylene group 2 is caused by the anisotropy effect, induced by the aromatic groups of the thiacalix[4]arene

platform in the 1,3-alternate conformation. Since both **4a** and **12b** have the same peak order for the crown-ether bridge protons (Figures 3.1 and 3.3), this tool can be used to determine the conformation. Additional proof was obtained from the NOE interactions between the ArH groups and both the benzyloxy groups and outer two peaks of the crown-ether bridge protons (1 and 2), and between the *tert*-butyl groups and the inner two peaks (3 and 4) of the crown-ether bridge. All these interactions are only possible in the 1,3-alternate conformation.

The cone conformer **18b** exhibits in its ^1H NMR spectrum three unsymmetrical peaks for the crown-ether bridge protons (1: 1: 2; Figure 3.3). COSY coupling between the two downfield shifted peaks shows that they belong to the first two methylene groups of the crown-ether bridge (1 and 2). Using COSY correlations it is possible to differentiate between the 1,3-alternate and cone conformer based on the difference in peak order of the crown-ether bridge protons (1)-(3)-(4)-(2) and (1)-(2)-(3,4),³⁰ respectively (for numbers see Figures 3.2 and 3.3). NOESY experiments of the cone conformer **18b**, show interactions between the ArH protons of the, chemically different, aromatic groups of the thiacalix[4]arene platform. In addition, interactions between the methylene group of the benzyl substituents and the crown-ether bridge are shown in the spectrum. These interactions can only occur in the cone conformation and are proof for this conformation. Based on the X-ray crystal structure, interactions were expected between the benzyloxy groups and the crown-ether bridge, but none were observed. Apparently, in solution the benzyloxy groups point outwards.

The ^1H NMR spectrum of the 1,3-thiacalix[4]crown-5 diethyl ester **13b** shows two ArH and two *tert*-butyl peaks. The crown-ether bridge peak order of (1)-(3)-(4)-(2) was similar to that of **12b** (Figure 3.3), indicating a 1,3-alternate conformation, which was confirmed by its X-ray crystal structure (not depicted).

1,3-Dipropoxythiacalix[4]crown-5 was obtained in all three conformers, viz. 1,3-alternate, partial cone, and cone. The 1,3-alternate **11b** and cone **17b** derivatives, both having two ArH (Figure 3.4) and two *tert*-butyl signals in their ^1H NMR spectra, could be distinguished using the pattern and peak order of the crown-ether bridge protons. Due to the absence of a C_2 -symmetry axis the partial cone conformation **15a** can be distinguished by the four ArH signals (1: 1: 1: 1; Figure 3.4) and the three *tert*-butyl

signals (1: 2: 1). In addition, the upfield shift, due to the anisotropic effect, of the signal belonging to the propoxy group of the rotated aryl ring is a strong indication for the partial cone conformation.

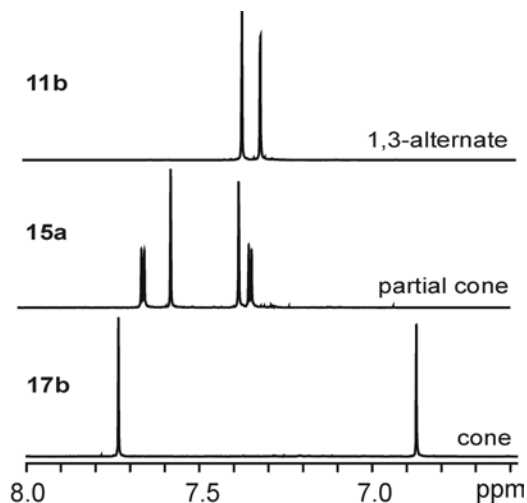


Figure 3.4. ^1H NMR region of the ArH peaks of the 1,3-dipropoxythiacalix[4]-crown-5, 1,3-alternate **11b** (top), partial cone **15a** (middle), and cone **17b** (bottom; CHCl_3 peak at 7.26 ppm has been removed).

Bridging **6-9** with pentaethylene glycol ditosylate (**2c**) gave rise to a different conformational outcome, compared to that obtained with **2b** (Table 3.2). As with the crown-5 derivatives, two distinctly different ^1H NMR spectra were observed for the crown-ether bridges of the 1,3-alternate and cone conformers. 1,3-bis(benzyloxy)thiacalix[4]crown-6 could only be obtained in the 1,3-alternate **12c** and the cone **18c** conformation, probably because of the substituent size. COSY experiments revealed that the outer peaks of the crown-ether bridge region, in the 1,3-alternate conformation, couple with each other. Consequently, they correspond to the first and second methylene protons of the crown-ether bridge, respectively, giving a (1)-(5)-(3,4)-(2)³⁰ peak order. In the cone conformation, the two downfield shifted peaks correspond to the first two methylene protons of the crown-ether bridge [(1)-(2)-(5)-(3)-(4)]. Since both conformers behave in a similar manner as their crown-5 analogs, the crown-ether bridge peak order can be applied to differentiate between the cone and 1,3-alternate crown-6

conformers. 1,3-thiacalix[4]crown-6 diethyl ester can have three conformers: 1,3-alternate **13c**, partial cone **16a**, and cone **19a**. The 1,3-alternate and cone conformers could be distinguished by two peaks for the ArH and *t*-butyl protons, and their crown-ether bridge peak order, and the partial cone conformer could be distinguished by the splitting pattern (1: 1: 1: 1) of its ArH protons. In analogy, 1,3-dipropoxythiacalix[4]crown-6 products, having two ArH and two *tert*-butyl signals, were assigned to the 1,3-alternate **11c**¹⁰ and cone **17c** conformers.

The 1,3-thiacalix[4]crown-4 derivatives (**11a**, **12a**, and **13a**) have two peaks for both the ArH and *t*-butyl protons, indicating either a cone or 1,3-alternate conformation. Furthermore, the hydrogens of the bridging crown-ether units exhibit almost the same chemical shifts [3.7-4.1 (m, 4H), 3.4-3.6 (m, 4H), 2.5 (s, 4H) ppm] suggesting they all have a conformation, in which there is no influence of the substituents. COSY NMR spectra of the crown-4 derivatives exhibit peak orders similar to those of the cone crown-5 conformers [(1)-(2)-(3)].^{30,31} However, in this case NOE interactions between the crown-ether bridge and the ArH protons of the thiacalix[4]arene platform were observed. These interactions are only possible in the 1,3-alternate conformation (see discussion **12b**). The ¹H NMR spectra of the crude reaction mixtures of 1,3-bis(benzyloxy)- and 1,3-dipropoxythiacalix[4]crown-4 exhibit an additional set of signals, of which the ArH peaks have similarities to those of the cone crown-5 isomer **17b** (approximately at 7.7 and 6.9 ppm; Figure 3.5). Therefore, it is assumed that the signals correspond to the cone conformer.

3.2.4.3 Conformationally Flexible Dihydroxy- and Dimethoxythiacalix[4]monocrowns

1,3-Dihydroxythiacalix[4]crowns can be considered as borderline, between rigid and flexible, thiacalix[4]crowns. Although the size of the hydroxyl groups allows rotation through the annulus, hydrogen-bonding²¹ can stabilize the cone conformation. COSY couplings found for 1,3-dihydroxythiacalix[4]crown-5 and -6 (**3b,c**) show that they have the crown-ether bridge peak order corresponding to that of a cone conformation. The X-ray crystal structure of **3c** showed a pinched cone conformation with stabilizing hydrogen bonds between phenolic hydrogens and one of the oxygens of the crown-ether bridge (Figure 3.5). Unlike the other crown-4 derivatives **11a**, **12a**, and **13a**, the peaks of the

dihydroxythiacalix[4]crown-4 conformer (**3a**), peak order (1,2,3), lie downfield [4.76 (t, 4 H), 4.25 (t, 4 H), 3.91 (s, 4 H) ppm]. NOE interactions, ArH/ ArH and OH/ crown-ether bridge, confirmed a cone conformation of **3a**.

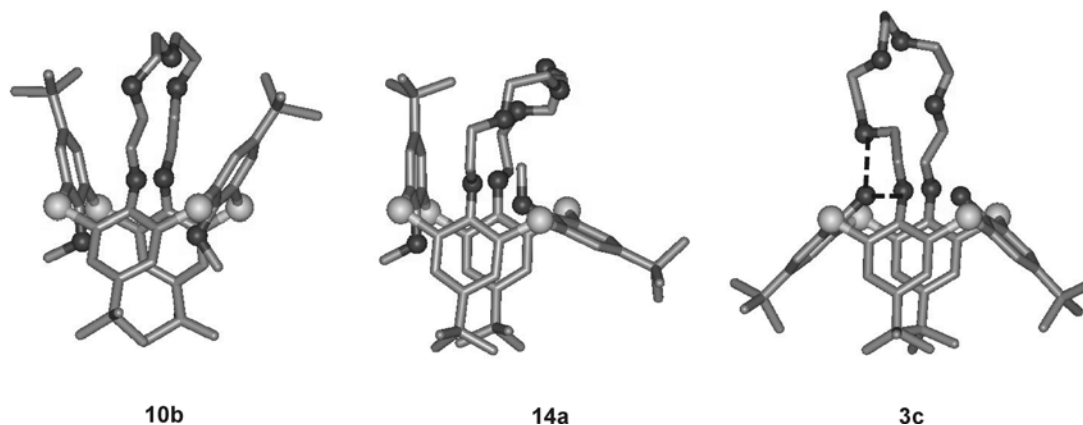


Figure 3.5. X-ray crystal structures of flexible thiacalix[4]crown: 1,3-alternate 1,3-dimethoxythiacalix[4]crown-5 (**10b**; left), partial cone 1,3-dimethoxythiacalix[4]crown-6 (**14a**; middle), and cone 1,3-dihydroxythiacalix[4]crown-6 (**3c**; right). Dotted lines depict H-bonds observed for the hydroxy group of **3c**.

Temperature dependent ^1H NMR studies were performed to study the possible conformational flexibility of the 1,3-dihydroxythiacalix[4]crowns (**3a-c**). Samples of **3a-c** measured in CDCl_3 (steps of ten degrees; temperatures range 223-323 K), showed no conformational changes. In CD_2Cl_2 (223-313 K) changes in the ^1H NMR spectrum of **3a** are observed. The ArH, *tert*-butyl, Ar-O- CH_2 , and OH peaks shift downfield upon increasing the temperature; at lower temperature the two ArH peaks are closer (Figure 3.6). The temperature dependent, linear shifts may indicate a fast exchange between a non-hydrogen bonded cone and a hydrogen bonded pinched cone conformation. The reason that only **3a** and not **3b,c** exhibits this behavior may be caused by the smaller crown-size of **3a**. Smaller crown-sizes favor a pinched cone conformation, due to the formation of stabilizing hydrogen bonds.

The ^1H NMR spectrum of the rotationally flexible²¹ 1,3-dimethoxythiacalix[4]crown-5, in CDCl_3 at 298 K, shows only two peaks for the ArH, the

tert-butyl, and the crown-ether bridge hydrogens (1:3). COSY correlations revealed an intermediate peak order [(1)-(2,3,4)].³⁰ In CD₂Cl₂ the resolution of the crown-ether bridge area is better, showing a similar peak order [(1)-(3)-(4)-(2)] as **12b**, which suggests a 1,3-alternate conformation. Both an X-ray crystal structure and NOE interactions, verify the 1,3-alternate conformation (**10b**; Figure 3.5). The 1,3-dimethoxythiacalix[4]crown-6 conformer, gives an order of the crown-ether bridge protons [(1)-(2)-(3,4,5)] similar to cone compound **18c**. NOE interactions, however, reveal that it has a 1,3-alternate conformation (**10c**). Surprisingly, crystallization of **10c** from CH₂Cl₂/ hexane gave exclusively single crystals of **14a**, the X-ray crystal structure of which clearly proved the partial cone conformation (Figure 3.5). Furthermore, redissolving the crystals of **14a** in CDCl₃ gave a ¹H NMR spectrum identical to that of 1,3-alternate conformer **10c**. Since the anisole units are mobile,²¹ this gives rise to a different conformation in the solid state and in solution. 1,3-Dimethoxythiacalix[4]crown-4 has a similar ¹H NMR spectrum as **11a**, **12a**, and **13a**, suggesting a 1,3-alternate conformation **10a**, which was confirmed with ROESY NMR.

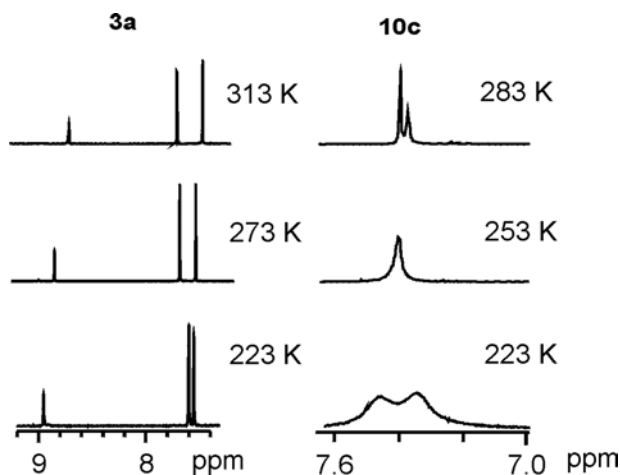


Figure 3.6. Temperature dependent ¹H NMR studies: left OH and ArH peaks of cone 1,3-dihydroxythiacalix[4]crown-4 **3a** (top to bottom: 313 K, 273 K, and 223 K) in CD₂Cl₂, right ArH peaks of 1,3-alternate 1,3-dimethoxythiacalix[4]crown-6 **10c** in CDCl₃ (top to bottom: 283 K, 253 K, 223 K; CHCl₃ peak at 7.26 ppm has been removed).

Temperature dependent ^1H NMR studies of 1,3-dimethoxythiacalix[4]crowns (**10a-c**), in the range 223-323 K, in CDCl_3 only revealed shifts for **10c** (Figure 3.6). Although no conformational interconversion was observed, even upon heating for 24 h at 407 K ($\text{CDCl}_2\text{CDCl}_2$), the shifts are probably the result of the presence of two 1,3-alternate conformers. This was confirmed by observed NOE interactions and relates to the pinched-cone pinched-cone transitions observed by Čajan *et al.*³² for tetrapropoxythiacalix[4]arenes.

Lang *et al.* have reported that propoxy groups are small enough to rotate through the thiacalix[4]arene annulus at elevated temperatures.¹⁹ Therefore, solutions of 1,3-alternate conformers **11a-c** in $\text{CDCl}_2\text{CDCl}_2$ were heated at 407 K for 24 h.³³ Surprisingly, this did not give rise to any change in their conformation, indicating a high stability for the 1,3-alternate conformers.

3.4 Conclusions

This chapter describes the first synthesis of several thiacalix[4](bis)crown conformers, viz. the 1,2-alternate thiacalix[4]biscrowns (**5**), the partial cone (**14-16**), and cone conformers of thiacalix[4]monocrowns (**3**, **17-19**). Both the cation of the base and the length of the oligoethylene glycol used, have a distinct influence on the outcome of the bridging reaction of thiacalix[4]arene. The structural assignment of the different thiacalix[4]crown conformers was mainly based on X-ray crystal structures, supported by different ^1H NMR techniques. The ArH peaks and the order of the peaks of the crown-ether bridge, determined with COSY NMR, is very characteristic for a particular conformation. The ^1H NMR spectra of the conformationally flexible 1,3-dihydroxy- (**3**), 1,3-dimethoxy- (**10**) and 1,3-dipropoxythiacalix[4]crowns (**11**) showed no conformational changes between 223 and 323 K (**3,10**) and after heating for 24 h at 407 K (**3,10,11**). The ArH peaks and the crown-ether bridge peak order provide conformational ‘signatures’ of the different conformers, that can act as a practical tool in the assignment of conformations of thiacalix[4]crowns.

3.5 Experimental

General Methods. All solvents were purified by standard laboratory procedures. All other chemicals were analytically pure and used without further purification, except for pentaethylene glycol di-*p*-toluenesulfonate, which was prepared from pentaethylene glycol and tosyl chloride obtained from Across. Acetonitrile, acetone and dimethylformamide were dried over molecular sieves. *t*-Butylthiacalix[4]arene (**1**) was prepared according to a literature procedure.³⁴ All reactions were carried out under an inert argon atmosphere. Thin-layer chromatography was performed on aluminum sheets precoated with silica gel 60 F254 (E. Merck); spots were visualized by UV-Absorbancy. Chromatographic separations were performed on silica gel 60 (E. Merck, 0.040-0.063 mm, 230-240 mesh). Melting points are uncorrected.

MALDI-TOF mass spectra were recorded on a PerSpective Biosystem Voyager-De-RP spectrometer. ¹H NMR spectra were obtained on a Varian INOVA 300 spectrometer; ¹³C NMR spectra were obtained from a Varian Unity 400 spectrometer. Spectra were recorded at 25 °C in CDCl₃ and referenced to the (residual) solvent peak (¹³CDCl₃). The 2D DQF-COSY spectra (300 MHz) consisted of 1024 data points in *t*₂ and 256 increments in *t*₁. The ROESY spectra (400 MHz) were acquired with a mixing time of 400 ms, 1024 data points in *t*₂ and 128 increments in *t*₁, or 2984 data points in *t*₂ and 256 increments in *t*₁.

General Procedure for the Direct Formation of 25,27-Difunctionalized and 25,26,27,28-Tetrafunctionalized 5,11,17,23-Tetra-*tert*-butyl-2,8,14,20-tetrathiacalix[4]arenes monocrown-n (n=4 or 5). To a suspension of *p-t*-butylthiacalix[4]arene **1** (0.73 g, 1 mmol) in CH₃CN (40 mL) were added MCO₃ (M⁺ = Na⁺, K⁺, and Cs⁺) and 1 equiv of tetra-, pentaethylene glycol di-*p*-toluenesulfonate (**2a,b**). The solution was refluxed for 11 d (**3b**), 6 h (**5a**), and 12 h (**5b**). Subsequently, the solvent was evaporated and CH₂Cl₂ was added (for the reaction mixtures containing 1,2-alternate thiacalix[4]biscrowns **5a,b** chloroform was used). The solution was washed twice with 10% HCl and once with water and evaporated to dryness, whereupon, the crude reaction mixture was purified further.

5,11,17,23-Tetra-*tert*-butyl-26,28-dihydroxy-2,8,14,20-tetrathiacalix[4]arene-monocrown-5, cone (3b). A suspension of **1** and **2b** (0.53 g, 1.0 mmol) in CH₃CN was

added NaCO₃ (1.3 g, 12 mmol). Column chromatography (CH₂Cl₂/ MeOH 10/1), afforded **3b** (87 mg, 10%): mp 233-234 °C; ¹H NMR δ 8.06 (s, 2 H), 7.68 (s, 4 H), 6.94 (s, 4 H), 4.78 (t, 4 H, *J* = 5.5 Hz), 4.17 (t, 4 H, *J* = 5.7 Hz), 3.91 (m, 4 H), 3.82 (m, 4 H), 1.37 (s, 18 H), 0.82 (s, 18 H); ¹³C NMR δ 155.5, 147.4, 134.1, 132.2, 128.6, 121.6, 72.5, 70.3, 70.0, 69.2, 33.7, 33.5, 30.6, 30.2; MALDI-TOF *m/z*: 901.0 [M+Na]⁺, calcd 901.3 [M+Na]⁺. Anal. Calcd for C₄₈H₆₂O₇S₄ · 0.7 H₂O: C, 64.67; H, 7.16. Found: C, 64.49; H, 7.04.

5,11,17,23-Tetra-*tert*-butyl-2,8,14,20-tetrathiacalix[4]arene-biscrown-4, 1,2-alternate (5a). A suspension of **1** and **2a** (0.92 g, 2.0 mmol) in CH₃CN was added CsCO₃ (1.3 g, 4 mmol). Precipitation from a MeOH/acetone 3/1 mixture yielded **5a** (720 mg, 74%): mp > 250 °C; ¹H NMR δ 7.77 (d, 4 H, *J* = 2.6 Hz), 7.52 (d, 4 H, *J* = 2.6 Hz), 4.06 (m, 4 H), 3.85 (m, 4 H), 3.45 (m, 11 H), 3.23 (m, 4 H), 1.37 (s, 36 H); ¹³C NMR δ 157.2, 145.9, 133.9, 129.4, 129.4, 128.2, 71.9, 69.6, 68.4, 33.9, 30.9; MALDI-TOF *m/z*: 971.0 [M+H]⁺, calcd 971.3 [M+H]⁺. Anal. Calcd for C₅₂H₆₈O₈S₄ · 0.2 CHCl₃: C, 64.41; H, 7.06. Found: C, 64.18; H, 6.73.

5,11,17,23-Tetra-*tert*-butyl-2,8,14,20-tetrathiacalix[4]arene-biscrown-5, 1,3-alternate (4a) and 1,2-alternate (5b). A suspension of **1** and **2b** (0.53 g, 1.0 mmol) in CH₃CN was added CsCO₃ (1.3 g, 4 mmol). Fractional precipitation from a MeOH/acetone 3/1 mixture yielded: **4a** (16 mg, 15%) and **5b** (28 mg, 27%). **4a** mp > 250 °C (lit.⁹ mp > 250 °C). The spectral data are identical to those reported.⁹ **5b** mp > 250 °C; ¹H NMR δ 7.72 (d, 4 H, *J* = 2.4 Hz), 7.56 (d, 4 H, *J* = 2.4 Hz), 4.25 (t, 2 H, *J* = 6.9 Hz), 4.22 (t, 2 H, *J* = 5.9 Hz), 3.35-3.70 (m, 12 H), 3.12 (t, 2 H, *J* = 6.2 Hz), 3.09 (t, 2 H, *J* = 6.4 Hz), 1.37 (s, 36 H); ¹³C NMR δ 156.8, 145.6, 133.8, 130.3, 128.8, 128.4, 71.2, 70.9, 69.8, 68.9, 33.9, 30.9; MALDI-TOF *m/z*: 1037.5 [M+H]⁺, calcd 1037.4 [M+H]⁺. Anal. Calcd for C₅₆H₇₆O₁₀S₄: C, 64.83; H, 7.38. Found: C, 64.78; H, 7.38.

General Procedure for the Formation of 25,27-Difunctionalized 5,11,17,23-Tetra-*tert*-butyl-2,8,14,20-tetrathiacalix[4]arenes monocrown-*n* (*n*=4, 5 or 6). To a suspension of 1,3-dialkoxythiacalix[4]arenes (**6-9**) in CH₃CN, were added 4 equiv of K₂CO₃ and 1 equiv of tetra-, penta-, or hexaethylene glycol di-*p*-toluenesulfonate (**2a-c**). The mixture was refluxed for 5 d (12 h in case of **9**). CH₃CN was removed and the residue extracted with CH₂Cl₂/CHCl₃. The solution was washed twice with 10% HCl and

water, and dried on MgSO₄. Solvents were removed under reduced pressure and the residue was triturated with MeOH to remove unreacted glycol di-*p*-toluenesulfonates, yielding after drying white solids.

5,11,17,23-Tetra-*tert*-butyl-25,27-dimethoxy-2,8,14,20-tetrathiacalix[4]arene-monocrown-4, 1,3-alternate (10a). A suspension of **6** (1.50 g, 2.0 mmol) in CH₃CN (100 mL) was reacted with **2a** (0.92 g, 2.0 mmol). After trituration with MeOH, the residue was triturated with CH₂Cl₂ to give **10a** (1.50 g, 87%): mp > 250 °C; ¹H NMR δ 7.49 (s, 4H), 7.30 (s, 4H), 4.10 (t, 4H, *J* = 4.0 Hz), 3.54 (t, 4H, *J* = 4.0 Hz), 3.32 (s, 6H), 2.51 (s, 4H), 1.33 (s, 18H), 1.30 (s, 18H); ¹³C NMR δ 157.6, 156.3, 146.3, 145.9, 130.0, 129.3, 127.2, 126.1, 71.0, 70.3, 69.0, 55.7, 34.4, 34.2, 31.4, 31.2; MALDI-TOF *m/z*: 863.9 [M+H]⁺, 885.8 [M+Na]⁺, 901.8 [M+K]⁺, calcd 863.3 [M+H]⁺. Anal. Calcd for C₄₈H₆₂O₆S₄: C, 66.78; H, 7.24. Found: C, 66.94; H, 6.95.

5,11,17,23-Tetra-*tert*-butyl-25,27-dimethoxy-2,8,14,20-tetrathiacalix[4]arene-monocrown-5, 1,3-alternate (10b)¹⁰. A suspension of **6** (1.50 g, 2.0 mmol) in CH₃CN (100 mL) was reacted with **2b** (1.05 g, 2.0 mmol) to give **10b** (1.68 g, 93%): mp > 250 °C (lit.¹⁰ mp 266-268 °C). The spectral data are identical to those reported.¹⁰

5,11,17,23-Tetra-*tert*-butyl-25,27-dimethoxy-2,8,14,20-tetrathiacalix[4]arene-monocrown-6, 1,3-alternate (10c)¹⁰. A suspension of **6** (1.75 g, 2.3 mmol) in CH₃CN (100 mL) was reacted with **2c** (1.26 g, 2.3 mmol). After trituration with MeOH, column chromatography (SiO₂, 2% acetone in CH₂Cl₂) was performed to give **10c** (1.23 g, 59%): mp > 250 °C (lit.¹⁰ mp 272-274 °C). The spectral data are identical to those reported.¹⁰

5,11,17,23-Tetra-*tert*-butyl-25,27-dipropoxy-2,8,14,20-tetrathiacalix[4]arene-monocrown-4, 1,3-alternate (11a). A suspension of **7** (0.50 g, 0.6 mmol) in CH₃CN (50 mL) was reacted with **2a** (0.28 g, 0.6 mmol). After trituration with MeOH, column chromatography (SiO₂, EtOAc/hexane 0.5/9.5) was performed to give **11a** (0.33 g, 58%): mp > 250 °C; ¹H NMR δ 7.37 (s, 4H), 7.31 (s, 4H), 4.00-4.03 (m, 4H), 3.70-3.76 (m, 4H), 3.52 (t, 4H, *J* = 4.0 Hz), 2.48 (s, 4H), 1.31 (s, 18H), 1.26 (s, 18H), 0.80-0.92 (m, 4H), 0.65 (t, 6H, *J* = 7.3 Hz); ¹³C NMR δ 158.0, 156.0, 145.9, 145.7, 128.6, 127.8, 126.8, 71.1, 70.0, 69.5, 68.6, 34.4, 34.2, 31.4, 31.2, 30.2, 29.7, 21.3, 9.7; MALDI-TOF *m/z*: 919.6 [M+H]⁺, 941.6 [M+Na]⁺, 957.5 [M+K]⁺, calcd 919.4 [M+H]⁺. Anal. Calcd for C₅₂H₇₀O₆S₄ · 0.3 H₂O: C, 67.52; H, 7.62. Found: C, 67.50; H, 7.46.

5,11,17,23-Tetra-*tert*-butyl-25,27-dipropoxy-2,8,14,20-tetrathiacalix[4]arene-monocrown-5, 1,3-alternate (11b)¹⁰, partial cone (15a), and cone (17b). A suspension of **7** (0.50 g, 0.6 mmol) in CH₃CN (50 mL) was reacted with **2b** (0.30 g, 0.6 mmol). After trituration with MeOH, column chromatography (SiO₂, EtOAc/hexane 0.5/9.5) was performed to give **11b**¹⁰ (0.35 g, 59%), **15a** (9 mg, 2%), and **17b** (50 mg, 8%). **11b**: mp > 250 °C (lit.¹⁰ mp 262-264 °C). The spectral data are identical to those reported.¹⁰ **15a**: mp > 250 °C; ¹H NMR δ 7.63 (d, 2H, *J* = 2.2 Hz), 7.55 (s, 2H), 7.35 (s, 2H), 7.32 (d, 2H, *J* = 2.2 Hz), 4.00-4.06 (m, 8H), 3.74-3.76 (m, 4H), 3.51-3.59 (m, 6H), 3.09 (t, 2H, *J* = 6.2 Hz), 1.85-1.97 (m, 2H), 1.42 (s, 9H), 1.28 (s, 18H), 1.06 (s, 9H), 1.03 (t, 3H, *J* = 7.5 Hz), 0.38-0.49 (m, 2H), 0.02 (t, 3H, *J* = 7.3 Hz); ¹³C NMR δ 158.1, 157.7, 146.4, 146.0, 145.9, 134.0, 131.1, 129.9, 129.4, 128.9, 128.0, 127.7, 79.2, 73.6, 71.2, 71.0, 70.6, 70.3, 34.3, 34.1, 31.4, 31.3, 31.0, 29.7, 23.1, 22.2, 10.6, 10.0; MALDI-TOF *m/z*: 963.4 [M+H]⁺, 985.4 [M+Na]⁺, 1001.4 [M+K]⁺, calcd 963.4 [M+H]⁺. Anal. Calcd for C₅₄H₇₄O₇S₄: C, 67.32; H, 7.74. Found: C, 67.24; H, 7.69. **17b**: mp > 250 °C; ¹H NMR δ 7.70 (s, 4H), 6.84 (s, 4H), 4.55-4.61 (m, 4H), 4.25-4.31 (m, 4H), 3.90 (t, 4H, *J* = 7.0 Hz), 3.82 (s, 8H), 1.89-2.01 (m, 4H), 1.34 (s, 18H), 1.10 (t, 6H, *J* = 7.5 Hz), 0.82 (s, 18H); ¹³C NMR δ 160.8, 157.9, 146.1, 145.8, 135.3, 132.5, 131.0, 128.7, 79.3, 72.9, 71.5, 71.0, 69.6, 34.4, 33.8, 31.5, 31.3, 30.9, 23.4, 10.8; MALDI-TOF *m/z*: 963.6 [M+H]⁺, 985.6 [M+Na]⁺, 1001.6 [M+K]⁺, calcd 963.4 [M+H]⁺. Anal. Calcd for C₅₄H₇₄O₇S₄: C, 67.32; H, 7.74. Found: C, 67.47; H, 7.99.

5,11,17,23-Tetra-*tert*-butyl-25,27-dipropoxy-2,8,14,20-tetrathiacalix[4]arene-monocrown-6, 1,3-alternate (11c)¹⁰. A suspension of **7** (0.36 g, 0.4 mmol) in CH₃CN (50 mL) was reacted with **2c** (0.22 g, 0.4 mmol). After trituration with MeOH, column chromatography (SiO₂, 2% acetone in CH₂Cl₂) was performed to give **11c** (0.25 g, 57%): mp > 250 °C (lit.¹⁰ mp 280-282 °C). The spectral data are identical to those reported.¹⁰

25,27-Bis(benzyloxy)-5,11,17,23-tetra-*tert*-butyl-2,8,14,20-tetrathiacalix[4]-arene-monocrown-4, 1,3-alternate (12a). A suspension of **8** (0.40 g, 0.4 mmol) in CH₃CN (50 mL) was reacted with **2a** (0.18 g, 0.4 mmol). After trituration with MeOH, column chromatography (SiO₂, CH₂Cl₂/hexane 1/1) was performed to give **12a** (0.15 g, 33%): mp > 250 °C; ¹H NMR δ 7.39 (s, 4H), 7.07-7.18 (m, 6H), 7.11 (s, 4H), 6.85-6.88 (m, 4H), 5.09 (s, 4H), 4.02-4.05 (m, 4H), 3.52-3.60 (m, 4H), 2.58 (s, 4H), 1.36 (s, 18H),

0.85 (s, 18H); ^{13}C NMR δ 157.7, 155.5, 146.2, 146.2, 137.3, 129.3, 128.8, 127.9, 127.8, 127.7, 127.3, 126.9, 71.2, 70.0, 69.9, 68.6, 34.4, 33.8, 31.4, 30.7; MALDI-TOF m/z : 1015.9 $[\text{M}+\text{H}]^+$, 1037.9 $[\text{M}+\text{Na}]^+$, calcd 1015.4 $[\text{M}+\text{H}]^+$. Anal. Calcd for $\text{C}_{60}\text{H}_{70}\text{O}_6\text{S}_4$: C, 70.97; H, 6.95. Found: C, 70.82; H, 6.74.

25,27-Bis(benzyloxy)-5,11,17,23-tetra-tert-butyl-2,8,14,20-tetrathiacalix[4]-arene-monocrown-5, 1,3-alternate (12b) and cone (18b). A suspension of **8** (0.50 g, 0.6 mmol) in CH_3CN (50 mL) was reacted with **2b** (0.30 g, 0.6 mmol). After trituration with MeOH, column chromatography (SiO_2 , CH_2Cl_2 /hexane 1/1) was performed to give **12b** (0.21 g, 33%). Eluent change to 5% acetone in CH_2Cl_2 gave **18b** (0.12 g, 20%). **12b**: mp > 250 °C; ^1H NMR δ 7.41 (s, 4H), 7.09 (t, 2H, $J = 7.4$ Hz), 7.03 (s, 4H), 6.98 (t, 4H, $J = 7.5$ Hz), 6.84 (d, 4H, $J = 7.6$ Hz), 5.03 (s, 4H), 3.94 (t, 4H, $J = 8.1$ Hz), 3.60-3.67 (m, 4H), 3.36-3.44 (m, 4H), 3.05 (t, 4H, $J = 8.2$ Hz), 1.38 (s, 18H), 0.85 (s, 18H); ^{13}C NMR δ 156.1, 155.9, 146.2, 146.1, 137.4, 128.5, 127.8, 127.5, 127.4, 127.2, 127.0, 126.8, 73.6, 71.4, 70.4, 70.1, 65.4, 34.4, 33.8, 31.5, 30.8; MALDI-TOF m/z : 1059.5 $[\text{M}+\text{H}]^+$, 1081.4 $[\text{M}+\text{Na}]^+$, 1097.4 $[\text{M}+\text{K}]^+$, calcd 1059.4 $[\text{M}+\text{H}]^+$. Anal. Calcd for $\text{C}_{62}\text{H}_{74}\text{O}_7\text{S}_4$: C, 70.29; H, 7.04. Found: C, 69.99; H, 7.26. **18b**: mp 248-252 °C; ^1H NMR δ 7.69 (s, 4H), 7.60 (d, 4H, $J = 6.2$ Hz), 7.28-7.39 (m, 6H), 6.86 (s, 4H), 4.99 (s, 4H), 4.45-4.51 (m, 4H), 3.99-4.05 (m, 4H), 3.41-3.44 (m, 8H), 1.33 (s, 18H), 0.84 (s, 18H); ^{13}C NMR δ 160.6, 157.1, 146.1, 137.1, 135.2, 132.6, 130.9, 129.6, 129.0, 128.3, 128.0, 79.0, 73.0, 71.1, 70.6, 69.3, 34.3, 33.9, 31.4, 30.9; MALDI-TOF m/z : 1059.7 $[\text{M}+\text{H}]^+$, 1081.6 $[\text{M}+\text{Na}]^+$, 1097.6 $[\text{M}+\text{K}]^+$, calcd 1059.4 $[\text{M}+\text{H}]^+$. Anal. Calcd for $\text{C}_{62}\text{H}_{74}\text{O}_7\text{S}_4$: C, 70.29; H, 7.04. Found: C, 70.06; H, 7.27.

25,27-Bis(benzyloxy)-5,11,17,23-tetra-tert-butyl-2,8,14,20-tetrathiacalix[4]-arene-monocrown-6, 1,3-alternate (12c) and cone (18c). A suspension of **8** (1.0 g, 1.1 mmol) in CH_3CN (75 mL) was reacted with **2c** (0.60 g, 1.1 mmol). After trituration with MeOH, column chromatography (SiO_2 , CH_2Cl_2 /hexane 1/1) was performed to give **12c** (0.29 g, 24%), eluent change to 10% acetone in CH_2Cl_2 gave **18c** (0.25 g, 20%). **12c**: mp 227-230 °C; ^1H NMR δ 7.43 (s, 4H), 7.12 (d, 2H, $J = 7.3$ Hz), 7.07 (s, 4H), 7.03 (t, 4H, $J = 7.3$ Hz), 6.88 (d, 4H, $J = 7.0$ Hz), 5.06 (s, 4H), 3.96 (t, 4H, $J = 7.3$ Hz), 3.59 (s, 4H), 3.52 (s, 8H), 3.06 (t, 4H, $J = 7.5$ Hz), 1.38 (s, 18H), 0.87 (s, 18H); ^{13}C NMR δ 156.4, 156.1, 146.4, 146.1, 137.4, 128.7, 127.8, 127.6, 127.2, 126.8, 71.5, 71.4, 70.8, 70.2, 69.5,

66.8, 34.4, 33.8, 31.4, 30.7; MALDI-TOF m/z : 1103.7 $[M+H]^+$, 1125.6 $[M+Na]^+$, 1141.6 $[M+K]^+$, calcd 1103.5 $[M+H]^+$. Anal. Calcd for $C_{64}H_{78}O_8S_4$: C, 69.66; H, 7.12. Found: C, 69.56; H, 7.10. **18c**: mp 229-234 °C; 1H NMR δ 7.67 (s, 4H), 7.58-7.61 (m, 4H), 7.31-7.41 (m, 6H), 6.87 (s, 4H), 5.01 (s, 4H), 4.43-4.48 (m, 4H), 3.95-4.00 (m, 4H), 3.56 (s, 8H), 3.52-3.55 (m, 4H), 3.37-3.41 (m, 4H), 1.32 (s, 18H), 0.84 (s, 18H); ^{13}C NMR δ 160.5, 157.2, 146.2, 137.1, 135.2, 132.7, 131.0, 129.5, 129.1, 128.3, 128.1, 79.0, 72.8, 70.9, 70.5, 69.6, 34.4, 33.9, 31.4, 30.9; MALDI-TOF m/z : 1103.5 $[M+H]^+$, 1125.5 $[M+Na]^+$, 1141.4 $[M+K]^+$, calcd 1103.5 $[M+H]^+$. Anal. Calcd for $C_{64}H_{78}O_8S_4$: C, 69.66; H, 7.12. Found: C, 69.75; H, 7.23.

5,11,17,23-Tetra-*tert*-butyl-25,27-bis[(ethoxycarbonyl)methoxy]-2,8,14,20-tetrathiacalix[4]arene-monocrown-4, 1,3-alternate (13a). A suspension of **9** (0.30 g, 0.3 mmol) in CH_3CN (30 mL) was reacted with **2a** (0.14 g, 0.3 mmol). After trituration with MeOH, column chromatography (SiO_2 , 10% acetone in CH_2Cl_2) was performed to give **13a** (98 mg, 29%): mp 213-217 °C; 1H NMR δ 7.35 (s, 4H), 7.32 (s, 4H), 4.41 (s, 4H), 4.08 (q, 4H, $J = 7.1$ Hz), 4.01-4.04 (m, 4H), 3.47-3.50 (m, 4H), 2.57 (s, 4H), 1.32 (s, 18H), 1.24 (s, 18H), 1.78 (t, 6H, $J = 7.3$ Hz); ^{13}C NMR δ 167.7, 157.7, 154.2, 146.4, 146.1, 129.8, 128.4, 127.3, 127.2, 71.2, 70.1, 68.9, 64.8, 60.1, 34.4, 34.1, 31.4, 31.0, 14.0; MALDI-TOF m/z : 1007.9 $[M+H]^+$, 1029.9 $[M+Na]^+$, 1045.9 $[M+K]^+$, calcd 1007.4 $[M+H]^+$. Anal. Calcd for $C_{54}H_{70}O_{10}S_4$: C, 64.38; H, 7.00. Found: C, 64.20; H, 6.82.

5,11,17,23-Tetra-*tert*-butyl-25,27-bis[(ethoxycarbonyl)methoxy]-2,8,14,20-tetrathiacalix[4]arene-monocrown-5, 1,3-alternate (13b). A suspension of **9** (0.50 g, 0.5 mmol) in CH_3CN (50 mL) was reacted with **2b** (0.25 g, 0.5 mmol) to give **13b** (0.42 g, 71%): mp > 250 °C; 1H NMR δ 7.36 (s, 4H), 7.34 (s, 4H), 4.36 (s, 4H), 4.06 (q, 4H, $J = 7.2$ Hz), 3.75-3.80 (m, 4H), 3.53-3.56 (m, 4H), 3.39-3.41 (m, 4H), 3.12-3.16 (m, 4H), 1.35 (s, 18H), 1.23 (s, 18H), 1.16 (t, 6H, $J = 7.1$ Hz); ^{13}C NMR δ 167.9, 156.9, 154.3, 146.2, 129.5, 128.3, 127.4, 127.0, 72.8, 70.9, 70.5, 67.6, 65.2, 60.1, 34.3, 34.1, 31.4, 31.0, 29.7, 23.7, 14.1; MALDI-TOF m/z : 1051.8 $[M+H]^+$, 1068.8 $[M+Na]^+$, 1089.7 $[M+H]^+$, calcd 1051.4 $[M+H]^+$. Anal. Calcd for $C_{56}H_{74}O_{11}S_4 \cdot 0.5 H_2O$: C, 63.43; H, 7.13. Found: C, 63.43; H, 7.36.

5,11,17,23-Tetra-*tert*-butyl-25,27-bis[(ethoxycarbonyl)methoxy]-2,8,14,20-tetrathiacalix[4]arene-monocrown-6, 1,3-alternate (13c). A suspension of **9** (0.30 g, 0.3 mmol) in CH₃CN (30 mL) was reacted with **2c** (0.16 g, 0.3 mmol). After trituration with MeOH, column chromatography (SiO₂, EtOAc/hexane 1/9) was performed to give **13c** (60 mg, 16%): mp > 250 °C; ¹H NMR δ 7.39 (s, 4H), 7.37 (s, 4H), 4.39 (s, 4H), 4.09 (q, 4H, *J* = 7.1 Hz), 3.74 (t, 4H, *J* = 6.6 Hz), 3.55 (s, 4H), 3.48-3.51 (m, 4H), 3.42-3.45 (m, 4H), 3.21 (t, 4H, *J* = 6.8 Hz), 1.33 (s, 18H), 1.24 (s, 18H), 1.18 (t, 6H, *J* = 7.1 Hz); ¹³C NMR δ 167.6, 157.0, 154.3, 145.8, 130.2, 128.2, 127.4, 127.0, 70.9, 70.7, 70.6, 69.5, 68.8, 65.2, 59.9, 33.9, 33.7, 30.9, 30.6, 29.3, 13.6; MALDI-TOF *m/z*: 1095.8 [M+H]⁺, 1117.8 [M+Na]⁺, 1133.8 [M+K]⁺, calcd 1095.4 [M+H]⁺. Anal. Calcd for C₅₈H₇₈O₁₂S₄: C, 63.59; H, 7.18. Found: C, 63.70; H, 7.18.

General Procedure for the Indirect Formation of 5,11,17,23-Tetra-*tert*-butyl-25,27-dihydroxy-2,8,14,20-tetrathiacalix[4]arene-monocrown-*n* (*n* = 4, 5, or 6). A suspension of 1,3-dimethoxy-*p-tert*-butylthiacalix[4]arene-monocrown-*n* (**10a-c**) and 5.5 equiv of CH₃SNa or C₂H₅SNa in DMF was heated at 80 °C for 5 d. DMF was removed under reduced pressure and the residue was redissolved in CH₂Cl₂/CHCl₃. The organic layer was washed with 1 N HCl (2 x 20 mL) and dried on MgSO₄. The solvents were removed and the residue was purified by column chromatography and/or precipitation from MeOH, yielding white solids.

5,11,17,23-Tetra-*tert*-butyl-25,27-dihydroxy-2,8,14,20-tetrathiacalix[4]arene-monocrown-4, cone (3a)²⁶. A suspension of **10a** (0.50 g, 0.6 mmol) in DMF (50 mL) was reacted with C₂H₅SNa (0.28 g, 3.3 mmol). Column chromatography (SiO₂, EtOAc/hexane 1/9) was performed to give **3a** (87 mg, 18%): mp > 250 °C (lit.²⁷ mp 272-273 °C). The spectral data are identical to those reported.²⁷

5,11,17,23-Tetra-*tert*-butyl-26,28-dihydroxy-2,8,14,20-tetrathiacalix[4]arene-monocrown-5, cone (3b). A suspension of **10b** (0.50 g, 0.55 mmol) in DMF (25 mL) was reacted with CH₃SNa (0.21 g, 3.0 mmol). Column chromatography (SiO₂, EtOAc/hexane 1/9), followed by precipitation from MeOH, gave **3b** (120 mg, 25%): mp 233-234 °C (lit.²⁶ mp 240-243 °C). The spectral data are identical to those reported above.

5,11,17,23-Tetra-*tert*-butyl-26,28-dihydroxy-2,8,14,20-tetrathiacalix[4]arene-monocrown-6 cone (3c). A suspension of **10c** (0.30 g, 0.26 mmol) in DMF (30 mL) was

reacted with C₂H₅SNa (0.12 g, 1.4 mmol) to give **3c** (39 mg, 16%): mp 175-185 °C; ¹H NMR δ 8.04 (s, 2H), 7.66 (s, 4H), 6.92 (s, 4H), 4.75 (t, 4H, *J* = 4.4 Hz), 4.13 (t, 4H, *J* = 4.6 Hz), 3.85-3.88 (m, 4H), 3.79-3.82 (m, 4H), 3.74 (s, 4H), 1.33 (s, 18H), 0.77 (s, 18H); ¹³C NMR δ 156.0, 147.9, 142.5, 134.6, 132.6, 129.1, 122.2, 73.8, 71.0, 70.9, 70.8, 34.2, 34.0, 31.5, 30.7; MALDI-TOF *m/z*: 923.3 [M+H]⁺, 945.3 [M+Na]⁺, calcd 923.4 [M+H]⁺. Anal. Calcd for C₅₀H₆₆O₈S₄: C, 65.04; H, 7.20; S, 13.89. Found: C, 64.97; H, 7.13; S, 13.83.

X-ray Crystallographic Data. Crystal data for **3c**, **4a**, **5b**, **10b**, **12b**, **14a**, and **18b**. Diffraction data were collected at 150 K on a Nonius KappaCCD diffractometer on rotating anode ($\lambda_{MoK\alpha} = 0.71073 \text{ \AA}$). All structures were solved using direct methods (SHELXS86³⁵) and refined on F² (SHELXL-97³⁶). The structures contained a number of disordered moieties that could be satisfactorily described with two-site disorder models: *tert*-butyl groups in **3c**, **4a**, **5b**, **12b**, **13b**, **14a**, and **18b**; crown ether moieties in **10b** and **14a**; and benzyloxy groups in **18b**. Severely disordered solvent molecules in structures **10b**, **12b**, **13b**, and **18b** were treated with corrections based on numerical Fourier transformations of the solvent area (SQUEEZE³⁷). Ordered non-hydrogen atoms were refined with anisotropic displacement parameters. Hydrogen atoms were included on calculated positions riding on their carrier. Full details of the structure determinations are given in the supporting information.

Compound **3c**: C₅₀H₆₆O₈S₄, *M_r* = 923.3, triclinic, $P\bar{1}$ (no. 2) with *a* = 13.7693(10), *b* = 18.219(2), *c* = 20.773 (2) Å, α = 77.239 (15), β = 88.394 (12), γ = 86.938 (12) deg, *V* = 5074.5 (8) Å³, *Z* = 4, *RI*[14423 *I* > 2σ(*I*)] = 0.0650, *wR2* (23162 refl.) = 0.1903.

Compound **4a**: C₅₆H₇₆O₁₀S₄, *M_r* = 1037.4, orthorhombic, *Pbca* (no. 61) with *a* = 16.7260(10), *b* = 17.4914(10), *c* = 38.238(2) Å, *V* = 11187.0(11) Å³, *Z* = 8, *RI*[7795 *I* > 2σ(*I*)] = 0.052, *wR2* (10221 refl.) = 0.130.

Compound **5b**: C₅₆H₇₆O₁₀S₄, *M_r* = 1037.4, triclinic, $P\bar{1}$ (no. 2) with *a* = 10.4720(10), *b* = 11.2486(15), *c* = 11.4484(15) Å, α = 88.533(10), β = 84.495(10), γ = 84.610(10)°, *V* = 1336.2(3) Å³, *Z* = 1, *RI*[for 4526 *I* > 2σ(*I*)] = 0.055, *wR2* (6070 refl.) = 0.155.

Compound **10b**: C₅₀H₆₆O₇S₄, $M_r = 907.3$, orthorhombic, *Pnma* (no. 62) with $a = 28.704$ (2), $b = 12.6928$ (10), $c = 14.2236$ (10) Å, $V = 5182.1$ (7) Å³, $Z = 4$, $RI[4732 I > 2\sigma(I)] = 0.0613$, $wR2$ (6218 refl.) = 0.1646.

Compound **12b**: C₆₂H₇₄O₇S₄, $M_r = 1059.5$, monoclinic, *P2₁/c* (no. 14) with $a = 15.327$ (2), $b = 15.272$ (2), $c = 27.561$ (4) Å, $\beta = 96.322$ (12) deg, $V = 6412.1$ (15) Å³, $Z = 4$, $RI[7483 I > 2\sigma(I)] = 0.0766$, $wR2$ (11606 refl.) = 0.1796.

Compound **13b** (not depicted in the text): C₅₆H₇₄O₁₁S₄, $M_r = 1051.4$, monoclinic, *P2₁/c* (no. 14) with $a = 40.260$ (5), $b = 14.164$ (3), $c = 29.4749$ (10) Å, $\beta = 93.712$ (12) deg, $V = 16773$ (4) Å³, $Z = 8$, $RI[15976 I > 2\sigma(I)] = 0.1004$, $wR2$ (30234 refl.) = 0.2966.

Compound **14a**: C₅₂H₇₀O₈S₄, $M_r = 951.4$, monoclinic, *P2₁/c* (no. 14) with $a = 15.2781$ (10), $b = 12.2052$ (15), $c = 28.622$ (2) Å, $\beta = 103.12$ (2) deg, $V = 5197.9$ (8) Å³, $Z = 4$, $RI[7745 I > 2\sigma(I)] = 0.0645$, $wR2$ (11884 refl.) = 0.1882.

Compound **18b**: C₆₂H₇₄O₇S₄, $M_r = 1059.5$, triclinic, $P\bar{1}$ (no. 2) with $a = 13.986$ (2), $b = 14.416$ (2), $c = 33.061$ (6) Å, $\alpha = 92.229$ (16), $\beta = 91.131$ (14), $\gamma = 99.872$ (10) deg, $V = 6559.8$ (18) Å³, $Z = 4$, $RI[7675 I > 2\sigma(I)] = 0.1007$, $wR2$ (15964 refl.) = 0.3031.

References

1. Bilyk, A.; Hall, A. K.; Harrowfield, J. M.; Hosseini, M. W.; Skelton, B. W.; White, A. H. *Inorg. Chem.* **2001**, *40*, 672-686.
2. Iki, N.; Miyano, S. *J. Inclusion Phenom. Macrocyclic Chem.* **2001**, *41*, 99-105.
3. Matsumiya, H.; Terazono, Y.; Iki, N.; Miyano, S. *J. Chem. Soc., Perkin Trans. 2* **2002**, 1166-1172.
4. Bernardino, R. J.; Costa Cabral, B. J. *J. Mol. Struct. (Theochem)* **2001**, *549*, 253-260.
5. Iki, N.; Kumagai, H.; Morhashi, N.; Ejima, K.; Hasewaga, M.; Miyanari, S.; Miyano, S. *Tetrahedron Lett.* **1998**, *39*, 7559-7562.
6. Casnati, A.; Pochini, A.; Ungaro, R.; Ugozzoli, F.; Arnaud, F.; Fanni, S.; Schwing, M. J.; Egberink, R. J. M.; de Jong, F.; Reinhoudt, D. N. *J. Am. Chem. Soc.* **1995**, *117*, 2767-2777.
7. Casnati, A.; Pochini, A.; Ungaro, R.; Bocchi, C.; Ugozzoli, F.; Egberink, R. J. M.; Struijk, H.; Lugtenberg, R.; de Jong, F.; Reinhoudt, D. N. *Chem. Eur. J.* **1996**, *2*, 182-191.
8. Lamare, V.; Dozol, J. F.; Thuéry, P.; Nierlich, M.; Asfari, Z.; Vicens, J. *J. Chem. Soc., Perkin Trans. 2* **2001**, 1920-1926.
9. Grün, A.; Csokai, V.; Parlagh, G.; Bitter, I. *Tetrahedron Lett.* **2002**, *43*, 4153-4156.
10. Csokai, V.; Grün, A.; Parlagh, G.; Bitter, I. *Tetrahedron Lett.* **2002**, *43*, 7627-7629.
11. Lee, J. K.; Kim, S. K.; Bartsch, R. A.; Vicens, J.; Miyano, S.; Kim, J. S. *J. Org. Chem.* **2003**, *68*, 6720-6725.
12. Narumi, F.; Masumura, N.; Morohashi, N.; Kameyama, H.; Miyano, S. *J. Chem.*

- Soc., Perkin Trans. 1* **2002**, 1843-1844.
13. Gutsche, C. D.; Dhawan, B.; Levine, J. A.; No, K. H.; Bauer, L. J. *Tetrahedron* **1983**, *39*, 409-426.
 14. Jaime, C.; de Mendoza, J.; Prados, P.; Nieto, P. M.; Sánchez, C. J. *Org. Chem.* **1991**, *56*, 3372-3376.
 15. Lhoták, P.; Himl, M.; Stibor, I.; Petrickova, H. *Tetrahedron Lett.* **2002**, *43*, 9621-9624.
 16. Iki, N.; Narumi, F.; Fujimoto, T.; Morohashi, N.; Miyano, S. *J. Chem. Soc., Perkin Trans. 2* **1998**, 2745-2750.
 17. Akdas, H.; Mislin, G.; Graf, E.; Hosseini, M. W.; De Cain, A.; Fischer, J. *Tetrahedron Lett.* **1999**, *40*, 2113-2116.
 18. Stoikov, I. I.; Omran, O. A.; Solovieva, S. E.; Latypov, S. K.; Enikeev, K. M.; Gubaidullin, A. T.; Antipin, I. S.; Kononov, A. I. *Tetrahedron* **2003**, *59*, 1469-1476.
 19. Lang, J.; Vlach, J.; Dvoráková, H.; Lhoták, P.; Himl, M.; Hrabal, R.; Stibor, I. *J. Chem. Soc., Perkin Trans. 2* **2001**, 576-580.
 20. Weber, D.; Gruner, M.; Stoikov, I. I.; Antipin, I. S.; Habicher, W. D. *J. Chem. Soc., Perkin Trans. 2* **2000**, 1741-1744.
 21. Lhoták, P.; Kaplánek, L.; Stibor, I.; Lang, J.; Dvoráková, H.; Hrabal, R.; Sýkora, J. *Tetrahedron Lett.* **2000**, *41*, 9339-9344.
 22. Iki, N.; Morohashi, N.; Narumi, F.; Fujimoto, T.; Suzuki, T.; Miyano, S. *Tetrahedron Lett.* **1999**, *40*, 7337-7341.
 23. An attempt to synthesize a cone derivative using **9** and **2b** with NaH (4 equiv) gave poor conversion after 5 days and was therefore abandoned.
 24. The ¹H NMR spectrum of the crude reaction mixture shows the presence of an additional conformer. Due to the behavior observed for the crystals of **14a** the partial cone conformation can be excluded.
 25. Yields are low due to loss of product during column chromatography.
 26. Csokai, V.; Grün, A.; Bitter, I. *Tetrahedron Lett.* **2003**, *44*, 4681-4684.
 27. Ferguson, G.; Lough, A. J.; Notti, A.; Pappalardo, S.; Parisi, M. F.; Petringa, A. J. *Org. Chem.* **1998**, *63*, 9703-9710.
 28. Canceill, J.; Lacombe, L.; Collet, A. *Chem. Commun.* **1987**, 219-221.
 29. Scheerder, J.; Vreekamp, R. H.; Engbersen, J. F. J.; Verboom, W.; van Duynhoven, J. P. M.; Reinhoudt, D. N. *J. Org. Chem.* **1996**, *61*, 3476-3481.
 30. Methylene groups are numbered from the thiacalix[4]arene platform and the 'peak order' refers to the sequence in which resonances are found in the spectrum when moving from low- to high field.
 31. Without two distinctly different spectra of two pure conformers, or an X-ray crystal structure, it was not possible to use the crown-ether bridge peak order to assign the conformations.
 32. Cajan, M.; Lhoták, P.; Lang, J.; Dvoráková, H.; Stibor, I.; Koca, J. *J. Chem. Soc. Perkin Trans. 2* **2002**, 1922-1929.
 33. Groenen, L. C.; van Loon, J. D.; Verboom, W.; Harkema, S.; Casnati, A.; Ungaro, R.; Pochini, A.; Uguzzoli, F.; Reinhoudt, D. N. *J. Am. Chem. Soc.* **1991**, *113*, 2385-2392.
 34. Kumagai, H.; Hasegawa, M.; Miyanari, S.; Sugawa, Y.; Sato, Y.; Hori, T.; Ueda, S.;

- Kamiyama, H.; Miyano, S. *Tetrahedron Lett.* **1997**, *38*, 3971-3972
35. Sheldrick, G. M. SHELXS86 Program for crystal structure determination. University of Göttingen, Germany, 1986.
 36. Sheldrick, G. M. SHELXL-97 Program for crystal structure refinement. University of Göttingen, Germany, 1997.
 37. Spek, A. L. *J. Appl. Crystallogr.* **2003**, *36*, 7-13.

Chapter 4

Ionizable (Thia)calix[4]crowns as Highly Selective Ra^{2+} Extractants*

Abstract: The Ra^{2+} selectivity of the ionizable (thia)calix[4]crowns (**1-4**) was determined in the presence of a large excess of the most common alkali and alkaline earth cations. Selective Ra^{2+} (2.9×10^{-8} M) extraction occurs even at extremely high M^{n+}/Ra^{2+} ratios of 3.5×10^7 [$M^{n+} = Na^+, K^+, Rb^+, Cs^+, Mg^{2+}, Ca^{2+},$ and Sr^{2+} ; (1 M)] and an extractant concentration of 10^{-4} M. The selectivity coefficients $\log(K_{ex}^{Ra}/K_{ex}^M)$ are about 3.5 for Mg^{2+} , Ca^{2+} , and Sr^{2+} . In the presence of Ba^{2+} , which has very similar chemical properties to Ra^{2+} , only the thiacalix[4]crown-6 derivative **4** showed a Ra^{2+} selectivity, with a Ba^{2+}/Ra^{2+} ratio of up to 3.5×10^5 . In addition to the remarkable Ra^{2+} selectivities, the effective pH range (pH 8-13) of the thiacalix[4]crown dicarboxylic acids (**3** and **4**) allows for full regeneration of the extractants at lower pH values (pH < 6).

* Parts of this chapter have been published in: Van Leeuwen, F. W. B.; Verboom, W.; Shi, X.; Davis, J. T.; Reinhoudt, D. N. *J. Am. Chem. Soc.* **2004**, *126*, 16575-16581; Van Leeuwen, F. W. B.; Beijleveld, H.; Miermans, C. J. H.; Huskens, J.; Verboom, W.; Reinhoudt, D. N. *submitted for publication*.

4.1 Introduction

Due to the presence of large quantities of alkali¹ and alkaline earth cations^{2,3} in “produced water” streams of the TENORM generating industries, selective removal of Ra²⁺ demands highly selective Ra²⁺ extraction methods. The main challenge is the development of re-usable extractants, which have a sufficiently high Ra²⁺ selectivity and are effective in low concentrations compared to the bulk of the waste.

This chapter will focus on Ra²⁺ extractants, using the synergism of acidic groups and a crown ether, for size-dependent selectivity, brought together on a (thia)calix[4]arene platform.^{4,7} Calix[4]arene-based crown ether derivatives are known to provide highly selective extractants for a variety of cations.^{8,9} Ungaro et al.¹⁰ have previously functionalized calix[4]crown-5 with additional carboxylic acid groups to give efficient extractants (**1**) for Ca²⁺, Sr²⁺ and Ba²⁺. Chen et al.⁷ have shown that an excess of the corresponding calix[4]crown-6 dicarboxylic acid (**2**) can be used to extract Ra²⁺ effectively from a mixture of alkaline earth cations.¹¹ Extractant **2** exhibited a higher Ra²⁺ selectivity than a 16-crown-5-ether functionalized with one carboxylic acid group⁶ and a podant functionalized with two carboxylic acid moieties.⁷

An alternative to the conventional calix[4]crowns are the thiacalix[4]crowns, as described in Chapter 3.¹²⁻¹⁶ One of the differences is the increased cavity size of the thiacalix[4]arene platform, which will influence the complexation of smaller cations.^{16,17}

In this Chapter, the synthesis of the *p-tert-butylthiacalix[4]crown* dicarboxylic acids (**3** and **4**) is described. Their complexation behavior is compared with that of the calix[4]crown dicarboxylic acids (**1** and **2**; Chart 4.1). Changing the platform from a calix[4]arene (**1** and **2**) to a thiacalix[4]arene (**3** and **4**) results in significant improvements of the Ra²⁺ selectivities.

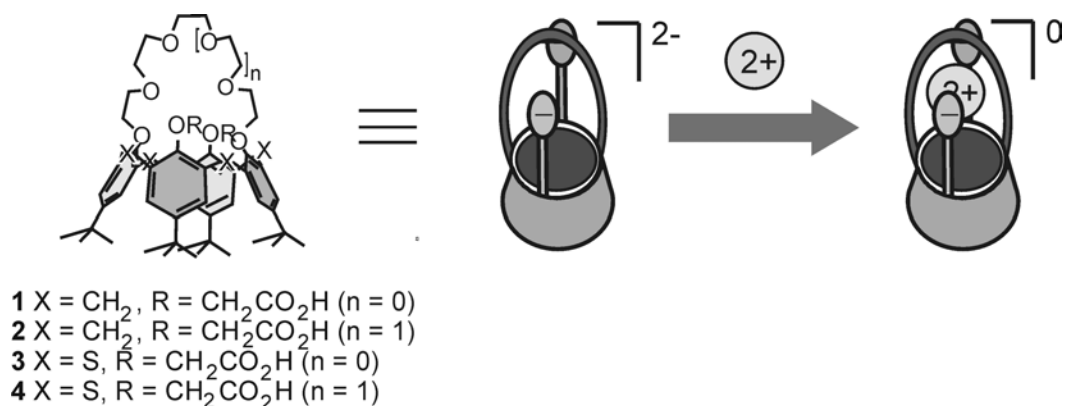
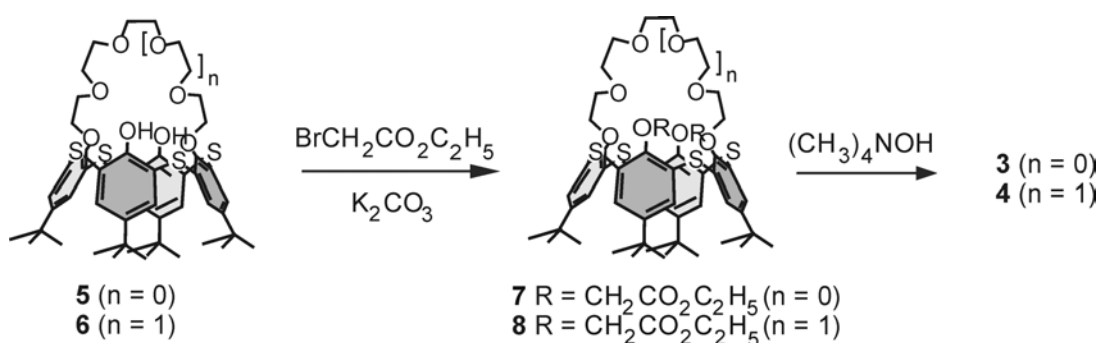


Chart 4.1

4.2 Results and Discussion

4.2.1 Synthesis

Reaction of thiacalix[4]crowns **5**¹² and **6**¹² with 2 equiv of ethyl bromoacetate in the presence of 1 equiv of K_2CO_3 gave the thiacalix[4]crown dicarboxylic esters **7** and **8** in 58% and 49% yield, respectively (Scheme 4.1). The presence two ArH and two *tert*-butyl peaks in the ^1H NMR spectra of **7** and **8** together with crown-ether bridge peak orders of (1)-(2)-(3)-(4) and (1)-(2)-(3)-(4)-(5),^{12,18} respectively, suggest the cone conformation in analogy with Chapter 3. Subsequent hydrolysis of the ethyl esters of **7** and **8** with tetramethylammonium hydroxide afforded the respective carboxylic acids **3** and **4** in near quantitative yields.



Scheme 4.1

4.2.2 Extraction of Alkali(ne Earth) Cations by (Thia)calix[4]crown Dicarboxylic Acids

The relative extraction capacities of **1**, **2**, **3**, and **4** towards the alkali and alkaline earth cations Cs^+ , Mg^{2+} , Ca^{2+} , Sr^{2+} , and Ba^{2+} were determined using non-competitive liquid-liquid extraction experiments at an equimolar salt to extractant ratio, using equal volumes of both the aqueous and the organic phase (Table 4.1).

Table 4.1. Extraction percentages [$p_M = [\text{M}^{2+}]_{\text{org}}/[\text{M}^{2+}]_{\text{tot}}$ (%)] of $^{137}\text{Cs}^+$, Mg^{2+} , Ca^{2+} , $^{90}\text{Sr}^{2+}$, and $^{133}\text{Ba}^{2+}$ at pH 8.9, determined both with tracers and Inductively Coupled Plasma-Mass Spectrometry (ICP-MS).^a

Extractant	$^{137}\text{Cs}^{+b}$ (%)	Mg^{2+} (%)	Ca^{2+} (%)	Sr^{2+} (%)	Ba^{2+} (%)
1	0.2	3	70	99	99
2	0.1	3	30	83	99
3	0.8	4	20	60	80
4	0.2	3	20	10	95

^a Non-competitive conditions, equal concentrations of [L] and $[\text{M}^{2+}]$ (10^{-4} M), in equal volumes of the organic (extractant in CH_2Cl_2 ; 1 mL) and aqueous phases (nitrate salt in pH 8.9 tris-HCl buffer; 1 mL). ^b Extraction percentages were determined by measuring the activity of the $^{137}\text{Cs}^+$ tracer in both the organic and aqueous phase.

Extraction experiments with Cs^+ showed hardly any $^{137}\text{Cs}^+$ extraction (< 1%) for all four extractants (**1-4**). Although, the size of Cs^+ (1.67- 1.88 Å),¹⁹ is similar to Ra^{2+} (1.48–1.70 Å),¹⁹ this monovalent cation does not effectively bind to the extractants **1-4**. The smallest and hardest alkaline earth cation, Mg^{2+} , gave low extraction percentages (< 5%) with all four extractants studied. In addition to a high Ca^{2+} extraction (70%), calix[4]crown-5 extractant **1** gave near-quantitative extraction of Sr^{2+} and Ba^{2+} . Increasing the crown-ether bridge to crown-6 (**2**) reduces the extraction of Ca^{2+} and Sr^{2+} to 30% and 83%, respectively. A similar reduction of the extraction of Ca^{2+} and Sr^{2+} was observed going from calix[4]arene (**1** and **2**) to thiacalix[4]arene (**3** and **4**). It is clear that extractants with two anionic groups disfavor the extraction of monovalent cations similar in size to Ra^{2+} . Furthermore, the cavity size of the (thia)calix[4]crowns influences the extraction of the smaller alkaline earth cations.

Due to its radiotoxic nature Ra^{2+} concentrations of 10^{-4} M are not desirable to work with.²⁰ For this reason Ba^{2+} was used as a model for Ra^{2+} .²¹ Solutions of $Ba(NO_3)_2$ (concentrations $0.2 - 3 \times 10^{-4}$ M), spiked with $^{133}Ba^{2+}$ tracer, were extracted with a constant extractant concentration of 10^{-4} M.

Ba^{2+} extraction percentages obtained for the extractants **1**, **2**, **3**, and **4** are close to 100% extraction for a 1:1 stoichiometry (Figure 4.1). Therefore, it is assumed that the (thia)calix[4]crowns **1-4** also bind Ra^{2+} in a 1:1 binding stoichiometry.

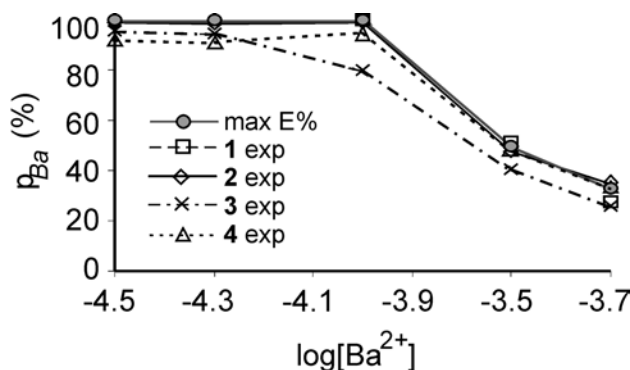


Figure 4.1. Ba^{2+} extraction percentages [$p_{Ba} = [^{133}Ba^{2+}]_{org}/[^{133}Ba^{2+}]_{tot}$ (%)] for extractants **1-4** (10^{-4} M) as a function of the $Ba(NO_3)_2$ concentration. The line through the closed circles gives the extraction percentages calculated for a 1:1 $[BaL]^0$ complex. The experiments were performed with equal volumes of the organic and aqueous phases (1 mL).

4.2.3 Precipitation of Ra^{2+}

During blank Ra^{2+} extraction experiments (no extractant present in the organic phase) performed in the presence of varying concentrations of alkali and alkaline earth metal nitrates, a deficit in detected Ra^{2+} cations, as compared to the actual amount added, was observed. Experiments showed a decrease of Ra^{2+} cations in the aqueous phase (Figure 4.2); however, Ra^{2+} cations could not be detected in the organic phase.²² This suggests that under these extraction conditions Ra^{2+} salts precipitates on the glass wall of the vials used, which would be a form of “scale/sludge formation” similar to that causing contamination of production pipes in industry (see Chapter 2). To obtain insight into the

influence of the different competing cations and their abundance on this “precipitation” of Ra^{2+} salts, reduction of the Ra^{2+} concentration ($[\text{Ra}^{2+}]_{\text{add}} = 2.9 \times 10^{-8} \text{ M}$) was monitored in the presence of varying concentrations of different salts ($M = \text{Na}^+, \text{K}^+, \text{Rb}^+, \text{Cs}^+, \text{Mg}^{2+}, \text{Ca}^{2+}, \text{Sr}^{2+}, \text{and Ba}^{2+}$).

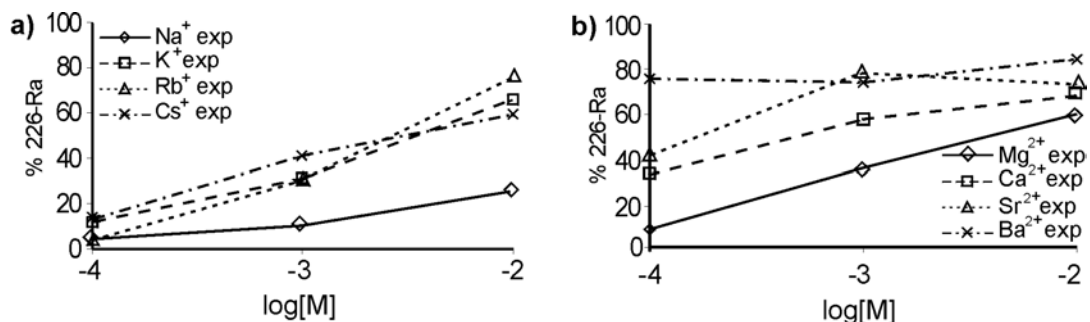


Figure 4.2. Ra^{2+} % present in aqueous solutions $[= [\text{Ra}^{2+}]_{\text{solv}}/[\text{Ra}^{2+}]_{\text{add}} (\%)]$ with varying concentrations of alkali(ne earth) cations at blank conditions. Different salt concentrations $M^n(\text{NO}_3)_n$ [(a) $M = \text{Na}^+, \text{K}^+, \text{Rb}^+, \text{and Cs}^+$; (b) $M = \text{Mg}^{2+}, \text{Ca}^{2+}, \text{Sr}^{2+}, \text{and Ba}^{2+}$] and fixed Ra^{2+} ($[\text{Ra}^{2+}]_{\text{add}} = 2.9 \times 10^{-8} \text{ M}$) concentrations were used.

Monovalent alkali cations (Figure 4.2a) gave rise to large reductions of Ra^{2+} cations in solutions with low concentrations of alkali cations ($< 10^{-3} \text{ M}$). In particular, the presence of the smallest and hardest cation (Na^+) caused a significant loss of Ra^{2+} cations, even at 10^{-2} M . The other cations ($\text{K}^+, \text{Rb}^+, \text{and Cs}^+$) gave smaller losses at concentrations of 10^{-2} M and a highly similar Ra^{2+} “precipitation” behavior.

In the case of the alkaline earth cations (Figure 4.2b), the detected reductions of $[\text{Ra}^{2+}]$ was significantly lower than that observed with the alkali cations. This may be a result of the similar chemistry of the alkaline earth cations, including Ra^{2+} . As a result Ba^{2+} , the cation most similar to Ra^{2+} , caused the smallest loss of Ra^{2+} cations. Nevertheless, the smaller and harder alkaline earth cations, viz. $\text{Mg}^{2+}, \text{Ca}^{2+}$, and to a lesser extent Sr^{2+} , showed significant “precipitation” of Ra^{2+} at the lower salt concentrations (Figure 4.2b ($\log[M] < -2$)). At salt concentrations of 10^{-2} M the “precipitation” of Ra^{2+} salts significantly decreased in all cases.

The “deficiency” data (Figure 4.2) suggest that in extraction experiments (vide infra), the actual amount of Ra²⁺ cations present in solution can be somewhat lower than the amount (2.9×10^{-8} M) of Ra²⁺ cations added. However, it was found that the extractants used (**1-4**) provide not only excellent Ra²⁺ selective extractants, but also for the greater part reduce the amount of Ra²⁺ salt precipitates.

4.2.4 Competitive Ra²⁺ Extraction Experiments in the Presence of Alkali(ne Earth) Cations

To assess the Ra²⁺ ($[^{226}\text{Ra}^{2+}] = 2.9 \times 10^{-8}$ M) extraction behavior in competition with alkali or alkaline earth cations, Ra²⁺ extractions were performed with 10^{-4} M extractant and in the presence of an excess of the competing cations Na⁺, K⁺, Rb⁺, or Cs⁺ (10^{-4} – 1 M; Figure 4.3) and Mg²⁺, Ca²⁺, Sr²⁺, or Ba²⁺ (10^{-5} – 1 M; Figures 4.4).

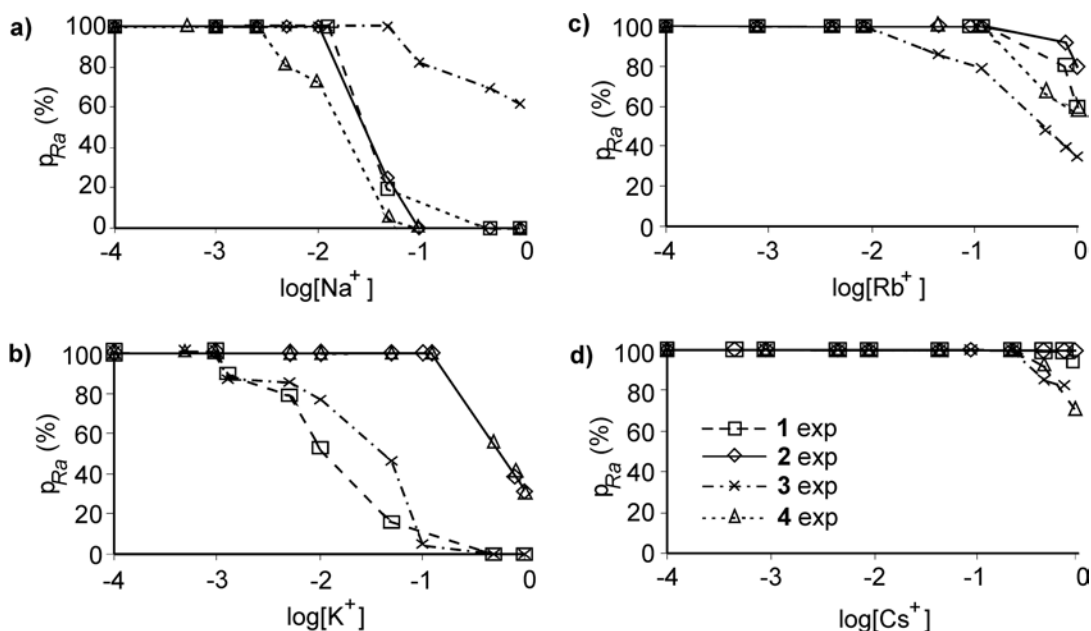


Figure 4.3. Ra²⁺ extraction percentages [$p_{\text{Ra}} = [^{226}\text{Ra}^{2+}]_{\text{org}}/[^{226}\text{Ra}^{2+}]_{\text{tot}}$ (%)] for extractants **1-4** (10^{-4} M), as a function of the M(NO₃) [$M = \text{Na}^+$ (a), K⁺(b), Rb⁺(c), and Cs⁺(d)] concentration, with 2.9×10^{-8} M Ra²⁺. The experiments were performed with equal volumes of the organic and aqueous phases (1 mL).

Competition experiments with Ra²⁺ and Na⁺ revealed that the (thia)calix[4]crown dicarboxylic acids **1**, **2**, and **4** cease to extract Ra²⁺ at 10^{-1} M Na⁺, which means at a 3.5 x

10^6 excess of Na^+ (Figure 4.3a). This suggests $[\text{2Na}^+\cdot(\text{L})^{2-}]^0$ salt formation.⁴ This is consistent with the white soapy third phase, that was observed in between the organic and aqueous phase, while all Ra^{2+} remains in solution.²³ However, the thiacalix[4]crown-5 derivative **3** extracts Ra^{2+} (~ 70%) even in the presence of 1 M Na^+ (a 3.5×10^7 excess of Na^+ compared to Ra^{2+}).

In the presence of K^+ , both crown-5 derivatives **1** and **3** ceased to extract Ra^{2+} at 10^{-1} M K^+ (Figure 4.3b). The crown-6 derivatives **2** and **4**, however, extract ~40% of Ra^{2+} even at a $\text{K}^+/\text{Ra}^{2+}$ ratio of 3.5×10^7 (1 M K^+). Apparently, both crown-5 derivatives favor the formation of neutral $[\text{2K}^+\cdot(\text{L})^{2-}]^0$ salts, whereas the crown-6 derivatives do not.

Independent of the cavity size, Rb^+ competes significantly less than K^+ for all extractants (Figure 4.3c), all four extractants still showed ~60% Ra^{2+} extraction even at 1 M Rb^+ .

The presence of Cs^+ cations does not seem to perturb the Ra^{2+} extraction, not even at a $\text{Cs}^+/\text{Ra}^{2+}$ ratio of 3.5×10^7 (Figure 4.3d), a result which is consistent with the low $^{133}\text{Cs}^+$ affinity (< 2%) found at $[\text{Cs}^+] = 10^{-4}$ M (see section 4.2.2).

In summary, the (thia)calix[4]arene derivatives **1-4** (10^{-4} M) extract Ra^{2+} in the presence of huge excesses of competing alkali cations, even up to $\text{M}^+/\text{Ra}^{2+}$ ratios of 3.5×10^7 , at 1 M of competing cations (Figure 4.3). The competition increases with the charge density of the competing cations ($\text{Cs}^+ > \text{Rb}^+ \gg \text{K}^+, \text{Na}^+$).

The experimentally obtained Ra^{2+} extraction curves, obtained with the divalent alkaline earth cations are shown in Figure 4.4. The corresponding selectivity coefficients are reported in Table 4.2.

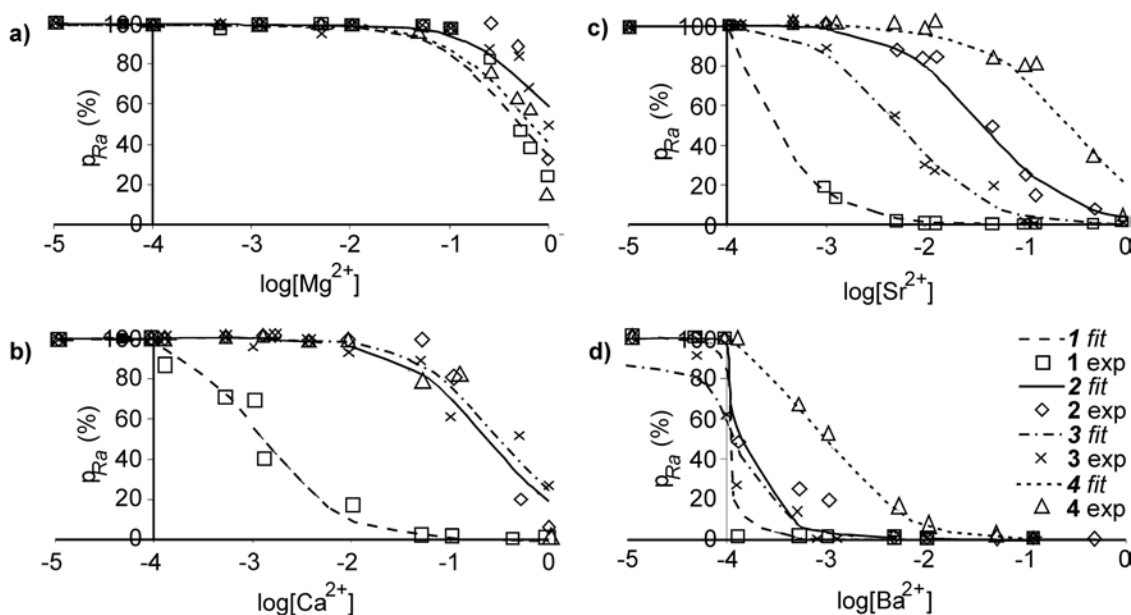


Figure 4.4. Ra²⁺ extraction percentages [$p_{Ra} = [^{226}\text{Ra}^{2+}]_{\text{org}}/[^{226}\text{Ra}^{2+}]_{\text{tot}}$ (%)] for extractants **1-4** (10^{-4} M), as a function of the $M(\text{NO}_3)_2$ [$M = \text{Mg}^{2+}$ (a), Ca^{2+} (b), Sr^{2+} (c), or Ba^{2+} (d)] concentration, with 2.9×10^{-8} M Ra²⁺. The experiments were performed with equal volumes of the organic and aqueous phases (1 mL).

Comparison of the extraction constants of the competing alkaline earth cations and of Ra²⁺ enables the quantification of the differences in extraction efficiency between the extractants **1-4**.

Since the pK_a of tris(hydroxymethyl)aminoethane (tris) is 8.1²⁴ and all the extraction experiments were performed at pH 8.9 ($[\text{tris}]_{\text{tot}} = 5.0 \times 10^{-2}$ M), $[\text{Htris}^+]_{\text{aq}} = 6.8 \times 10^{-3}$ M. Consequently, the uncomplexed ligands ($[\text{L}]_{\text{tot}} = 10^{-4}$ M) in the organic phase are assumed to exist as (Htris)₂L salts. Assuming a 1:1 complex stoichiometry (Figure 4.1), the equilibrium for the extraction of the competing divalent cations can be written as equation 1, with equation 2 describing the corresponding extraction constants.



$$K_{\text{ex}}^{\text{M}} = \frac{[\text{ML}]_{\text{org}}[\text{Htris}^+]_{\text{aq}}^2}{[\text{M}^{2+}]_{\text{aq}} [(\text{Htris})_2\text{L}]_{\text{org}}} \quad (2)$$

Because of the equal volumes used, a decrease of $[M^{2+}]_{\text{aq}}$ in the aqueous phase leads to an equal increase of $[ML]_{\text{org}}$ in the organic phase, allowing for direct comparison of the concentrations of the two phases. This results in equations 3 and 4 for the mass balances of M^{2+} and L, respectively.

$$[M^{2+}]_{\text{tot}} = [M^{2+}]_{\text{aq}} + [ML]_{\text{org}} \quad (3)$$

$$[L]_{\text{tot}} = [(H\text{tris})_2L]_{\text{org}} + [ML]_{\text{org}} \quad (4)$$

If the extraction percentages obtained for the competing cations (see Table 4.1) are incorporated as $p_M = [ML]_{\text{org}}/[M^{2+}]_{\text{tot}}$ then $[ML]_{\text{org}}$ is equal to $p_M[M^{2+}]_{\text{tot}}$, and $[M^{2+}]_{\text{aq}} = (1-p_M)[M^{2+}]_{\text{tot}}$.

The extraction percentages of M^{2+} (Table 4.1) provide single-point indications of K_{ex}^M , which allows calculation of p_M at other $[M^{2+}]_{\text{tot}}$. For Ba^{2+} , for which extraction is quantitative using the (thia)calix[4]crowns **1**, **2**, and **4** (see Table 4.1), the p_M values at other $[\text{Ba}^{2+}]_{\text{tot}}$ are based on this quantitative extraction behavior, applying the 1:1 stoichiometry found above (calculated and shown in Figure 4.1).

When the Ra^{2+} experiments, in competition with the divalent cations Mg^{2+} , Ca^{2+} , Sr^{2+} , and Ba^{2+} (Figure 4.4), are modeled, additional equilibria and mass balances have to be considered. The extraction equilibrium and its extraction constant are given in equations 5 and 6, respectively. The Ra^{2+} mass balance is given in equation 7, and the ligand mass balance (equation 4) is now expanded to equation 8.



$$K_{\text{ex}}^{\text{Ra}} = [\text{Ra}L]_{\text{org}}[H\text{tris}^+]_{\text{aq}}^2/[\text{Ra}^{2+}]_{\text{aq}}[(H\text{tris})_2L]_{\text{org}} \quad (6)$$

$$[\text{Ra}^{2+}]_{\text{tot}} = [\text{Ra}^{2+}]_{\text{aq}} + [\text{Ra}L]_{\text{org}} \quad (7)$$

$$[L]_{\text{tot}} = [(H\text{tris})_2L]_{\text{org}} + [ML]_{\text{org}} + [\text{Ra}L]_{\text{org}} \quad (8)$$

However, because of the small amount of $[\text{Ra}^{2+}]_{\text{tot}}$ (2.9×10^{-8} M), $[\text{Ra}L]_{\text{org}}$ can be neglected in equation 8. Similar to p_M for the competing cations, p_{Ra} is defined as $[\text{Ra}L]_{\text{org}}/[\text{Ra}^{2+}]_{\text{tot}}$, resulting in $[\text{Ra}L]_{\text{org}} = p_{\text{Ra}}[\text{Ra}^{2+}]_{\text{tot}}$, and $[\text{Ra}^{2+}]_{\text{aq}} = (1-p_{\text{Ra}})[\text{Ra}^{2+}]_{\text{tot}}$. Thus the $K_{\text{ex}}^{\text{Ra}}/K_{\text{ex}}^M$ ratio (equation 9) can be written as equation 10.

$$K_{\text{ex}}^{\text{Ra}}/K_{\text{ex}}^{\text{M}} = ([\text{RaL}]_{\text{org}}/[\text{Ra}^{2+}]_{\text{aq}})([\text{M}^{2+}]_{\text{aq}}/[\text{ML}]_{\text{org}}) \quad (9)$$

$$K_{\text{ex}}^{\text{Ra}}/K_{\text{ex}}^{\text{M}} = (p_{\text{Ra}}/p_{\text{M}})(1-p_{\text{M}})/(1-p_{\text{Ra}}) \quad (10)$$

Since the K_{ex}^{M} values are based on single concentrations, and because constants for some metals (Mg^{2+} , Ba^{2+}) cannot be determined accurately anyway, only $K_{\text{ex}}^{\text{Ra}}/K_{\text{ex}}^{\text{M}}$ ratios are given. These ratios are then obtained by fitting calculated p_{Ra} values to the experimentally determined values (Figure 4.4), using a non-linear least squares fitting procedure. The $\log(K_{\text{ex}}^{\text{Ra}}/K_{\text{ex}}^{\text{M}})$ ratios are given in Table 4.2.

Table 4.2 shows that the differences in Ra^{2+} selectivity of the four extractants are only evident in the case of the larger alkaline earth cations Ca^{2+} , Sr^{2+} , and Ba^{2+} , where the selectivity coefficient observed for Mg^{2+} gave an average of 4.0 for all four extractants. In the case of Ca^{2+} only the extractant with the smallest cavity, calix[4]crown-5 dicarboxylic acid (**1**), gives a relatively low selectivity coefficient (1.1), where the others maintain selectivity coefficients of about 3.4.

Table 4.2. The Ra^{2+} Selectivity Coefficients ($\log(K_{\text{ex}}^{\text{Ra}}/K_{\text{ex}}^{\text{M}})$) for the Extractants **1-4** in the Presence of Mg^{2+} , Ca^{2+} , Sr^{2+} , and Ba^{2+} cations.

Extractants	$\log(K_{\text{ex}}^{\text{Ra}}/K_{\text{ex}}^{\text{Mg}})$	$\log(K_{\text{ex}}^{\text{Ra}}/K_{\text{ex}}^{\text{Ca}})$	$\log(K_{\text{ex}}^{\text{Ra}}/K_{\text{ex}}^{\text{Sr}})$	$\log(K_{\text{ex}}^{\text{Ra}}/K_{\text{ex}}^{\text{Ba}})$
1	3.7	1.1	0.3	-1.3
2	4.2	3.4	2.6	-0.5
3	4.2	3.5	1.7	-0.5
4	3.8	3.3	3.4	+0.9

With Sr^{2+} and Ba^{2+} , the positive influences of both the larger crown-6-ether bridge size and the larger thiacalix[4]arene-cavity size on the Ra^{2+} selectivity is evident. With Sr^{2+} , the selectivities ($K_{\text{ex}}^{\text{Ra}}/K_{\text{ex}}^{\text{Ca}}$) of the crown-6 derivatives (**2** and **4**) are 212 and 52 times larger, respectively, than those of the corresponding crown-5 derivatives (**1** and **3**). Furthermore, both thiacalix[4]arene derivatives (**3** and **4**) give an improved $\text{Ra}^{2+}/\text{Sr}^{2+}$ selectivity over their parent calix[4]arene derivatives (**1** and **2**), 25- and 6-fold respectively. In the case of Ba^{2+} , thiacalix[4]crown-6 derivative **4** is the only extractant

studied that actually prefers Ra^{2+} over Ba^{2+} , exhibiting a 25-fold improvement of the Ra^{2+} selectivity compared to the known calix[4]crown-6 derivative **2**. This makes **4** the most Ra^{2+} selective of the four extractants studied; it gives Ra^{2+} extraction up to $[\text{M}^{2+}]/[\text{Ra}^{2+}]$ ratios of 3.5×10^7 for Mg^{2+} , Ca^{2+} and Sr^{2+} (1 M), and a $[\text{Ba}^{2+}]/[\text{Ra}^{2+}]$ ratio of 3.5×10^5 ($[\text{Ba}^{2+}] = 10^{-2}$ M).

4.2.5 Dissolution of Precipitated Ra^{2+} Salts

In section 4.2.3, it was demonstrated that Ra^{2+} cations have the tendency to form insoluble salts at the extraction conditions used, causing a loss of Ra^{2+} .²² In the present study only the least Ra^{2+} selective extractant, **1**, gave significant losses of Ra^{2+} at lower concentrations of the competing alkali(ne earth) cations (Figure 4.5),²⁵ making **1** less suited for Ra^{2+} extraction. However, the quantitative amount of Ra^{2+} cations present in solution in the case of the (thia)calix[4]crowns **2**, **3**, and **4**, shows that these extractants are able to fully dissolve precipitated Ra-salts, a result that further strengthens their potential as selective Ra^{2+} extractants in waste stream applications.

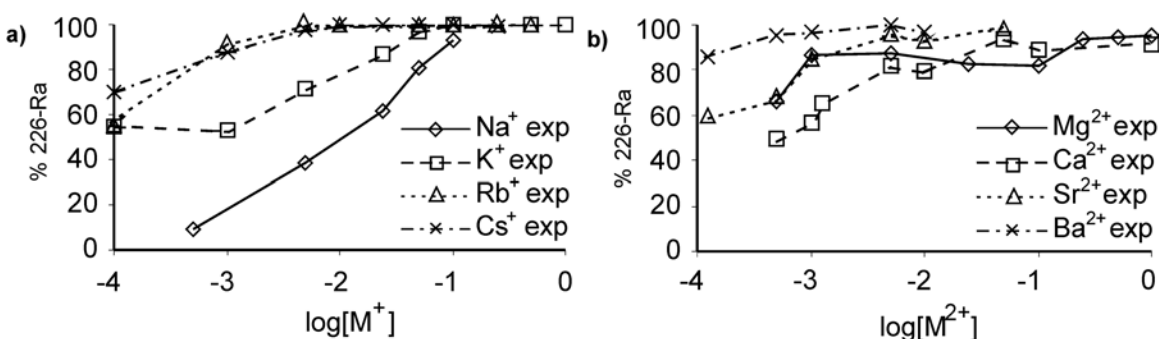


Figure 4.5. Ra^{2+} % present $[= [^{226}\text{Ra}^{2+}]_{\text{solv}}/[^{226}\text{Ra}^{2+}]_{\text{add}} (\%)]$ versus $[\text{M}^{n+}]$ after extractions with calix[4]crown-5 derivative **1**; (a) with competing alkali cations and (b) alkaline earth cations.

4.2.6 Effective pH Range of Thiacalix[4]crown-6 Dicarboxylic Acid (**4**)

Since thiacalix[4]crown-6 dicarboxylic acid (**4**) is the best overall Ra^{2+} extractant, only in this case the effective pH range was determined (Figure 4.6); because the extractants **3** and **4** are very related, differences in their pH profiles are not expected.

Thiacalix[4]crown-6 **4** still extracts Ra^{2+} above pH 11, this pH range gives an improvement over that reported for the corresponding calix[4]crown-6 derivative **2**,⁷ with which Ra^{2+} extraction ceases at pH 11. Below pH 6 the carboxylic acid groups are protonated, and consequently neutral complexes cannot be formed and Ra^{2+} extraction ceases.

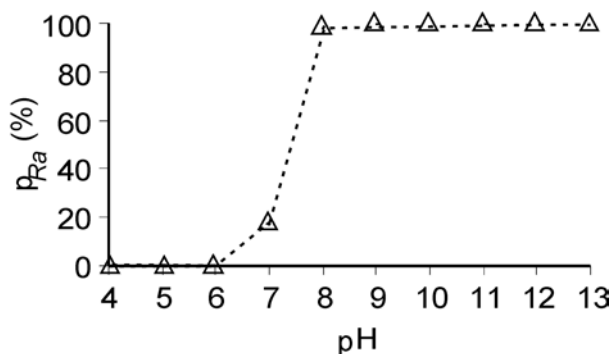


Figure 4.6. pH dependent Ra^{2+} extraction curve of thiacalix[4]crown-6 dicarboxylic acid (**4**).

4.2.7 Loading and Regeneration of Thiacalix[4]crown-6 Dicarboxylic Acid (**4**) by pH Variation

The pH dependent effectiveness of thiacalix[4]crown-6 dicarboxylic acid (**4**) allows for loading and regeneration; **4** can be loaded with Ba^{2+} above pH 7, while stripping takes place at lower pH values ($pH < 6$) (Figure 4.7).

Extraction experiments were performed with thiacalix[4]crown-6 dicarboxylic acid (**4**) (10^{-3} M) in $CDCl_3$ using a ten-fold excess of $Ba(NO_3)_2$ (10^{-2} M), so that complex formation could be accurately monitored with 1H NMR spectroscopy. The difference between the two 1H NMR spectra and the fact that in both cases the methylene hydrogens adjacent to the carboxylic acid groups only give one signal, indicate that in the Ba^{2+} -complex ($[Ba^{2+} \cdot (4)^{2-}]^0$) both carboxylic acid groups participate in the complexation of Ba^{2+} cations. Moreover, significant shifts of all the crown-ether bridge peaks indicate the full involvement of the crown-6-ether bridge in binding Ba^{2+} cations and thus suggests quantitative complex formation.

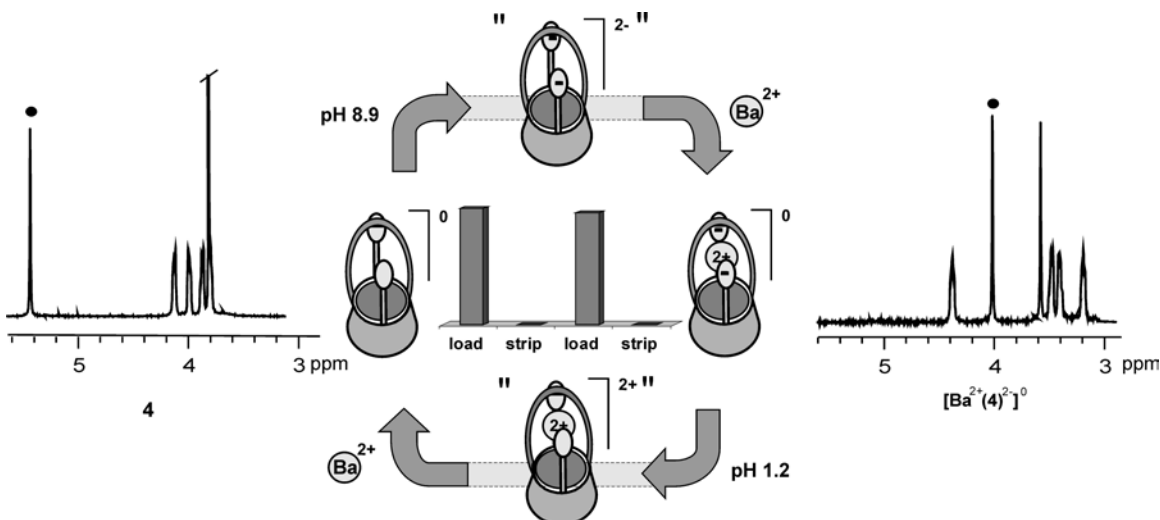


Figure 4.7. The pH dependent loading (pH 8.9) and stripping (pH 1.2) of thiacalix[4]crown-6 dicarboxylic acid (**4**). Parts of the ^1H NMR spectra of thiacalix[4]crown-6 dicarboxylic acid (**4**) (left) and its Ba^{2+} complex $[\text{Ba}^{2+}\cdot(\mathbf{4})^{2-}]^0$ (right). The COSY NMR spectra of **4** and $[\text{Ba}^{2+}\cdot(\mathbf{4})^{2-}]^0$ show no couplings for the marked peak, which indicates that it belongs to the methylene protons next to the carboxylic acid groups.

Washing the organic phase containing the $[\text{Ba}^{2+}\cdot(\mathbf{4})^{2-}]^0$ complex with water of pH 1.2 quantitatively stripped Ba^{2+} , giving free extractant **4** (Figure 4.7), while reloading the stripped organic phase again gave full conversion to $[\text{Ba}^{2+}\cdot(\mathbf{4})^{2-}]^0$. This result clearly proves the possibility to recycle thiacalix[4]crown-6 dicarboxylic acid (**4**) and thus underlines its practical applicability.

4.3 Conclusions

The thiacalix[4]crown dicarboxylic acids **3** and, in particular, **4** have significantly improved Ra^{2+} selectivities over their corresponding calix[4]crown derivatives **1** and **2**, respectively. Extremely high Ra^{2+} selectivities were found, using a 10^4 excess of $[\text{M}^{n+}]$ (M^{n+} = alkali and alkaline earth cations) to [extractant]; 3.5×10^7 excess of Na^+ , K^+ , Rb^+ , Cs^+ , Mg^{2+} , Ca^{2+} , and Sr^{2+} (1 M) and a 3.5×10^5 excess of Ba^{2+} (10^{-2} M), compared to Ra^{2+} (2.9×10^{-8} M). In addition, precipitated Ra^{2+} salts could be fully dissolved by the thiacalix[4]crowns **3** and **4**, which may suggest that these extractants can re-dissolve Ra from industrial precipitates. Consequently, thiacalix[4]crown-6 dicarboxylic acid (**4**) is

the best Ra²⁺ extractant reported so far. The obtained extremely high Ra²⁺/Mⁿ⁺ (n = 1 and 2) selectivities for common competing cations, using an excess of [Mⁿ⁺] to fully recyclable extractant, is a significant step towards the removal of Ra²⁺ cations from waste streams under waste conditions.

4.4 Experimental

4.4.1 Synthesis

General Methods. The preparation of calix[4]crown dicarboxylic acids (**1**¹⁰ and **2**⁷) was done according to literature procedures. All solvents were purified by standard laboratory procedures. All other chemicals were analytically pure and used without further purification. Acetonitrile and toluene were dried on molecular sieves, whereas dry THF was obtained by distillation over sodium. *tert*-Butylthiacalix[4]crown-5 and -6 (**5** and **6**) were prepared according to recently described procedures.^{12,26} All reactions were carried out under an inert argon atmosphere. All NMR experiments were performed in CDCl₃. MALDI-TOF experiments were performed with a dithranol matrix.

Thin-layer chromatography was performed on aluminum sheets precoated with silica gel 60 F254 (E. Merck); spots were visualized by UV-absorbency. Chromatographic separations were performed on silica gel 60 (E. Merck, 0.040-0.063 mm, 230-240 mesh) or on preparative thin layer chromatography (Silica gel 60 F₂₅₄, 2mm). Melting points are uncorrected.

MALDI-TOF mass spectra were recorded on a PerSpective Biosystem Voyager-De-RP spectrometer. ¹H NMR spectra were obtained on a Varian INOVA 300 spectrometer; ¹³C NMR spectra were obtained from a Varian Unity 400 spectrometer. Spectra were recorded at 25 °C in CDCl₃ and referenced to the (residual) solvent peak (¹³CDCl₃).

5,11,17,23-Tetra-*tert*-butyl-26,28-bis[(ethoxycarbonyl)methoxy]-2,8,14,20-tetrathiacalix[4]arene monocrown-5 (7). A suspension of **5** (420 mg, 0.48 mmol), ethyl bromoacetate (160 mg, 0.96 mmol), and K₂CO₃ (66 mg, 0.48 mmol) in CH₃CN (75 mL) was refluxed for 24 h. Subsequently, the CH₃CN was removed and the residue extracted with CH₂Cl₂ (75 mL). The solution was washed with 10% HCl (2 x 100 mL) and water (2 x 100 mL), and dried with MgSO₄. After evaporation of the solvent the residue was

purified by column chromatography (SiO₂, EtOAc/hexane 1/3) to give **7** (289 mg, 58%): mp 196-199 °C; ¹H NMR δ 7.36 (s, 4H), 7.25 (s, 4H), 5.49 (s, 4H), 4.45 (t, 4H, *J* = 6.2 Hz), 4.15 (q, 4H, *J* = 7.3 Hz), 4.12 (t, 4H, *J* = 6.2 Hz), 3.78-3.80 (m, 4H), 3.72-3.73 (m, 4H), 1.21 (t, 6H, *J* = 7.1 Hz), 1.13 (s, 18H), 1.03 (s, 18H); ¹³C NMR δ 169.9, 159.0, 157.3, 145.8, 145.4, 129.2, 129.1, 73.4, 70.6, 70.3, 69.8, 69.6, 59.9, 33.7, 33.6, 30.8, 30.7, 13.8; MALDI-TOF *m/z*: 1050.8 [M]⁺, 1072.8 [M+Na]⁺, 1088.8 [M+K]⁺, calcd. 1050.4 [M]⁺. Anal. Calcd for C₅₆H₇₄O₁₁S₄: C, 63.97; H, 7.09. Found: C, 63.57; H, 6.96.

5,11,17,23-Tetra-*tert*-butyl-26,28-bis[(ethoxycarbonyl)methoxy]-2,8,14,20-tetrathiacalix[4]arene monocrown-6 (8). A suspension of **6** (360 mg, 0.39 mmol), ethyl bromoacetate (137 mg, 0.82 mmol), and K₂CO₃ (51 mg, 0.37 mmol) in CH₃CN (120 mL) was refluxed for 64 h. Subsequently, the acetonitrile was removed and the residue extracted with CH₂Cl₂ (120 mL). The solution was washed with 10% HCl (2 x 150 mL) and water (2 x 150 mL), and dried with MgSO₄. After evaporation of the solvent the residue was purified by column chromatography (SiO₂, EtOAc/hexane 2/3) to give **8** (427 mg, 49%): mp 118-120 °C; ¹H NMR δ 7.58 (s, 4H), 7.00 (s, 4H), 4.93 (s, 4H), 4.53 (t, 4H, *J* = 7.0 Hz), 4.16-4.25 (m, 8H), 3.82-3.85 (m, 4H), 3.75-3.79 (m, 4H), 3.75 (s, 4H), 1.28 (t, 6H, *J* = 7.0 Hz), 1.25 (s, 18H), 0.91 (s, 18H); ¹³C NMR δ 169.2, 160.2, 156.9, 146.3, 146.2, 135.1, 133.0, 130.5, 128.8, 73.5, 71.9, 71.0, 70.8, 70.7, 70.0, 60.8, 34.2, 33.9, 31.3, 30.9, 14.2; MALDI-TOF *m/z*: 1094.4 [M]⁺, 1116.4 [M+Na]⁺, 1132.4 [M+K]⁺, calcd. 1094.4 [M]⁺. Anal. Calcd for C₅₈H₇₈O₁₂S₄ • 0.2 CH₂Cl₂: C, 63.59; H, 7.18. Found: C, 63.01; H, 6.96.

General Procedure for the Hydrolysis of 7 and 8. To a suspension of thiacalix[4]crown-6 dicarboxylic esters **7** or **8** in THF/H₂O (1/1) was added an excess of tetramethylammonium hydroxide (TMAH) (25%) in MeOH, whereupon the mixture was refluxed for 12 hours. The organic solvents were removed, the water layer was extracted with CH₂Cl₂ (100 mL) and washed with 10% HCl (2 x 100 mL), the organic layer was dried with MgSO₄, and the solvent was removed.

5,11,17,23-Tetra-*tert*-butyl-26,28-bis(carboxymethoxy)-2,8,14,20-tetrathiacalix[4]arene monocrown-5 (3). Reaction of **7** (773 mg, 0.74 mmol) and TMAH (7 mL) in THF/H₂O (30 mL) yielded **3** (698 mg, 95%): mp 247-250 °C; ¹H NMR δ 7.74 (s, 4H), 7.02 (s, 4H), 5.79 (s, 4H), 4.29-4.32 (m, 4H), 3.99-4.02 (m, 4H), 3.79 (q,

8H, $J = 6.0$ Hz), 1.35 (s, 18H), 0.84 (s, 18H); ¹³C NMR δ 171.2, 158.4, 157.7, 147.1, 147.0, 135.6, 134.1, 129.3, 128.0, 75.2, 70.7, 69.7, 34.4, 33.9, 31.4, 30.7; MALDI-TOF m/z : 994.1 [M]⁺, 1016.1 [M+Na]⁺, 1032.1 [M+K]⁺, calcd. 994.3 [M]⁺. Anal. Calcd for C₅₂H₆₆O₁₁S₄: C, 62.75; H, 6.68. Found: C, 62.56; H, 6.79.

5,11,17,23-Tetra-*tert*-butyl-26,28-bis(carboxymethoxy)-2,8,14,20-tetrathiacalix[4]arene monocrown-6 (4). Reaction of **8** (209 mg, 0.19 mmol) and TMAH (2 mL) in THF/H₂O (20 mL) yielded **4** (189 mg, 94%): mp 226-229 °C; ¹H NMR δ 7.75 (s, 4H), 6.94 (s, 4H), 5.43 (s, 4H), 4.11-4.13 (m, 4H), 3.98-4.00 (m, 4H), 3.86-3.89 (m, 4H), 3.81 (s, 4H), 3.78-3.79 (m, 4H), 1.35 (s, 18H), 0.85 (s, 18H); ¹³C NMR δ 170.5, 169.5, 159.2, 157.8, 147.1, 135.9, 133.3, 129.7, 128.4, 71.6, 71.0, 70.8, 70.2, 34.4, 34.0, 31.4, 30.8; MALDI-TOF m/z : 1038.1 [M]⁺, 1060.1 [M+Na]⁺, 1076.1 [M+K]⁺, calcd. 1038.4 [M]⁺. Anal. Calcd for C₅₄H₇₀O₁₂S₄: C, 62.40; H, 6.79. Found: C, 62.51; H, 6.71.

4.4.2 Extraction

Materials. Tris(hydroxymethyl)aminoethane (tris) 99.8+% was obtained from Alrich. The acids (concentrated HCl and HNO₃) and CH₂Cl₂ were of p.a. grade and used as received. The nitrate salts of K⁺ ($\geq 99.5\%$) and Rb⁺ (p.a.) were obtained from Fluka Chemie and Na⁺ (p.a.), Cs⁺ (99%), Mg²⁺ (p.a.), Ca²⁺ (p.a.), Sr²⁺ (p.a.), and Ba²⁺ (p.a.) were obtained from Acros Organics. ¹³³Ba²⁺ stock solutions were obtained from Isotope Products Europe Blaseg GmbH. ²²⁶Ra²⁺ stock solutions were purchased from AEA Technology QSA GmbH; ²²⁶Ra was used due to its long half-life ($t_{1/2} = 1.6 \times 10^3$ y). **(Note: ²²⁶Ra has a very high radiotoxicity and should be handled with care and under radionuclear supervision)**

Solutions. All basic experiments were performed using an aqueous phase with pH 8.9 (tris-HCl buffer) and an organic phase containing 10⁻⁴ M extractant in CH₂Cl₂. The different nitrate salt concentrations were obtained by diluting stock solutions to the required concentration. From a carrier free stock solution of ¹³⁷Cs⁺, a dilution of 9.8 kBq/g in 0.1 M HCl was made. From a 10 μ g Ba²⁺/mL carrier containing stock solution of ¹³³Ba²⁺ in 0.1 M HCl, a dilution of 45.18 kBq/g in water was made. From a carrier free stock solution of ²²⁶Ra²⁺ in 0.5 M HCl, a dilution of 1.2 kBq/g (1.4 x 10⁻⁶ M) in 0.1 M HNO₃ was made.

General Extraction Procedures. Equal volumes (1.0 mL) of the organic and aqueous solutions were transferred into a screw cap vial with a volume of 4 mL. The samples were shaken (1500 rpm) at ambient temperatures (22-24 °C) for 1 h to ensure complete settling of the two-phase equilibration. After extraction, the solutions were disengaged by centrifugation (1600 rpm for 5 min) and aliquots (0.5 mL) of the organic and aqueous phases were pipetted out. Experiments were performed in duplicate; average values are reported, with an estimated error of 10-15%.

ICP-MS Monitored Extraction Procedures. The solvent of the aliquot taken from the organic phase was evaporated and the residue destructed in 0.5 mL of concentrated HNO₃. The cation concentrations were measured on a Perkin-Elmer Sciex Elan 6000 ICP-MS instrument, using a Cross-flow nebulizer. The extraction percentage is defined as 100% times the ratio of cation concentration in the organic phase ($[M_o]$) and the added cation concentration ($[M_{add}]$) (eq 11).

$$E\% = 100\%([M_o]/[M_{add}]) \quad (11)$$

Non-competitive ICP-MS (Table 4.1). In the non-competitive extraction experiments the salt concentrations ($M(NO_3)_2$; $M = Mg^{2+}$, Ca^{2+} , Sr^{2+} , and Ba^{2+}) were equal to those of the extractants (10^{-4} M).²⁷

Tracer Monitored Extraction Procedures. The extraction percentages were determined using the appropriate tracer in individual $M^n(NO_3)_n$ ($M = Cs^+$, Sr^{2+} , or Ba^{2+}) solutions. In each case individual salt concentrations (10^{-4} M) were equal to that of the extractant concentration (10^{-4} M). The obtained extraction percentage are defined as 100% times the ratio of activity in the organic phase (A_o) and the total activity ($A_o + A_{aq}$) (eq 12).

$$E\% = 100\%(A_o/(A_o + A_{aq})) \quad (12)$$

¹³⁷Cs Tracer Experiments (Table 4.1). The Cs⁺ extraction percentages were determined using 20 μL of ¹³⁷Cs⁺ tracer (196 Bq; 4.6×10^{-10} M). The gamma-activity was determined using a NaI scintillation counter.

¹³³Ba Tracer Experiments (Figure 4.1). In ¹³³Ba²⁺ extraction experiments the Ba(NO₃)₂ concentration was varied slightly compared to the extractant concentration (10⁻⁴ M). But in this case, 10 μL of ¹³³Ba tracer (452 Bq; 3.6 x 10⁻¹⁰ M) were added. The gamma-activity was determined using a NaI scintillation counter.

²²⁶Ra²⁺ Extraction Procedures. In the case of the ²²⁶Ra²⁺ extraction experiments, to the aqueous phase 20 μL of ²²⁶Ra²⁺ tracer (240 Bq; 2.9 x 10⁻⁸ M) were added. The gamma-activity was determined with a Ge(Li) scintillation counter.

Competitive ²²⁶Ra²⁺ Extraction Curves (single competing cation; Figures 4.3 and 4.4; Table 4.2). In the competitive extraction experiments, aqueous phase pH 8.9 (tris-HCl), the ratio of competing Mⁿ(NO₃)_n (M = Na⁺, K⁺, Rb⁺, Cs⁺, Mg²⁺, Ca²⁺, Sr²⁺, and Ba²⁺) salt concentrations compared to a fixed extractant concentration (1 mL; 10⁻⁴ M) was altered to provide competing cation-concentration dependent extraction curves.

Precipitation Experiments (Figures 4.1 and 4.4). Extraction experiments were performed as described above, but in this case the total amount of detected ²²⁶Ra²⁺ tracer was determined. The organic phase contained no extractant (blank) or 10⁻⁴ M extractant in dichloromethane. The ²²⁶Ra²⁺ percentage is defined as 100% times the ratio of ²²⁶Ra²⁺ detected in the aqueous phase (A_{aq}) and the amount of ²²⁶Ra²⁺ added (A_{add}) (eq 13).

$$Ra\% = 100\%(A_{aq}/A_{add}) \quad (13)$$

Extraction vs. pH Curves (Figure 4.6). Experiments were performed using fixed concentrations of **4** (10⁻⁴ M) and ²²⁶Ra²⁺ (2.9 x 10⁻⁸ M). The pH values were set using different buffer solutions: pH 4-6: HCl, pH 7-10: tris-HCl, and pH 10-13: tris-(CH₃)₃NOH.

¹H NMR Monitored Loading and Stripping Experiments (Figure 4.7). Loading experiments (30 min) were performed with **4** (3 mL; 10⁻³ M) in CDCl₃ and a ten-fold excess of Ba(NO₃)₂ (10⁻² M) in water at pH 8.9 (tris-HCl) so that complex formation could be monitored via ¹H NMR spectroscopy of a 1 mL sample of the organic phase. Removing the aqueous phase, followed by adding a strip solution at pH 1.2 (HCl) allowed for full regeneration of the starting material, which followed from the ¹H NMR spectrum determined with ¹H NMR of a 1 mL aliquot, after shaking for 15 min.

References

1. Whaley, T. P. in *Comprehensive Inorganic Chemistry Vol. 1*; Bailar, J. C.; Emelús, H. J.; Nylom, Sir R.; Trotman-Dickenson, A. F. (Eds), 1th ed., Pergamon Press: New York, **1973**, p. 36.
2. Wiegand, J.; Feige, S. *Origin of Radium in High-Mineralized Waters* IAEA; Vienna, 2002.
3. Bostick, D. T.; Luo, H.; Hindmarsh, B. *Characterization of Soluble Organics in Produced water*; ORNL/TM-2001/78, 2001.
4. McDowell, W. J.; Arndsten, B. A.; Case, G. N. *Solvent Extr. Ion Exch.* **1989**, *7*, 377-393.
5. Dietz, M. L.; Chiariza, R.; Horwitz, E. P. *Anal. Chem.* **1997**, *69*, 3028-3037.
6. Beklemishev, M. K.; Elshani, S.; Wai, C. M. *Anal. Chem.* **1994**, *66*, 3521-3527.
7. Chen, X. Y.; Ji, M.; Fisher, D. R.; Wai, C. M. *Inorg. Chem.* **1999**, *38*, 5449-5452.
8. Casnati, A.; Pochini, A.; Ungaro, R.; Ugozzoli, F.; Arnaud, F.; Fanni, S.; Schwing, M. J.; Egberink, R. J. M.; de Jong, F.; Reinhoudt, D. N. *J. Am. Chem. Soc.* **1995**, *117*, 2767-2777.
9. Casnati, A.; Pochini, A.; Ungaro, R.; Bocchi, C.; Ugozzoli, F.; Egberink, R. J. M.; Struijk, H.; Lugtenberg, R.; de Jong, F.; Reinhoudt, D. N. *Chem. Eur. J.* **1996**, *2*, 182-191.
10. Ungaro, R.; Pochini, A.; Andreetti, G. D. *J. Inclusion Phenom. Macrocyclic Chem.* **1984**, *2*, 199-206.
11. This compound has been used as reference compound, due to the impressive results reported by Chen et al.¹² However, in order to directly compare its Ra²⁺ extraction data to that of the other extractants, the extraction behavior of this known Ra²⁺ extractant has been studied more extensively, and under different conditions as previously reported.
12. Chapter 3 and Van Leeuwen, F. W. B.; Beijleveld, H.; Kooijman, H.; Spek, A. L.; Verboom, W.; Reinhoudt, D. N. *J. Org. Chem.* **2004**, *69*, 3928-3936.
13. Bilyk, A.; Hall, A. K.; Harrowfield, J. M.; Hosseini, M. W.; Skelton, B. W.; White, A. H. *Inorg. Chem.* **2001**, *40*, 672-686.
14. Iki, N.; Miyano, S. *J. Inclusion Phenom. Macrocyclic Chem.* **2001**, *41*, 99-105.
15. Matsumiya, H.; Terazono, Y.; Iki, N.; Miyano, S. *J. Chem. Soc., Perkin Trans. 2* **2002**, 1166-1172.
16. Bernardino, R. J.; Costa Cabral, B. J. *J. Mol. Struct. (Theochem)* **2001**, *549*, 253-260.
17. Lamare, V.; Dozol, J. F.; Thuéry, P.; Nierlich, M.; Asfari, Z.; Vicens, J. *J. Chem. Soc., Perkin Trans. 2* **2001**, 1920-1926.
18. The crown-ether bridge methylene peaks are counted from the thiacalix[4]arene platform (see Chapter 3). The conformations have been verified by NOESY NMR spectra of **3** and **4**.
19. Shannon, R. D. *Acta Cryst. A* **1976**, *32*, 751-767.
20. A concentration of 10⁻⁴ M Ra²⁺ corresponds to an activity of 8.3 GBq.
21. Moon, D. S.; Burnett, W. C.; Nour, S.; Horwitz, P.; Bond, A. *Appl. Rad. Isot.* **2003**, *59*, 255-262.
22. McDowell et al.⁴ suggested that Ra²⁺ cations could be lost by precipitation with metal hydroxides. Solubility products of M(OH)₂ salts, in the alkaline earth cation series, decrease in the order Ba²⁺(3.2 x 10⁻¹ M) > Sr²⁺ (2.5 x 10⁻¹ M) > Ca²⁺(3.0 x 10⁻²

M)[>] Mg²⁺ (4.1 x 10⁻⁴ M), which is in line with the Ra²⁺ (%) found (Figure 4.2b). Furthermore, precipitation of RaCl₂ (below 0.7 x 10⁻³ [M²⁺] the tris-HCl buffer causes an excess of Cl⁻ anions) seems unlikely to cause the loss of Ra²⁺ since the solubility product of RaCl₂ is 0.87 M. Goodenough, R.D.; Stenger, V.A. in *Comprehensive Inorganic Chemistry Vol. 1*; Bailar, J. C.; Emeléus, H. J.; Nylom, Sir R.; Trotman-Dickenson, A. F. (Eds), 1th ed., Pergamon Press: New York, **1973**, p. 625.

23. Calix[4]crown-5 dicarboxylic acid (**1**) showed a loss of ²²⁶Ra²⁺ cations, a result that is discussed further along this paper.
24. Kearns, A.; Cole, L.; Haws, C. R.; Evans, D. E. *Plant Physiol. Biochem.* **1998**, *36*, 879-887.
25. Since the concentration of [RaL]_{org} can be neglected in equation 7, and the selectivity coefficient is not influenced by the fact that p_{Ra} is determined by $[\text{RaL}]_{\text{org}}/([\text{RaL}]_{\text{org}} + [\text{Ra}^{2+}]_{\text{aq}})$, rather than $[\text{RaL}]_{\text{org}}/[\text{Ra}^{2+}]_{\text{tot}}$. The precipitation of Ra²⁺ salts does not influence the selectivity coefficients obtained (Table 4.2).
26. Bitter I.; Csokai V. *Tetrahedron Lett.* **2003**, *44*, 2261-2265.
27. The isotope ⁴³Ca was corrected for the interference of the doubly charged isotope ⁸⁸Sr.

Chapter 5

Thiacalix[4]arene Derivatives as Ra^{2+} Extractants: a Systematic Study on the Requirements for ${}^2\text{Ra}^{2+}$ Extraction*

Abstract: The synthesis and NOE-based structural characterization of thiacalix[4]arene tricarboxylic acid (**7**), thiacalix[4]crown-5 and -6 monocarboxylic acids (**2** and **5**), and the bis(N-methylsulfonyl)thiacalix[4]crowns-5 and -6 (**4a,b**) is described. The Ra^{2+} selectivity coefficients, $\log (K_{\text{ex}}^{\text{Ra}}/K_{\text{ex}}^{\text{M}})$, of the new thiacalix[4]arene derivatives are compared directly with those of thiacalix[4]crown-5 and -6 (**1a,b**), thiacalix[4]crown-5 and -6 dicarboxylic acids (**3a,b**), and thiacalix[4]arene di- and tetracarboxylic acid (**6** and **8**). Thiacalix[4]arene dicarboxylic acid (**6**) already exhibits a high Ra^{2+} selectivity, but this is significantly improved in the case of **3b**, having an additional crown-(6-)ether bridge. The covalent combination of a crown ether and carboxylic acid substituents as in the thiacalix[4]arenes **2**, **3a,b**, **4a,b**, and **5** gives a better Ra^{2+} selectivity in the presence of Sr^{2+} or Ba^{2+} than mixtures of dibenzo-21-crown-7 and thiacalix[4]arene dicarboxylic acid (**6**) or of pentadecanoic acid and thiacalix[4]crown-6 (**1b**).

* This chapter has been submitted for publication: Van Leeuwen, F. W. B.; Beijleveld, H.; Velders, A. H.; Huskens, J.; Verboom, W.; Reinhoudt, D. N.

5.1 Introduction

In order to transfer Ra^{2+} efficiently from an aqueous into an organic medium, the extractant needs to neutralize the divalent cation and to meet its coordination preference (see Chapter 2).¹ In a recent study by Hendriksen et al.² aminocarboxylic acids,³ tetraazacyclododecane tetracetic acid, and calix[4]arene tetracarboxylic acid have been used for Ra^{2+} extraction. However, most work on Ra^{2+} extraction is focused on so-called synergistic extraction, using mixtures of crown ethers and an acid for neutralization.^{1,4-9} Alternatively, Bartsch et al.¹⁰ functionalized crown ethers with acidic groups.¹¹⁻¹³ In Chapter 4 the excellent Ra^{2+} complexation properties of the thiacalix[4]crown dicarboxylic acids (**3a,b**) are reported.¹⁴

In this chapter a systematic study of the influence of the different structural elements of thiacalix[4]crown dicarboxylic acids on the Ra^{2+} selectivity is described. The following structural variations were studied: (i) the crown ether size, (ii) the number and type of acidic groups, and (iii) the covalent attachment of acidic groups vs. mixtures of ligands and acids (Chart 5.1). Finally, the synthesis of new trisubstituted thiacalix[4]arenes is described.

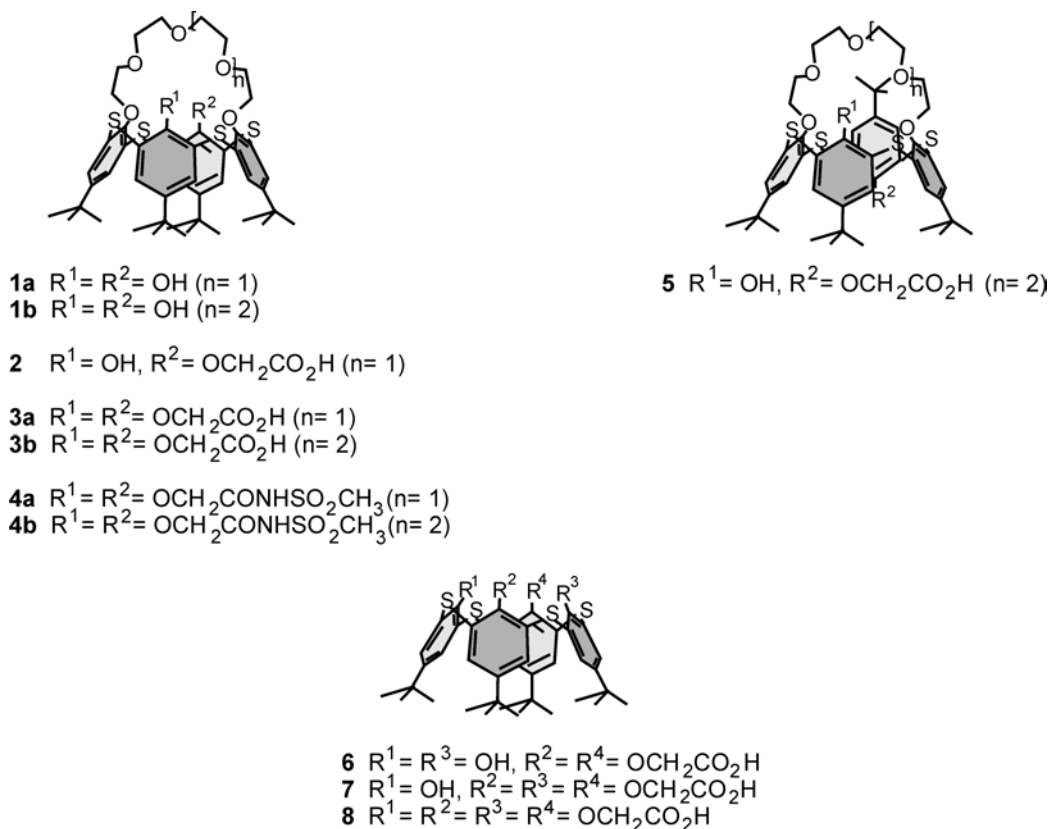
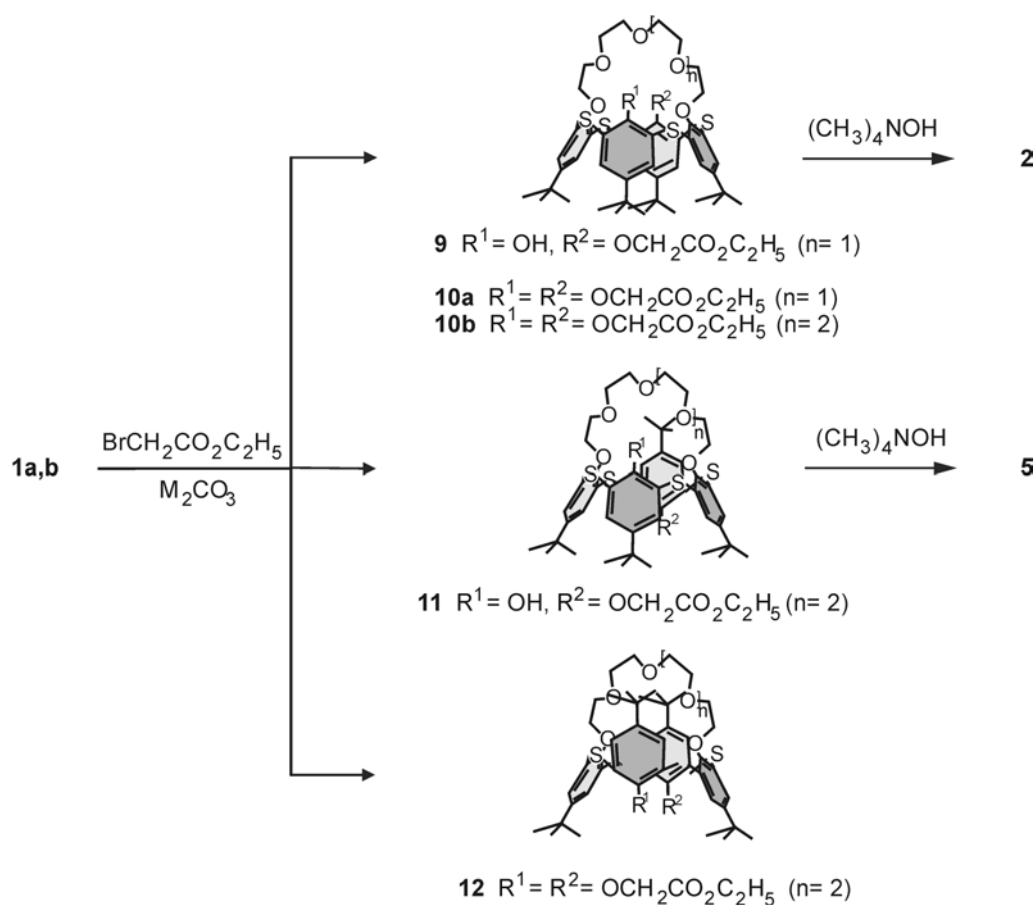


Chart 5.1

5.2 Results and Discussion

5.2.1 Synthesis and Characterization of Extractants 2-8



Scheme 5.1

The thiacalix[4]crown monocarboxylic acids (**2** and **5**) were synthesized starting from dihydroxy thiacalix[4]crowns **1a,b** (Scheme 5.1). Reaction of thiacalix[4]crown-5 (**1a**)^{15,16} with ethyl bromoacetate in the presence of Na_2CO_3 (0.5 equiv) in refluxing acetonitrile for 64 h gave a mixture of unreacted **1a** (~30%), cone thiacalix[4]crown-5 monoethyl ester (**9**), and cone thiacalix[4]crown-5 diethyl ester (**10a**) (~10%).¹⁷ From this mixture, **9** was isolated in 59% yield. The corresponding reaction of thiacalix[4]crown-6 (**1b**)¹⁶ using K_2CO_3 (2 equiv) as a base gave a mixture of cone thiacalix[4]crown-6 diethyl ester (**10b**),¹⁴ partial cone thiacalix[4]crown-6 monoethyl ester **11**, and the 1,3-alternate thiacalix[4]crown-6 diethyl ester (**12**) (~10%),¹⁶ from which **10b** and **11** were isolated in 38% and 19% yield, respectively.¹⁸

Hydrolysis of the esters **9** and **11** with tetramethylammonium hydroxide afforded the thiacalix[4]crown monocarboxylic acids (**2** and **5**) in 81% and 85% yield,

respectively. The thiacalix[4]crown dicarboxylic acids (**3a,b**) were prepared as described in Chapter 4.¹⁴

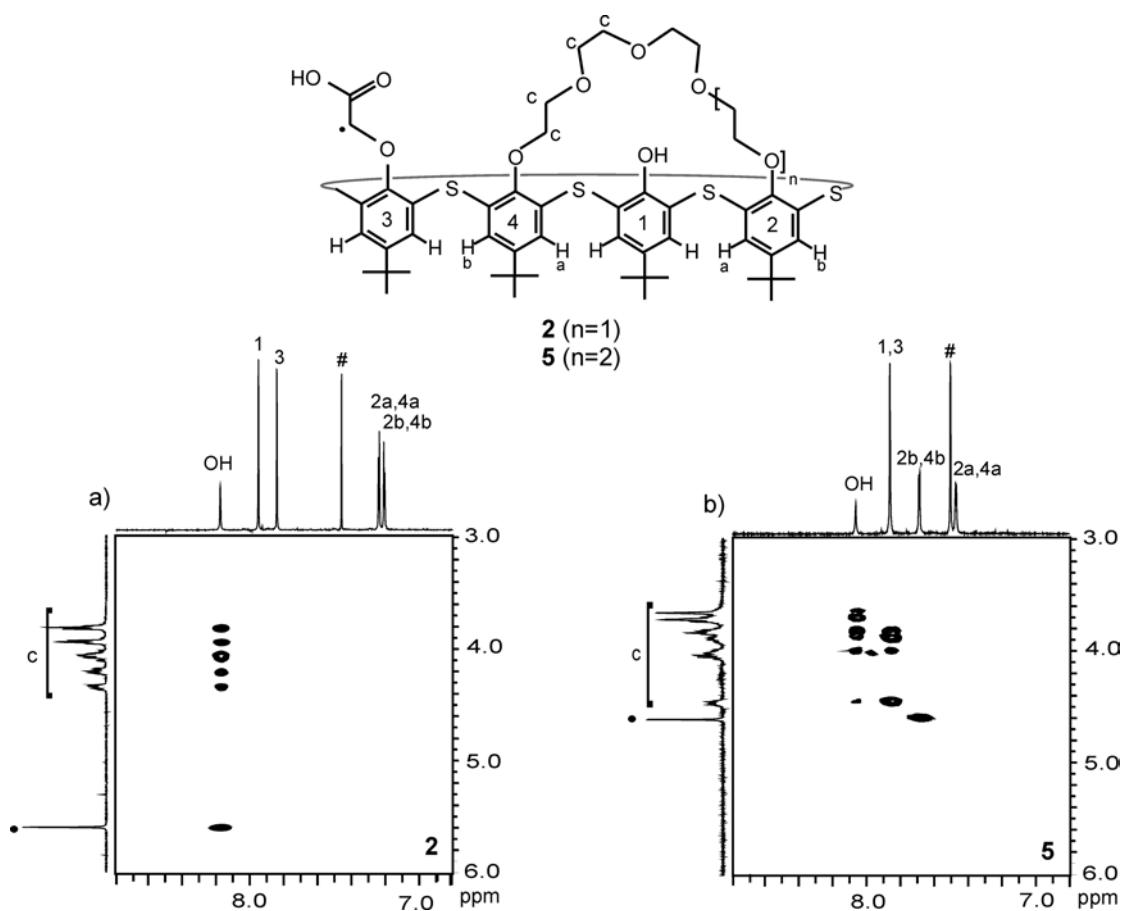
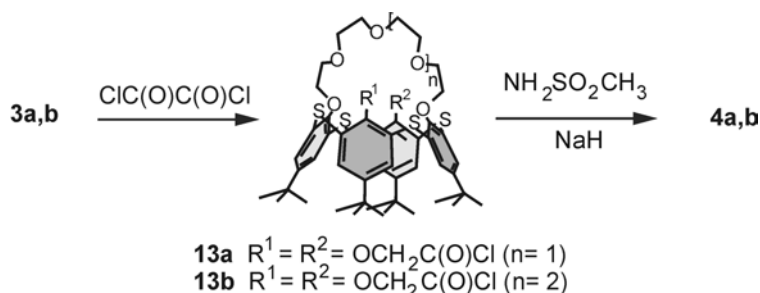


Figure 5.1. ROESY (a) and NOESY (b) spectra of the thiacalix[4]crown monocarboxylic acids [**2**; cone; and **5**; partial cone], respectively, in CDCl₃ at 25 °C. The resonances of CHCl₃ are indicated with #.

In their ¹H NMR spectra, the thiacalix[4]crown monocarboxylic acids (**2** and **5**) show two singlets and two doublets for the ArH peaks of which the two singlets in **5** overlap (Figure 5.1b). On the basis of the symmetry the doublets can be assigned to the ArH2a/ArH4a and ArH2b/ArH4b protons of the crown-ether bridge containing aryl groups, while the protons of the other two aryl groups (ArH1a,b and ArH3a,b) give singlets. A significant difference in the ¹H NMR spectra of **2** and **5** (the relative shifts of the ArH2b/ArH4b resonances) points to a difference in conformation. The conformations of **2** and **5** have unambiguously been determined via ROESY and NOESY NMR spectroscopy (Figure 5.1).¹⁹

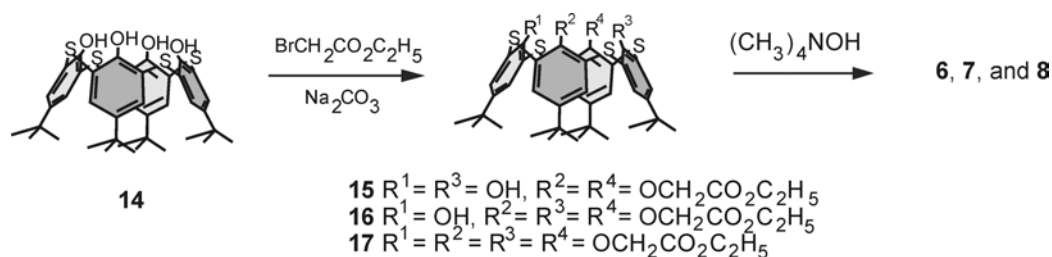
Most characteristic for thiacalix[4]crown-5 monocarboxylic acid (**2**) is the presence of NOE cross peaks between the OH resonance with both methylene resonances of the crown-ether bridge and that of the methylene group adjacent to the carboxylic acid moiety (see Figure 5.1a). This indicates that thiacalix[4]crown-5 monocarboxylic acid (**2**) is in the cone conformation.

NOESY experiments performed on the thiacalix[4]crown-6 monocarboxylic acid (**5**) revealed strong couplings between the methylene protons next to the carboxylic acid moiety and the ArH2b/ArH4b protons (Figure 5.1b).²¹ The ArH3 peak²⁰ shows NOE interactions with the crown-ether bridge, while the ArH1 peak interacts with the ArH2a/ ArH4a peak (not shown in Figure 5.1b).²¹ Furthermore, the OH resonance shows NOESY couplings with the protons of the crown-ether bridge, but not with the methylene protons adjacent to the carboxylic acid moiety (see Figure 5.1b). All these NOE interactions indicate that compound **5** has the partial-cone conformation, in which the carboxylic acid group is situated on the opposite side of both the crown-ether bridge and the OH group.



Scheme 5.2

The cone thiacalix[4]crown bis(methylsulfonyl carboxamides) (**4a,b**) were prepared in 58% and 60% yield, respectively, by reaction of the corresponding cone crown dicarboxylic acids **3a,b** (see Chapter 4) with 2.5 equiv of oxalyl chloride to give the acid chlorides **13a,b**, followed by reaction with 2.5 equiv of methanesulfonamide in the presence of 10 equiv of NaH in THF (Scheme 5.2). The formation of **4a,b** clearly followed from the presence of characteristic signals for the methylsulfonyl groups at δ 3.19 and 3.24 ppm, respectively, in the ^1H NMR spectra.



Scheme 5.3

For comparison, the thiacalix[4]arene di- (**6**),²² tri- (**7**), and tetracarboxylic acids (**8**)²² were synthesized. Reaction of thiacalix[4]arene (**14**) with 3 equiv of ethyl bromoacetate in the presence of 1.5 equiv of Na_2CO_3 in acetone gave a mixture of the esters **15-17** (Scheme 5.3), from which **16** was obtained in 7% yield. Subsequent hydrolysis of the ester groups in **16** with tetramethylammonium hydroxide gave thiacalix[4]arene tricarboxylic acid **7** in 92% yield.

Indicative for the cone conformation of **16** are the NOE couplings between the four ArH resonances and the NOE couplings between the -OH resonance and all three the - OCH_2CO_2 - methylene resonances, which were similar to those observed for the cone thiacalix[4]crown-5 monocarboxylic acid (**2**) (see Figure 5.1a).²³

5.2.2 The Role of Covalently Attached Carboxylic Acid Groups

It is not a priori obvious that the covalent combination of carboxylic acids and the thiacalix[4]crown-6 platform (**3b**) binds Ra^{2+} better than a mixture of the thiacalix[4]crown-6 (**1b**) with pentadecanoic acid or of thiacalix[4]arene dicarboxylic acid (**6**) with dibenzo-21-crown-7. Therefore, the Ra^{2+} extraction behavior of the different systems was studied in standard competition experiments in the presence of an excess of Ca^{2+} , Sr^{2+} , or Ba^{2+} ($10^{-4} - 1 \text{ M}$; Figure 5.2).²⁴ The experiments were performed using equal volumes of the organic and aqueous phases.

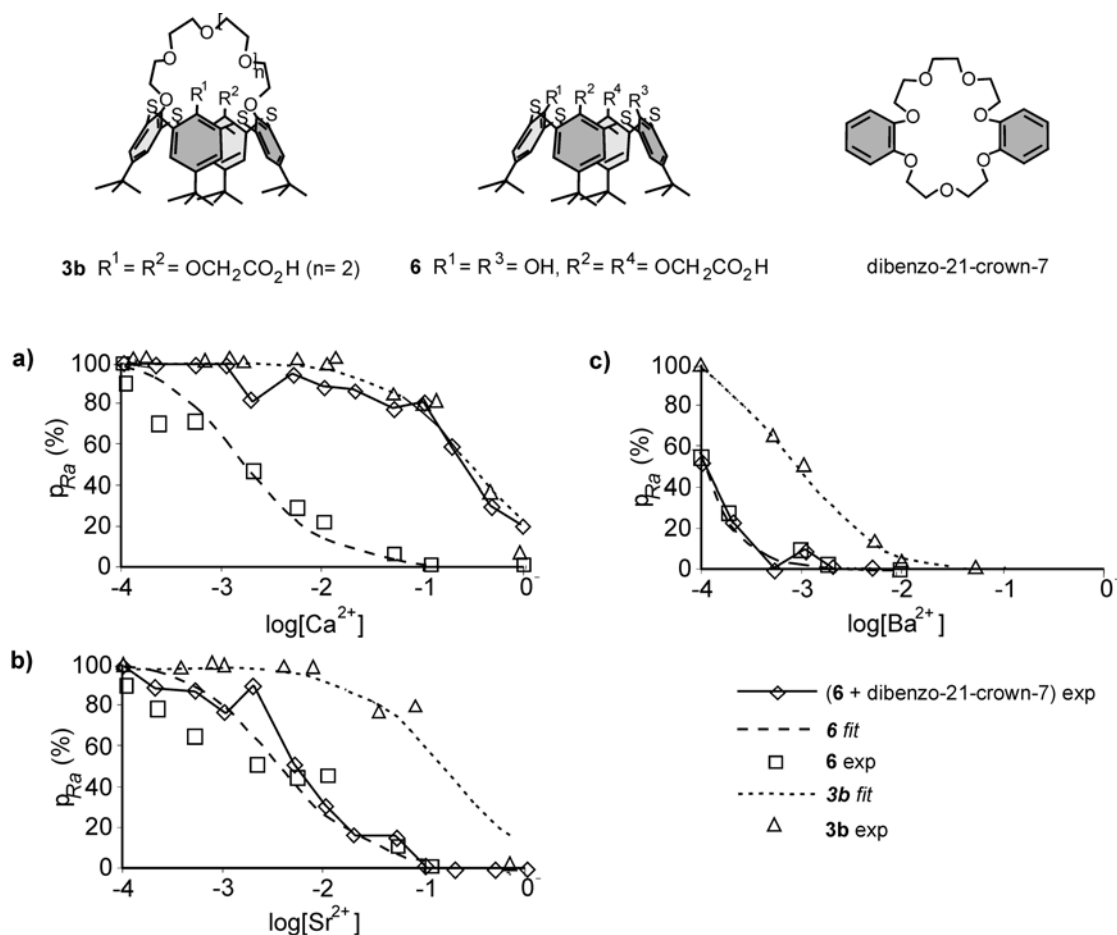


Figure 5.2. Ra^{2+} extraction percentages [$p_{\text{Ra}} = [\text{Ra}^{2+}]_{\text{org}}/[\text{Ra}^{2+}]_{\text{tot}}$ (%)] for different ratios of extractant [$L = \mathbf{3b}$, $\mathbf{6}$, and $\mathbf{6} + \text{dibenzo-21-crown-7}$] to $\text{M}(\text{NO}_3)_2$ [$\text{M}^{2+} = \text{Ca}^{2+}$ (a), Sr^{2+} (b), or Ba^{2+} (c)], and fixed extractant ($[\mathbf{3b}] = [\mathbf{6}] = [\text{dibenzo-21-crown-7}] = 10^{-4}$ M; 1 mL of CH_2Cl_2), and $[\text{Ra}^{2+}]_{\text{tot}}$ (2.9×10^{-8} M; pH 8.9 tris-HCl) concentrations.

Figure 5.2 shows that dibenzo-21-crown-7, a crown ether known for its optimal crown-cavity¹ to Ra^{2+} radius²⁵ fit, only improves the Ra^{2+} selectivity of the thiacalix[4]arene dicarboxylic acid (**6**) in the presence of Ca^{2+} cations. For Ca^{2+} the Ra^{2+} extraction curve of this mixture is identical to that of thiacalix[4]crown-6 dicarboxylic acid (**3b**;¹⁴ Figure 5.2a). (Dibenzo-)21-crown-7-ethers clearly favor binding of Ra^{2+} over Ca^{2+} , a result that agrees with data published by Chiarizia et al.⁷ In the presence of Sr^{2+} and Ba^{2+} there is no influence of dibenzo-21-crown-7 on the Ra^{2+} extraction by **6** (Figure 5.2b and c). These data support the literature results,^{4,7} where it is demonstrated that when the radius of the competing cations²⁵ increases, the influence of a 21-crown-7 ether on the Ra^{2+} selectivity diminishes in a synergistic

mixture with acids ($\text{Ca}^{2+} \gg \text{Sr}^{2+} > \text{Ba}^{2+}$). Nevertheless, thiacalix[4]crown-6 dicarboxylic acid (**3b**)¹⁴ still allows for separation of Ra^{2+} from Sr^{2+} and Ba^{2+} . These results clearly show the improved Ra^{2+} selectivity of thiacalix[4]crown-6 dicarboxylic acid (**3b**) over a mixture of thiacalix[4]arene dicarboxylic acid (**6**) and dibenzo-21-crown-7.

The other combination, thiacalix[4]crown-6 (**1b**) and two equiv of pentadecanoic acid,²⁶ did not extract Ra^{2+} ion in competition with Ca^{2+} , Sr^{2+} , and Ba^{2+} .²⁷ So it can be concluded that the mixture of thiacalix[4]arene dicarboxylic acid (**6**) and dibenzo-21-crown-7 is far more Ra^{2+} selective than the mixture of thiacalix[4]crown-6 (**1b**) and pentadecanoic acid.

5.2.3 Ra^{2+} Extraction by Thiacalix[4]arene Derivatives **3**, **3a,b**, **4a,b**, **5**, **6**, **7**, and **8**.

The influence of the different structural elements of thiacalix[4]crown dicarboxylic acids, on the Ra^{2+} selectivity was determined based on the extraction behavior of thiacalix[4]crown monocarboxylic acids (**2** and **5**), thiacalix[4]crown dicarboxylic acids (**3a,b**), thiacalix[4]crown bis(methylsulfonyl) carboxamides (**4a,b**), thiacalix[4]arene dicarboxylic acids (**6**), thiacalix[4]arene tricarboxylic acid (**7**), and thiacalix[4]arene tetracarboxylic acid (**8**). First the extraction strengths of the alkaline earth cations Ca^{2+} , Sr^{2+} , and Ba^{2+} by these extractants were determined using both inductively coupled plasma-mass spectrometry (ICP-MS) and radiotracers.

The extraction constants (K_{ex}^{M}) of the competing cations Ca^{2+} , Sr^{2+} , and Ba^{2+} were obtained by a non-linear least squares fitting procedure with five experimental points in the range of $(0.2 - 5) \times 10^{-4}$ M of M^{2+} cations (Table 5.1). The complete models and extraction curves are given in the appendix of this chapter.

For the thiacalix[4]crown monocarboxylic acids **2** and **5** the extraction curves obtained for Ca^{2+} , Sr^{2+} , and Ba^{2+} suggest a 1:1 complex stoichiometry. Consequently, the extraction constant of M^{2+} (Ca^{2+} , Sr^{2+} , and Ba^{2+}) can be expressed as in equation 1.

$$K_{\text{ex}}^{\text{M}} = \frac{[\text{MLX}]_{\text{org}}[\text{Htris}^+]_{\text{aq}}}{[\text{M}^{2+}]_{\text{aq}}[\text{HtrisL}]_{\text{org}}[\text{X}^-]_{\text{aq}}} \quad (1)$$

For the extractants with two or three carboxylic acids **3a,b**,¹⁴ **4a,b**, **6**, and **7**, the 1:1 complex stoichiometry was determined in the same way. The extraction constant of M^{2+} can be expressed as in equation 2.¹⁴

$$K_{\text{ex}}^{\text{M}} = [\text{ML}]_{\text{org}}[\text{Htris}^+]_{\text{aq}}^2/[\text{M}^{2+}]_{\text{aq}}[(\text{Htris})_2\text{L}]_{\text{org}} \quad (2)$$

The Ca²⁺, Sr²⁺, and Ba²⁺ extraction data of thiacalix[4]arene tetracarboxylic acid (**8**) suggests a 1:2 (ML₂) complex stoichiometry. Consequently, the extraction constant of M²⁺ is expressed as in equation 3.

$$K_{\text{ex}}^{\text{M}} = [\text{M}((\text{Htris}^+)_3\text{L})_2]_{\text{org}}[\text{Htris}^+]_{\text{aq}}^2/[\text{M}^{2+}]_{\text{aq}}[(\text{Htris})_4\text{L}]_{\text{org}}^2 \quad (3)$$

Since the extraction constants (K^M_{ex}) reported in Table 5.1 do not have the same dimensions, a direct comparison between the K^M_{ex} values of the different extractants is not possible.

Table 5.1. Extraction constants^a of extractants **2**, **3a,b**, **4a,b**, **5**, **6**, **7**, and **8**.^{28,29}

Extractant	K ^{Ca} _{ex}	K ^{Sr} _{ex}	K ^{Ba} _{ex}
2	3.8 x 10 ⁴ M ⁻¹	3.2 x 10 ⁴ M ⁻¹	3.7 x 10 ⁴ M ⁻¹
5	1.2 x 10 ⁴ M ⁻¹	< 6.5 x 10 ² M ⁻¹ ^b	< 1.0 x 10 ³ M ⁻¹ ^b
3a	1.2 M	3.7 M	23 M
3b	< 9.5 x 10 ⁻¹ M ^b	1.9 x 10 ⁻¹ M	> 50 M ^c
4a	1.2 M	< 3.2 x 10 ⁻¹ M ^b	2.0 M
4b	1.0 M	< 6.5 x 10 ⁻² M ^b	< 5.7 x 10 ⁻¹ M ^b
6	21 M	7.2 x 10 ¹ M	23 M
7	54 M	5.8 M	6.0 M
8	7.6 x 10 ³	1.6 x 10 ⁷	2.1 x 10 ⁶

^a Liquid-liquid extractions with extractant (10⁻⁴ M; 1 mL of CH₂Cl₂) and M(NO₃)₂ salts (M²⁺ = Ca²⁺, Sr²⁺, and Ba²⁺; (0.2 - 5) x 10⁻⁴ M; 1 mL of pH 8.9 tris-HCl buffer). ^b This value indicates an upper limit, due to the very low extraction percentages obtained. ^c This value indicates a lower limit, due to the very high extraction percentages obtained.

With the stoichiometries and K_{ex}^{M} values of the different extractants, the Ra^{2+} selectivity coefficients were determined from competition experiments performed under standard conditions (see above). Representative Ra^{2+} extraction curves are depicted in Figure 5.2 (6) and Figure 5.3 (2, 3a,b, and 5).

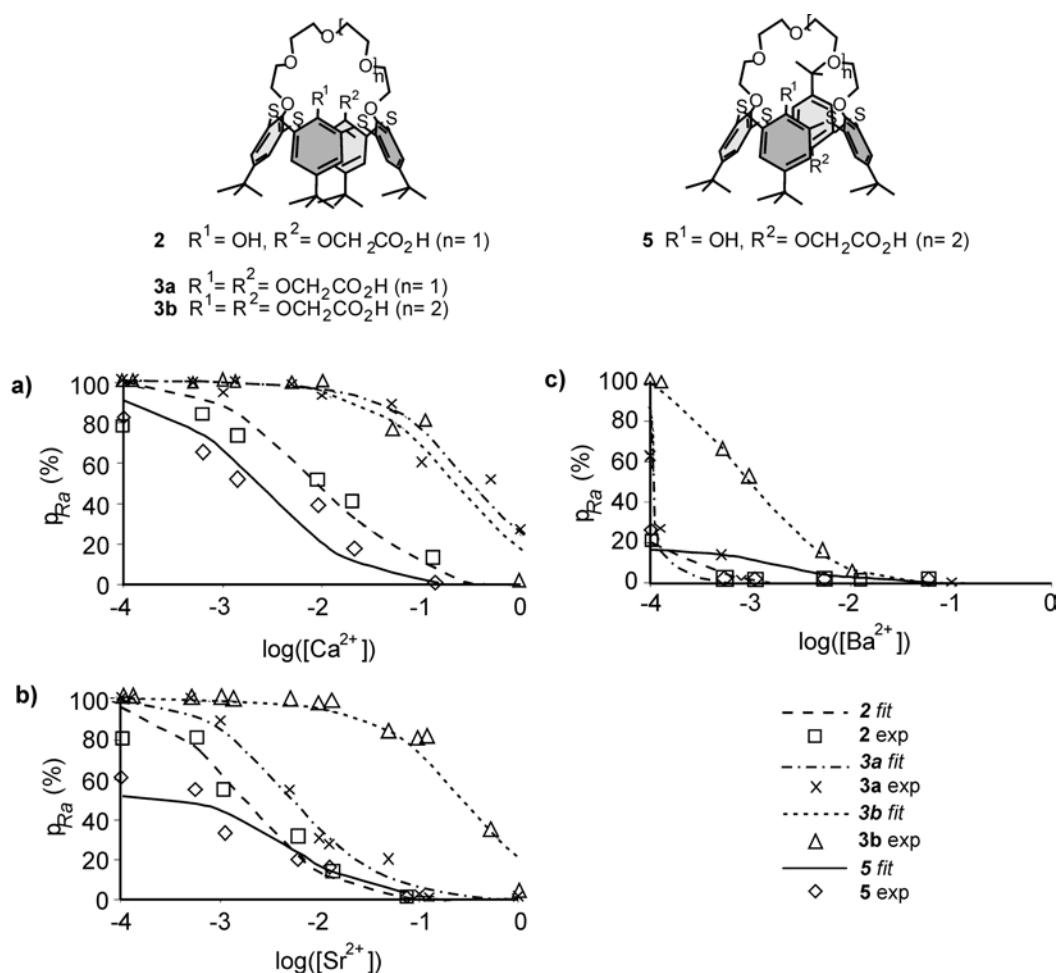


Figure 5.3. Ra^{2+} extraction percentages [$p_{\text{Ra}} = [\text{Ra}^{2+}]_{\text{org}}/[\text{Ra}^{2+}]_{\text{tot}}$ (%)] for extractants 2, 3a,b, and 5 (10^{-4} M), as a function of the $\text{M}(\text{NO}_3)_2$ [$\text{M}^{2+} = \text{Ca}^{2+}$ (a), Sr^{2+} (b), or Ba^{2+} (c)] concentration, with 2.9×10^{-8} M Ra^{2+} .

If the extraction percentages of the competing cations, calculated with K_{ex}^{M} , are incorporated in the equations 1-3 as $p_{\text{M}} = [\text{ML}]_{\text{org}}/[\text{M}^{2+}]_{\text{tot}}$ and the experimentally determined Ra^{2+} extraction percentages as $p_{\text{Ra}} = [\text{Ra}^{2+}]_{\text{org}}/[\text{Ra}^{2+}]_{\text{tot}}$, the $K_{\text{ex}}^{\text{Ra}}/K_{\text{ex}}^{\text{M}}$ values can be determined using a fitting procedure of the extraction curves of Ra^{2+} (see equation 4).¹⁷

$$K_{\text{ex}}^{\text{Ra}}/K_{\text{ex}}^{\text{M}} = (p_{\text{Ra}}/p_{\text{M}})(1-p_{\text{M}})/(1-p_{\text{Ra}}) \quad (4)$$

The $K_{\text{ex}}^{\text{Ra}}/K_{\text{ex}}^{\text{M}}$ values allow for a direct comparison of the Ra²⁺ selectivity coefficients of the different extractants used (Table 5.2).

Table 5.2. Selectivity coefficients ($\log(K_{\text{ex}}^{\text{Ra}}/K_{\text{ex}}^{\text{M}})$), obtained under standard conditions, of extractants **2**, **3a,b**, **4a,b**, **5**, **6**, **7**, and **8**.³⁰

Extractant	$\log(K_{\text{ex}}^{\text{Ra}}/K_{\text{ex}}^{\text{Ca}})$	$\log(K_{\text{ex}}^{\text{Ra}}/K_{\text{ex}}^{\text{Sr}})$	$\log(K_{\text{ex}}^{\text{Ra}}/K_{\text{ex}}^{\text{Ba}})$
2	1.7	1.1	< -0.77 ^a
3a	3.5	1.7	-0.45
3b	3.3	3.4	0.92
4a	1.9	1.1	-0.060
4b	1.6	1.5	1.1
5	1.1	1.2	< 0.34 ^a
6	1.2	1.5	-0.36
7	-1.2	0.22	-0.18
8	< -0.56 ^a	< -1.2 ^a	< -0.45 ^a

^a These values indicate upper limits, due to the low Ra²⁺ extraction percentages obtained.

The influence of the number of carboxylic acid substituents, the conformation, and the crown bridge on the Ra²⁺ selectivity of a thiacalix[4]crown was deduced from the Ra²⁺ extraction abilities of thiacalix[4]crown monocarboxylic acids (**2** and **5**) and thiacalix[4]crown dicarboxylic acids (**3a,b**) (Figure 5.3; Table 5.2).

The Ca²⁺, Sr²⁺, and Ba²⁺ extraction constants of the cone (**2**) and partial cone (**5**) thiacalix[4]crown monocarboxylic acids differ; **5** has significantly lower K_{ex}^{M} values for Sr²⁺ and Ba²⁺ (Table 5.1). Surprisingly, in the presence of Ca²⁺ their Ra²⁺ selectivity coefficients [$\log(K_{\text{ex}}^{\text{Ra}}/K_{\text{ex}}^{\text{M}})$] clearly differ, 1.7 and 1.1, respectively, while with Sr²⁺ the difference is minor, 1.1 and 1.2, respectively (Table 5.2). With Ba²⁺ both thiacalix[4]crown-6 derivatives **3b** and **5** are Ra²⁺ selective, with $\log(K_{\text{ex}}^{\text{Ra}}/K_{\text{ex}}^{\text{Ba}})$ values of 0.92 and <0.34³¹, respectively, whereas both thiacalix[4]crown-5 derivatives **2** and **3a** favor Ba²⁺ over Ra²⁺. Nevertheless, in the presence of Ca²⁺ and Sr²⁺, both thiacalix[4]crown monocarboxylic acids (**2** and **5**)

give significantly lower Ra^{2+} selectivity coefficients than the thiacalix[4]crown dicarboxylic acids (**3a,b**).¹⁴ Comparison of the latter two compounds, which both have the cone conformation, shows a clear influence of the size of the crown-ether bridge size, with the highest $\log (K_{\text{ex}}^{\text{Ra}}/K_{\text{ex}}^{\text{M}})$ values for thiacalix[4]crown-6 dicarboxylic acid (**3b**).

The Ra^{2+} extraction of partial cone thiacalix[4]crown-6 monocarboxylic acid (**5**), together with the complete lack of Ra^{2+} extraction in the case of thiacalix[4]crown-6 (**1b**), indicates that a carboxylic acid group at the opposite side of the thiacalix[4]arene platform can still partially neutralize Ra^{2+} cations complexed in the crown-ether bridge. This was supported by NOE spectra of the $[\text{Ba}^{2+} \cdot \mathbf{5} \cdot \text{Pic}]^0$ complex.³²

Apparently, the co-extraction of an anion, needed in the case of the thiacalix[4]crown monocarboxylic acids (**2** and **5**), has a negative influence on the Ra^{2+} selectivity coefficients, compared to thiacalix[4]crown dicarboxylic acids (**3a,b**).

Hendriksen et al. have reported that a calix[4]arene platform functionalized with four carboxylic acid moieties gives stable Ra^{2+} complexes.² Therefore, the effect of the number of carboxylic acid groups on the Ra^{2+} extraction was studied. The Ra^{2+} selectivity coefficients of thiacalix[4]arene di- (**6**; Figure 5.2a), tri- (**7**), and tetracarboxylic acid (**8**) are given in Table 5.2.

Since thiacalix[4]arene tetracarboxylic acid (**8**) shows near quantitative extraction of Sr^{2+} and Ba^{2+} (Table 5.1), but poor Ra^{2+} selectivity coefficients, it seems that four carboxylic acid groups have a negative influence on the Ra^{2+} selectivity. Thiacalix[4]arenes with two and three carboxylic acid moieties (**6** and **7**) are rather effective extractants for Ca^{2+} and Sr^{2+} (Table 5.1), but still show Ra^{2+} extraction. Only thiacalix[4]arene dicarboxylic acid (**6**) has a Ra^{2+} selectivity in the presence of Ca^{2+} , while thiacalix[4]arene tricarboxylic acid (**7**) and dicarboxylic acid (**8**) show a Ra^{2+} selectivity in the presence of Sr^{2+} . The Ra^{2+} selectivity coefficients of thiacalix[4]arene dicarboxylic acid (**6**) towards Ca^{2+} and Sr^{2+} , 1.2 and 1.5, respectively, are similar to those of the thiacalix[4]crown monocarboxylic acids (**2** and **5**; Table 5.2). This suggests that the presence of two carboxylic acid substituents on a platform is as favorable for the Ra^{2+} selectivity as the combination of a crown-(6-)ether bridge and one carboxylic acid moiety. However, thiacalix[4]arene dicarboxylic acid (**6**) is not $\text{Ra}^{2+}/\text{Ba}^{2+}$ selective, in contrast to thiacalix[4]crown-6 monocarboxylic acid (**5**).

Compared to thiacalix[4]crown-5 dicarboxylic acid (**3a**), only the Ra²⁺/Ca²⁺ selectivity of thiacalix[4]arene dicarboxylic acid (**6**) is significantly lower (214 times). On the other hand, thiacalix[4]crown-6 dicarboxylic acid (**3b**), shows significantly higher Ra²⁺ selectivities than **6** for all competing cations.

Thiacalix[4]crown bis(methylsulfonyl carboxamides) (**4a,b**) could provide alternatives for the known thiacalix[4]crown dicarboxylic acids (**3a,b**).¹⁴ Their Ra²⁺ selectivities were determined under standard conditions (Table 5.2; for Ra²⁺ extraction curves see Appendix Chapter 5). However, the extraction constants of the thiacalix[4]crown bis(methylsulfonyl carboxamides) (**4a**), and in particular (**4b**), for Sr²⁺ and Ba²⁺, are considerably lower than those of the thiacalix[4]crown dicarboxylic acids (**3a,b**; Table 5.1). In competition experiments with Ca²⁺, thiacalix[4]crown bis(methylsulfonyl carboxamides) (**4a,b**) give significantly lower Ra²⁺ selectivity coefficients than the thiacalix[4]crown dicarboxylic acids (**3a,b**), viz. 1.9 and 1.6 vs. 3.5 and 3.3, respectively. In the presence of Sr²⁺ only thiacalix[4]crown-6 dicarboxylic acid (**3b**) gives a significantly higher selectivity coefficient than **4a** and **4b** (3.4 vs. 1.1 and 1.5, respectively). In the case of thiacalix[4]crown bis(methylsulfonyl carboxamides) (**4a,b**), no distinct crown-ether size influence could be observed in the presence of Ca²⁺ and Sr²⁺. However, the crown-6 derivative **4b** has a Ra²⁺/Ba²⁺ selectivity (1.1),³¹ which is slightly higher than that of the thiacalix[4]crown-6 dicarboxylic acid **3b** (0.95). In general, the thiacalix[4]crown bis(methylsulfonyl carboxamides) (**4a,b**) show lower selectivities than the thiacalix[4]crown dicarboxylic acids (**3a,b**).

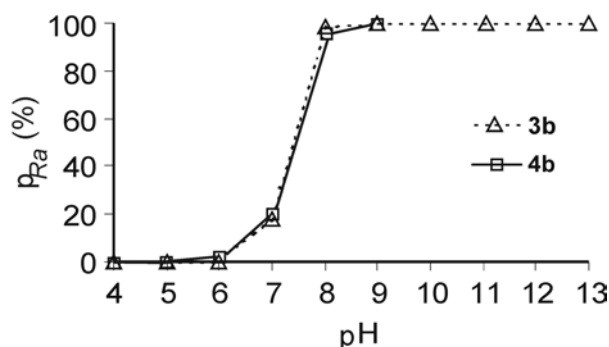


Figure 5.4. pH dependent Ra²⁺ extraction curve of thiacalix[4]crown-6 dicarboxylic acid (**3b**) and thiacalix[4]crown-6 bis(methylsulfonyl carboxamide) (**4b**).

The difference in acidity of methylsulfonyl carboxamide, compared with carboxylic acid groups, might have enlarged the effective pH range.³³ However, the non-competitive Ra^{2+} extraction with **3b** and **4b** gave identical curves over a pH range of 4 - 9 (Figure 5.4).¹⁴

5.3 Conclusions

The results of this systematic study clearly show the advantage of bringing together the crown ether and acid components of a synergistic system on a molecular platform, resulting in much higher Ra^{2+} extraction efficiencies and selectivities. The use of a thiacalix[4]arene with two carboxylic acid groups already gives a high Ra^{2+} selectivity, a result that is further improved by the introduction of a crown-(6-)ether bridge at the thiacalix[4]arene platform. The latter significantly improves the Ra^{2+} selectivity compared to that of the mixtures consisting of thiacalix[4]arene dicarboxylic acid (**6**) and dibenzo-21-crown-7, or thiacalix[4]crown-6 (**1b**) and pentadecanoic acid. The thiacalix[4]crown-6 dicarboxylic acid (**3b**), is unambiguously the best Ra^{2+} selective extractant in the presence of Ca^{2+} , Sr^{2+} , or Ba^{2+} .

5.4 Experimental

5.4.1 Synthesis

General Methods. All solvents were purified by standard laboratory procedures. All other chemicals were analytically pure and used without further purification. Acetonitrile, acetone, and toluene were dried on molecular sieves, whereas dry THF was obtained after distillation over sodium. *t*-Butylthiacalix[4]crown-5 and -6 (**1a,1b**; Chapter 3), *t*-butylthiacalix[4]crown-5 and -6 dicarboxylic ethyl esters (**10a,b**; Chapter 4), *t*-butylthiacalix[4]crown-5 and -6 dicarboxylic acid (**3a,b**; Chapter 4), *t*-butylthiacalix[4]arene dicarboxylic ethyl ester (**15**), *t*-butylthiacalix[4]arene dicarboxylic acid (**6**), *t*-butylthiacalix[4]arene tetracarboxylic ethyl ester (**17**), and *t*-butylthiacalix[4]arene tetracarboxylic acid (**8**) were prepared according to the reported procedure.^{14-16,22} Except for the hydrolysis, all reactions were carried out under an inert argon atmosphere. MALDI-TOF experiments were performed with a dithranol matrix.

MALDI-TOF mass spectra were recorded on a PerSpective Biosystem Voyager-De-RP spectrometer. ¹H NMR spectra were obtained on a Varian INOVA 300 spectrometer; ¹³C NMR spectra were obtained from a Varian Unity 400

spectrometer. Spectra were recorded at 25 °C in CDCl₃ and referenced to the (residual) solvent peak (¹³CDCl₃). The HH-NOESY and ROESY spectra (recorded at the 400 MHz spectrometer) were acquired using the standard Varian pulse sequences with mixing times ranging from 100 to 500 ms, 1024 to 2048 data points in *t*₂ and 128 to 256 increments in *t*₁.

Thin-layer chromatography was performed on aluminium sheets precoated with silica gel 60 F254 (E. Merck); spots were visualized by UV-absorbance. Chromatographic separations were performed on silica gel 60 (E. Merck, 0.040-0.063 mm, 230-240 mesh) or with preparative thin layer chromatography (Silica gel 60 F₂₅₄, 2mm). Melting points are uncorrected.

5,11,17,23-Tetra-*tert*-butyl-26-[(ethoxycarbonyl)methoxy]-2,8,14,20-tetra-thiacalix[4]arenemonocrown-5 (9). A suspension of **1a** (200 mg, 0.23 mmol), ethyl bromoacetate (38 mg, 0.23 mmol), and Na₂CO₃ (12 mg, 0.11 mmol) in CH₃CN (40 mL) was refluxed for 64 h. Subsequently, the CH₃CN was removed and the residue dissolved in CH₂Cl₂ (50 mL). The solution was washed with 10% HCl (2 x 100 mL) and water (2 x 100 mL), and dried on MgSO₄. After evaporation of the solvent the residue was separated by column chromatography (SiO₂, EtOAc/hexane 2/3) to give **9** (130 mg, 59%): mp 241-243 °C; ¹H NMR δ 8.32 (s, 1H), 7.48 (s, 2H), 7.29 (s, 2H), 7.22 (s, 4H), 5.40 (s, 2H), 4.63-4.70 (m, 2H), 4.44-4.37 (m, 2H), 4.01-4.22 (m, 6H), 3.77-3.97 (m, 8H), 1.26 (t, 3H, *J* = 7.3 Hz), 1.23 (s, 9H), 1.06 (s, 9H), 0.99 (s, 18H); ¹³C NMR δ 170.0, 158.1, 157.2, 156.5, 147.0, 146.2, 142.0, 134.6, 134.5, 134.1, 133.4, 129.9, 129.5, 121.8, 74.7, 70.5, 70.3, 70.0, 69.8, 60.5, 34.1, 34.0, 31.3, 31.2, 31.0, 14.2; MALDI-TOF *m/z*: 965.9 [M+H]⁺, 987.9 [M+Na]⁺, 1003.8 [M+K]⁺, calcd 965.4 [M]⁺. Anal. Calcd for C₅₂H₆₈O₉S₄: C, 64.70; H, 7.10. Found: C, 64.38; H, 7.00.

5,11,17,23-Tetra-*tert*-butyl-26-[(ethoxycarbonyl)methoxy]-2,8,14,20-tetra-thiacalix[4]arenemonocrown-6 (11). A suspension of **1b** (479 mg, 0.52 mmol), ethyl bromoacetate (182 mg, 1.09 mmol), and K₂CO₃ (68 mg, 0.49 mmol) in CH₃CN (160 mL) was refluxed for 24 h. Subsequently, the CH₃CN was removed and the residue dissolved in CH₂Cl₂ (150 mL). The solution was washed with 10% HCl (2 x 150 mL) and water (2 x 150 mL), and dried on MgSO₄. After evaporation of the solvent the residue was separated by column chromatography (SiO₂, EtOAc/hexane 2/3) to give **10b**¹⁴ (218 mg, 38%). Subsequent eluent change to EtOAc yielded **11** (100 mg, 19%): mp 174-179 °C; ¹H NMR δ 7.83 (s, 1H), 7.61 (s, 4H), 7.44 (d, 2H, *J* =

2.6 Hz), 7.23 (d, 2H, $J = 2.6$ Hz), 4.59 (s, 2H), 4.44 (m, 2H), 3.96-4.05 (m, 4H), 3.78-3.91 (m, 6H), 3.64-3.73 (m, 10H), 1.43 (s, 9H), 1.33 (s, 9H), 1.07 (s, 18H), 0.99 (t, 3H, $J = 7.1$ Hz); ^{13}C NMR δ 167.8, 157.1, 156.9, 156.6, 146.9, 146.6, 141.8, 134.7, 133.9, 132.7, 131.2, 129.0, 128.4, 127.0, 121.6, 73.4, 71.1, 70.9, 70.7, 69.9, 67.1, 60.4, 34.5, 34.1, 34.0, 31.5, 30.9, 13.8; MALDI-TOF m/z : 1008.6 $[\text{M}]^+$, 1030.6 $[\text{M}+\text{Na}]^+$, 1046.6 $[\text{M}+\text{K}]^+$, calcd 1008.4 $[\text{M}]^+$. Anal. Calcd for $\text{C}_{54}\text{H}_{72}\text{O}_{10}\text{S}_4$: C, 64.25; H, 7.19. Found: C, 64.21; H, 7.19.

5,11,17,23-Tetra-*tert*-butyl-25,26,27-tris[(ethoxycarbonyl)methoxy]-2,8,14,20-tetrathiacalix[4]arene (16). A suspension of **14** (1.0 g, 1.39 mmol), ethyl bromoacetate (689 mg, 4.17 mmol), and Na_2CO_3 (220 mg, 2.02 mmol) in dry acetone (50 mL) was refluxed for 24 h. Subsequently, the acetone was removed and the residue, containing a mixture of the esters **15**, **16**, and **17**, dissolved in CH_2Cl_2 (75 mL). The solution was washed with 10% HCl (2 x 100 mL) and water (2 x 100 mL), and dried on MgSO_4 . After evaporation of the solvent the residue was separated by column chromatography (SiO_2 , CH_2Cl_2) to give **16** (95 mg, 7%): mp 134-137 °C; ^1H NMR δ 7.61 (s, 2H), 7.58 (s, 2H), 7.01 (d, 2H, $J = 2.6$ Hz), 6.98 (d, 2H, $J = 2.6$ Hz), 5.34 (s, 2H), 5.22 (s, 2H), 5.17 (s, 2H), 4.83 (s, 1H), 4.77 (s, 1H), 4.28-4.36 (m, 6H), 4.13 (q, 2H, $J = 7.2$ Hz), 1.18-1.37 (m, 9H), 1.30 (s, 9H), 1.26 (s, 9H), 0.86 (s, 18H); ^{13}C NMR δ 169.6, 169.1, 168.5, 168.2, 157.2, 156.4, 156.1, 148.6, 148.1, 147.4, 146.5, 142.1, 135.2, 134.4, 133.7, 133.0, 132.4, 129.9, 128.9, 127.1, 121.6, 71.7, 71.5, 71.4, 71.2, 68.6, 34.2, 33.9, 31.8, 31.7, 31.5, 31.4, 31.2, 31.1, 31.0, 30.7, 30.6, 30.2, 14.6, 14.27, 14.1, 13.9, 13.8; MALDI-TOF m/z : 978.6 $[\text{M}]^+$, 1001.5 $[\text{M}+\text{Na}]^+$, 1017.5 $[\text{M}+\text{K}]^+$, calcd 978.4 $[\text{M}]^+$. Anal. Calcd for $\text{C}_{52}\text{H}_{66}\text{O}_{10}\text{S}_4$: C, 63.77; H, 6.79. Found: C, 63.75; H, 7.00.

General Hydrolysis Procedure. To a suspension of **9**, **11**, or **16** in THF/ H_2O (1/1) was added an excess of tetramethylammonium hydroxide (TMAH) (25%) in MeOH, whereupon the mixture was refluxed for 12 h. The organic solvents were removed and the residue was dissolved in CH_2Cl_2 (100 mL). The solution was washed with 10% HCl (2 x 100 mL), dried with MgSO_4 , whereupon the solvent was removed.

5,11,17,23-Tetra-*tert*-butyl-26-carboxymethoxy-2,8,14,20-tetrathiacalix[4]arenemonocrown-5 (2). Reaction of **9** (81 mg, 84 μmol) and TMAH (1.5 mL) in THF/ H_2O (20 mL) yielded **2** (64 mg, 81%): mp >250 °C; ^1H NMR δ 7.97 (s, 1H), 7.75 (s, 2H), 7.64 (s, 2H), 7.03 (d, 2H, $J = 2.6$ Hz), 7.00 (d, 2H, $J = 2.6$ Hz), 5.58

(s, 2H), 4.31-4.37 (m, 2H), 4.24 (m, 2H), 4.00-4.23 (m, 4H), 3.95 (t, 4H, $J = 5.3$ Hz), 3.78-3.88 (m, 4H), 1.35 (s, 9H), 1.33 (s, 9H), 0.83 (s, 18H); ¹³C NMR δ 171.1, 158.1, 157.2, 156.5, 147.6, 147.4, 142.0, 135.7, 134.3, 133.7, 133.5, 129.4, 129.0, 127.8, 122.0, 71.4, 70.7, 70.0, 69.8, 34.4, 34.1, 31.5, 31.3, 30.7, 29.7; MALDI-TOF m/z : 937.8 [M+H]⁺, 959.7 [M+Na]⁺, 975.7 [M+K]⁺, calcd 937.3 [M+H]⁺. Anal. Calcd for C₅₀H₆₄O₉S₄: C, 64.07; H, 6.88. Found: C, 63.95; H, 6.91.

5,11,17,23-Tetra-*tert*-butyl-26-carboxymethoxy-2,8,14,20-tetrathiacalix[4]arenemonocrown-6 (5). Reaction of **11** (85 mg, 84 μ mol) and TMAH (1.5 mL) in THF/H₂O (16 mL) yielded **5** (70 mg, 85%): mp 241-244 °C; ¹H NMR δ 7.81 (s, 1H), 7.62 (s, 2H), 7.54 (s, 2H), 7.45 (d, 2H, $J = 2.6$ Hz), 7.30 (d, 2H, $J = 2.6$ Hz), 4.59 (s, 2H), 4.28-4.34 (m, 2H), 4.11-4.18 (m, 2H), 3.73-3.83 (m, 6H), 3.72-3.61 (m, 10H), 1.43 (s, 9H), 1.33 (s, 9H), 1.13 (s, 18H); ¹³C NMR δ 167.3, 156.9, 156.5, 153.0, 148.6, 148.4, 142.7, 135.9, 133.5, 130.1, 129.0, 128.9, 128.8, 126.4, 121.2, 73.3, 71.0, 70.9, 70.8, 69.6, 64.4, 34.7, 34.3, 34.1, 31.4, 30.8, 29.7; MALDI-TOF m/z : 980.0 [M+H]⁺, 1002.9 [M+Na]⁺, 1018.9 [M+K]⁺, calcd 980.4 [M+H]⁺. Anal. Calcd for C₅₂H₆₈O₁₀S₄: C, 63.64; H, 6.98. Found: C, 63.71; H, 6.91.

5,11,17,23-Tetra-*tert*-butyl-25,26,27-tris(carboxymethoxy)-2,8,14,20-tetrathiacalix[4]arene (7). Reaction of **16** (263 mg, 269 μ mol) and TMAH (2.5 mL) in THF/H₂O (20 mL) yielded **7** (221 mg, 92%): mp > 250 °C; ¹H NMR δ 7.61 (dd, 4H, $J = 2.6$ and 2.6 Hz), 7.38 (s, 2H), 7.16 (s, 2H), 5.97 (s, 1H), 5.91 (s, 1H), 4.78 (m, 2H), 4.62 (s, 1H), 4.57 (s, 1H), 1.22 (s, 18H), 1.11 (s, 9H), 0.92 (s, 9H); ¹³C NMR δ 174.5, 170.2, 158.8, 155.0, 148.1, 143.2, 135.5, 134.6, 133.9, 129.2, 128.9, 128.8, 120.8, 34.3, 33.9, 31.6, 31.3, 30.9, 30.5, 29.6; MALDI-TOF m/z : 894.3 [M]⁺, 917.4 [M+Na]⁺, 933.3 [M+K]⁺, calcd 894.3 [M]⁺. Anal. Calcd for C₄₆H₅₄O₁₀S₄: C, 61.72; H, 6.08. Found: C, 61.44; H, 6.10.

General Procedure for the Preparation of *N*-methylsulfonyl Carboxamides 4a,b. To a solution of **3a,b** in dry toluene (10 mL) was added oxalyl chloride (2.5 equiv). The solution was refluxed for 12 h, whereupon the toluene was removed at reduced pressure. The residue was dissolved in dry THF (20 mL) and the resulting solution added to a suspension of NaH (60% dispersion in mineral oil) (10 equiv) and methanesulfonamide (2.5 equiv) in dry THF (5 mL). The mixture was stirred at room temperature for 72 h. Excess NaH was carefully neutralized by adding

water. After the work up as described for the general hydrolysis procedure, preparative thin layer chromatography (SiO₂, EtOAc) was performed to yield **4a,b**.

5,11,17,23-Tetra-tert-butyl-26,28-bis[(methylsulfonyl)carbamoylmethoxy]-2,8,14,20-tetrathiacalix[4]arenemonocrown-5 (4a). Reaction of **3a** (185 mg, 0.19 mmol), oxalyl chloride (69 mg, 54 mmol), sodium hydride (87 mg, 1.86 mmol), and methanesulfonamide (52 mg, 55 mmol) gave **4a** (125 mg, 58%): mp >250 °C; ¹H NMR δ 11.27 (s, 2H), 7.73 (s, 4H), 7.00 (s, 4H), 5.83 (s, 4H), 4.31-4.33 (m, 4H), 4.06-4.08 (m, 4H), 3.85-3.86 (m, 4H), 3.77-3.79 (m, 4H), 3.19 (s, 6H), 1.35 (s, 18H), 0.84 (s, 18H); ¹³C NMR δ 169.9, 158.2, 157.5, 147.0, 146.9, 135.4, 134.2, 129.5, 128.0, 74.7, 71.1, 70.6, 70.4, 41.5, 34.4, 33.9, 31.4, 30.7, 29.7; MALDI-TOF *m/z*: 1148.4 [M]⁺, 1170.4 [M+Na]⁺, 1186.4 [M+K]⁺, calcd. 1148.3 [M]⁺. Anal. Calcd for C₅₄H₇₂N₂O₁₃S₆ • 0.7 H₂O: C, 55.81; H, 6.37. Found: C, 55.78; H, 6.23.

5,11,17,23-Tetra-tert-butyl-26,28-bis[(methylsulfonyl)carbamoylmethoxy]-2,8,14,20-tetrathiacalix[4]arenemonocrown-6 (4b). Reaction of **3b** (80 mg, 77 μmol), oxalyl chloride (25 mg, 0.19 mmol), sodium hydride (31 mg, 0.77 mmol), and methanesulfonamide (19 mg, 0.19 mmol) gave **4b** (55 mg, 60%): mp >250 °C; ¹H NMR δ 11.11 (s, 2H), 7.71 (s, 4H), 6.92 (s, 4H), 5.66 (s, 4H), 4.14-4.17 (m, 4H), 4.03-4.06 (m, 4H), 3.86-3.90 (m, 4H), 3.77-3.81 (m, 4H), 3.75 (s, 4H), 3.24 (s, 6H), 1.35 (s, 18H), 0.85 (s, 18H); ¹³C NMR δ 169.5, 158.5, 157.4, 147.0, 146.8, 135.8, 133.3, 129.3, 128.1, 76.4, 71.0, 70.7, 70.5, 70.4, 70.2, 41.3, 34.4, 34.0, 31.4, 30.8, 29.7; MALDI-TOF *m/z*: 1191.9 [M]⁺, 1213.9 [M+Na]⁺, 1229.9 [M+K]⁺, 1235.9 [M+2Na]⁺, 1251.9 [M+Na+K]⁺, 1257.9 [M+2K]⁺, calcd. 1192.4 [M]⁺. Anal. Calcd for C₅₆H₇₆N₂O₁₄S₆: C, 56.35; H, 6.42. Found: C, 56.10; H, 6.49.

[Ba²⁺•5•Pic]⁰ complex formation. A mixture of **5** (9.8 mg, 10⁻² mmol), Ba(NO₃) (29 mg, 10⁻¹ mmol) and LiPic (24 mg, 10⁻¹ mmol) in CH₂Cl₂/acetonitrile 1/1 (5 mL) was stirred at 40 °C for 1 h. The solvents were evaporated and the residue dissolved in CDCl₃ (1 mL), after which the solution was filtered.

5.4.2 Extraction

Materials. The acids (concentrated HCl and HNO₃) and CH₂Cl₂ were of p.a. grade and used as received. The nitrate salts of Ca²⁺ (p.a.), Sr²⁺ (p.a.), and Ba²⁺ (p.a.) were purchased from Acros Organics. ⁹⁰Sr²⁺ isotope solutions were purchased from Amersham UK. ¹³³Ba²⁺ isotope solutions were purchased from Isotope Products

Europe Blaseg GmbH. Ra²⁺ stock solutions were purchased from AEA Technology QSA GmbH; ²²⁶Ra was used because of its long half-life ($t_{1/2} = 1.6 \times 10^3$ y). (**Note: ²²⁶Ra has a very high radiotoxicity and should be handled with care and under radionuclear supervision**)

Solutions. All basic experiments were performed using an aqueous phase with pH 8.9 (tris-HCl buffer) and an organic phase containing 10⁻⁴ M of extractant in CH₂Cl₂. The different nitrate salt concentrations were obtained by diluting stock solutions to the required concentration. From a carrier free stock solution of ⁹⁰Sr²⁺, a dilution of 2.5 MBq/g was made in 0.1 M HNO₃. From a 10 µg Ba²⁺/mL carrier containing stock solution of ¹³³Ba²⁺ in 0.1 M HCl, a dilution of 45.18 kBq/g was made in water. From a carrier free stock solution of ²²⁶Ra²⁺ in 0.5 M HCl, a dilution of 1.2 kBq/g (1.4 x 10⁻⁶ M) was made in 0.1 M HNO₃.

General Extraction Procedures. Equal volumes (1.0 mL) of the organic and aqueous solutions were transferred into a screw cap vial with a volume of 4 mL. The samples were shaken (1500 rpm) at ambient temperatures (22-24 °C) for 1 h to ensure complete settling of the two-phase equilibration. After extraction, the solutions were disengaged by centrifugation (1600 rpm for 5 min) and aliquots (0.5 mL) of the organic and aqueous phases were pipetted out. Experiments were performed in duplicate; average values are reported, with an estimated error of 10-15%.

Non-competitive Extraction Experiments (Table 5.1). In the non-competitive extraction experiments the concentration of [M(NO₃)₂] (M²⁺ = Ca²⁺, Sr²⁺, and Ba²⁺) was varied (0.2-3) x 10⁻⁴ M compared to the extractant concentration (10⁻⁴ M).³⁴

ICP-MS Monitored Extraction Procedures (Table 5.1). The solvent of the aliquot taken from the organic phase was evaporated and the residue destructed in 0.5 mL of concentrated HNO₃. The cation concentrations were measured on a Perkin Elmer Sciex Elan 6000 ICP-MS instrument, using a cross flow nebulizer.³⁴ The extraction percentage is defined as 100% times the ratio of cation concentration in the organic phase ([M_o]) and the added cation concentration ([M_{add}]) (eq 5).

$$E\% = 100\%([M_o]/[M_{add}]) \quad (5)$$

Tracer Monitored Extraction Procedures (Table 5.1). The extraction percentages were determined using the appropriate tracer in individual $M(\text{NO}_3)_n$ [$M = \text{Sr}^{2+}$ ($^{90}\text{Sr}^{2+}$), or Ba^{2+} ($^{133}\text{Ba}^{2+}$)] solutions. In the case of $\text{Sr}(\text{NO}_3)_2$ the extraction percentages were determined using 2.5 μL of $^{90}\text{Sr}^{2+}$ tracer (616 Bq). The activity was determined using a liquid scintillation counter to detect the Cherenkov radiation. In the case of $\text{Ba}(\text{NO}_3)_2$ the extraction percentages were determined using 10 μL of ^{133}Ba tracer (452 Bq). The gamma-activity was determined using a NaI scintillation counter. The obtained extraction percentages are defined as 100% times the ratio of the activity in the organic phase (A_o) and the total activity ($A_o + A_{aq}$) (eq 6).

$$E\% = 100\%(A_o/(A_o + A_{aq})) \quad (6)$$

Competitive Ra^{2+} Extraction Curves (single competing cation; (Figures 5.2 and 5.3 and Table 5.2). In the competitive extraction experiments, aqueous phase pH 8.9 (tris-HCl), the ratio of competing $M^n(\text{NO}_3)_n$ ($M = \text{Ca}^{2+}$, Sr^{2+} , and Ba^{2+}) salt concentrations compared to a fixed extractant concentration (1 mL; 10^{-4} M) was altered to provide competing cation-concentration dependent extraction curves. To the aqueous phase 20 μL of $^{226}\text{Ra}^{2+}$ tracer (240 Bq) were added and the gamma-activity was determined with a Ge(Li) scintillation counter. The obtained extraction percentages are defined as 100% times the ratio of activity in the organic phase (A_o) and the total activity ($A_o + A_{aq}$) (eq 6).

Extraction vs. pH Curves (Figure 5.4). Experiments were performed using fixed concentrations **3b** and **4b** of (10^{-4} M) and $^{226}\text{Ra}^{2+}$ (2.9×10^{-8} M). The pH values were set using different buffer solutions: pH 4-6: HCl, pH 7-10: tris-HCl, and pH 10-13: tris-(CH_3)₃NOH.

References

1. Bond, A. H.; Dietz, M. L.; Chiarizia, R. *Ind. Eng. Chem. Res.* **2000**, *39*, 3442-3464.
2. Hendriksen, G.; Hoff, P.; Larsen, R. H. *Appl. Rad. Isot.* **2002**, *56*, 667-671.
3. Sekine, T.; Kawashima, Y.; Unnai, T.; Sakairi, M. *Bull. Chem. Soc. Jpn.* **1968**, *41*, 3013-3015.
4. McDowell, W. J. *Sep. Sci. Technol.* **1988**, *23*, 1251-1268.
5. McDowell, W. J.; Moyer, B. A.; Case, G. N.; Case, F. I. *Solvent Extr. Ion Exch.* **1986**, *4*, 217-236.
6. McDowell, W. J.; Arndsten, B. A.; Case, G. N. *Solvent Extr. Ion Exch.* **1989**, *7*, 377-393.

7. Chiarizia, R.; Horwitz, E. P.; Dietz, M. L.; Cheng, Y. D. *Reactive and Functional Polymers* **1998**, *38*, 249-255.
8. Dietz, M. L.; Chiarizia, R.; Horwitz, E. P. *Anal. Chem.* **1997**, *69*, 3028-3037.
9. Rajec, P.; Mikulaj, V.; Švec, V. *J. Radioanal. Nucl. Chem.* **1997**, *219*, 123-125.
10. Strzelbicki, J.; Bartsch, R. A. *Anal. Chem.* **1981**, *53*, 2247-2250.
11. Beklemishev, M. K.; Elshani, S.; Wai, C. M. *Anal. Chem.* **1994**, *66*, 3521-3527.
12. Chu, T. C.; Lin, C. C. *Appl. Radiat. Isot.* **2001**, *55*, 609-616.
13. Chen, X. Y.; Ji, M.; Fisher, D. R.; Wai, C. M. *Inorg. Chem.* **1999**, *38*, 5449-5452.
14. Chapter 4 and Van Leeuwen, F. W. B.; Beijleveld, H.; Miermans, C. J. H.; Huskens, J.; Verboom, W.; Reinhoudt, D. N. *submitted for publication*.
15. Bitter, I.; Csokai, V. *Tetrahedron Lett.* **2003**, *44*, 2261-2265.
16. Chapter 3 and Van Leeuwen, F. W. B.; Beijleveld, H.; Kooijman, H.; Spek, A. L.; Verboom, W.; Reinhoudt, D. N. *J. Org. Chem.* **2004**, *69*, 3928-3936.
17. The difference in reactivity of the two hydroxyl groups of a thiacalix[4]crown may allow for selective functionalization, a feature that could be useful for the preparation of mixed substituent thiacalix[4]crowns.
18. Attempts to form the cone crown-6 monoester with Na₂CO₃ as a base (2 equiv) only gave partial conversion of thiacalix[4]crown-6 (**1b**) to the partial cone thiacalix[4]crown-6 monoester (**11**). The preferred formation of partial cone **11** is rather surprising, since a crown-5-ether bridge only allows for the formation of the monoester in the cone conformation (**9**).
19. All conformational assignments are fully confirmed by NOESY data, including the NOE interactions of the *t*-butyl group resonances.
20. In the ¹H NMR spectra of **7** the ArH1 and ArH3 peaks perfectly overlap.
21. The NOE couplings between the ArH peaks allows to discriminate the low field peaks to ArH2a/ArH4a and as a consequence the upfield peaks to ArH2b/ArH4b.
22. Iki, N.; Morohashi, N.; Narumi, F.; Fujimoto, T.; Suzuki, T.; Miyano, S. *Tetrahedron Lett.* **1999**, *40*, 7337-7341.
23. Due to the sharper OH resonance found for the thiacalix[4]arene tricarboxylic ester (**15**), with respect to the corresponding thiacalix[4]arene tricarboxylic acid (**7**), compound **15** was used to assign their conformation.
24. Due to the lack of differences in extraction behavior, described in Chapter 4 for the competition of Mg²⁺ cations, only Ca²⁺, Sr²⁺, and Ba²⁺ were used as competing cations in this work.
25. Shannon, R. D. *Acta Cryst. A* **1976**, *32*, 751-767.
26. To determine whether pentadecanoic acid is lipophilic enough to remain in the organic phase, its presence in the organic phase was verified with ¹H NMR spectroscopy after extraction with a tris-HCl buffer of pH 8.9. Furthermore, a clear organic/aqueous phase separation was obtained after the extraction experiments.
27. Thiacalix[4]crown-5 and -6 (**1a,b**) alone did not give any⁺ extraction under the conditions studied.
28. At lower salt concentrations (< 10⁻³ M) a third phase was observed with these extractants.
29. Since the thiacalix[4]crowns **1a,b** showed no Ra²⁺ affinity under the standard conditions used, their extraction constants for Ca²⁺, Sr²⁺, and Ba²⁺ were not determined.
30. Since the concentration of [Ra²⁺]_{org} can maximally be 2.9 x 10⁻⁸ M, compared to a [L] of 10⁻⁴ M, the selectivity coefficients are not influenced by the fact that *p*_{Ra} is determined by [Ra²⁺]_{org}/([Ra²⁺]_{org} + [Ra²⁺]_{aq}), rather than

$[\text{}^{226}\text{Ra}^{2+}]_{\text{org}}/[\text{}^{226}\text{Ra}^{2+}]_{\text{tot}}$. The precipitation of Ra^{2+} salts does not influence the selectivity coefficients obtained and as such is not discussed.

31. The relatively high Ra^{2+} selectivity coefficients are mainly caused by the low Ba^{2+} extraction constants.
32. Partial cone thiacalix[4]crown-6 monocarboxylic acid (**5**) shows NOE cross peaks between the *t*-butyl3 resonances of the inversed aromatic unit of the thiacalix[4]arene and the crown-ether bridge, while its $[\text{Ba}^{2+}\cdot\mathbf{5}\cdot\text{Pic}^-]^0$ complex does not. Nonetheless, NOE interactions between the resonances of the methylene group adjacent to the carboxylic acid moiety and ArH2 and ArH4 (strong) and *t*-butyl2 and *t*-butyl4 (weak) resonances, still confirm the partial cone conformation. Furthermore, the ArH2b and ArH4b peaks shift down field significantly (0.3 ppm) for the $[\text{Ba}^{2+}\cdot\mathbf{5}\cdot\text{Pic}^-]^0$ complex. These NMR data suggest outward rotation of the *t*-butyl1 peak, to allow for inward rotation of the carboxylic acid group. To the best of our knowledge this is the first example that in the partial cone conformation a carboxylic acid moiety rotates into the cavity to interact with a cation at the other side of the thiacalix[4]arene platform.
33. Talanova, G. G.; Hwang, H.-S.; Talanov, V. S.; Bartsch, R. A. *Chem. Commun.* **1998**, 419-420.
34. The isotope ^{43}Ca was corrected for the interference of the doubly charged isotope ^{88}Sr .

Appendix Chapter 5

Derivation of Extraction Constants and Ra^{2+} Selectivity Coefficients *

A.1 Introduction

Based on the Ca^{2+} , Sr^{2+} , and Ba^{2+} extraction data, the complex stoichiometries of the extractants described in Chapter 5 are reported. These stoichiometries are used to derive the extraction constants (K_{ex}^{M} ; $\text{M} = \text{Ca}^{2+}$, Sr^{2+} , Ba^{2+} , and Ra^{2+}), allowing for the determination of Ra^{2+} selectivity coefficients ($K_{\text{ex}}^{\text{Ra}}/K_{\text{ex}}^{\text{M}}$). In turn, these Ra^{2+} selectivity coefficients enable a direct comparison of the Ra^{2+} extraction data of extractants with different complexation stoichiometries is possible.

A.2 General

Comparison of the extraction constants of the competing cations (Ca^{2+} , Sr^{2+} , and Ba^{2+}) and of Ra^{2+} , allows the quantification of the differences between the various extractants used (**2**, **3a,b**, **4a,b**, **5**, **6**, **7**, and **8**). In order to obtain these extraction constant ratios, several equilibria have to be considered.

Since the $\text{p}K_{\text{a}}$ of tris is 8.1¹ and all the competition experiments were performed at pH 8.9 ($[\text{tris}]_{\text{tot}} = 5.0 \times 10^{-2}$ M), $[\text{Htris}^+]_{\text{aq}} = 6.8 \times 10^{-3}$ M. Consequently, because of the basic nature of the aqueous phase, the uncomplexed ligands ($[\text{L}]_{\text{tot}} = 10^{-4}$ M) in the organic phase are assumed to exist as neutral (Htris)L, (Htris)₂L, (Htris)₃L, or (Htris)₄L salts, depending on the charge of the ligand.

* This Appendix has been submitted for publication: Van Leeuwen, F. W. B.; Beijleveld, H.; Velders, A. H.; Huskens, J.; Verboom, W.; Reinhoudt, D. N.

A.3 Singly Charged Extractants, 1: 1 Stoichiometry (2 and 5)

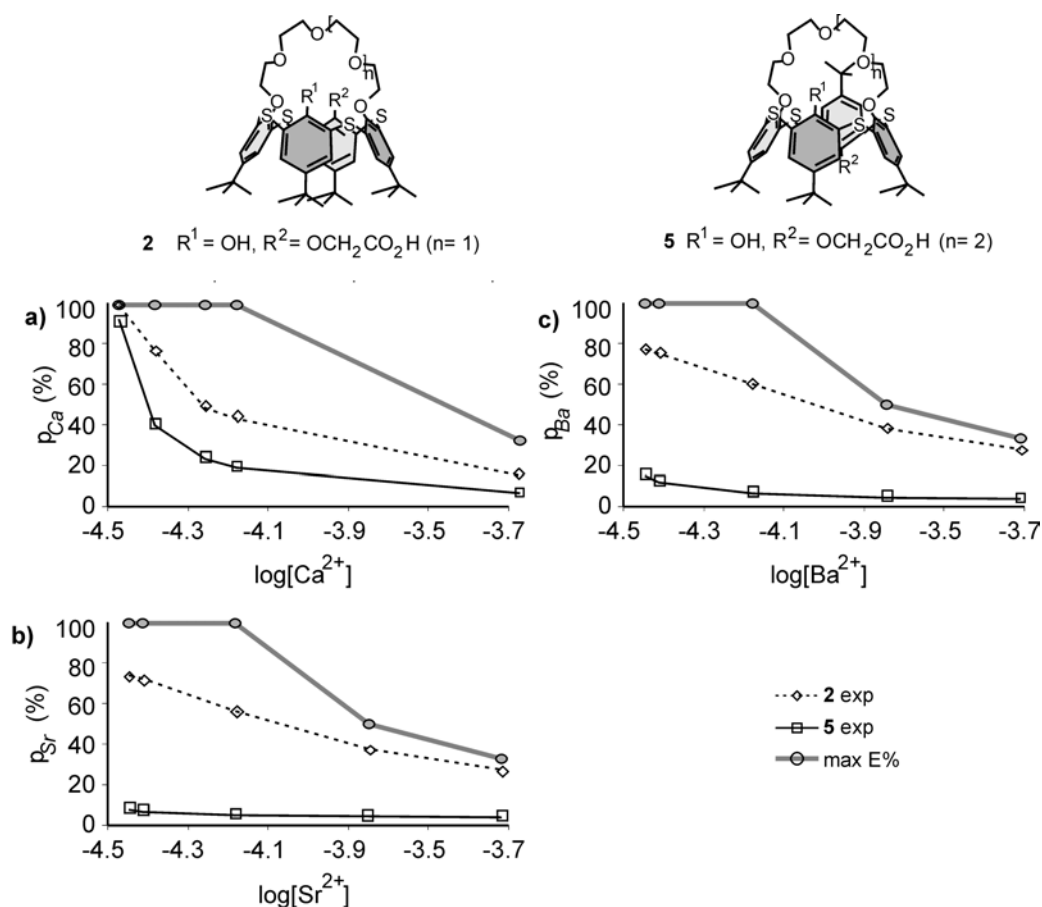
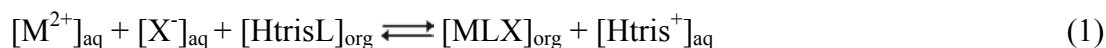


Figure A.1. M^{2+} extraction percentages ($p_M = [M^{2+}]_{\text{org}}/[M^{2+}]_{\text{tot}}(\%)$) for extractants **2** and **5** (10^{-4} M; 1 mL of CH_2Cl_2) as a function of $\log[M^{2+}]$ ($M^{2+} = \text{Ca}^{2+}$ (a), Sr^{2+} (b), and Ba^{2+} (c); 1 mL of water pH 8.9 tris-HCl buffer). The line through the circles gives the extraction percentages calculated for the full complex formation of a 1:1 $[M^{2+} \cdot (L) \cdot X^-]^0$ complex.

Extraction of M^{2+} cations by the singly charged thiocalix[4]crown monocarboxylic acids (**2** and **5**) is shown in Figure A.1. The best fits were obtained assuming a 1:1 complex stoichiometry, the maximal extraction percentages are depicted in Figure A.1, and therefore the equilibrium for the extraction of the divalent cations can be written as equation 1, with equation 2 describing the corresponding extraction constant.



$$K_{ex}^M = [MLX]_{org}[Htris^+]_{aq}/[M^{2+}]_{aq}[HtrisL]_{org}[X^-]_{aq} \quad (2)$$

Because of the equal volumes used, a decrease of $[M^{2+}]_{aq}$ in the aqueous phase leads to an equal increase of $[ML]_{org}$ in the organic phase, allowing for direct comparison of the concentrations of the two phases. This results in the equations 3 and 4 for the mass balances of M^{2+} and L, respectively.

$$[M^{2+}]_{tot} = [M^{2+}]_{aq} + [MLX]_{org} \quad (3)$$

$$[L]_{tot} = [(Htris)_2L]_{org} + [MLX]_{org} \quad (4)$$

The extraction percentages obtained for the competing cations (see Figure A.1) are incorporated as $p_M = [MLX]_{org}/[M^{2+}]_{tot}$, therefore, $[MLX]_{org}$ is equal to $p_M[M^{2+}]_{tot}$, and $[M^{2+}]_{aq} = (1-p_M)[M^{2+}]_{tot}$.

The extraction percentages of the competing M^{2+} cations in a concentration range of $(0.2 - 3.0) \times 10^{-4}$ M are provided in Figure A.1. From these extraction curves, K_{ex}^M can be obtained by fitting calculated p_M values to the experimentally determined values (Table 5.2), using a non-linear least squares fitting procedure.

When the Ra^{2+} experiments, in competition with the divalent cations Ca^{2+} , Sr^{2+} , and Ba^{2+} (Figure 5.3), are modelled, additional equilibria and mass balances have to be considered. The extraction equilibrium for Ra^{2+} and its extraction constant are given in equations 5 and 6, respectively. The Ra^{2+} mass balance is given in equation 7, and the ligand mass balance (equation 4) is now expanded to equation 8.



$$K_{ex}^{Ra} = [RaLX]_{org}[Htris^+]_{aq}/[Ra^{2+}]_{aq}[HtrisL]_{org}[X^-]_{aq} \quad (6)$$

$$[Ra^{2+}]_{tot} = [Ra^{2+}]_{aq} + [RaLX]_{org} \quad (7)$$

$$[L]_{tot} = [(Htris)_2L]_{org} + [MLX]_{org} + [RaLX]_{org} \quad (8)$$

However, because of the small amount of $[Ra^{2+}]_{tot}$ (2.9×10^{-8} M), $[RaL]_{org}$ can be neglected in equation 8. Similar to p_M for the competing cations, p_{Ra} is defined as $[RaLX]_{org}/[Ra^{2+}]_{tot}$, resulting in $[RaLX]_{org} = p_{Ra}[Ra^{2+}]_{tot}$, and $[Ra^{2+}]_{aq} = (1-p_{Ra})[Ra^{2+}]_{tot}$. Thus the K_{ex}^{Ra}/K_{ex}^M ratio (equation 9) can be written as equation 10.

$$K_{\text{ex}}^{\text{Ra}}/K_{\text{ex}}^{\text{M}} = ([\text{RaLX}]_{\text{org}}/[\text{Ra}^{2+}]_{\text{aq}})([\text{M}^{2+}]_{\text{aq}}/[\text{MLX}]_{\text{org}}) \quad (9)$$

$$K_{\text{ex}}^{\text{Ra}}/K_{\text{ex}}^{\text{M}} = (p_{\text{Ra}}/p_{\text{M}})(1-p_{\text{M}})/(1-p_{\text{Ra}}) \quad (10)$$

Since the K_{ex}^{M} values of the different extractants have different dimensions, only $K_{\text{M}}^{\text{Ra}}/K_{\text{ex}}^{\text{M}}$ ratios are given. These ratios are obtained by fitting calculated p_{Ra} values to the experimentally determined values (Figure 5.3), using a non-linear least squares fitting procedure.

A.4 Doubly or Triply Charged Extractants, 1: 1 Stoichiometry (3a,b, 4a,b, 6, and 7)

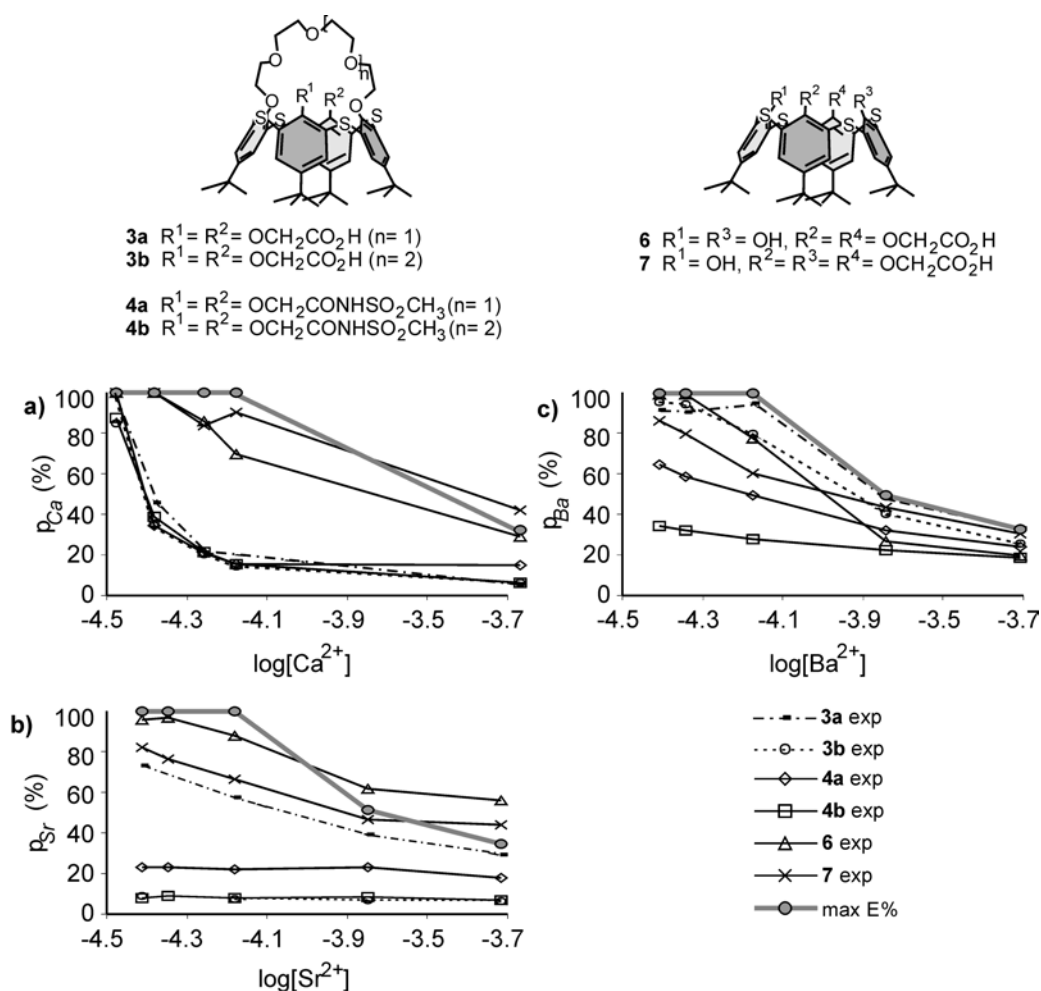


Figure A.2. M^{2+} extraction percentages ($p_M = [\text{M}^{2+}]_{\text{org}}/[\text{M}^{2+}]_{\text{tot}}$ (%)) for extractants **3a,b**, **4a,b**, **6**, and **7** (10^{-4} M; 1 mL of CH_2Cl_2) as a function of $\log[M^{2+}]$ ($M^{2+} = \text{Ca}^{2+}$ (a), Sr^{2+} (b), and Ba^{2+} (c); 1 mL of water pH 8.9 tris-HCl buffer). The line through the circles gives the extraction percentages calculated for a 1:1 $[\text{M}^{2+} \cdot (\text{L}^{2-})]^0$ complex.

In Chapter 4 the equations used to determine the extraction constants and selectivity coefficient of the divalently charged thiacalix[4]crown dicarboxylic acids (**3a,b**) are described.² For thiacalix[4]crown bis(methylsulfonyl) carboxamides (**4a,b**), thiacalix[4]arene dicarboxylic acid (**6**), and thiacalix[4]arene tricarboxylic acid (**7**) the same equations can be used, which results in equation 10 for the Ra^{2+} selectivity coefficient. Here only the extraction behavior of **3a,b**, **4a,b**, **6**, and **7** towards Ca^{2+} , Sr^{2+} , and Ba^{2+} are depicted in Figure A.2, as well as the Ra^{2+} extraction curves of **4a,b** and **7** (Figure A.3).

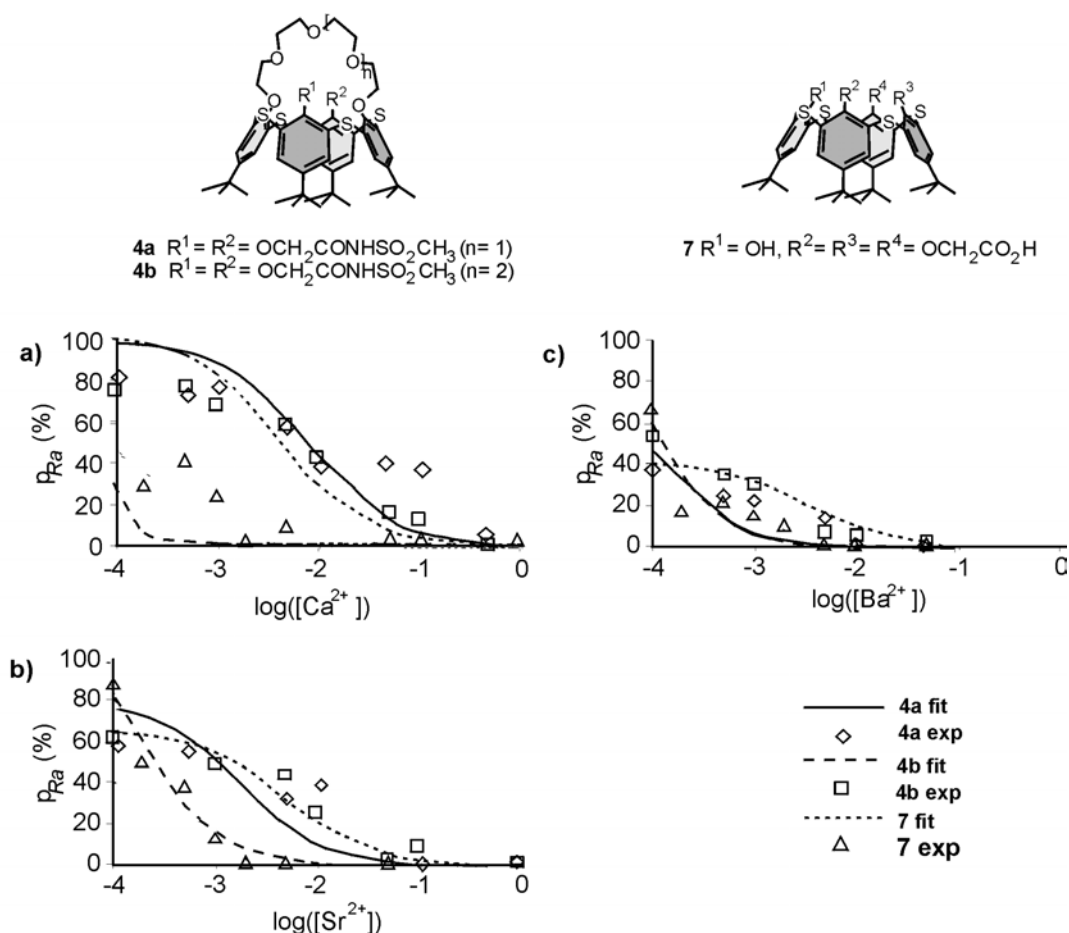


Figure A.3. Ra^{2+} extraction percentages ($p_{Ra} = [^{226}Ra^{2+}]_{org}/[^{226}Ra^{2+}]_{tot}$ (%)) for extractants **4a** (a), **4b** (b), and **7** (c) (10^{-4} M; 1 mL of CH_2Cl_2), as a function of the $M(NO_3)_2$ concentration ($M^{2+} = Ca^{2+}$, Sr^{2+} , or Ba^{2+} ; 1 mL of water pH 8.9 tris-HCl buffer), with 2.9×10^{-8} M Ra^{2+} .

A.5 Quadruply Charged Extractants, 1: 2 Stoichiometry (8)

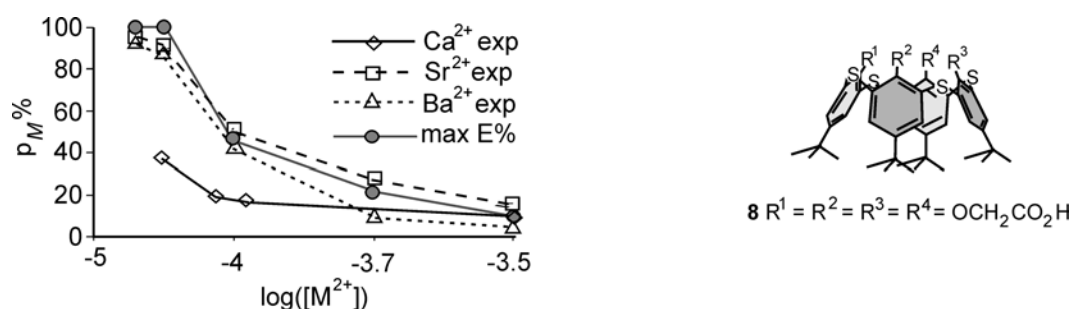
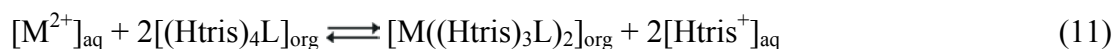


Figure A.4. M^{2+} extraction percentages ($p_M = [M^{2+}]_{\text{org}}/[M^{2+}]_{\text{tot}}$ (%)) recorded with **8** at different extractant to $M(\text{NO}_3)_2$ ratios ($M^{2+} = \text{Ca}^{2+}$, Sr^{2+} , and Ba^{2+} ; 1 mL of pH 8.9 tris-HCl buffer), using a fixed extractant (10^{-4} M; 1 mL of CH_2Cl_2). The line through circles shows the maximal extraction percentage expected for a 1:2 $[M^{2+} \cdot (\text{Htris})_3\text{L}]_2^0$ complex stoichiometry.

Surprisingly, extraction data obtained for the thiocalix[4]arene tetracarboxylic acid (**8**), with the competing cations Ca^{2+} , Sr^{2+} , and Ba^{2+} (Figure A.4) suggest a 1:2 (ML_2) complex stoichiometry. Models based on a 1:1 and 2:1 stoichiometries or a combination, did not give proper fits. As a result thereof, the equilibrium for the extraction of the divalent cations can be written as equation 11, with equation 12 describing the corresponding extraction constant.



$$K_{\text{ex}}^M = [M((\text{Htris})_3\text{L})_2]_{\text{org}} [\text{Htris}^+]_{\text{aq}}^2 / [M^{2+}]_{\text{aq}} [(\text{Htris})_4\text{L}]_{\text{org}}^2 \quad (12)$$

Because of the equal volumes used, a decrease of $[M^{2+}]_{\text{aq}}$ in the aqueous phase leads to an equal increase of $[M((\text{Htris})_3\text{L})_2]_{\text{org}}$ in the organic phase, allowing for direct comparison of the concentrations of the two phases. This results in the equations 13 and 14 for the mass balances of M^{2+} and L, respectively.

$$[M^{2+}]_{\text{tot}} = [M^{2+}]_{\text{aq}} + [M((\text{Htris})_3\text{L})_2]_{\text{org}} \quad (13)$$

$$[L]_{\text{tot}} = [(\text{Htris})_4\text{L}]_{\text{org}} + 2[M((\text{Htris})_3\text{L})_2]_{\text{org}} \quad (14)$$

The extraction percentages obtained for the competing cations (see Table 1) are incorporated in equations 12-14 as $p_M = [M((Htris)_3L)_2]_{org}/[M^{2+}]_{tot}$, $[M((Htris)_3L)_2]_{org} = p_M[M^{2+}]_{tot}$, and $[M^{2+}]_{aq} = (1-p_M)[M^{2+}]_{tot}$.

The extraction percentages of the competing M^{2+} cations in a concentration range of $(0.2-3.0) \times 10^{-4}$ M are provided in Figure A.4. From these extraction curves, K_{ex}^M can be obtained by fitting calculated p_M values to the experimentally determined values (Table 5.2), using a non-linear least squares fitting procedure.

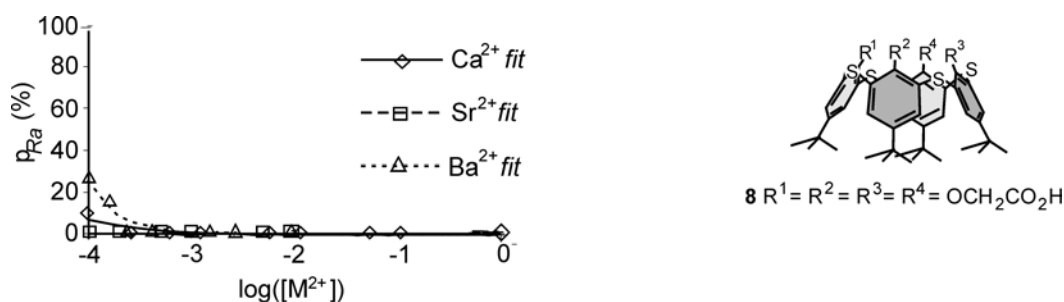
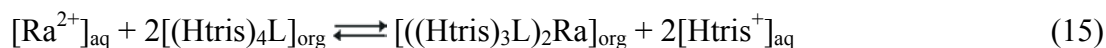


Figure A.5. Ra^{2+} extraction percentages (p_{Ra} (%)) for extractant **8** (10^{-4} M; 1 mL of CH_2Cl_2), as a function of the $M(NO_3)_2$ concentration ($M = Ca^{2+}$, Sr^{2+} , or Ba^{2+} ; 1 mL of water pH 8.9 tris-HCl buffer), with 2.9×10^{-8} M Ra^{2+} . The fitted curves are depicted.

When the Ra^{2+} experiments, in competition with the divalent cations Ca^{2+} , Sr^{2+} , and Ba^{2+} (Figure A.5), are modelled, additional equilibria and mass balances have to be considered. The extraction equilibrium and its extraction constant are given in equations 15 and 16, respectively. The Ra^{2+} mass balance is given in equation 17, and the ligand mass balance (equation 4) is now expanded to equation 18.



$$K_{ex}^{Ra} = [Ra((Htris)_3L)_2]_{org}[Htris^+]_{aq}^2/[Ra^{2+}]_{aq}[(Htris)_4L]_{org}^2 \quad (16)$$

$$[Ra^{2+}]_{tot} = [Ra^{2+}]_{aq} + [Ra((Htris)_3L)_2]_{org} \quad (17)$$

$$[L]_{tot} = [(Htris)_4L]_{org} + 2[M((Htris)_3L)_2]_{org} + 2[Ra((Htris)_3L)_2]_{org} \quad (18)$$

However, because of the small amount of $[Ra^{2+}]_{tot}$ (2.9×10^{-8} M), $[RaL]_{org}$ can be neglected in equation 18. Similar to p_M for the competing cations, p_{Ra} is defined as

$[\text{RaL}]_{\text{org}}/[\text{Ra}^{2+}]_{\text{tot}}$, resulting in $[\text{RaL}]_{\text{org}} = p_{Ra}[\text{Ra}^{2+}]_{\text{tot}}$, and $[\text{Ra}^{2+}]_{\text{aq}} = (1-p_{Ra})[\text{Ra}^{2+}]_{\text{tot}}$. Thus the $K_{\text{ex}}^{\text{Ra}}/K_{\text{ex}}^{\text{M}}$ ratio (equation 19) can be written as equation 20.

$$K_{\text{ex}}^{\text{Ra}}/K_{\text{ex}}^{\text{M}} = ([\text{Ra}((\text{Htris})_3\text{L})_2]_{\text{org}}/[\text{Ra}^{2+}]_{\text{aq}})([\text{M}^{2+}]_{\text{aq}}/[\text{M}((\text{Htris})_3\text{L})_2]_{\text{org}}) \quad (19)$$

$$K_{\text{ex}}^{\text{Ra}}/K_{\text{ex}}^{\text{M}} = (p_{Ra}/p_M)(1-p_M)/(1-p_{Ra}) \quad (20)$$

Since the K_{ex}^{M} values of the different extractants have different dimensions, only $K_{\text{M}}^{\text{Ra}}/K_{\text{ex}}^{\text{M}}$ ratios are given. These ratios are obtained by fitting calculated p_{Ra} values to the experimentally determined values (Figure A.5), using a non-linear least squares fitting procedure.

References

1. Kearns, A.; Cole, L.; Haws, C. R.; Evans, D. E. *Plant Physiol. Biochem.* **1998**, *36*, 879-887.
2. Equations previously derived in Chapter 4.

Chapter 6

Selective Ra^{2+} Extractants Provided by Self-assembly of Guanosine and Isoguanosine Derivatives*

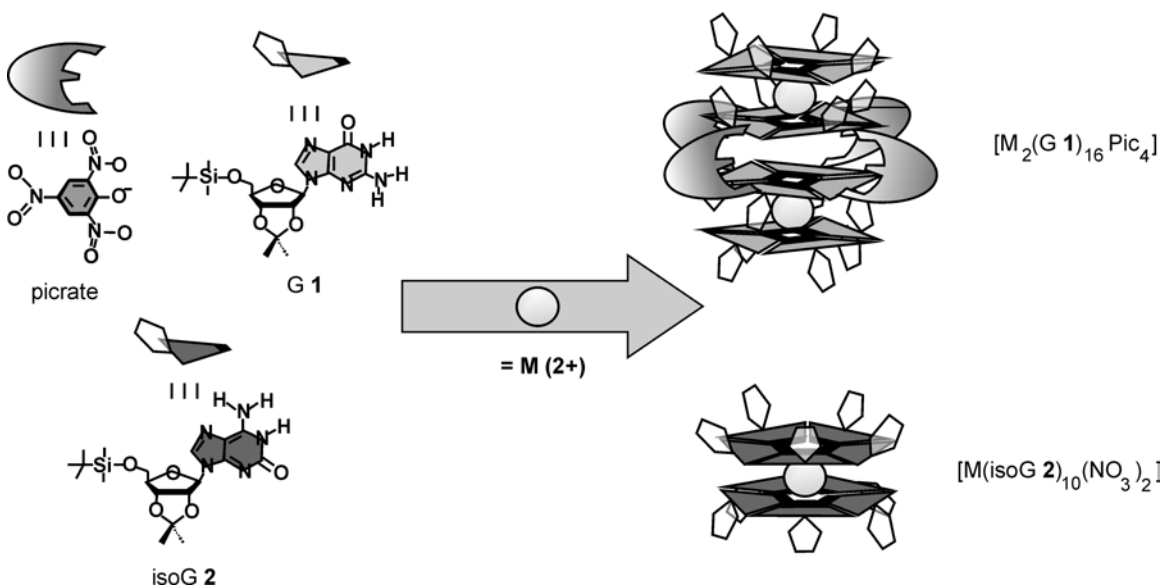
Abstract: The self-assembled guanosine (G 1)-based hexadecamers and isoguanosine (isoG 2)-based decamers are excellent Ra^{2+} selective extractants even in the presence of excess alkali (Na^+ , K^+ , Rb^+ , and Cs^+) and alkaline earth (Mg^{2+} , Ca^{2+} , Sr^{2+} , and Ba^{2+}) cations over the pH range of 3-11. G 1 requires additional picrate anions to provide a neutral assembly, whereas the isoG 2 assembly extracts Ra^{2+} cations without any such additives. Both G 1-Picrate and isoG 2 assemblies show Ra^{2+} extraction even at a 0.35×10^6 fold excess of Na^+ , K^+ , Rb^+ , Cs^+ , Mg^{2+} , or Ca^{2+} (10^{-2} M) to Ra^{2+} (2.9×10^{-8} M) and at a hundred-fold salt to extractant excess. In the case of the G 1-Picrate assembly, more competition was observed from Sr^{2+} and Ba^{2+} , as extraction of Ra^{2+} ceased at a $\text{M}^{2+}/\text{Ra}^{2+}$ ratio of 10^6 and 10^4 , respectively. With the isoG 2 assembly Ra^{2+} extraction also occurred at a $\text{Sr}^{2+}/\text{Ra}^{2+}$ ratio of 10^6 , but ceased at a 10^6 excess of Ba^{2+} . The results clearly demonstrate the power of molecular self-assembly for the construction of highly selective extractants.

* This chapter has been published in: Van Leeuwen, F. W. B.; Verboom, W.; Shi, X.; Davis, J. T.; Reinhoudt, D. N. *J. Am. Chem. Soc.* **2004**, *126*, 16575-16581.

6.1 Introduction

The known Ra^{2+} extraction procedures (Chapter 2) mainly use crown ether-like compounds with ionizable groups that allow for overall neutrality of the resulting salt-crown complexes,¹⁻⁴ a conventional approach described in Chapters 2, 4, and 5. However, the drawbacks to these crown ethers as extractants include the considerable effort often required for their synthesis and the limitation that they function only above pH 6,³ since cation extraction depends on the ionization state of the acidic groups.

Nature uses molecular self-assembly to form many receptors and this would also provide a powerful tool for the formation of selective extractants.⁵ Guanosine-rich nucleic acids are well known to coordinate alkali and alkaline earth cations using the G-quartet motif.^{6,7} Synthetic guanosine derivatives also form highly organized and well characterized structures in the presence of a range of monovalent and divalent cations.⁸



Scheme 6.1. The cation induced self-assembly of guanosine (G 1) and picrate giving a $[2M^{2+} \cdot (G\ 1)_{16} \cdot 4Pic^-]$ complex, which corresponds to a 8:1 extractant-cation stoichiometry. The cation induced self-assembly of isoguanosine (isoG 2) giving a 10:1 stoichiometry. These stoichiometries are based on their Ba^{2+} and Cs^+ complexes, respectively.^{10,11}

As schematically depicted in Scheme 6.1, X-ray crystallography has shown that the guanosine (G **1**) derivative forms non-covalent assemblies stabilized by picrate, that are based on (G **1**)₈-M⁺⁽⁺⁾ octamers, while the isoguanosine (isoG **2**) derivative forms decamers in the presence of a templating cation. The G **1** assembly has a relatively high K⁺, Sr²⁺, and Ba²⁺ affinity,^{9,10} whereas the isoG **2** assembly shows strongest affinity for the larger Cs⁺ and Ba²⁺ cations.^{11,12} This cation binding selectivity is attributed to the geometry of the hydrogen bond donors and acceptors: G **1** forms tetramers, whereas isoG **2** prefers to form hydrogen-bonded pentamers in the presence of the cation template. In addition, recent calculations on a series of (isoG)_n-M⁺ complexes support our experimental observations that (isoG)₅-M⁺ pentamers are favored over the (isoG)₄-M⁺ tetramers by the alkali metal cations larger than Li⁺.¹³ The macrocycle cavity size of these self-assembled extractants determines the cation binding selectivity.

In separations of Group I and II cations, selectivity is often controlled by the extractant cavity size. A self-assembled receptor with multiple oxygen donors and a cavity that fits the Ra²⁺ coordination sphere is a logical start for identifying Ra²⁺ extractants. Since G **1**-Picrate and isoG **2** assemblies were shown to possess high affinities for cations similar to Ra²⁺, we reasoned they might be excellent candidates for Ra²⁺ coordination.

In this Chapter, the extremely high Ra²⁺ extraction selectivity of assemblies formed by the lipophilic nucleosides G **1** and isoG **2**, even in the presence of alkali and alkaline earth cations and over a wide pH range is reported.

6.2 Results and Discussion

6.2.1 Non-competitive Ra²⁺ Extraction Experiments

To evaluate the Ra²⁺ extraction ability of G **1** and isoG **2** assemblies, liquid-liquid extractions were first performed under non-competitive conditions. In each experiment the aqueous phase contained the same concentration of added Ra²⁺ cations ($[^{226}\text{Ra}^{2+}]_{\text{add}} = 2.9 \times 10^{-8}\text{M}$) and the organic phase contained 10⁻⁴ M of self-assembled extractant, assuming complete formation of the (G **1**)₈-M²⁺ and the (isoG **2**)₁₀-M²⁺ complexes. The G **1** assembly only extracted Ra²⁺ cations when picrate anions were present in the aqueous phase (100% extraction). In marked contrast, the isoG **2** assembly extracted 100% of the

Ra²⁺ cations, both with and without picrate anions in the aqueous phase. These extraction results are consistent with previous findings that additional “stabilizing” picrate anions are needed for the formation of neutral G-quadruplex structures using G **1**,^{9,10} whereas cation-templated formation of the isoG **2** decamer is known to be anion independent.^{11,12}

6.2.2 Binding Potential of G **1**-Picrate and IsoG **2** Assemblies for Divalent Alkaline Earth Cations

To study whether G **1**-Picrate and isoG **2** assemblies have a binding affinity for alkaline earth cations (Mg²⁺, Ca²⁺, Sr²⁺, and Ba²⁺) the relative extraction ability of G **1**-picrate and isoG **2** assemblies under non-competitive conditions, using non-radioactive nitrate salts (10⁻⁴ M), were determined with Inductively Coupled Plasma-Mass Spectrometry (ICP-MS). The results are summarized in Table 6.1.

Table 6.1. Extraction percentages [$p_M = [M^{2+}]_{\text{org}}/[M^{2+}]_{\text{tot}}$ (%)] of Mg²⁺, Ca²⁺, Sr²⁺, and Ba²⁺ cations by G **1**-Picrate and isoG **2** assemblies, at an equimolar self-assembled extractant to cation concentration (10⁻⁴ M), determined by ICP-MS.^a

Extractant	Mg ²⁺ (%)	Ca ²⁺ (%)	Sr ²⁺ (%)	Ba ²⁺ ^b (%)
G 1 -Picrate	2	39	90	84
IsoG 2	1	57	32	48

^a In all cases metal nitrate salts were used. ^b Extraction percentages were verified under identical conditions with a ¹³³Ba tracer.

The G **1**-Picrate assembly shows high relative extraction abilities for Sr²⁺ and Ba²⁺, compared to Ca²⁺ and Mg²⁺ cations. In the case of the isoG **2** assembly generally a lower extraction ability is observed, which may be due to the lack of a lipophilic anion such as picrate to facilitate partitioning of metal ions into the organic phase. However, the isoG **2** assembly still allows about 50% extraction of Ca²⁺ and Ba²⁺ cations under these conditions.

6.2.3 Competitive Ra^{2+} Extraction Experiments in the Presence of Alkaline Earth Cations

In order to determine whether Ra^{2+} would be extracted in competition with Mg^{2+} , Ca^{2+} , Sr^{2+} , and Ba^{2+} , extractions were performed under the same conditions as were used for the ICP-MS analyzed extractions (Table 6.1). For these Ra^{2+} extraction experiments a ratio of Ra^{2+} cations to competing alkaline earth cations of $2.9 \times 10^{-8} \text{ M}$ to 10^{-4} M was used. After adding the Ra^{2+} cations, extraction experiments with G 1-Picrate and isoG 2 assemblies revealed high Ra^{2+} selectivities with all four competing cations. This means that both nucleosides are able to selectively extract Ra^{2+} from a 3.5×10^3 fold excess of Mg^{2+} , Ca^{2+} , Sr^{2+} , and Ba^{2+} cations (Figure 6.1; $\log[\text{M}^{2+}] = -4$).

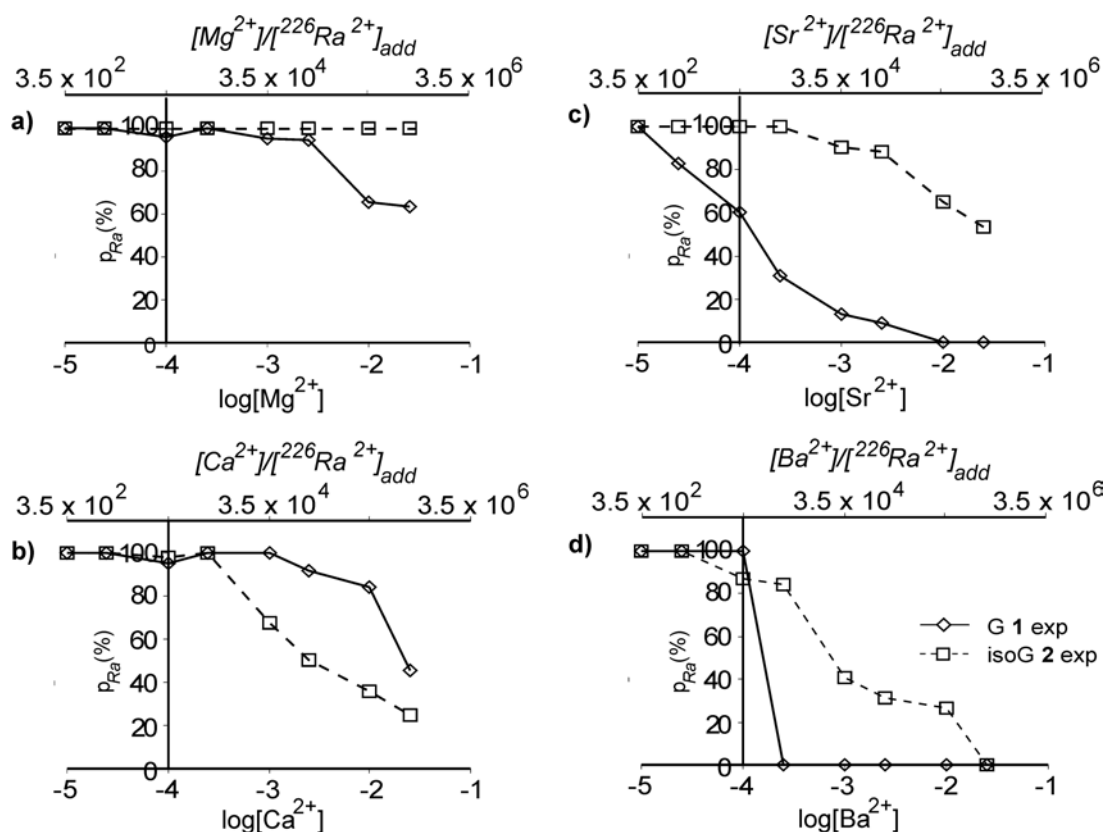


Figure 6.1. Ra^{2+} extraction percentages [$p_{\text{Ra}} = [^{226}\text{Ra}^{2+}]_{\text{org}}/[^{226}\text{Ra}^{2+}]_{\text{tot}}$ (%)] for different ratios of extractant to $\text{M}(\text{NO}_3)_2$ ($\text{M} = \text{Mg}^{2+}$ (a), Ca^{2+} (b), Sr^{2+} (c), or Ba^{2+} (d)), using fixed extractant ($[(\text{G } 1)_8 + 2(\text{Pic}^-)] = [(\text{isoG } 2)_{10}] = 10^{-4} \text{ M}$), and Ra^{2+} ($2.9 \times 10^{-8} \text{ M}$) concentrations. The $\log[\text{M}^{2+}]$ values correlate directly with $[\text{M}^{2+}]/[^{226}\text{Ra}^{2+}]_{\text{add}}$ values; $-4 = 3.5 \times 10^3$, $-3 = 3.5 \times 10^4$, $-2 = 3.5 \times 10^5$, and $-1.6 = 0.8 \times 10^6$.¹⁴

To determine the range in which G **1**-Picrate and isoG **2** assemblies are effective Ra^{2+} extractants, competition experiments with the single cations (Mg^{2+} , Ca^{2+} , Sr^{2+} , and Ba^{2+}) were carried out. The smallest of the alkaline earth cations Mg^{2+} showed high $\text{Ra}^{2+}/\text{Mg}^{2+}$ extraction selectivities for both the G **1**-Picrate and isoG **2** assemblies. At a 10^6 fold excess of Mg^{2+} to Ra^{2+} cations (salt to extractant ratio of 240), 63% of the Ra^{2+} cations were still extracted (Figure 6.1a; $\log[\text{Mg}^{2+}] = -1.6$) by the G **1**-picrate assembly. However, the isoG **2** assembly (without added picrate) did not show any interference in its Ra extraction percentage by Mg^{2+} , which is a common cation in saline waters containing Ra^{2+} .¹⁵ The isoG **2** assembly can quantitatively remove Ra^{2+} cations from solutions containing more than a million-fold excess of Mg^{2+} cations, and the G **1**-Picrate assembly maintains a significant Ra^{2+} selectivity under identical conditions.

At a $\text{Ca}^{2+}/\text{Ra}^{2+}$ ratio of 10^6 , 45% and 25% of the Ra^{2+} cations were still extracted by both the G **1**-Picrate and isoG **2** assemblies, respectively (Figure 6.1b; $\log[\text{Ca}^{2+}] = -1.6$). These comparative extraction data show that assemblies of both the lipophilic nucleosides G **1** and isoG **2** are able to selectively remove Ra^{2+} from a million-fold excess of Ca^{2+} cations.

In the presence of Sr^{2+} cations, the isoG **2** assembly shows a remarkable Ra^{2+} cation selectivity (53%; $\text{Sr}^{2+}/\text{Ra}^{2+} = 10^6$), but the G **1**-Picrate assembly fails to extract Ra^{2+} above a ratio of 10^5 (Figure 6.1c). This results in a more than hundred-fold higher selectivity in the case of the isoG **2** assembly, allowing for Ra^{2+} extraction at a million-fold excess of competing Sr^{2+} cations.

In the case of Ba^{2+} , the cation most similar in size to Ra^{2+} ,²² the $\text{Ra}^{2+}/\text{Ba}^{2+}$ extraction selectivities are significantly lower for both extractants (Figure 6.1d). Whereas the G **1**-Picrate assembly shows a sharp drop as soon as the Ba^{2+} concentration exceeds that of [(G **1**)₈] (at a $\text{Ba}^{2+}/\text{Ra}^{2+}$ ratio of 3.5×10^3 ; Figure 6.1d; $\log[\text{Ba}^{2+}] = -4$), the isoG **2** assembly continues extracting Ra^{2+} up to a ratio of 10^6 . The ability to differentiate between the similar chemical properties and sizes of Ba^{2+} (1.35-1.61 Å) and Ra^{2+} (1.48-1.70 Å)¹⁶ cations suggests that the self-assembled extractants prepared from isoG **2** are excellent $\text{Ra}^{2+}/\text{Ba}^{2+}$ selective extractants.

In comparing the Mg²⁺, Ca²⁺, Sr²⁺, Ba²⁺, and Ra²⁺ selectivities and the relative extraction ability of the G **1**-Picrate assembly, a trend related to the cation size can be observed. The G **1**-Picrate assembly has the highest affinity for Sr²⁺ and Ba²⁺ (Table 6.1), which is in direct agreement with previous findings that G **1** based octamers have the optimal coordination sphere for Sr²⁺ and Ba²⁺ cations.¹² Therefore, the lowest Ra²⁺ selectivities were observed in competition experiments with these cations (Figures 6.1c and d). In the case of Mg²⁺ and Ca²⁺ hardly any affinity of the G **1**-Picrate assembly was observed (Table 6.1); as a consequence, very high Ra²⁺ selectivities by the G **1**-Picrate assembly were obtained for these cations (Figures 6.1a and b). While the isoG **2** assembly shows relatively low extraction abilities for the alkaline earth cations (Table 6.1), it has impressive Ra²⁺ selectivities in their presence (Figure 6.2; Scheme 6.2). This indicates that the isoG **2** decamer has a preference for binding the “largest” Ra²⁺ (1.48-1.70 Å) cations, over the smaller alkaline earth cations (0.52-1.61 Å). This is consistent with the isoG **2** assembly being a Cs⁺ (1.67-1.88 Å)¹⁶ selective extractant in the presence of the smaller alkali cations.¹⁷

In addition to the high selectivities reported in the presence of the other alkaline earth cations, the presence of G **1** and isoG **2** in the organic phase greatly reduced the deficit of detectable Ra²⁺ cations (Figure 6.2a-c), as compared to that reported for the blank experiments (see Chapter 4).

With Mg²⁺ cations the presence of G **1** and isoG **2** still allows for the detection of nearly all the Ra²⁺ cations (> 80%) at 10⁻⁴ M, which is a considerable improvement to the 10% of Ra²⁺ detected under blank conditions. IsoG **2** continues to show a near quantitative presence of Ra²⁺ cations with Ca²⁺, Sr²⁺, and Ba²⁺ cations. In the case of G **1**, the presence of Ca²⁺ and Sr²⁺ cations gave similar amounts of detected Ra²⁺ cations as was reported for the blank experiments, while the presence of Ba²⁺ cations gave near quantitative amounts (> 80%) of detected Ra²⁺ cations. These findings suggest that precipitation of Ra²⁺ salts is significantly prevented by the nucleosides used. The G **1**-picrate assembly and, in particular, the isoG **2** assembly are not only very selective Ra²⁺ extractants but they can also prevent “Ra-scale formation” from solutions containing an excess of alkaline earth cations.

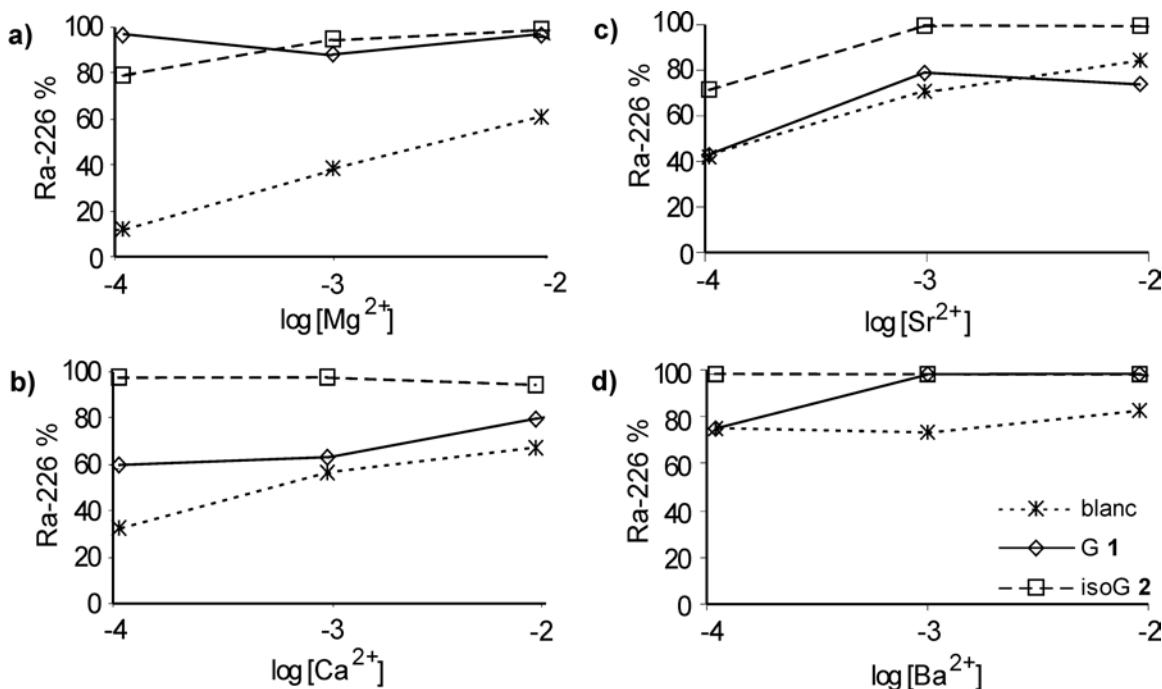


Figure 6.2. Ra^{2+} % present solution $[= [^{226}\text{Ra}^{2+}]_{\text{sol}}/[^{226}\text{Ra}^{2+}]_{\text{add}} (\%)]$ with varying concentrations of alkaline earth cations, after extraction with **G 1**-Picrate and **isoG 2**. Different salt concentrations $\text{M}(\text{NO}_3)_n$ [$\text{M}^{2+} = \text{Mg}^{2+}$ (a), Ca^{2+} (b), Sr^{2+} (c), or Ba^{2+} (d)], fixed extractant ($[(\text{G } \mathbf{1})_8 + 2(\text{Pic}^-)] = [(\text{isoG } \mathbf{2})_{10}] = 10^{-4}$ M) and Ra^{2+} (2.9×10^{-8} M) concentrations were used.

6.2.4 Competitive Ra^{2+} Extraction Experiments in the Presence of Alkali Cations

Since Ra^{2+} -containing waters also contain relatively high concentrations of alkali cations,¹⁵ and previous work^{9,10} has shown that both the **G 1**-Picrate and **isoG 2** assemblies have high affinities for some of these cations, competitive extraction experiments with alkali cations were performed (Figure 6.3).

For both self-assembled systems of the nucleosides, **G 1** and **isoG 2**, the Ra^{2+} extraction efficiency does not seem to be perturbed by the presence of Na^+ , even at a $\text{Na}^+/\text{Ra}_{\text{add}}^{2+}$ ratio of 0.35×10^6 ; The **isoG 2** assembly showed only a slight drop in Ra^{2+} extraction at this point. Furthermore, both nucleosides extracted significant percentages of Ra^{2+} cations in the presence of high concentrations of competing K^+ , Rb^+ , and Cs^+ cations. Figure 6.3 shows that impressive Ra^{2+} extraction percentages were obtained for

both the G **1**-picrate assembly [K⁺ (54%), Rb⁺ (64%), Cs⁺ (87%)] and the isoG **2** assembly [K⁺ (66%), Rb⁺ (56%), Cs⁺ (18%)], even at [M⁺]/[²²⁶Ra²⁺]_{add} ratios of 0.35 x 10⁶. Since the lipophilic G **1**-Picrate assembly was shown to have a high K⁺ affinity,⁹ and the isoG **2** assembly a high Cs⁺ affinity,^{12,17} it is understandable that these particular alkali cations interfere the most with Ra²⁺ extraction.

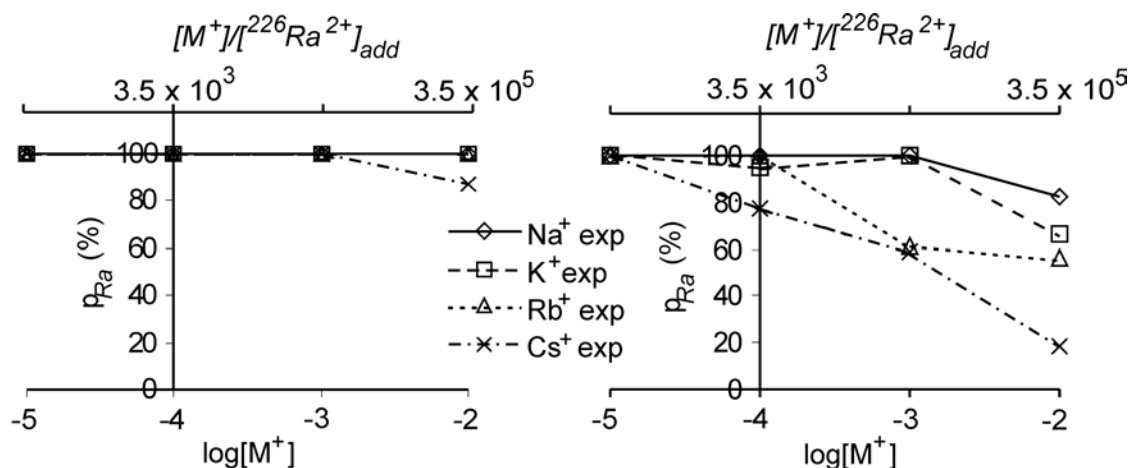


Figure 6.3. Ra²⁺ extraction percentages [$p_{Ra} = [^{226}\text{Ra}^{2+}]_{\text{org}}/[^{226}\text{Ra}^{2+}]_{\text{tot}}$ (%)] for different ratios of extractant (L) to M(NO₃) (M = Na⁺, K⁺, Rb⁺, and Cs⁺), using fixed extractant ([G **1**]₈ + 2(Pic⁻)] (a) and [isoG **2**]₁₀] (b); both 10⁻⁴ M, and Ra²⁺ (2.9 x 10⁻⁸ M) concentrations. The $\log[M^+]$ values correlate directly with $[M^+]/[^{226}\text{Ra}^{2+}]_{\text{add}}$ values; -4 = 3.5 x 10³, -3 = 3.5 x 10⁴, -2 = 3.5 x 10⁵, and -2.4 = 0.8 x 10⁶.¹⁸

In accordance with its high Ra²⁺ selectivity in the presence of alkali cations, the G **1**-Picrate assembly shows, in all cases, near quantitative percentages of detected Ra²⁺ cations, which is a significant improvement to the amounts found under blank conditions (no extractant used; see Chapter 4). The isoG **2** assembly, however, still shows a loss of Ra²⁺ cations in the presence of Na⁺, K⁺, and, in particular, Cs⁺ cations. As the isoG **2**-assembly has its Ra²⁺ extraction considerably interfered with by the presence of Cs⁺ cations, the loss of Ra²⁺ cations can be attributed to its lower Ra²⁺ selectivity in the presence of these cations (Figure 6.4a-c).

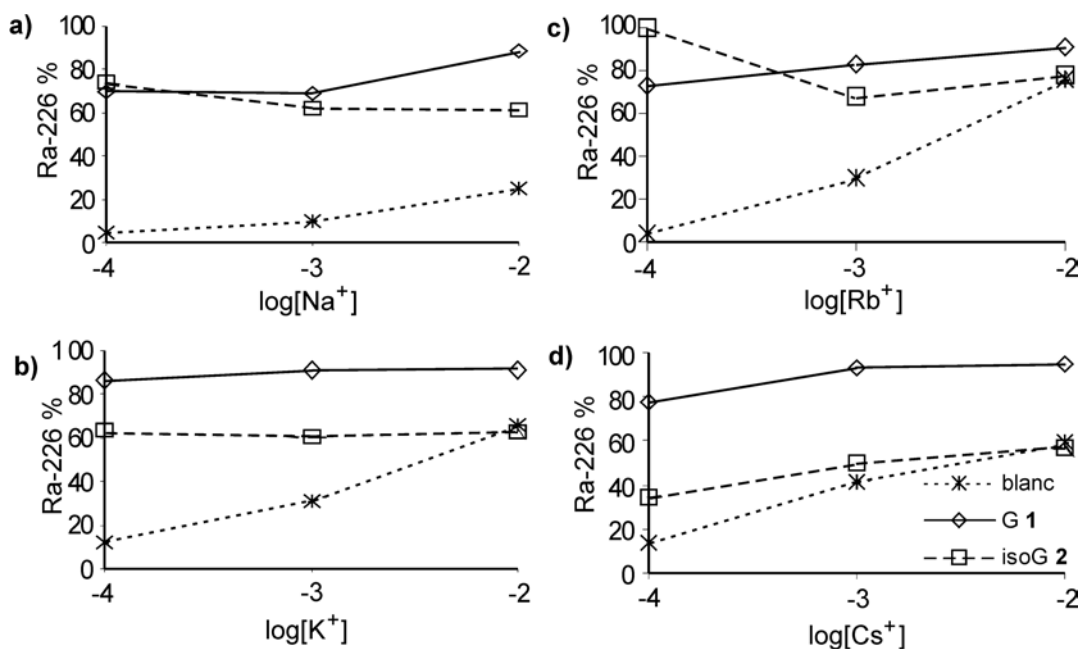
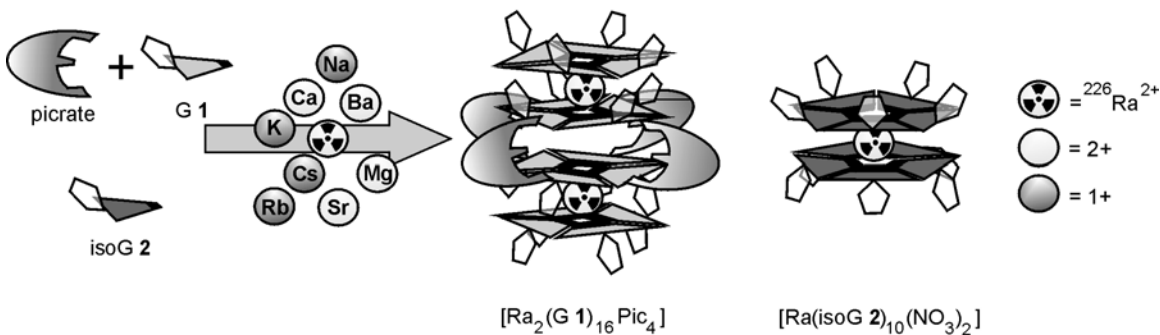


Figure 6.4. Ra^{2+} % present in solution $[= [^{226}\text{Ra}^{2+}]_{\text{solv}}/[^{226}\text{Ra}^{2+}]_{\text{add}} (\%)]$ with varying concentrations of alkali cations, after extraction with G 1-Picrate and isoG 2. Different salt concentrations $\text{M}(\text{NO}_3)_n$ [$\text{M}^+ = \text{Na}^+$ (a), K^+ (b), Rb^+ (c), or Cs^+ (d)], fixed extractant ($[(\text{G } 1)_8 + 2(\text{Pic}^-)] = [(\text{isoG } 2)_{10}] = 10^{-4}$ M) and Ra^{2+} (2.9×10^{-8} M) concentrations were used.

Extraction of Ra^{2+} by G 1-Picrate and isoG 2 assemblies occurs even in the presence of a 0.35×10^6 fold excess of monovalent alkali cations. Additionally, Ra^{2+} “precipitation” is significantly prevented by the presence of both G 1 and isoG 2. Clearly, the noncovalent assemblies formed by G 1 and isoG 2 are much more favorable at binding divalent Ra^{2+} cations than monovalent alkali cations (Scheme 6.2).



Scheme 6.2

6.2.5 Determination of the Effective pH Range

The pH profiles for Ra²⁺ extraction by G **1**-Picrate and isoG **2** assemblies, obtained under non-competitive conditions, indicate that both these nucleosides are effective Ra²⁺ extractants between pH 3 and 11 (Figure 6.5).

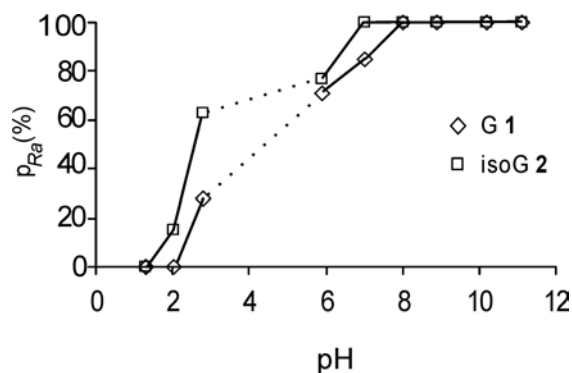


Figure 6.5. Influence of the pH on the Ra²⁺ extraction of G **1**-picrate and isoG **2** assemblies.¹⁹

Between pH 2 and pH 8 the extraction efficiency shows an upward trend for both the G **1**-Picrate and the isoG **2** assemblies and above pH 8 the Ra²⁺ extraction becomes quantitative. This significantly improves the effective pH region compared to that reported by Chen et al. for self-neutralizing systems (pH 6-11) viz. *p*-*tert*-butylcalix[4]arene-crown-6-dicarboxylic acid, *p*-*tert*-butylcalix[4]arene-crown-6-dihydroxamic acid, a 17-crown-5 ether with one pendant carboxylic acid group, and an acyclic polyether with two pendant carboxylic acid groups.³ In order to verify the results obtained with the low Ra²⁺ concentrations used ($[L]/[^{226}\text{Ra}^{2+}_{\text{add}}] = 3.5 \times 10^3$), extraction experiments were performed using an 4×10^2 excess of Ba²⁺ nitrate and two equivalents of Lithium Picrate in the case of G **1**. These experiments were monitored by ¹H NMR spectroscopy for the formation of the corresponding G **1**-picrate and isoG **2** assemblies. The hexadecameric assembly of G **1**, $2\text{Ba}^{2+} \cdot [\text{G } \mathbf{1}]_{16} \cdot 4\text{Pic}^-$, was shown to be stable between pH 2 and 11. Below pH 2, the picrate (pK_a = 0.38 in water)²⁰ peak and signals for $2\text{Ba}^{2+} \cdot [\text{G } \mathbf{1}]_{16} \cdot 4\text{Pic}^-$ broaden and NMR signals for “free” G **1** are observed. Above pH 11, NMR signals for the G-quadruplex $2\text{Ba}^{2+} \cdot [\text{G } \mathbf{1}]_{16} \cdot 4\text{Pic}^-$ could no longer be

observed.²¹ Characteristic NMR signals for the isoG **2** decamer, $\text{Ba}^{2+}\cdot[\text{isoG } \mathbf{2}]_{10}$, were also observed between pH 3 and 11. Below pH 3, an additional NH signal appeared and only partial complex formation was observed, while above pH 11, the characteristic NH signals of the decamer $\text{Ba}^{2+}\cdot[\text{isoG } \mathbf{2}]_{10}$ were no longer present.²² Assembly formation is clearly influenced by the presence of charges on the nucleoside monomers, as generated by protonation or deprotonation of the NH groups. Nevertheless, the effective pH range covers a broad region, making assemblies of G **1** and isoG **2** widely applicable extractants.

6.3 Conclusions

The noncovalent assemblies formed by G **1** and isoG **2** show high Ra^{2+} selectivities in the presence of divalent alkaline earth cations. Where G **1** requires the presence of a lipophilic anion before giving a high Ra^{2+} selectivity in the case of Mg^{2+} and Ca^{2+} , isoG **2** gives high selectivities in the presence of Mg^{2+} , Ca^{2+} , Sr^{2+} , and Ba^{2+} , without any additional additives.²³ Furthermore, a remarkable Ra^{2+} preference in the presence of monovalent alkali cations, “precipitation preventing/dissolving” characteristics, and a broad effective pH range were observed for both G **1** and isoG **2**. The ability to quantitatively and selectively extract a highly toxic radioisotope from a solution containing a million-fold excess of other cations shows the power and potential of using molecular self-assembly to construct highly selective receptors.

6.4 Experimental Section

Materials. The preparation of G **1**⁹ and isoG **2**²⁴ was performed according to literature procedures. Tris(hydroxymethyl)aminoethane (tris) 99.8+% was ordered from Aldrich. Concentrated HCl and HNO_3 acids and CH_2Cl_2 were of p.a. grade and used as received. The nitrate salts of K^+ ($\geq 99.5\%$), Rb^+ (p.a.) were purchased from Fluka Chemie and Na^+ (p.a.), Cs^+ (99%), Mg^{2+} (p.a.), Ca^{2+} (p.a.), Sr^{2+} (p.a.), and Ba^{2+} (p.a.) were purchased from Acros Organics. $^{133}\text{Ba}^{2+}$ stock solutions were purchased from Isotope Products Europe Blaseg GmbH. $^{226}\text{Ra}^{2+}$ stock solutions were purchased from AEA Technology QSA GmbH; ^{226}Ra was used because of its long half-life ($t_{1/2} = 1.6 \times 10^3$ y).

(Note: ²²⁶Ra has a very high radiotoxicity and should be handled with care and under radionuclear supervision)

Solutions. All basic experiments were performed using an aqueous phase with pH 8.9 (tris-HCl buffer) and an organic phase containing 10⁻⁴ M of extractant in CH₂Cl₂. The extractant concentrations of the organic solutions were based on the amount of “free” extractant needed to complex one alkaline earth cation [(G **1**)₈, (isoG **2**)₁₀]. The different nitrate salt concentrations were obtained by diluting stock solutions to the required concentration. From a 10 µg Ba²⁺/mL carrier containing stock solution of ¹³³Ba²⁺ in 0.1 M HCl, a dilution of 45.18 kBq/g in water was made. From a carrier free stock solution of ²²⁶Ra²⁺ in 0.5 M HCl, a dilution of 1.2 kBq/g (1.4 x 10⁻⁶ M) in 0.1 M HNO₃ was made.

General Extraction Procedures. Equal volumes (1.0 mL) of the organic and aqueous solutions were transferred into a screw cap vial with a volume of 4 mL. The samples were shaken (1500 rpm) at ambient temperatures (22-24 °C) for 1 h to ensure complete settling of the two-phase equilibration. In the case of the G **1** extraction experiments two molar equivalents, compared to [(G **1**)₈], of LiPic were added to allow for full extraction. After extraction, the solutions were disengaged by centrifugation (1600 rpm for 5 min) and aliquots (0.5 mL) of the organic and aqueous phases were pipetted out. Experiments were performed in duplicate; average values are reported, with an estimated error of 10-15%.

ICP-MS Monitored Extraction Procedures. The solvent of the aliquot taken from the organic phase was evaporated and the residue destructed in 0.5 mL of concentrated HNO₃. The cation concentrations were measured on a Perkin Elmer Sciex Elan 6000 ICP-MS instrument, using a Cross flow nebulizer. The extraction percentage is defined as 100% times the ratio of cation concentration in the organic phase ([M_o]) and the added cation concentration ([M_{add}]) (equation 1).²⁵

$$E\% = 100\%([M_o]/[M_{add}]) \quad (1)$$

Non-competitive ICP-MS (Table 6.1). In the non-competitive extraction experiments the salt concentrations (M(NO₃)₂; M= Mg²⁺, Ca²⁺, Sr²⁺, and Ba²⁺) were equal to those of the extractants (10⁻⁴ M) and were verified by their mass-balances.

^{133}Ba Tracer Experiments (Table 6.1). In $^{133}\text{Ba}^{2+}$ extraction experiments the exact conditions were used as described above for the ICP-MS experiments. But in this case, 10 μL of ^{133}Ba tracer (452 Bq) were added. The gamma-activity was determined using a NaI scintillation counter. The obtained extraction percentage is defined as 100% times the ratio of $^{133}\text{Ba}^{2+}$ activity in the organic phase (A_o) and the total $^{133}\text{Ba}^{2+}$ activity ($A_o + A_{aq}$) (equation 2).

$$E\% = 100\%(A_o/(A_o + A_{aq})) \quad (2)$$

Ra^{2+} Extraction Procedures. In the case of the Ra^{2+} extraction experiments, to the aqueous phase 20 μL of $^{226}\text{Ra}^{2+}$ tracer (240 Bq) were added. The gamma-activity was determined with a Ge(Li) scintillation counter. The obtained extraction percentage is defined as 100% times the ratio of $^{226}\text{Ra}^{2+}$ activity in the organic phase (A_o) and the total $^{226}\text{Ra}^{2+}$ activity ($A_o + A_{aq}$) (equation 2).

Non-competitive Ra^{2+} Extractions. In the non-competitive extraction experiments the aqueous phase only contained $^{226}\text{Ra}^{2+}$ cations in 1 mL of pH 8.9 tris-HCl buffer. In order to determine the influence of picrate anions on the extraction behavior of the G 1 and isoG 2 assemblies, additional experiments were performed in which two molar equivalents of LiPic (2×10^{-4} M) were added to the aqueous phases.

Competitive $^{226}\text{Ra}^{2+}$ Extraction Curves (single competing cation; Figures 6.1 and 6.3). In the competitive extraction experiments, aqueous phase pH 8.9 (tris-HCl), the ratio of competing $\text{M}^n(\text{NO}_3)_n$ ($\text{M} = \text{Na}^+, \text{K}^+, \text{Rb}^+, \text{Cs}^+, \text{Mg}^{2+}, \text{Ca}^{2+}, \text{Sr}^{2+}, \text{and Ba}^{2+}$) salt concentrations compared to a fixed extractant concentration (1 mL; 10^{-4} M) was altered to provide competing cation-concentration dependent extraction curves.

Precipitation Experiments with G 1 and isoG 2 (Figure 6.2 and 6.4). Extraction experiments were performed under competitive conditions. In an aqueous phase pH 8.9 (tris-HCl), the ratio of competing $\text{M}(\text{NO}_3)_n$ ($\text{M} = \text{Na}^+, \text{K}^+, \text{Rb}^+, \text{Cs}^+, \text{Mg}^{2+}, \text{Ca}^{2+}, \text{Sr}^{2+}, \text{and Ba}^{2+}$) salt concentrations was altered compared to a fixed extractant concentration (1 mL; 10^{-4} M) in the organic phase. The detectable amount of $^{226}\text{Ra}^{2+}$ tracer was determined and the $^{226}\text{Ra}^{2+}$ percentages obtained with G 1 and isoG 2, were

defined as 100% times the ratio of the sum of ²²⁶Ra²⁺ in the aqueous and organic phase ($A_{aq} + A_o$), and the amount of ²²⁶Ra²⁺ added (A_{add}) (equation 3).

$$Ra\% = 100\% \cdot ((A_{aq} + A_o) / A_{add}) \quad (3)$$

Extraction vs. pH Curves (Figure 6.5). Experiments were performed using a fixed extractant (G **1**)₈ or (isoG **2**)₁₀ concentration of 10⁻⁴ M and a fixed ²²⁶Ra²⁺ concentration (2.9 x 10⁻⁸ M). The pH values were set using different buffer solutions: pH 1-3; glycerol-LiCl-HCl (G **1**) and HCl (isoG **2**),²⁶ pH 6-7; imidazol-HCl, pH 8-10; tris-HCl, and pH 10-13; tris-(CH₃)₃NOH.

¹H NMR Monitored Extraction Experiments. Using the same buffer solutions as mentioned above, solid phase extraction experiments of Ba(NO₃)₂ (0.1 g; 3.8 x 10⁻⁴ mol) were performed with a 1 mL, buffer containing, aqueous phase and a 1.0 mL organic phase, containing 10⁻³ M of extractant. ¹H NMR spectra were obtained on a Varian INOVA 300 spectrometer

References

1. McDowell, W. J.; Arndsten, B. A.; Case, G. N. *Solv. Extract. Ion Exch.* **1989**, *7*, 377-393.
2. Dietz, M. L.; Chiarizia, R.; Horwitz, E. P. *Anal. Chem.* **1997**, *69*, 3028-3037.
3. Chen, X. Y.; Ji, M.; Fisher, D. R.; Wai, C. M. *Inorg. Chem.* **1999**, *38*, 5449-5452.
4. Beklemishev, M. K.; Elshani, S.; Wai, C. M. *Anal. Chem.* **1994**, *66*, 3521-3527.
5. Whitesides, G. M.; Grzybowski, B. *Science* **2002**, *295*, 2418-2421.
6. Laughlan, G.; Murchie, A. I. H.; Norman, D. G.; Moore, M. H.; Moody, P. C. E.; Lilley, D. M. J.; Luisi, B. *Science* **1994**, *265*, 520-524.
7. Deng, J.; Xiong, Y.; Sundaralingam, M. *Proc. Nat. acad. Sci. U.S.* **2001**, *98*, 13665-13670.
8. Davis, J. T. *Angew. Chem. Int. Ed.* **2004**, *43*, 668-698.
9. Forman, S. L.; Fettingner, J. C.; Pieraccini, S.; Gottarelli, G.; Davis, J. T. *J. Am. Chem. Soc.* **2000**, *122*, 4060-4067.
10. Shi, X. D.; Mullaugh, K. M.; Fettingner, J. C.; Jiang, Y.; Hofstadler, S. A.; Davis, J. T. *J. Am. Chem. Soc.* **2003**, *125*, 10830-10841.
11. a) Cai, M. M.; Marlow, A. L.; Fettingner, J. C.; Fabris, D.; Haverlock, T. J.; Moyer, B. A.; Davis, J. T. *Angew. Chem. Int. Ed.* **2000**, *39*, 1283-1288. b) Shi, X.; Fettingner, J. C.; Cai, M. M.; Davis, J. T. *Angew. Chem. Int. Ed.*, **2000**, *39*, 3124-3127.
12. Lee, S. C.; Lamb, J. D.; Cai, M. M.; Davis, J. T. *J. Inclusion Phenom. Macrocyclic Chem.* **2001**, *40*, 51-57; The Ra²⁺ selectivity of the isoG **2** assembly is in agreement with competitive liquid membrane experiments, showing that the isoG **2** assembly

transports Ba^{2+} nitrate across supported liquid membranes much faster than it does the corresponding Na^+ and K^+ nitrate salts.

13. Meyer, M.; Suhnel, J. *J. Phys. Chem. A* **2003**, *107*, 1025-1031.
14. At concentrations $> 10^{-2}$ M the total detected amount of Ra^{2+} cations was almost equal to that originally added ($^{226}\text{Ra}^{2+}$)_{add}, which means that there are no losses due to Ra^{2+} salt precipitation.
15. Wiegand, J.; Feige, S. *Origin of Radium in High-Mineralized Waters* IAEA: Vienna, **2002**.
16. Shannon, R. D. *Acta Cryst. A* **1976**, *32*, 751-767.
17. Davis, J. T.; Tirumala, S. K.; Marlow, A. L. *J. Am. Chem. Soc.* **1997**, *119*, 5271-5272.
18. At concentrations of 10^{-2} M the total detected amount of Ra^{2+} cations with G **1** was almost equal to that originally added (Ra^{2+})_{add}, whereas isoG **2** still showed $^{226}\text{Ra}^{2+}$ salt precipitation.
19. Due to the competitive nature of the available buffers between pH 3 and 6, the $^{226}\text{Ra}^{2+}$ extraction percentages could not be accurately determined in this region. Therefore, the results are extrapolated from those obtained at pH 3 and 6.
20. Botoshansky, M.; Herbststein, F. H.; Kapon, M. *Acta Cryst. B* **1994**, *32*, 191-200.
21. Rogstad, K. N.; Jang, Y. H.; Sowers, L. C.; Goddard, W. A. *Chem. Res. Toxicol.* **2003**, *16*, 1455-1462; The loss of the G **1** complex stability below pH 2 and above pH 11 appears to match the guanosine pKa values ($\text{NH1} = 9.65$ and $\text{NH7/NH3} = 3.2$) determined in water.
22. Jang, Y. H.; Goddard, W. A.; Noyes, K. T.; Sowers, S. H.; Chung, D. S. *J. Phys. Chem. B* **2003**, *107*, 344-357; The loss of the isoG **2** complex stability below pH 3 and above pH 11 appears to match the isoguanosine pKa values ($\text{NH1} = 11.1$, and $\text{NH3} = 3.8$) determined in water.
23. A direct comparison with the extractants described in chapter 4, suggests that these systems are less Ra^{2+} selective.
24. Davis, J. T.; Tirumala, S.; Jenssen, J. R.; Radler, E.; Fabris, D. *J. Org. Chem.* **1995**, *60*, 4167-4176.
25. The isotope ^{43}Ca was corrected for the doubly charged interference of the isotope ^{88}Sr .
26. Below pH 3, G **1** seemed to have its Ra^{2+} extraction interfered by HCl, whereas isoG **2** had its Ra^{2+} extraction interfered by glycerol-HCl-LiCl.

Chapter 7

Selective Removal of Ra^{2+} from Produced Waters of the Gas Industry*

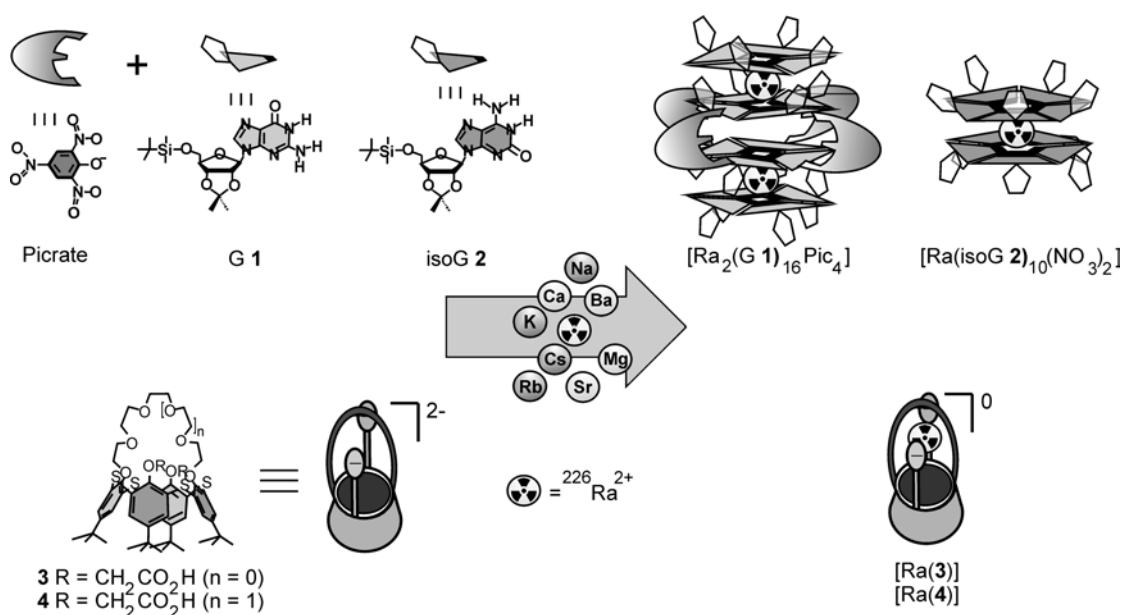
Abstract: The Ra^{2+} selectivity of both the self-assembled guanosine (G 1-Picrate) and isoguanosine (isoG 2) systems and the ionizable thiacalix[4]crown dicarboxylic acids 3 and 4 was determined in gas-field produced water and a metal ion-containing model solution. Seven gas-field produced water samples have been analyzed. From a representative sample (K5D; $[M_{tot}] = 0.14\text{ M}$), the thiacalix[4]arene derivative tcc5da 3 (10^{-4} M) extracts 60% of the Ra^{2+} content. Extractions performed with the model solution ($^M\text{K5D}$) indicate that in K5D there is significant competition in Ra^{2+} extraction due to the organic constituents of K5D, in particular with self-assembled extractants G 1-Picrate and isoG 2. Nevertheless, all four extractants extract Ra^{2+} both from the produced water K5D and the model solution $^M\text{K5D}$, even with a 100-fold excess of $[M_{tot}]/[\text{extractant}]$. The extracted Ra^{2+} cations could effectively be stripped from the extractants by washing with water of pH 2. The results obtained with these extractants, especially tcc5da 3, clearly demonstrate their potential for selective removal of Ra^{2+} from gas-field produced waters.

* This chapter has been submitted for publication: Van Leeuwen, F. W. B.; Miermans, C. J. H.; Beijleveld, H.; Tomasberger, T.; Davis, J. T.; Verboom, W.; Reinhoudt, D. N.

7.1 Introduction

Sedimentary rocks containing oil and gas deposits have a high concentration of the naturally occurring¹ nuclides ^{238}U and ^{232}Th and contain large quantities of Ra^{2+} holding formation water.²⁻⁴ When the oil and gas are transported to the surface, Ra^{2+} is introduced into the environment.⁵ Consequently, the oil and gas industries have to deal with the problem of “technologically enhanced naturally occurring radioactive material” (TENORM) (see Chapter 2).^{6,7}

A significant challenge is the selective extraction of Ra^{2+} (average concentration 5.9 – 9.0 Bq/L)⁵ from e.g. gas-field produced waters containing a large excess of other, mainly alkali(ne earth), cations,⁹ and anions e.g. SO_4^{2-} , Cl^- , and HCO_3^- .⁸ These waters also contain excesses of organic species, such as oil, monocyclic aromatic hydrocarbons, and fatty acids.^{9,10} In addition, commonly used water-soluble scale inhibitors such as different types of phosph(on)ates, carboxylates, and sulfonates can be present.⁸



Scheme 7.1

In the Chapters 4 and 6, both the noncovalent self-assembly of **G 1**-Picrate and **isoG 2** subunits¹¹ and the covalent self-neutralizing thiacalix[4]crown dicarboxylic acids (**3** and **4**)¹² are reported to be excellent Ra^{2+} selective extractants. In this chapter the use of highly Ra^{2+} selective extractants, **1-4** (Scheme 7.1), in actual gas-field

produced water conditions is described. To the best of our knowledge this is the first time that Ra²⁺ removal from produced water has been addressed with selective extractants.

7.2 Results and Discussion

7.2.1 Metal ion Constituents of Gas-field Produced Water

First, seven different samples from gas-wells at the Dutch continental shelf were analyzed using Inductively Coupled Plasma-Mass Spectrometry (ICP-MS) and a Flame Photometer.

Table 7.1. Metal ion content of seven produced water samples: range-, average-, and sample K5D- metal ion concentrations.^{a,13}

Metal ion	Range [M]	Average [M]	K5D [M]
Ti ^b	$9.4 \times 10^{-10} - 1.1 \times 10^{-6}$	2.3×10^{-7}	3.3×10^{-7}
Mn ^b	$2.3 \times 10^{-6} - 5.0 \times 10^{-4}$	9.6×10^{-5}	1.2×10^{-4}
Fe ^b	$2.6 \times 10^{-4} - 5.4 \times 10^{-3}$	1.4×10^{-3}	1.5×10^{-3}
Co ^b	$1.4 \times 10^{-7} - 5.6 \times 10^{-7}$	3.1×10^{-7}	2.3×10^{-7}
Ni ²⁺	$0 - 1.7 \times 10^{-6}$	9.0×10^{-7}	1.1×10^{-7}
Cu ^b	$8.8 \times 10^{-9} - 1.4 \times 10^{-6}$	3.8×10^{-7}	3.2×10^{-7}
Zn ²⁺	$0 - 2.3 \times 10^{-3}$	3.9×10^{-4}	3.9×10^{-4}
Cd ²⁺	$4.5 \times 10^{-11} - 3.3 \times 10^{-6}$	5.5×10^{-7}	4.9×10^{-7}
Ti ³⁺	$3.6 \times 10^{-10} - 7.4 \times 10^{-7}$	1.3×10^{-7}	1.7×10^{-7}
Pb ^b	$0 - 1.6 \times 10^{-4}$	2.4×10^{-5}	1.3×10^{-5}
Mg ²⁺	$0 - 5.0 \times 10^{-2}$	9.9×10^{-3}	1.5×10^{-2}
Ca ²⁺	$2.1 \times 10^{-6} - 3.8 \times 10^{-1}$	7.2×10^{-2}	1.1×10^{-1}
Sr ²⁺	$6.3 \times 10^{-8} - 6.2 \times 10^{-3}$	1.1×10^{-3}	1.5×10^{-3}
Ba ²⁺	$3.5 \times 10^{-8} - 1.4 \times 10^{-4}$	2.5×10^{-5}	1.8×10^{-5}
Na ⁺	$3.1 \times 10^{-4} - 2.1$	4.1×10^{-1}	5.7×10^{-1}
K ⁺	$6.1 \times 10^{-6} - 4.1 \times 10^{-3}$	1.4×10^{-3}	2.3×10^{-3}
Total		5.0×10^{-1}	7.0×10^{-1}

^a Determined with ICP-MS and in the case of Na⁺ and K⁺ a Flame Photometer

^b These metal ions can be present in a number of valencies.

Table 7.1 clearly shows the wide variety of cations present in the produced waters. Apart from traces of transition and other heavy metals (total 2×10^{-3} M) significant quantities of alkali(ne earth) cations are present (total 7×10^{-1} M). Of the latter the alkali cation Na^+ is by far the most abundant. Of the alkaline earth cations Ca^{2+} is the most abundant, followed by Mg^{2+} , Sr^{2+} , and Ba^{2+} . Based on the average metal ion concentrations, one produced water sample (K5D) was selected for further extraction experiments.

7.2.2 Ra^{2+} Extraction from a Produced Water Sample

To assess the $\text{Ra}^{2+}/M_{\text{tot}}$ separation from gas-field produced waters, liquid-liquid extractions were performed with 10^{-4} M extractant [(G **1**)₈, (isoG **2**)₁₀, **3**, and **4**]. This extractant concentration allows for a direct comparison with results described in Chapters 4 and 6, dealing with the $\text{Ra}^{2+}/M_{\text{single}}$ selectivity in the alkali(ne earth) cation series.^{11,12} A number of dilution steps were performed (5 - 100 times; samples K5D_{1/5} - K5D_{1/100}), to determine the Ra^{2+} extraction over $[M_{\text{tot}}]/[L]$ ratios ranging from 1400 to 70.

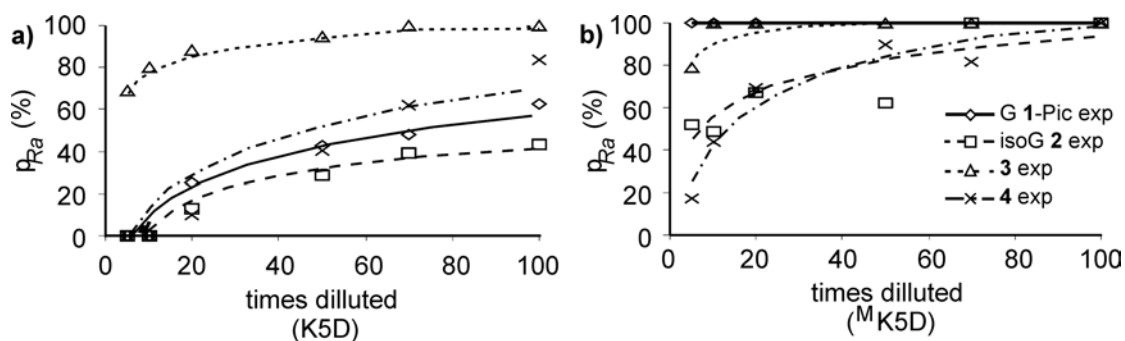


Figure 7.1. Ra^{2+} extraction percentages ($p_{\text{Ra}} = \frac{[^{226}\text{Ra}^{2+}]_{\text{org}}}{[^{226}\text{Ra}^{2+}]_{\text{tot}}}$ (%)) versus times of dilution: (a) produced water sample K5D and (b) metal ion-based model solution ^MK5D. Extraction percentages were determined using fixed extractant ($[(\text{G } \mathbf{1})_8 + 2(\text{Pic}^-)] = [(\text{isoG } \mathbf{2})_{10}] = [\mathbf{3}] = [\mathbf{4}] = 10^{-4}$ M), and $\text{Ra}^{2+}_{\text{add}}$ (2.9×10^{-8} M) concentrations.

The extraction data (Figure 7.1a) show that with thiacalix[4]crown-5 dicarboxylic acid (**3**), about 70% of Ra^{2+} can be extracted from K5D_{1/5}, whereas K5D_{1/70} and higher allow for quantitative extraction of Ra^{2+} . The other three

extractants, G **1**-Picrate, isoG **2**, and thiacalix[4]crown-6 dicarboxylic acid (**4**), only extract Ra²⁺ from the samples K5D_{1/20} - K5D_{1/100}. In the case of K5D_{1/100}, these extractants only give Ra²⁺ extraction percentages of 43%, 62%, and, 83% respectively. These results clearly show that thiacalix[4]crown-5 dicarboxylic acid (**3**) is the best Ra²⁺ extractant under these conditions.

To study the influence that the metal ions in K5D have on the Ra²⁺ extraction, extractions were performed with a metal ion-based model solution (^MK5D). This model solution contains the same concentration of the major metal ions present in produced water sample K5D, *viz.* Na⁺, K⁺, Mg²⁺, Ca²⁺, Sr²⁺, Ba²⁺, Fe³⁺, Mn²⁺, Zn²⁺, and Pb²⁺ (Table 7.1), resulting in a total metal ion concentration ([M_{tot}]) of 0.70 M.

The highest Ra²⁺ extraction percentages were obtained with G **1**-Picrate and thiacalix[4]crown-5 dicarboxylic acid (**3**), showing (near) quantitative Ra²⁺ extraction from ^MK5D_{1/5} (Figure 7.1b). This means that 10⁻⁴ M of extractant is able to extract 2.8 x 10⁻⁸ M Ra²⁺ from a total salt concentration of 0.14 M ([M_{tot}]/5). Surprisingly, the extractants reported to have the highest *overall* Ra²⁺ selectivities in the alkali(ne earth) series, isoG **2** (Chapter 6) and thiacalix[4]crown-6 dicarboxylic acid (**4**; Chapter 4), gave the poorest results with K5D and ^MK5D. Apparently, for these extractants there is more competition by the other cations present.¹⁴ Nevertheless, from ^MK5D_{1/70}, all four extractants quantitatively extracted Ra²⁺. This means that they can extract Ra²⁺ at a [M_{tot}]/[L] ratio of 100.

The extractants with the highest Ra²⁺/Na⁺_{single} selectivity (G **1**-Pic and thiacalix[4]crown-5 dicarboxylic acid (**3**); Chapters 4 and 6) show the highest Ra²⁺ extraction from ^MK5D (Figure 7.1b).^{11,12,15} In ^MK5D_{1/5} the concentrations of the other alkali(ne earth) cations (Table 7.1), in particular that of the second most abundant cation Ca²⁺ (1.1 x 10⁻¹ M), are below the previously determined thresholds for Ra²⁺ extraction (see Chapters 4 and 6). Of the extractants used, the lowest Ra²⁺/Ca²⁺ separation in the presence of only Ca²⁺ as competing cation has been reported in Chapter 6 for isoG **2**; at 2.4 x 10⁻² M Ca²⁺_{single} still 30% of Ra²⁺ is extracted.¹¹ Apparently, Na⁺, the most abundant cation in the solutions extracted here, is the metal ion that causes the competition in the Ra²⁺ extraction.

The extraction data of K5D (Figure 7.1a) clearly show a lower Ra²⁺ extraction efficiency than the ^MK5D model solution (Figure 7.1b). An increased competition in Ra²⁺ extraction is observed for all four extractants, however, it is most pronounced with G **1**-Picrate. Since the cationic content has been determined for a wide range of

metal ions, this indicates that either anionic or organic constituents of K5D have a negative influence on the Ra^{2+} extraction. The anions are assumed to have no effect on the extraction behavior, since G 1-Picrate,¹¹ thiacalix[4]crown dicarboxylic acids (**3** and **4**)¹² provide their own anionic groups for neutralization; the extraction behavior of isoG **2** is even anion independent.¹⁶⁻¹⁸ Therefore, organic pollutants are assumed to cause competition in the Ra^{2+} extraction. A result that is in agreement with the formation of a “soapy” third phase, when the K5D sample is diluted less than 70 times, while the ^MK5D does not show such a behavior. Consequently, the extractants G 1-Picrate, isoG **2**, and thiacalix[4]crown-6 dicarboxylic acid (**4**) might be much more effective in water streams, which do not contain competing organic constituents, but have Na^+ , Mg^{2+} , and Ca^{2+} as the main competing ions.¹⁹⁻²³

7.2.3 Stripping of the Organic Phases

Efficient extraction of Ra^{2+} depends on effective stripping from the organic phases into another aqueous solution. Therefore, Ra^{2+} stripping experiments were performed with samples of the organic phases obtained after the Ra^{2+} extraction experiments (see above; Figure 7.1). Average stripping percentages are shown in Figure 7.2.

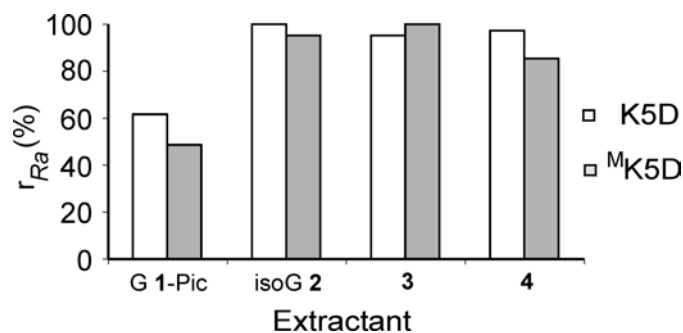


Figure 7.2. The average Ra^{2+} recovery ($r_{\text{Ra}} = \frac{[^{226}\text{Ra}^{2+}]_{\text{aq}}}{[^{226}\text{Ra}^{2+}]_{\text{tot}}} (\%)$) from G 1-Picrate, isoG **2**, and thiacalix[4]crown dicarboxylic acids **3** and **4**. Stripping of a 1 mL organic phase occurred with a 1 mL pH 2 aqueous phase (HCl).²⁴

The stripping experiments show that while G 1-Picrate only gives ~50% recovery, the other three extractants, isoG **2**, and thiacalix[4]crown dicarboxylic acids (**3** and **4**), give near quantitative Ra^{2+} recoveries, under the conditions used. This

means that these extractants are not only able to selectively extract Ra²⁺ cations, but can also effectively be stripped of their radioactive radium content.²⁵

7.3 Conclusions

The noncovalent assemblies formed by G **1**-Picrate and isoG **2** and the self-neutralizing extractants thiacalix[4]crown dicarboxylic acids (**3** and **4**) show an impressive Ra²⁺ extraction from K5D gas-field produced water and its model solution ^MK5D. The most effective thiacalix[4]crown, thiacalix[4]crown-5 dicarboxylic acid (**3**), gives Ra²⁺ extraction (70%) from K5D_{1/5}, whereas the most effective self-assembled extractant, G **1**-Pic, gives quantitative extraction from ^MK5D_{1/5}. For the latter, the organic pollutants present in produced water sample K5D may cause significant competition in the Ra²⁺ extraction. The ability to selectively extract Ra²⁺ from a solution containing an excess of other metal ions, together with various anions and organic compounds, followed by the quantitative stripping of the Ra²⁺ content, shows the potential of these extractants in industrial Ra²⁺ separations.

7.4 Experimental section

Materials. The preparation of G **1**²⁶, isoG **2**²⁷, and thiacalix[4]crown dicarboxylic acids (**3** and **4**)¹¹ was performed according to literature procedures. Tris(hydroxymethyl)aminoethane (tris) 99.8+% was ordered from Aldrich. The concentrated HCl and HNO₃ acids and CH₂Cl₂ were of p.a. grade and used as received. The nitrate salts of K⁺ (≥99.5%), Rb⁺ (p.a.), and Mn²⁺ (≥ 97.0%) were purchased from Fluka Chemie and Na⁺ (p.a.), Cs⁺ (99%), Mg²⁺(p.a.), Ca²⁺ (p.a.), Sr²⁺ (p.a.), Ba²⁺ (p.a.), Cd²⁺ (98%), Zn²⁺ (98+%), Pb²⁺ (p.a.), and Fe³⁺ (> 99%) were purchased from Acros Organics. ²²⁶Ra²⁺ stock solutions were purchased from AEA Technology QSA GmbH; ²²⁶Ra was used because of its long half-life (t_{1/2} = 1.6 x 10³ y). **(Note: ²²⁶Ra has a very high radiotoxicity and should be handled with care and under radionuclear supervision)**

Solutions. All basic experiments were performed using an organic phase containing 10⁻⁴ M extractant in CH₂Cl₂. The extractant concentrations of the organic solutions were based on the amount of “free” extractant needed to complex one alkaline earth cation [(G **1**)₈, (isoG **2**)₁₀, **3**, and **4**]. Produced water samples were used as obtained from the gas-well. The K5D metal ion-based model solution was made using metal nitrate salts, Na⁺ (5.7 x 10⁻¹ M), K⁺ (2.3 x 10⁻³ M), Mg²⁺ (1.5 x 10⁻² M),

Ca²⁺ (1.1 x 10⁻¹ M), Sr²⁺ (1.5 x 10⁻³ M), Ba²⁺ (1.8 x 10⁻⁵ M), Fe³⁺ (1.5 x 10⁻³ M), Mn²⁺ (1.2 x 10⁻⁴ M), Zn²⁺ (3.9 x 10⁻⁴ M), and Pb²⁺ (1.3 x 10⁻⁵ M), in demi-water. Produced water (model solution) dilutes, 5, 20, 50, 70, and 100 times, were made in a pH 8.9 tris-HCl buffer.²⁸ From a carrier free stock solution of ²²⁶Ra²⁺ in 0.5 M HCl, a dilution of 1.2 kBq/g (1.4 x 10⁻⁶ M) in 0.1 M HNO₃ was made.

Determination of the Metal Ion Contents of Produced Water Samples (Table 7.1). The analysis of the Mg, Ca, Ba, Sr, Fe, Mn, Zn, Pb, U, Tl, Te, Cd, Ag, Mo, Cu, Ni, Co, Ti, and Be metal ion content was performed using a Perkin Elmer Sciex Instruments Elan 6000 Inductively Coupled Plasma Mass Spectrometer equipped with a Cross-flow nebulizer, a platinum sampler, and a skimmer cone. Analysis was performed with: Ge and Re as internal standards, a power of 900 W, a nebulizer gas flow of 0.87 L/min, a Plasma gas flow of 15 L/min, and a sample uptake of 1 mL/min.²⁹ The analysis of the Na and K metal ion content was performed using an Eppendorf ELEX 6361 flame photometer.

Ra²⁺ Extraction Procedures (Figure 7.1). Equal volumes (2.0 mL) of the organic and aqueous solutions were transferred into a screw cap vial with a volume of 4 mL. To determine the ²²⁶Ra²⁺ extraction, 40 µL of ²²⁶Ra²⁺ tracer (480 Bq) was added to the aqueous phase (2.9 x 10⁻⁸ M).³⁰ In the case of the G 1 extraction experiments two equiv, compared to [(G 1)₈], of LiPic were added to allow for full extraction.¹¹ The samples were shaken (1500 rpm) at ambient temperatures (22-24 °C) for 1 h to ensure complete settling of the two-phase equilibration. After extraction, the solutions were disengaged by centrifugation (1600 rpm for 5 min) and aliquots (0.5 mL) of the organic and aqueous phases were pipetted out for the determination of the ²²⁶Ra²⁺ extraction percentages. The gamma-activity was determined with a HPGe detector. The obtained extraction percentages are defined as 100% times the ratio of activity in the organic phase (A_o) and the total activity (A_o + A_{aq}) (equation 1), with an estimated error of 10-15%.^{11,12}

$$E\% = 100\%(A_o/(A_o + A_{aq})) \quad (1)$$

Ra²⁺ Stripping Procedures (Figure 7.2). From the remaining 1.5 mL organic phase, a 1.0 mL sample was removed and transferred into a new screw cap vial with a volume of 4 mL. Subsequently, 1.0 mL of pH 2 adjusted water (HCl) was added and the samples were shaken (1500 rpm) at ambient temperatures (22-24 °C) for 1 h to

ensure complete settling of the two-phase equilibration. After extraction, the solutions were disengaged by centrifugation (1600 rpm for 5 min) and an aliquot (0.5 mL) of the aqueous phases was pipetted out for the determination of the Ra²⁺ stripping percentages. The obtained extraction percentages are defined as 100% times the ratio of the ²²⁶Ra activity in the aqueous stripping phase (A_{strip}) and the original activity in the organic phase (A_{org}) (equation 2), with an estimated error of 10-15%.^{11,12}

$$E\% = 100\%(A_{\text{strip}}/A_{\text{org}}) \quad (2)$$

References

1. Kathren, R. L. *Appl. Radiat. Isot.* **1998**, *49*, 149-168.
2. UNSCEAR, *Sources and Effects of Ionizing Radiation*, United Nations, New York 1977.
3. Shawky, S.; Amer, H.; Nada, A. A.; Abd El-Maksound, T. M.; Ibrahiem, N. M. *Appl. Radiat. Isot.* **2001**, *55*, 135-139.
4. Greeman, D. J.; Rose, A. W.; Washington, J. W.; Dobos, R. R., Ciolkosz, E. J. *Appl. Geochem.* **1999**, *14*, 365-385.
5. Strålberg, E.; Smith Varskog, A. Th.; Raaum, A.; Varskog, P. *Naturally Occurring Radionuclides in the Marine Environment – and Overview of Current Knowledge with Emphasis the North Sea area*, 2003, ND/E-19/03.
6. Heaton, B.; Lambley, J. *Appl. Radiat. Isot.* **1995**, *46*, 577-581.
7. United States Environmental Protection Agency, Air and Radiation, *Evaluation of EPA's Guideline for Technologically Enhanced Naturally Occurring Radioactive Materials (TENORM)*, 2000, EPA 402-R-00-01.
8. He, S.; Kan, A. T.; Tomson, M. B. *Appl. Geochem.* **1999**, *14*, 17-25.
9. Van Hattum, B.; Cofino, W. P.; Feenstra, J. F. *Environmental Aspects of Produced Water Discharges from Oil and Gas Production on the Dutch Continental Shelf*, Institute for environmental studies, 1992.
10. Bostick, D. T.; Luo, H.; Hindmarsh, B. *Characterization of Soluble Organics in Produced Water*, ORNL/TM-2001/78, 2001.
11. Chapter 6: Van Leeuwen, F. W. B.; Verboom, W.; Shi, X.; Davis, J. T.; Reinhoudt, D. N. *J. Am. Chem. Soc.* **2004**, *126*, 16575-16581.
12. Chapter 4: Van Leeuwen, F. W. B.; Beijleveld, H.; Miermans, C. J. H.; Huskens, J.; Verboom, W.; Reinhoudt, D. N. *submitted for publication*.
13. Metal ions with an average concentration below 10⁻⁷ M are not reported. The Ra²⁺ concentrations were too low to be determined with a HPGE detector (counting time 2 days).
14. Competition by transition metal ions is not expected, since the extractants only have hard donor atoms.
15. Ra²⁺/Na⁺ selectivities of G **1**-Pic and isoG **2** were not determined above [Na⁺] = 10⁻² M.
16. Cai, M. M.; Marlow, A. L.; Fettingner, J. C.; Fabris, D.; Haverlock, T. J.; Moyer, B. A.; Davis, J. T. *Angew. Chem. Int. Ed.* **2000**, *39*, 1283-1288.
17. Shi, X.; Fettingner, J. C.; Cai, M. M.; Davis, J. T. *Angew. Chem. Int. Ed.* **2000**, *39*, 3124-3127.

18. At K5D_{1/100} and ^MK5D_{1/100} there still are distinct differences in the ²²⁶Ra²⁺ extraction behavior. Due to dilution in a tris-HCl buffer, [Cl⁻] is equal to [M_{tot}] in both samples (7 x 10⁻³ M).
19. Jiménez, A.; De La Montaña Rufo, M. *Water Research* **2002**, *6*, 1715-1724.
20. Rihs, S.; Condomines, M. *Chem. Geol.* **2002**, *182*, 409-421.
21. Somlai, J.; Horváth, B.; Kanyár, B.; Kovács, T.; Bodrogi, E.; Kávási, N. *J. Environ. Rad.* **2002**, *62*, 235-240.
22. Ogunleye, P. O.; Mayaki, M. C.; Amapu, I. Y. *J. Environ. Rad.* **2002**, *62*, 39-48.
23. Rutherford, P. M.; Dudas, M. J.; Arocena, J. M. *Sci. Total Environ.* **1996**, *180*, 201-209.
24. In Chapters 4 and 6 it has been shown that the Ra²⁺ extraction of all four extractants used cannot occur below pH 2. Therefore, this pH is considered to be low enough to quantitatively strip all Ra²⁺ cations.^{11,12}
25. In Chapter 4, the complete regeneration of tcc6da **4** (and tcc5da **3**) has been reported, indicating that after stripping these extractants can effectively be re-used for the extraction of Ra²⁺ from aqueous solutions with a pH above 7.
26. Forman, S. L.; Fettingner, J. C.; Pieraccini, S.; Gottarelli, G.; Davis, J. T. *J. Am. Chem. Soc.* **2000**, *122*, 4060-4067.
27. Davis, J. T.; Tirumala, S.; Jenssen, J. R.; Radler, E.; Fabris, D. *J. Org. Chem.* **1995**, *60*, 4167-4176.
28. Chapters 4 and 6 have shown that the extractants used only show quantitative Ra²⁺ extraction above pH 8.^{11,12}
29. Interference corrections were made for ⁴⁰Ca¹⁶OH⁺ on ⁵⁷Fe⁺, ⁴³Ca¹⁶O⁺ on ⁵⁹Co⁺, ⁴³Ca¹⁶O⁺ on ⁶⁰Ni⁺, sulfur on ⁶⁵Cu⁺ and ⁶⁶Zn⁺ and ⁸⁸Sr²⁺ on ⁴⁴Ca⁺.
30. Since experiments performed with half the amount of tracer still give the same extraction percentages, the [M_{tot}]/[L] ratio probably has a larger influence on the Ra²⁺ extraction than the concentration of ²²⁶Ra²⁺ tracer in the aqueous phase.

Outlook

Thiacalix[4]crown dicarboxylic acid- and (iso)guanosine-based extractants show extremely high Ra^{2+} selectivities as described in Chapters 4 and 6. Furthermore, both types of extractants give Ra^{2+} extraction from actual gas-field produced water (see Chapter 7). However, the results presented are based on fundamental investigations into the Ra^{2+} separation possibilities and these extractants do not provide a direct solution for the industries with a Ra^{2+} TENORM problem. Therefore, these extractants have to be adapted to be applicable in industrial water streams. Possible improvements are adapting of the effective pH range of the thiacalix[4]crown diacids or attachment of the extractants to a solid support.

The first improvement would be increasing of the effective pH range of the extractants. The pH range of common (oil and gas) produced waters lies between pH 3 and 8,¹⁻³ while the thiacalix[4]crown dicarboxylic acids (Chapter 4) are only effective above pH 6. Increasing the pH of these produced waters would increase the precipitation of metal hydroxides,⁴ resulting in enlarged amounts of contaminated scales and sludges.⁵ The thiacalix[4]crowns with methylsulfonyl carboxamide substituents, described in Chapter 5, were designed as extractant, which would extract Ra^{2+} over a wider pH range. However, this experiment did not provide the desired improvement of the effective pH range and furthermore it showed that increasing the steric hindrance caused by this acid substituent reduces the Ra^{2+} affinity/selectivity. Consequently, alternative acid groups should be both similar in size to a carboxylic acid group and provide an improved pH range; sulfonic acid and phosphonic acid substituents would meet both these requirements (Figure O.1).

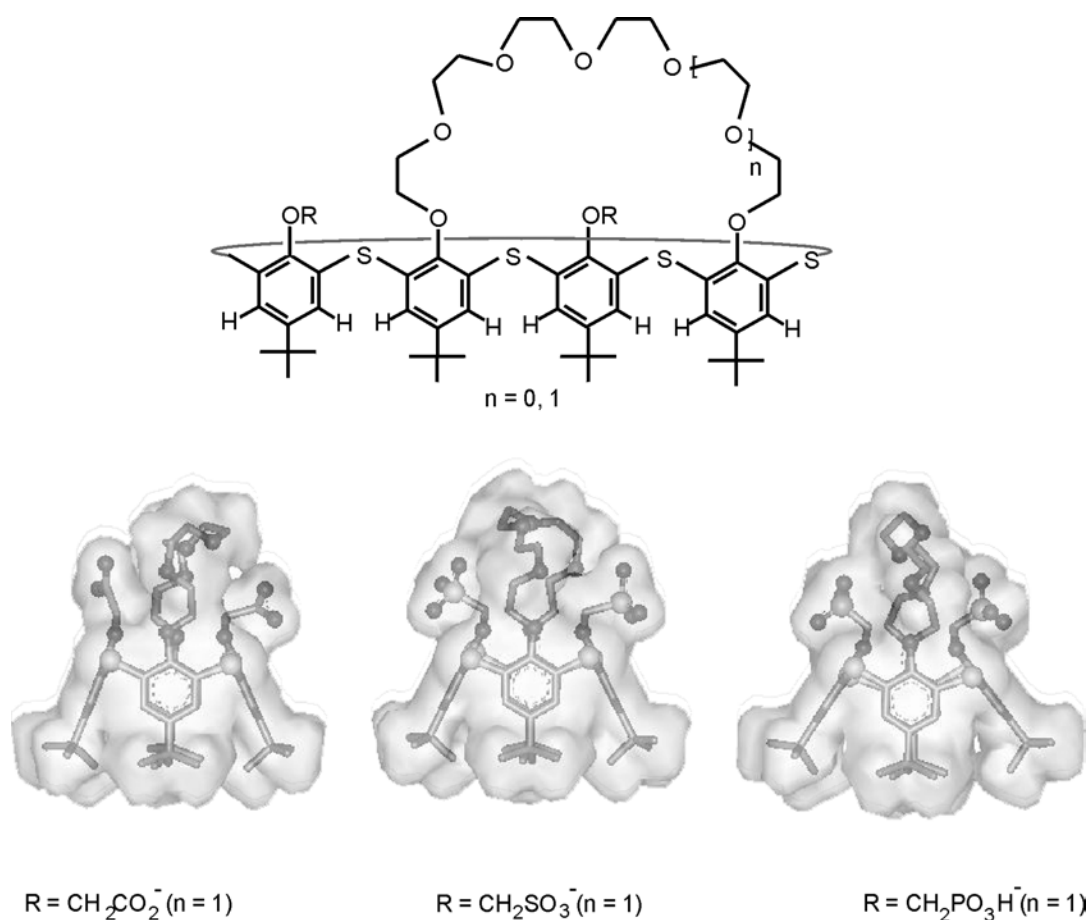


Figure O.1. Three different (deprotonated) thiacalix[4]crown diacids; molecular models show the similar sizes of the different substituents.

The second improvement would be immobilization of the extractants on a solid support, since liquid-liquid extraction is not very effective for the removal of traces of a pollutant from (bulky) industrial waste streams.⁶ Immobilization is easiest for the thiacalix[4]crown extractants, as these could be: (i) covalently attached, preferably via the upper rim of only one aryl unit of the platform, to a solid support, e.g. silica (Figure O.2 a),⁷ (ii) impregnated into a solid support or a membrane,^{8,9} or (iii) -perhaps a more ambitious suggestion - used as “ship in a bottle” systems in zeolites (Figure O.2b).¹⁰ However, for all these approaches steric restrictions of the thiacalix[4]arene platforms could significantly reduce the Ra^{2+} selectivity and should be minimized by e.g. only attaching one aryl unit to a solid support.

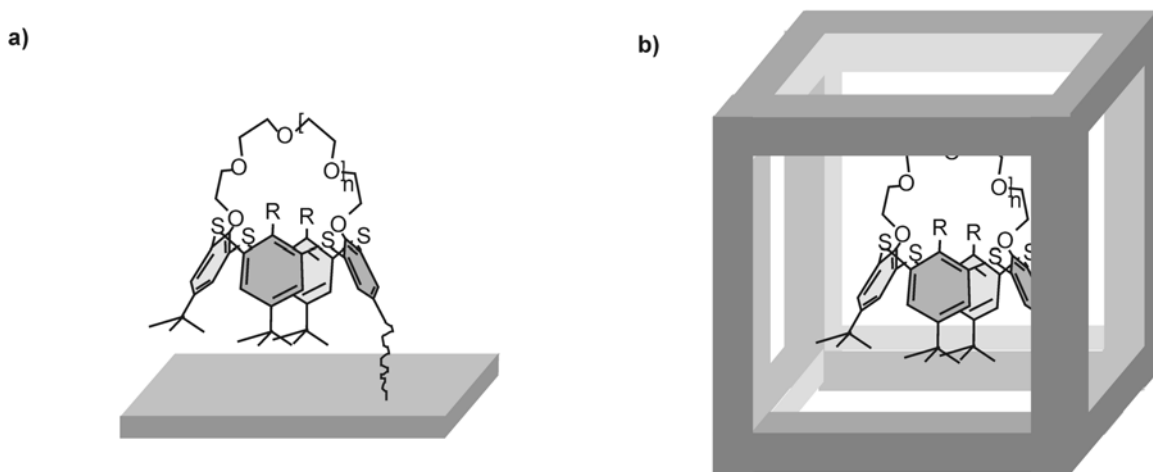


Figure O.2. Immobilization of thiacalix[4]crowns: a) on a solid support and b) in a cavity of a porous material/zeolite.

For the self-assembled systems of guanosine and isoguanosine (Chapter 6), immobilization is more difficult. Preformed complexes with a cation that binds less strongly than Ra^{2+} can be immobilized in membranes.¹¹ Since the self-assembled ionophores would have a higher selectivity for Ra^{2+} , these membranes can in theory extract Ra^{2+} from solutions containing a wide variety of metal ions (see Chapters 6 and 7). Another possibility for immobilization might be the formation of vesicle/micelle emulsions with single units of guanosine or isoguanosine,¹² allowing assemblies to be formed in-situ upon the complexation of Ra^{2+} cations. Filtration can then be used to separate the contaminated vesicles/micelles from the aqueous streams (Figure O.3). Since the self-assembled systems suffer from competition in the Ra^{2+} extraction from water-soluble organic compounds (see Chapter 7), they should not be applied in waste streams containing these organic pollutants.

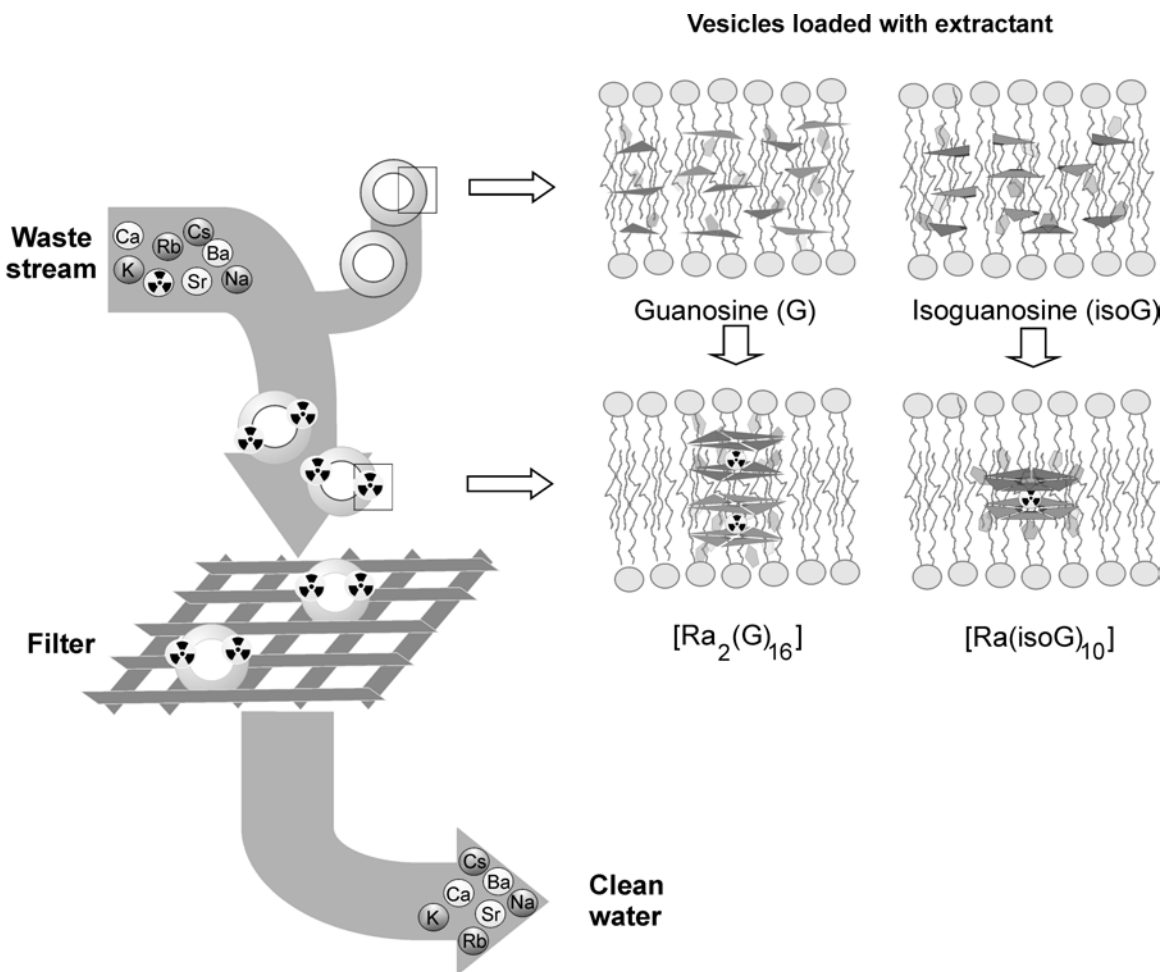


Figure O.3. Guanosine- and isoguanosine-loaded vesicles and their possible application in waste stream purification.

During the petroleum extraction process Ra^{2+} can precipitate with other alkaline earth cations and form contaminated scales and sludges (see Chapter 2). As a result the produced water effluents only contain a part of the Ra^{2+} brought to the surface.¹³ Therefore, the Ra^{2+} cations should ideally be extracted from the subsurface formation waters. Water-soluble extractants like EDTA, are currently introduced to these waters as anti-scaling agents⁵ and perhaps water-soluble derivatives of the in Chapter 4 described thiocalix[4]crowns could be used to prevent specific Ra^{2+} precipitation; assuming a similar kinetic stability of their Ra^{2+} complexes as has been reported for the calix[4]arene derivatives (see Chapter 2).^{14,15} Another way to make the extractants more effective

would be the overall prevention of scale formation, e.g. by not injecting sulfate-rich sea water into the well (Table 4; Chapter 2) or by decreasing the pH of injection water.⁵

References.

1. Bostick, D. T.; Luo, H.; Hindmarsh, B. Characterization of Soluble Organics in Produced water ORNL/TM-2001/78.
2. Cofino, W. P.; Slager, L. K.; van Hattum, B. *Environmental aspects of produced water discharges from oil and gas production on the Dutch Continental Shelf Part I. Overview of surveys on the composition of produced waters conducted on the Dutch Continental Shelf*. Institute for environmental studies Vrije Universiteit Amsterdam; commissioned by the Netherlands Oil and Gas Exploration and Producing Association (NOGEP), 1992.
3. McFarlane, J.; Bostick, D. T.; Luo, H. *Characterization and modeling of produced water* (www.ornl.gov/divisions/nuclear_science_technology/pprf/index).
4. McDowell, W. J.; Arndsten, B. A.; Case, G. N. *Solvent Extr. Ion Exch.* **1989**, *7*, 377-393.
5. Crabtree, M.; Eslinger, D.; Flecher, P.; Miller, M.; Johnson, A.; King, G. *Oilfield Review* **1999**, 30-45.
6. Kentisch, S. E.; Stevens, G. W. *Chem. Eng. J.* **2001**, *84*, 149-159.
7. Izatt, R. M.; Bradshaw, J. S.; Bruening, R. L. *Pure Appl. Chem.* **1996**, *68*, 1237-1241.
8. Benzi, P.; Reghetti, R.; Volpe, P. *J. Radioanal. Nucl. Chem. Lett.* **1992**, *164*, 211-220.
9. Casnati, A.; Pochini, A.; Ungaro, R.; Ugozzoli, F.; Arnaud, F.; Fanni, S.; Schwing, M.-J.; Egberink, R. J. M.; de Jong, F.; Reinhoudt, D. N. *J. Am. Chem. Soc.* **1995**, *117*, 2767-2777.
10. Corma, A.; Garcia, H. *Eur. J. Inorg. Chem.* **2004**, 1143-1164.
11. Lee, S. C.; Lamb, J. D.; Cai, M. M.; Davis, J. T. *J. Incl. Phenom.* **2001**, *40*, 51-57.
12. Ten Cate, M. G. J.; Crego-Calama, M.; Reinhoudt, D. N. *J. Am. Chem. Soc.* **2004**, *126*, 10840-10841.
13. Sorbie, K. S.; Mackay, E. J. *J. Pet. Sci. Eng.* **2000**, *27*, 85-106.
14. Chen, X. Y.; Ji, M.; Fisher, D. R.; Wai, C. M. *Inorg. Chem.* **1999**, *38*, 5449-5452.
15. Hendriksen, G.; Hoff, P.; Larsen, R. H. *Appl. Rad. Isot.* **2002**, *56*, 667-671.

Summary

This thesis describes the design and selectivity of new Ra^{2+} extractants. The results presented provide insight in both the requirements needed to give Ra^{2+} selectivity and in the achievable $\text{Ra}^{2+}/\text{M}^{n+}$ (M^{n+} = alkali(ne earth) cation) separations.

Chapter 1 gives a general introduction into molecular recognition and the need for selective extraction of radioactive contaminants. Chapter 2 describes the industries and conditions in which the naturally occurring Ra^{2+} nuclides are encountered as well as their toxic nature. In addition, various known Ra^{2+} extraction techniques are discussed, with the emphasis on organic extractants.

In Chapter 3, the bridging of thiacalix[4]arene derivatives with oligoethylene glycol ditosylates is described. The conformation of the resulting thiacalix[4](bis)crowns depends on the base and oligoethylene glycol ditosylates used. The conformational assignment relies on several X-ray crystal structures and extensive 2-D ^1H NMR studies. This chapter provides the (synthetic) background necessary for the synthesis and characterization of the extractants described in Chapter 4 and 5.

Chapter 4 describes the synthesis of thiacalix[4]crown dicarboxylic acids, and their Ra^{2+} selectivity in the presence of a large excess of the most common alkali(ne earth) cations. Thiacalix[4]crowns show significantly improved Ra^{2+} selectivities over their parent calix[4]crowns and of the two crown-ether bridge sizes (5 and 6), the crown-6 gives the highest overall Ra^{2+} selectivity. This results in Ra^{2+} extraction from $\text{M}^{n+}/\text{Ra}^{2+}$ ratios up to 3.5×10^7 (M^{n+} = Na^+ , K^+ , Rb^+ , Cs^+ , Mg^{2+} , Ca^{2+} , Sr^{2+} , or Ba^{2+}), using an excess of metal cation to extractant. In addition, the effective pH range (6-13) of thiacalix[4]crown-6 dicarboxylic acid allows for full regeneration of the extractants at acidic conditions.

Chapter 5 deals with the synthesis of (tri)substituted thiacalix[4]arene derivatives. Based on their Ra^{2+} selectivities and those of known thiacalix[4]arene derivatives, the optimal conditions are determined for the effective extraction of Ra^{2+} from solutions containing Ca^{2+} , Sr^{2+} , or Ba^{2+} . The results clearly show the advantage of bringing the Ra^{2+} extracting components of a synergistic system together on a

thiacalix[4]arene platform. This is exemplified by the in Chapter 4 reported thiacalix[4]crown-6 dicarboxylic acid, which is the best thiacalix[4]arene-based Ra^{2+} extractant under the conditions used.

In Chapter 6, the non-covalent assemblies formed by guanosine (hexadecamers) and isoguanosine (decamers) show Ra^{2+} extraction from $\text{M}^{n+}/\text{Ra}^{2+}$ ratios up to 10^6 ($\text{M}^{n+} = \text{Na}^+, \text{K}^+, \text{Rb}^+, \text{Cs}^+, \text{Mg}^{2+}, \text{Ca}^{2+}, \text{Sr}^{2+}, \text{or Ba}^{2+}$), using a similar deficiency of extractant as described in Chapter 4. These systems are effective over a broad pH range (3-11). Whereas guanosine requires the presence of a lipophilic picrate anion to form Ra^{2+} selective assemblies, the more Ra^{2+} selective isoguanosine gives high selectivities without any additives. The results clearly demonstrate the power of molecular self-assembly for the construction of selective extractants.

The last experimental chapter, Chapter 7, shows that the thiacalix[4]crowns and (iso)guanosines described in Chapters 4 and 6, respectively, are also able to effectively extract Ra^{2+} from mixed metal ion-containing gas-field produced water and an organic molecule free model solution. Surprisingly, the extractants reported in Chapters 4-6 have the highest *overall* Ra^{2+} selectivities in the alkali(ne earth) series, thiacalix[4]crown-6 dicarboxylic acid and isoguanosine gave the poorest results with the produced water and its model solution. This is caused by their relatively low $\text{Ra}^{2+}/\text{Na}^+$ selectivities, combined with the fact that Na^+ is the main competing cation in the gas-field produced water. The Ra^{2+} cations can be effectively stripped from the organic phases, underlining the potential for applications in industrial Ra^{2+} separation.

The outlook gives some suggestions for further improvements that can make the extractants described in Chapters 4, 6, and 7 better applicable in industrial Ra^{2+} -containing (aqueous) waste streams.

Overall it can be concluded that the Ra^{2+} selectivities of conventional crown ether/acid systems have been improved and a new non-covalent method for the formation of Ra^{2+} extractants is introduced. Furthermore, the potential use of organic extractants in industrial Ra^{2+} containing TENORM waste streams is made clear. Although the work presented in this thesis is of a fundamental nature, it clearly illustrates the headway made towards the separation of Ra^{2+} from waste streams containing significant excesses of competing cations.

Samenvatting

Dit proefschrift beschrijft de ontwikkeling en selectiviteit van nieuwe Ra^{2+} extractanten. De resultaten geven inzicht in zowel de vereisten waaraan extractanten moeten voldoen, als de haalbare $\text{Ra}^{2+}/\text{M}^{n+}$ (M^{n+} = (aard)alkalikation) scheidingen.

Hoofdstuk 1 geeft een algemene inleiding in moleculaire herkenning en het nut van de selectieve extractie van radioactieve vervuilingen. Hoofdstuk 2 beschrijft de industriën en condities waarin de van nature voorkomende Ra^{2+} nucliden gevonden worden. Daarnaast wordt hun toxiciteit behandeld en worden verscheidene Ra^{2+} -extractietechnieken besproken, met de nadruk op organische extractanten.

In Hoofdstuk 3 wordt het bruggen van thiacalix[4]arenen met oligoethyleenglycolditosylaten beschreven. De conformatie van de resulterende thiacalix[4]kronen hangt af van zowel het gebruikte oligoethyleenglycolditosylaats, als de gebruikte bazen. De conformaties zijn vastgesteld met behulp van verscheidene kristalstructuren en 2-D ^1H NMR studies.

Hoofdstuk 4 beschrijft de synthese van thiacalix[4]kroonethers met twee carbonzuurgroepen, alsmede hun Ra^{2+} selectiviteit in de aanwezigheid van een grote overmaat (aard)alkalikationen. Uit extractiestudies blijkt dat thiacalix[4]kroonethers ten opzichte van calix[4]kroonethers voor een significante verbetering van de Ra^{2+} selectiviteit zorgen en dat een kroon-6 relatief gezien de hoogste Ra^{2+} selectiviteit geeft. Dit resulteert in Ra^{2+} extractie uit mengsels met Na^+ , K^+ , Rb^+ , Cs^+ , Mg^{2+} , Ca^{2+} , Sr^{2+} of Ba^{2+} , tot $\text{M}^{n+}/\text{Ra}^{2+}$ verhoudingen van 3.5×10^7 en in de aanwezigheid van een overmaat metaal kationen ten opzichte van de hoeveelheid extractant. Daarnaast maakt het effectieve pH gebied (6-13) van de thiacalix[4]kroonetherdicarbonzuren volledige regeneratie mogelijk onder zure condities.

In Hoofdstuk 5 wordt de synthese van trigesubstitueerde thiacalix[4]arenen behandeld. Gebaseerd op hun Ra^{2+} selectiviteiten en die van bekende thiacalix[4]areen-derivaten zijn de optimale condities voor de effectieve extractie van Ra^{2+} uit oplossingen met Ca^{2+} , Sr^{2+} of Ba^{2+} bepaald. De resultaten geven duidelijk de verbetering in selectiviteit weer die verkregen wordt door de combinatie van een kroonether en een zuur op een thiacalix[4]areenplatform. Uit de resultaten blijkt dat

het thiacalix[4]kroon-6-dicarbonzuur, beschreven in Hoofdstuk 4, het beste op thiacalix[4]areen gebaseerde Ra^{2+} extractant is onder de gebruikte condities.

In Hoofdstuk 6 wordt de Ra^{2+} extractie van nietcovalente assemblages van guanosinederivaten (hexadecameren) en isoguanosinederivaten (decameren) beschreven. Deze extractanten geven Ra^{2+} extractie uit mengsels met Na^+ , K^+ , Rb^+ , Cs^+ , Mg^{2+} , Ca^{2+} , Sr^{2+} of Ba^{2+} , tot $\text{M}^{n+}/\text{Ra}^{2+}$ verhoudingen van 10^6 en gebruikmakend van een zelfde ondermaat extractant als in Hoofdstuk 4. Het effectieve pH-gebied van deze systemen ligt tussen pH 3 en 11. Waar guanosine additionele picraatanionen nodig heeft voor Ra^{2+} extractie, doet isoguanosine dit zonder extra toevoegingen. De resultaten tonen duidelijk de potentie van self-assemblage voor de vorming van selectieve extractanten.

In het laatste experimentele hoofdstuk, Hoofdstuk 7, wordt aangetoond dat de thiacalix[4]kroonethers en (iso)guanosines beschreven in de Hoofdstukken 4 en 6 ook in staat zijn om Ra^{2+} kationen effectief te extraheren uit productiewater van de gas-industrie, dat ook een mengsel van kationen in grote overmaat bevat. Een verbazingwekkend resultaat is dat de extractanten die de hoogste relatieve Ra^{2+} selectiviteit in de (aard)alkalikation series hebben (zie de Hoofdstukken 4 en 6), thiacalix[4]kroon-6-dicarbonzuur en isoguanosine, de slechtste resultaten geven met het productiewater en de modeloplossing waarin geen organische bestanddelen aanwezig zijn. Dit wordt veroorzaakt door de relatief lage $\text{Ra}^{2+}/\text{Na}^+$ selectiviteit van deze verbindingen, terwijl Na^+ het meest voorkomende concurrerende kation is. De geëxtraheerde Ra^{2+} kationen kunnen vervolgens effectief teruggeëxtraheerd worden uit de organische lagen, wat hun potentie voor industriële Ra^{2+} scheiding aantoont.

In de “outlook” worden wat suggesties gegeven voor verbeteringen die de extractanten beschreven in de Hoofdstukken 4, 6 en 7 beter toepasbaar kunnen maken in industriële Ra^{2+} houdende afvalstromen.

In het algemeen kan geconcludeerd worden dat de Ra^{2+} selectiviteiten van conventionele kroonether/zuur systemen zijn verbeterd en een nieuwe non-covalente methode voor de bereiding van Ra^{2+} extractanten is geïntroduceerd. Daarnaast is ook het potentiële gebruik van organische extractanten voor de extractie van Ra^{2+} uit industriële TENORM afvalstromen aangetoond. Ondanks de voornamelijk fundamentele aard van dit onderzoek, toont het duidelijk de vooruitgang die gemaakt is bij de scheiding van Ra^{2+} uit afvalstromen, waarin een grote overmaat van concurrerende kationen aanwezig is.

Acknowledgments/Dankwoord

The research described in this thesis could not have been performed without the help and/or support of the people acknowledged below.

Ik wil beginnen met het bedanken van mijn begeleiders David Reinhoudt en Wim Verboom voor de mogelijkheid om mijn promotieonderzoek binnen SMCT uit te voeren. David, we hebben elkaar in de afgelopen vier jaar weinig gezien, maar je was er altijd als het nodig was. Ik denk dat die momenten van grote invloed zijn geweest op dit proefschrift. Wim, in tegenstelling tot David was jij er altijd. Zonder jouw steun was het niet mogelijk geweest om dit proefschrift binnen de gestelde termijn tot een goed einde te brengen.

I want to thank the following people for their scientific contribution to the various chapters in this thesis. Jeff, what can I say, your sabbatical turned out to be the turning point during my Ph.D. Your endless enthusiasm made even the simplest of things “interesting”, not even mentioning the “amazing” stuff. Furthermore, entrusting me with the last of “your” (iso)guanosine derivatives, has allowed me to perform the studies described in Chapters 6 and 7. Jurriaan, jouw hulp met het fitten van de extractieconstanten uit de Hoofdstukken 4 en 5 was cruciaal voor de quantificering van de extractieresultaten. Aldrik, penso di essere stato fortunato perche’ le misure e la caratterizzazioni della mappa stellare NOE al NMR del Capitolo 5 sono state effettuate prima della sua rottura. Huub, jouw kundigheid in de ”zwarte magie” van de kristallografie heeft ons naast de X-rays in hoofdstuk 3 heel wat fancy self-assembly X-rays opgeleverd. Hans, as ie d’er nich wan’n west, had ik nô nog an de gang west met ‘t spul van thiocalix[4]areen oet de kapittels 3, 4 en 5.

The proofreaders, Clare, Alart, Aldrik, and Merce, thanks for the effort you all made in correcting my concept thesis.

Mijn dank gaat ook uit naar de Stichting Technische Wetenschappen (STW) voor de financiering, Kees Miermans en de afdeling IMLA van het RIZA voor de ICP-MS metingen, Martin Heus van Akzo Nobel voor de patentpogingen (het was erg leuk om ergens “de uitvinder” van te zijn), Total voor de productiewatersamples, NRG-FAI voor het beschikbaar stellen van de radionucleaire faciliteiten en Tanja

Tomasberger voor het verwerken van de eindeloze hoeveelheden ^{226}Ra samples die ik geproduceerd heb.

Ik wil “staf 2” en Marcel bedanken voor hun constante beschikbaarheid en ondergewaardeerde, maar essentiële, ondersteunende werkzaamheden. Ben, ie hebt mie ‘t twentse boetnlev’n biebracht. Ik hop dat’t altied zo (mooi) blif in Twente. Richard, ie hebt mie in veer jaor oaveral me hölp’n, wak mie mer wunsche kon en ie hept mie völ biebracht (oaver chemie). Ik bin na blier dat ie miene secondant wilt wenn.

Next to the people mentioned above, I had a nice time with Marcel, Jannie, Ron, Vera, Gerrit[†], Geert-Jan, Marco, Ronald, and Marga (at NRG) and with Alart, Wiljan, Thieme, Roel, Leon, Becky, Peter, Emiel, Frederieke, Jurjen, Bianca, Hannie, Carla, Jeroen, Fernando, Izabel, Barbara, Nancy, and some people I probably forgot to mention (at CT). Arjan, zonder jouw “Fijs kom je (ook) lunchen” was ik waarschijnlijk nooit van lab 52 afgekomen. Miguel, cuatro años mas tarde y a pesar the muchos “I don’t care” y “?”, ha sido y continua siendo muy divertido escribir junto a ti en la habitacion 1719. Monica, quando mi mancavano i miei bambini eri sempre lì per rallegrarmi.

Als ik na lange dagen in Petten moederziel alleen in “Leyden” kwam, was er altijd iemand om in “de Uil” een biertje mee te drinken; Toin, Ron, Theo, Rob en de anderen bedankt voor de relativerende momenten. Sjon, vroegâh stonde wè same op de "1e rè" in de scrum, nu zulle we zien of deize combinatie voâh een praumautiecommissie net zau effeksief is.

Ma, jouw eindeloze geduld voor de “ik zat te denken” momenten die ik als kind had heeft de basis gelegd voor mijn onderzoeksdrang. An, ik kijk uit naar de wetenschappelijke innovaties die jij hoogstwaarschijnlijk zal veroorzaken.

Mijn liefste Lieke, jij hebt de afgelopen tien jaar aan mijn zijde gestaan en bent altijd in mij blijven geloven. Hierdoor heb jij van alle benoemde mensen misschien wel de grootste bijdrage aan dit proefschrift geleverd.

Zoë en Sven, iedereen vraagt aan mij of het niet moeilijk is om te studeren/promoveren met kleine kinderen. Ik geloof echter dat ik het met jullie erg getroffen heb, want jullie glimlach maakt de zwaarste (werk)dag weer goed en jullie drang om nieuwe dingen te onderzoeken is mijn grootste inspiratie.